Chimeric Antigen Receptor (CAR) T-cell Immunotherapy for MUC1-positive Breast Cancer

Gavriil, Artemis

Awarding institution:
King's College London

Chimeric Antigen Receptor (CAR) T-cell Immunotherapy for MUC1-positive Breast Cancer

Artemis Gavriil
Student number: 1344584

Thesis submitted for the Degree of Doctor of Philosophy

Abstract

Cancer immunotherapy using chimeric antigen receptor (CAR) T-cells has shown exceptional promise in the treatment of patients with refractory B-cell malignancy. In this approach, patient-derived peripheral blood T-cells are engineered to express a cell surface receptor, which confers specificity for a tumour-associated (TA) antigen. Mucin-1 (MUC1) is a large transmembrane glycoprotein that is overexpressed in 90% of breast cancers. A further important characteristic of this mucin is the fact that it is under-glycosylated in cancer cells. This holds the potential for CAR T-cell mediated targeting of MUC1 epitopes in tumour-cells which are not exposed in normal cells. Antibodies such as TAB004 and HMFG2 are considered to bind preferentially to TA-MUC1. The aim of this PhD project was the development of a CAR T-cell approach for MUC1-positive breast cancer. Herein, the anti-tumour potential of a novel 2nd generation MUC1-specific CAR, named TAB28z, has been investigated. The binding domain of this CAR is derived from the TAB004 anti-MUC1 antibody. TAB28z is being compared with two other previously developed MUC1-specific CARs, H28z and HDF28z, both of which are derived from the HMFG2 antibody. TAB28z CAR T-cells demonstrated significant anti-tumour activity against MUC1-positive breast cancer cell lines in the *in vitro* setting. Nevertheless, it became apparent throughout this project that MUC1 expressed on activated T-cells is detected by both HMFG2-based and TAB004-based CAR T-cells during the T-cell expansion period. This background recognition resulted in tonic signalling by CARs, which was accompanied by constitutive production of IFN-γ, CAR T-cell enrichment, reduced T-cell expansion and a trend towards upregulation of T-cell activation and exhaustion markers. Despite these observations, the activity of the three MUC1-specific signalling CARs was investigated in two different breast cancer xenograft models. No significant anti-tumour responses were observed in either of the two models, which could possibly be attributed to the effects of tonic signalling.

Table of contents

Table of figures

Table of tables

Abbreviations

ACT	Adoptive T-cell therapy
ADCC	Antibody-dependent cell-mediated cytotoxicity
AICD	Activation-induced cell death
ALL	Acute lymphoblastic Leukaemia
APC	Antigen presenting cell
APC	Allophycocyanin
Asn	Asparagine
BCMA	B-cell maturation antigen
BLI	Bioluminescence imaging
BPDCN	Blastic plasmacytoid dendritic cell neoplasm
CA	Capsid
CAF	Cancer-associated fibroblasts
CAIX	Carbonic anhydrase IX
CAR	Chimeric antigen receptor
CCL2	C-C motif chemokine ligand 2
CEA	Carcinoembryonic antigen
CRS	Cytokine release syndrome
CT	Cytoplasmic tail
CTGF	Connective tissue growth factor
CTL	Cytotoxic T-lymphocytes
CTLA-4	Cytotoxic T-lymphocyte-associated antigen 4
DC	Dendritic cells
DLBCL	Diffuse large B-cell lymphoma
DMEM	Dulbecco's Modified Eagle Medium
dMMR	Mismatch repair deficiency
DMSO	Dimethyl Sulfoxide
DNA	Deoxyribonucleic acid
E. coli	*Escherichia Coli*
ECD	Extracellular domain
EDTA	Ethylenediaminetetraacetic acid

EGFR	Epidermal growth factor receptor
EGFRvIII	Epidermal growth factor receptor variant III
ELISA	Enzyme linked immunosorbent assay
ER	Endoplasmic reticulum
ER	Oestrogen receptor
FDA	Food and Drug Administration
Ffluc	firefly luciferase
FITC	Fluorescein isothiocyanate
FMO	Fluorescence minus one
FRα	Folate receptor-alpha
Gal	Galactose
GalNAc	N-acetylgalactosamine
GalNAcT	N-acetylgalactose aminyltransferase
GALV	Gibbon-Ape Leukaemia Virus
GD2	Diasialoganglioside-2
GI	Gastrointestinal
GlcNAc	N-acetyl glucosamine
Grb2	Growth factor receptor-bound protein 2
GSK3β	Glycogen synthase kinase 3β
GvHD	Graft versus host disease
HER	Human epidermal growth factor
HER-2	Human epidermal growth factor receptor 2
HMFG	Human milk fat globule
HRP	Horseradish peroxidase
i.p.	Intra-peritoneal
iCAR	Inhibitory chimeric antigen receptor
ICB	Immune checkpoint blockade
IDC-NST	Invasive ductal carcinoma of no special type
IDO	Indoleamine-pyrrole 2,3-dioxygenase
IFN-γ	Interferon γ
Ig	Immunoglobulin
IL	Interleukin

IL-2	Interleukin-2
IL6-R	Receptor of interleukin-6
IN	Integrase
ITAM	Immunoreceptor tyrosine-based activation motif
iTregs	Induced Tregs
IVIg	Intravenous immunoglobulin
LDH	Lactate dehydrogenase
mAb	Monoclonal antibody
MAGE	Melanoma-associated antigen
MAPK	Mitogen-activated protein kinase
MDSC	Myeloid derived suppressor cells
MHC	Major histocompatibility complex
MoMLV	Moloney murine leukaemia virus
mRNA	Messenger RNA
MSI-H	Microsatellite instability-high
MT-MMP	Membrane-type matrix metalloproteases
mTOR	Mammalian target of Rapamycin
MTT	3-(4,5-dimethylthiazol-2-yl)-2,5-diphenyltetrazolium bromide
MUC	Mucin
MUC1	Mucin-1
MUC1-C	MUC1 C-terminal subunit
MUC1-N	MUC1 N-terminal subunit
MVA	Modified virus of Ankara
NF-κB	Nuclear factor kappa B
NICE	National Institute for Health and Care Excellence
NSCLC	Non-small cell lung cancer
NSG	NOD *scid* gamma
nTregs	Natural Tregs
OD	Optical density
PARP1	Poly [ADP-ribose] polymerase 1
PBMCs	Peripheral blood mononuclear cells

PBS	Phosphate buffered saline
PCR	Polymerase Chain Reaction
PD-1	Programmed death-1
PDGFA	Platelet-derived growth factor-A
PDGFB	Platelet-derived growth factor-B
PD-L1	Program death ligand-1
PE	Phycoerythrin
PEI	Polyethylenimine
PFS	Progression-free survival
PHA	Phytohemagglutinin
PI3K	Phosphatidylinositol-3-Kinase
PR	Progesterone receptor
PR	Protease
ROR1	Receptor tyrosine kinase-like orphan receptor 1
RR	Relative risk
RT	Reverse transcriptase
RTK	Receptor tyrosine kinase
s.c.	Subcutaneous
scFv	Single chain variable fragment
SCID	Severe combined immunodeficiency
SCIg	Subcutaneous immunoglobulin
SD	Standard deviation
SEA	Sperm protein, enterokinase and agrin
SEM	Standard error of the mean
SLNB	Sentinel lymph node biopsy
Sos	Son of sevenless
ssRNA	Single-stranded RNA
ST	Sialyl T
ST3Gal I	α3-sialyltransferase
ST6GalNAc I	α6-sialyltransferase
STAT	Signal transducer and activator of transcription
STn	Sialyl Tn

SU	Surface envelope protein
synNotch	Synthetic Notch
T-DM1	Trastuzumab emtansine
TACE	Tumour necrosis factor-α enzyme
TAM	Tumour-associated macrophages
TAN	Tumour-associated neutrophils
TCR	T-cell receptor
Td	Tandem dimer
TGF	Transforming growth factor
TGF-α	Transforming growth factor-α
TILs	Tumour-infiltrating lymphocytes
TKIs	Tyrosine kinase inhibitors
TM	Transmembrane
TMB	3,3',5,5'-Tetramethylbenzidine
TNF-α	Tumour necrosis factor-α
Tregs	Regulatory T-cells
TRAC	T-cell receptor α constant
Tregs	Regulatory T-cells
TT	Tetanus toxoid
TTP	Time-to-progression
UEC	Uterine epithelial cells
VEGF	Vascular endothelial growth factor
VEGFA	Vascular endothelial growth factor-A
VNTR	Variable number tandem repeats
VSV-G	Vesicular stomatis virus G
WHO	World Healh Organisation
Zap-70	Zeta-chain associated protein 70
β-TrCP	β-transducin repeat containing
β1,3-Gal T	β1,3-galactose transferase
β1,6-C2GnT I	β1,6-N-acetyl glucosamine transferase
TAA	Tumour associated antigens

Acknowledgments

I would sincerely like to thank all the people who made the completion of this PhD possible. Firstly, I would like to express my sincere gratitude to my first supervisor Dr John Maher for his continuous support and guidance.

Additionally, I would like to thank my second supervisor Dr Sophie Papa and all the present and past members of the CAR Mechanics Group (Marc, Ana, Lynsey, Roseanna, Mustafa, Leena, Ben, Thivyan). I am also grateful to the members of the Breast Cancer Biology Group for sharing with me their scientific expertise (Professor Joy Burchell, Professor Joyce-Taylor Papadimitriou, Dr Richard Beatson and Dr Picco Gianfranco).

I am extremely thankful to my friends and excellent scientists Fiona Kogera and Dr Daniela Achkova for supporting me to every step throughout this PhD, in both personal and scientific level; and to every other friend and family member whose emotional support and indirect contribution is undeniable (Stefani, Christian, Elin, Evanna, Lambros, Tolis, Antonella and many more).

Lastly, there are no words to express my deepest gratitude to my parents, Paris and Fedra, and to my sister, Eleni. It is not an understatement to say that everything I have achieved is because of them.

This thesis is dedicated to my aunt, Maria,

who is battling Inflammatory Breast Cancer.

Chapter 1: Introduction

1.1 Breast Cancer

1.1.1 Epidemiology

Breast cancer is the most common malignancy in women, with 1.77 millions cases per year, and the second most diagnosed type of cancer worldwide, following lung cancer[1,2]. One in eight women will develop breast cancer during their lifetime. Additionally, breast cancer is the leading cause of cancer death in females in both developed and less developed countries, with 521,900 deaths reported worldwide in 2012[1]. Men can also develop breast cancer, accounting for 1% of all cases.

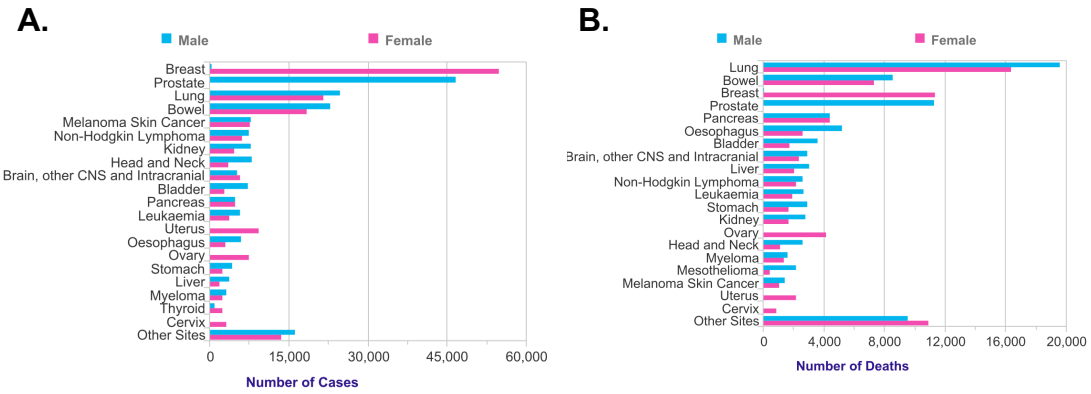

Figure 1.1: Breast cancer incidence and mortality in UK (2014). A) Twenty most common cancers in both males and females. B) Twenty most common cancer types responsible for cancer-associated deaths. Adapted from Cancer Research UK Statistics (http://www.cancerresearchuk.org/health-professional/cancer-statistics/mortality/common-cancers-compared#heading-Zero).

In the United Kingdom, breast cancer is the most common cancer in both women and men combined, accounting for the 15% of all cancer cases, and is the third leading cause of cancer deaths (8%) (Figure 1.1)[3,4]. Although

incidence has increased over time, mortality rates have declined substantially, with a 32% decrease since the early 1970s[5]. This is mainly attributed to the improvement of treatment options and to early detection[5].

1.1.2 Risk factors

Breast cancer is strongly associated with age with 48% of cases occurring at age 65 and above (Figure 1.2)[6].

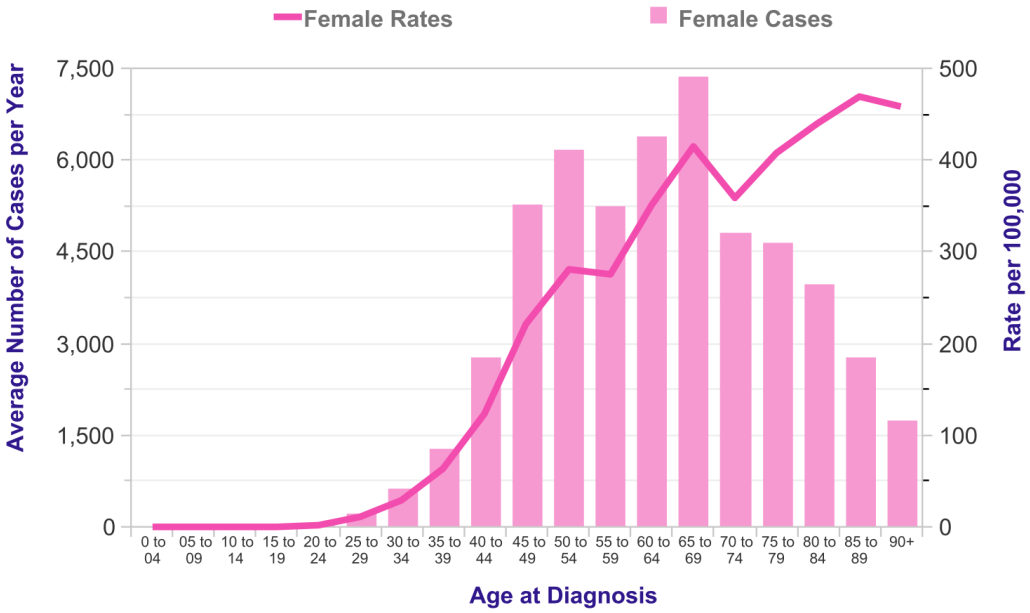

Figure 1.2: Breast cancer incidence in relation to age at diagnosis in females in UK (2014). *Adapted from Cancer Research UK Statistics (http://www.cancerresearchuk.org/health-professional/cancer-statistics/statistics-by-cancer-type/breast-cancer/incidence-in-situ#heading-One), accessed 20th August 2017).*

Other risks factors have been linked to the development of the disease, including hormonal factors, lifestyle and environmental factors and genetic predisposition. These are summarised in and have been reviewed by S.

Singletary[7]. The factors mentioned in the table below affect the risk of disease presentation at varying levels. For example, environmental and hormonal factors have a moderate influence with ~1.0-2.0 relative risk[7]. In contrast, BRCA1 and BRCA2 mutation are reported to substantially increase the risk for breast cancer, with >11-30 fold higher risk than background population rates[8].

Table 1.1: Risk factors associated with breast cancer.

Risk factor	Risk group/comments
Age	Risk increases with age.
Race/ethnicity[9,10]	White women are at increased risk in comparison with women from other race groups, such as Hispanic and African American.
Reproductive factors	
Age of menopause[11]	Increased risk if occurs after the age of 55.
Age of menarche[12]	Increased risk if occurs before the age of 12.
Pregnancy[13]	Nulliparous women are in higher risk.
Age of first full-term pregnancy[13,14]	Increased risk in women who gave birth ≥30 years of age.
Oophorectomy[12]	Decreased risk in premenopausal women.
Lifestyle and environmental factors	
Alcohol consumption[15]	Increased risk related to excessive consumption.
Body mass index (BMI)[16,17]	Increased risk in postmenopausal women with high BMI; protective in premenopausal women.
Radiation exposure[18,19]	Increased risk, especially in females treated in younger age. Latency period for cancer presentation is >30 years.
Physical activity[20]	Decreased risk, more apparent in pre-menopausal women.
Exogenous hormonal factors	
Hormone replacement therapy[21,22]	Increased risk in current or recently ceased users after 5 years or more of use.
Contraceptive pill[23]	Increased risk associated with medium and high-dose oestrogen contraceptives. Progesterone-based contraceptives also increase the risk. There are two types of progestin-based contraceptive pills. The estrane-type showed higher risk related to cumulative dose. By contrast, increased risk associated with gonane-based contraceptives did not correlate with dose.
Previous presentation of hyperplasia[24] **or breast cancer**	Increased risk.
Family History[25]	Increased risk if a first or/and second degree relative have had breast cancer.
Genetic mutations[8] (e.g BRCA1, BRCA2)	Increased risk. The relative risk (RR) for BRCA1 carriers is >30 fold at age <40 years old and 14-fild for individuals age >60. The RR for BRCA2-mutation carriers is 11-fold at all age groups.

1.1.3 Histological and molecular classification

Historically, breast cancer was considered as a single disease with distinct histological and morphological characteristics. Traditionally, classification of breast cancer types into subgroups was mainly based on the clinico-pathological characteristics of the disease such as histological type, involvement of lymph nodes, histological grade or presence of metastatic disease[26]. Predictive markers were also extensively used for the classification and selection of treatment, including the expression of oestrogen (ER) and progesterone (PR) receptors (for endocrine therapy), and HER-2 overexpression (for treatment with trastuzumab)[26].

Most of the attempts at histological-based classification of breast cancer have failed due to the fact that breast cancer is comprised by areas with distinct morphological characteristics[27]. This heterogeneity in breast carcinomas has been well documented by the World Health Organisation (WHO)[28]. The WHO has identified at least 38 different breast cancer types and subtypes, including 20 types of breast cancer and 18 special types[28]. Of all documented types, invasive ductal carcinoma of no special type (IDC-NST) appears to be the most commonly reported type (40-75%), while invasive lobular carcinoma accounts for 5-15% of all cases[28].

In recent years, with the advent of high throughput technologies, there has been a breakthrough in the understanding of the biology of breast cancer. Microarray-based studies that allow gene expression analysis revealed that breast cancer should not be considered as a single disease with various

subtypes but rather as a number of different diseases that affect the same anatomical side[29,30].

Perou *et al.* published the first study that provided a molecular classification of breast cancer based on gene expression patterns[31]. The first key observation was that ER-positive and ER-negative breast cancers are highly distinct tumours based on their gene expression profiles. Moreover, extensive work has revealed the presence of four different molecular subtypes of breast cancer, named as luminal (luminal A, B and C), HER-2 positive, basal-like and normal breast-like (intrinsic subtype classification)[31–34]. This molecular classification is of major clinical importance as each of these subtypes are reported to have different prognosis, incidence and response to treatment[32,34–38].

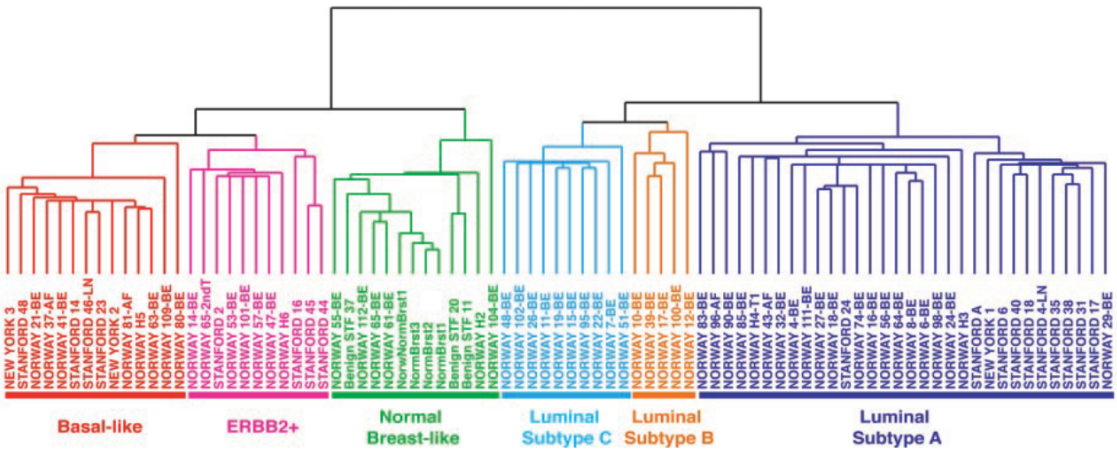

Figure 1.3: Molecular classification of breast cancer. 85 samples were used for the gene expression analysis. These included 78 malignant tumours, three benign tumours and four normal tissues. The tumour samples were divided into five (or six) subtypes based on differences in gene expression. The cluster dendrogram is showing the five (six) subtypes of tumours. basal-like – red; ERBB2^{+} – pink; normal breast-like – green; luminal subtype C - light blue; luminal subtype B – orange; luminal subtype A - dark blue. *Adapted from Sorlie et. al (2001)*[32].

As depicted in Figure 1.3, the distinct molecular types of breast cancer are split into two major branches, the ER-low to negative branch (basal-like, ErbB2$^+$, normal-like) and the ER-positive tumour types (luminal). The basal-like category is characterised by shorter overall survival and includes triple-negative breast cancer (ER-ve PR-ve HER-2-ve), which tends to be more aggressive than the other breast cancer types[32,34,39,40]. Additionally, this category includes cancers that carry a BRCA1 mutation[34]. The HER-2 category is characterized by amplification of the ErbB2 gene while the normal-like category exhibits higher expression of genes expressed in non-epithelial cells. The luminal category is divided into three different subtypes. The luminal A subtype occurs at the highest frequency (50-60%) and is characterised by high expression of ER and good prognosis. Subtypes B and C present moderate to low ER expression but once again may be distinguished based on their unique gene expression profiles [32].

Gene expression technology has also been used for the development of prognostic signatures which help to predict the outcome of the disease in individual patients and to distinguish which patients could benefit from endocrine or cytotoxic treatment. The most well-known platforms are the Oncotype DX and MammaPrint and both are considered useful tools in the clinic[40–42]. Notably, a study was conducted which compared the five most popular prognostic platforms: Oncotype DX, MammaPrint, intrinsic subtype classification, wound-response model and the two-gene ratio model[43]. Based on this study, all of the platforms (with the exception of the two-gene ratio model) showed agreement in the outcome predictions for individual patients[43].

1.1.4 Treatment strategies

1.1.4.1 National Institute for Health and Care Excellence (NICE) recommendations

According to the recommendations of the National Institute for Health and Care Excellence (NICE), the standard treatment for breast cancer differs for early and advanced disease[44,45]. In both cases, the treatment plan offered to each patient may include one or a combination of the following: surgery, chemotherapy, radiotherapy, endocrine therapy and biological therapy. Different combinations of these modalities of treatment may be used in the generation of a treatment plan for an individual breast cancer patient, depending on the tumour's clinico-pathological and molecular characteristics[44,45].

The diagnosis of breast cancer is generally based on clinical assessment followed by mammography, ultrasound imaging of the axilla, core biopsy and/or fine needle aspiration cytology[44,45]. In the case where the ultrasound reveals abnormal lymph nodes, then an ultrasound-guided needle biopsy may be performed in order to stage disease[44,45]. The most common technique of ultra-guided needle biopsy is sentinel lymph node biopsy (SLNB). This technique is based on the fact that tumour cells spread to the lymph nodes through the lymphatic system[46,47]. The sentinel lymph node is the first node which is infiltrated by tumour cells[46,47]. To perform SLNB, a radioactive element and/or a blue dye are injected in the breast near the tumour. These travel to the sentinel node via the lymphatic vessels which allows for the localisation of the sentinel node[48,47]. Afterwards, a gamma probe is used in

order to detect the radioactive nodes[48,49]. It is noteworthy that there can be more than one sentinel node. Lymph nodes that are radioactive or stained with the blue dye are excised and analysed for tumour cell infiltration[50].

Treatment of patients usually includes surgery, which can be either breast conserving or mastectomy. In breast conserving surgery, a tissue excision with minimum 2 mm radial margin is recommended[44,45]. In the case of patients with invasive breast cancer, the excised tissues are characterised for ER and HER-2 status. Additionally, an axillary lymph node dissection is performed in patients where the sentinel lymph node biopsy has previously revealed the presence of infiltrating tumour cells[44,45].

Breast cancer patients often also undergo neoadjuvant (administered before surgery) or adjuvant cytotoxic chemotherapy (administered after surgery)[44,45]. Usually a combination of two to three different drugs are used for chemotherapy treatment. Following surgery, patients with early invasive breast cancer are offered radiotherapy to the breast[44,45]. Patients with high risk of recurrence undergo radiotherapy targeted to the chest wall. Additionally, patient with positive lymph nodes are being offered additional radiotherapy to the axilla or to supraclavicular fossa[44,45]. If a patient undergoes chemotherapy after surgery, then the radiotherapy takes place post chemotherapy. Additionally, patients with HER-2-positive breast cancer can receive biological treatment, e.g trastuzumab[44,45].

The above treatments can be used in combination with endocrine therapy for ER+ve and/or PR+ve tumours. The agents usually used for this purpose include tamoxifen and aromatase inhibitors, such as letrozole, anastrozole and exemestane[44,45]. Tamoxifen is usually given to pre-

menopausal women while aromatase inhibitors are generally prescribed for post-menopausal women[44,45]. Tamoxifen acts as binding competitor of oestrogen to oestrogen receptor while aromatase inhibitors prevent the production of oestrogen[44,45].

1.1.4.2 Targeting DNA-repair mechanisms

In parallel with studies related to the molecular characterization of breast cancer, there have been many advances in the understanding of signalling pathways that are involved in tumour formation. This research has led to the emergence of several new targeted therapies for breast cancer in recent years. The hallmarks of tumour development include uncontrolled cell proliferation, genomic instability, cell metabolic changes and induction of angiogenesis[51]. Genetic instability is responsible for the generation of random mutations which cause either loss or gain of gene function. One well-known example is the inactivation of the BRCA1 or BRCA2 genes, both of which are normally involved in DNA repair. Inactivation of these genes leads to the accumulation of mutations in breast cells[52]. Germ-line mutations of these genes are associated with inherited predisposition to breast and ovarian cancer[53].

The enzyme, poly [ADP-ribose] polymerase 1 (PARP1) is also involved in the repair of DNA-single strand breaks. Inhibitors of PARP1 (PARPi) have been developed as a form of targeted therapy and they function by blocking the DNA repair mechanism of malignant cells which eventually causes the apoptosis of these cells[54]. PARP inhibitors appear to be particularly effective in patients carrying mutant BRCA1 and/or BRCA2 genes[55–58]. This has been

reported to be due to a synthetic lethal interaction[54,59]. Synthetic lethality, first described by Dobzhansky in 1946, is the phenomenon where a defect in a single gene does not result in significant cell damage[60,61]. Nevertheless, a defect in two distinct but complementary genes significantly increases cell damage[60].

1.1.4.3 Targeting tyrosine kinase receptors

A second important example stems from the fact that uncontrolled proliferation of breast cancer cells may be caused by signalling of tyrosine kinase receptors. The most representative example is HER-2 (ErbB2) which belongs to the human epidermal growth factor receptor (HER) family. Patients with HER-2 overexpression have poorer prognosis and they respond less well to standard treatment[62,63]. Many monoclonal antibodies have been produced and approved by the Food and Drug Administration (FDA) for treatment of HER-2 positive breast cancer. Trastuzumab (Herceptin) was the first such agent and even though it showed significant activity, a limited duration of response is frequently observed due to acquired resistance to the drug[64]. These observations led to the development of other HER-2 targeted therapies - either single or double targeting approaches[64]. These include antibody drug conjugates and tyrosine kinase inhibitors (TKIs).

Trastuzumab emtansine (T-DM1, Kadcyla™) is a HER-2 specific antibody drug conjugate which has been generated by conjugating trastuzumab with the DM1 cytotoxic agent[65]. It has been shown to have anti-tumour activity against both trastuzumab-resistant and lapatinib-resistant tumour cells, both *in vitro* and *in vivo*[65,66]. The potential of trastuzumab

emtansine as a monotherapy for HER-2 amplified breast cancer was confirmed in a recent Phase III clinical trial[67]. In that study, 991 breast cancer patients who have been previously treated with trastuzumab and taxane-based drug received either T-DM1 or lapatinib plus capecitabine[67]. Patients who received T-DM1 achieved significantly prolonged progression-free survival (PFS), with 9.6 months median PFS versus 6.4 months in patients treated with lapatinib plus capecitabine[67]. These results led to the approval of Trastuzumab emtansine by the FDA for the treatment of patients with metastatic HER-2 positive breast cancer and who have been previously been treated with trastuzumab and taxane-based drug[68].

Lapatinib (Tykerb) is an orally administered small molecule inhibitor with dual specificity for epidermal growth factor receptor (EGFR) and HER-2[69]. As with other TKIs, it functions by blocking auto-phosphorylation of the intracellular signalling domain of tyrosine kinases, thus preventing the activation of downstream signalling pathways[69,70]. Lapatinib is the only FDA-approved TKI for breast cancer. It was initially approved in 2007 to be used in combination with capecitabine (Xeloda) for the treatment of HER-2-positive breast cancer patients who have previously been treated with anthracycline, taxane, and trastuzumab-based drugs[71]. The approval was based on the results of a Phase III randomised clinical trial in which patients received capecitabine alone or in combination with lapatinib[72]. The combination of the two drugs resulted in a delay in disease progression, with median time-to-progression (TTP) of 27.1 weeks versus 18.6 weeks for patients treated with capecitabine alone[72]. Additionally, lapatinib was approved by FDA in 2010 as combination therapy with letrozole as first-line treatment of ER-positive and

HER-2-positive breast cancer[71]. The approval of lapatinib with letrozole was based on results showing that the PFS of patients who received the combination of two drugs was 8.3 months compared to 3 months for letrozole alone [73].

Monoclonal antibodies have also been produced in order to target vascular endothelial growth factor (VEGF), which is involved in the process of angiogenesis. Bevacizumab was initially proved to significantly improve the PFS of breast cancer patients when combined with chemotherapy[74]. These results led to the approval of bevacizumab by FDA in 2008 as a first-line treatment for patients with metastatic HER-2–positive breast cancer[75]. Nevertheless, additional studies did not confirm these findings[76,77]. For this reason, FDA re-considered its decision and eventually decided in 2011 to withdraw the recommendation of this drug for the treatment of metastatic breast cancer[78].

1.1.4.4 Immune checkpoint inhibitors

Other immunotherapeutic strategies are under investigation for the treatment of breast cancer. These include immune checkpoint inhibitors and chimeric antigen receptor (CAR) T-cells.

Different studies have shown expression of program death ligand-1 (PD-L1) in breast cancer clinical samples, indicating the rationale for its blockade with checkpoint inhibitors[79–83]. Interestingly, higher PD-L1 expression was observed in triple negative cell lines (TNBC) and in tumour samples with a triple negative phenotype[82,83]. PD-L1 and PD-L2 are ligands for the PD-1 immune checkpoint receptor, which is a negative-regulator of T-cell function.

The efficacy of either PD-L1 or PD-1 checkpoint inhibitors is being investigated in various clinical trials for patients with TNBC or hormone-positive breast cancer[84–87]. One example is the KEYNOTE-012 phase 1b trial, in which the activity of pembrolizumab, a PD-1 inhibitor, has been investigated[88]. In this study, patients with advanced, PD-L1-positive TNBC received pembrolizumab as monotherapy. The results were promising, with an 18.5% overall response rate[88]. Based on the results of this study, a Phase II clinical trial is currently ongoing (NCT02447003)[89].

Another negative regulator of T-cell activation is the cytotoxic T-lymphocyte–associated antigen 4 (CTLA-4). CTLA-4 is expressed on activated T-cells and provides a negative regulatory signal upon interaction with its ligands, CD80 and CD86, thus inhibiting T-cell activation. A variety of checkpoint inhibitors specific for CTLA-4 have been generated and some of these are being investigated in clinical trials for the management of breast cancer. In a Phase I clinical trial, 26 women with advanced breast cancer were treated with tremelimumab, an anti-CTLA-4 monoclonal antibody, in combination with hormonal therapy (exemestane)[90]. Although no complete responses were observed, 42% of the patients presented stable disease for ≥ 12 weeks[90]. Additionally, the combination of two distinct immune checkpoint inhibitors as potential treatment strategy for breast cancer is currently being investigated. In a single-arm Phase II clinical trial, patients with HER-2-negative metastatic breast cancer are being treated with tremelimumab in combination with durvalumab (MEDI4736)[91]. This clinical trial is currently ongoing (NCT02536794)[91].

1.1.4.5 Chimeric antigen receptor (CAR) T-cells

Chimeric antigen receptor (CAR) T-cell immunotherapy is a strategy whereby T-cells are engineered to express a synthetic receptor with specificity for an antigen expressed on the tumour cell surface. This immunotherapeutic strategy in analysed in depth in section 1.1.4.5. Numerous clinical trials are currently on-going in patients with breast cancer and these are listed in Table 1.2[92]. Antigens that are being targeted with CAR T-cells in these clinical trials include mesothelin, carcinoembryonic antigen (CEA), receptor tyrosine kinase-like orphan receptor 1 (ROR1), MUC1, HER-2 and CD133. However, no results are available as yet in regard to their efficacy or safety in breast cancer patients.

Table 1.2: Clinical trials investigating the efficacy and safety of chimeric antigen receptor (CAR) T-cells in breast cancer patients. The information provided in this table has been acquired from http://clinicaltrials.gov (*accessed 24th September 2017*)[92].

Antigen Targeted	Phase	Institution	Identifier
HER-2	I/II	Fuda Cancer Hospital, Guangzhou	NCT02547961
EpCAM	I	Sichuan University	NCT02915445
Mesothelin	I	Memorial Sloan Kettering Cancer Center	NCT02792114
cMET	Early I	University of Pennsylvania	NCT03060356
CEA	I	Southwest Hospital, China	NCT02349724
CD70	I/II	National Cancer Institute (NCI)	NCT02830724
ROR1	I	Fred Hutchinson Cancer Research Center, National Cancer Institute (NCI)	NCT02706392
MUC1	I/II	PersonGen BioTherapeutics (Suzhou) Co., Ltd.	NCT02839954
MUC1	I/II	PersonGen BioTherapeutics (Suzhou) Co., Ltd.	NCT02587689
HER-2	I/II	Southwest Hospital of Third Millitary Medical University	NCT02713984
Mesothelin	I	Chinese PLA General Hospital	NCT02580747
CD133	I	Chinese PLA General Hospital	NCT02541370

1.2 Mucin-1 (MUC1) as a target

The concept of targeted cancer therapies is based in the hypothesis that tumour cells have a distinct antigen expression profile, when compared to healthy cell types. An ideal target is considered to be an antigen (or a pattern of antigens) that is both overexpressed and exclusively present in the tumour cells but not in normal tissues. In addition, an antigen could be considered as a good target if it is immunogenic. Nevertheless, very few antigens are known to have these characteristics, allowing their classification as tumour associated antigens (TAAs). One of these TAAs is mucin-1 (MUC1), for the reasons that are explained in this section.

1.2.1 Mucins

Epithelial cells are found in various organs and tissues, such as in the gastrointestinal (GI) tract, the respiratory system, the liver, pancreas and the eye[93]. The epithelial lining of these tissues requires continuous protection due to the critical and dynamic functions that they are involved with (e.g. gas exchange, digestion and absorption of nutrients, lubrication of ocular surface etc) [93]. The contribution of mucins in this protection is vital as they cover the surface of epithelial cells with a mucosal gel-barrier[93]. Additionally, mucins "sense" changes in the external microenvironment and transmit this information to epithelial cells, leading to various cellular responses such as an increase in cell proliferation[94].

Mucins are glycoproteins characterized by high molecular weight and a large degree of glycosylation. In total, 21 different mucins have been identified with distinct tissue localization patterns (MUC1-MUC21). Mucins share a number of common characteristics such as the presence of a large extracellular domain that contains tandemly repeated elements. In addition, these molecules are typically rich in serine and threonine residues, allowing them to undergo extensive O-linked glycosylation[95]. Mucins can be classified into two categories, namely: secreted (e.g. MUC2, MUC5B, MUCB5C, MUC6, MUC19, MUC7, MUC20) and transmembrane types (e.g. MUC1, MUC3A, MUC3B, MUC4, MUC12, MUC13, MUC16 MUC17, MUC22). Both types of mucins have a major role in the protection of epithelial surfaces. The secreted mucins form a physical barrier through the formation of a mucus gel while the transmembrane mucins contribute to this barrier through their O-glycosylated ectodomain[94].

Secreted mucins can be further subdivided into gel-forming (MUC2, MUC5B, MUCB5C, MUC6, MUC19) and non-gel forming subtypes (MUC7, MUC20). While in the endoplasmic reticulum (ER), gel-forming mucins undergo homodimerisation through the formation of inter-molecular disulphide bonds[96]. These bonds are created between the amino and/or carboxyl termini of monomeric mucins in cysteine-rich domains[97]. Mucin homodimers undergo O-linked glycosylation in the Golgi apparatus and they connect further to each other, leading to the creation of multimeric chains[96,98]. These multimeric mucins are packed into granules and are transported to the surface of the epithelial cells[99,100]. Upon exocytosis, the granules are dispersed and the mucus gel is formed[99,100]. The ability of mucins to create homodimers is

responsible for the viscous properties of the mucus. Transmembrane mucins will be considered in the next section in the context of MUC1.

1.2.2 MUC1 in healthy tissues

1.2.2.1 MUC1: a membrane-tethered glycoprotein

The most extensively studied transmembrane mucin is MUC1 (also known as episialin, PEM, EMA, ECM, DF3 antigen and H23 antigen)[101]. MUC1 is a heavily glycosylated glycoprotein with its extracellular domain extending up to 200-500nm from the cell surface. MUC1 has been shown to be expressed in epithelial cells present in a variety of organs and tissues including lung, pancreas, oesophagus, duodenum, colon, kidney, seminal vesicle, prostate, cervix and endometrium and, to a lesser extent, in haematopoietic cells[102](Figure 1.4).

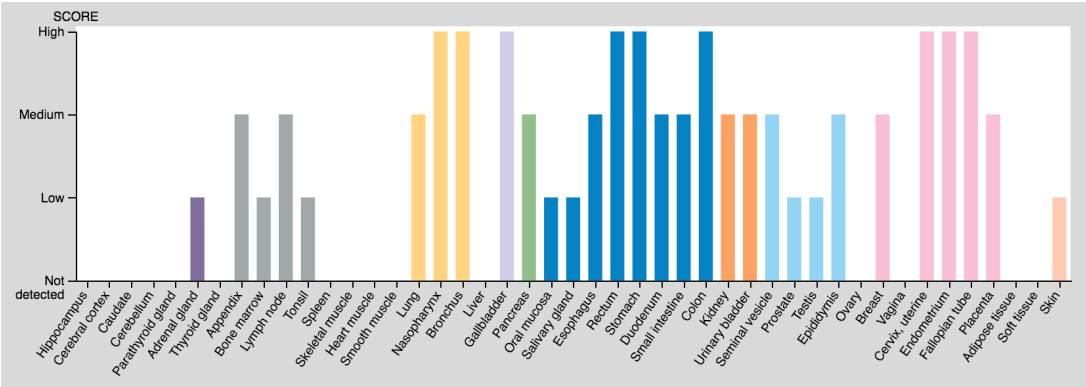

Figure 1.4: Protein expression of MUC1 in 44 different tissues types. The colour-coding scheme is based on common functional features of the tissues listed. Endocrine tissues, dark purple; bone marrow & immune cells, grey; lung, yellow; light purple, liver & gallbladder; pancreas, green; gastrointestinal track, dark blue; kidney & urinary bladder, dark orange; male tissues, light blue; female tissue, pink; skin, light orange. *From the Human Protein Atlas (http://www.proteinatlas.org/ENSG00000185499-MUC1/tissue, accessed 5th September 2017).*

1.2.2.2 Structure of MUC1

MUC1 is normally translated as a single polypeptide which undergoes auto-cleavage following translation to yield two subunits: the MUC1 N-terminal subunit (MUC1-N) and the MUC1 C-terminal subunit (MUC1-C). The two subunits remain attached to each other through non-covalent bonds[103]. The MUC1-N domain contains the variable number tandem repeats (VNTR) region and the SEA (sperm protein, enterokinase and agrin) domain (Figure 1.5). The SEA domain contains the GSVVV motif in which the auto-cleavage occurs[104].

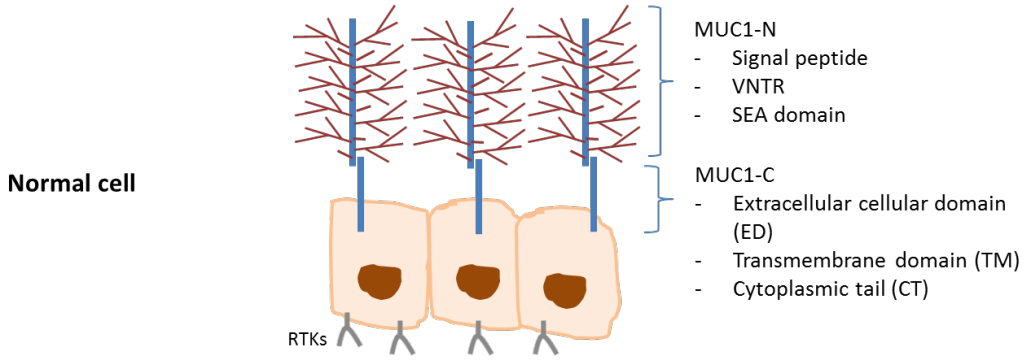

Figure 1.5: MUC1 structure as expressed in normal cells. The MUC1 glycoprotein is initially translated as a single polypeptide which then undergoes autocleavage, leading to the formation of an heterodimeric complex. This complex is comprised of the MUC1-N and the MUC1-C domains. The MUC1-N domain consists of the signal peptide, the VNTR region and the SEA domain. The VNTR region contains serine and threonine residues which become O-glycosylated. Different MUC1 glycoforms exist, depending on the type of the O-glycans present (e.g. core-1 glycans, core-2 glycans etc). The MUC1-C domain consists of the extracellular domain, the transmembrane region and the cytoplasmic tail. The latter delivers stress signals associated with cell proliferation and growth in order to restore the epithelium, in case of damage. In normal epithelial cells, MUC1 is localized on the apical membrane while various growth factors and tyrosine kinase receptors are localized on the basolateral surface.

Owing to genetic polymorphism, the VNTR region contains 25-125 repeats of a 20 amino acid sequence, mainly comprised of proline, serine and threonine residues. Serine and threonine residues serve as a scaffold for the attachment of O-glycans[105,106]. In addition to O-glycosylation, N-glycosylation is also observed at five asparagine residues which are present in the MUC1 heterodimer. Four of these residues are situated in the VNTR region and one in the SEA domain[107]. The molecular mass of MUC1 varies between 200 and 500kDA, depending on the extent of glycosylation and the number of tandem repeats present[95,108].

N-glycosylation occurs in the ER post auto-cleavage of MUC1 and is characterised by the addition of mannose-rich glycans to asparagine residues.

This glycosylation reaction is accomplished by N-acetylgalactose aminyltransferase (GalNAcT). The MUC1 heterodimer is then transferred to the Golgi apparatus where the N-glycans are further processed. In parallel, step by step O-glycolysation occurs. During this process, galactose, fucose, N-acetylgalactosamine (GalNAc) and/or sialic acid are attached to the hydroxyl group of a serine or threonine residue. The process of O-glycosylation will be further explained in section 1.2.3.2. An immature form of protein is released at the cell surface which is then re-internalised and re-surfaces through multiple cycles. Ultimately, a mature, fully sialylated protein is generated and is transported to the cell membrane[109]. The addition of a sialyl-residue is the last step in O-glycosylation.

The MUC1-C subunit consists of an extracellular domain (ECD-58 aa), transmembrane domain (TM-28 aa) and a cytoplasmic tail (CT-72 aa). Under normal conditions, MUC1 is expressed as heterodimeric molecule. In conditions of cellular stress or in malignancy, production of pro-inflammatory cytokines such as interferon-γ (IFN-γ) and tumour necrosis factor-α (TNF-α), lead to dissociation of the MUC1-C/MUC1-N complex and release of the MUC1-N domain from the MUC1-C (Figure 1.6). This process, known as ‘shedding’, is catalysed by enzymes with sheddase activity, such as tumour necrosis factor-α enzyme (TACE/ADAM17) and membrane-type matrix metalloproteases (MT-MMP)[110,111]. The MUC1-C domain, and in particular the cytoplasmic tail (CT) is responsible for promoting cell growth and survival signalling, enabling the repair of the epithelial layer when this is damaged. Further studies have demonstrated that this domain has a key role in tumourigenesis (reviewed by Donald W. Kufe)[112–115].

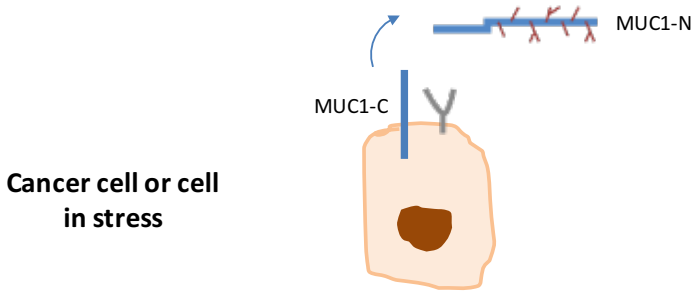

Figure 1.6: MUC1 shedding. In malignant or stressed cells, the MUC1-N domain is cleaved from MUC-C and is released into the bloodstream. Consequently, serum MUC1 measurement may be used as a biomarker to monitor disease status in breast cancer and pancreatic cancer patients (e.g. the CA15.3 test – see section 1.2.4).

1.2.2.3 Functions of MUC1

As MUC1 belongs to the family of mucins, its function involves the lubrication of epithelial cells and physical protection of epithelial cells from pathogens. In keeping with this, it has been shown that MUC1-deficient mice are more prone to bacterial infections, such as conjunctivitis and bacterial infections of the gastrointestinal tract[116,117]. Furthermore, MUC1-null mice develop chronic inflammation and infection of the lower reproductive tract caused by bacteria normally present in the flora[118]. It has been suggested that bacteria attach to the glycosylated chains of mucins, hindering their ability to penetrate tissues. Upon bacterial infection and in cell stress conditions, MUC1-CT becomes phosphorylated and regulates signalling pathways related to cell apoptosis and proliferation[119]. This process will be considered further in section 1.2.3.3. On the other hand, overexpressed and under-glycosylated MUC1 can drive chronic inflammation, such as inflammatory bowel disease (IBD), by recruiting cells of the innate immune system, such as dendritic cells and macrophages (see section 1.2.3 for details in MUC1 overexpression and aberrant glycosylation)[120]. This increase in MUC1

expression seems to be mediated by the production of pro-inflammatory cytokines upon initial inflammation[120].

MUC1 is also characterized by anti-adhesion properties, an effect that is attributed to steric hindrance caused by its large extracellular domain[121,122]. In relation to this, it has been reported that downregulation of MUC1 expression in uterine epithelial cells (UEC) is essential for embryonic implantation[123].

The role of MUC1 in tumourigenesis as well as its interaction with immune compartments is described in the section 1.2.3.3.

1.2.3 MUC1 in cancer

1.2.3.1 Overexpression

MUC1 has been found to be overexpressed in 90% of breast cancers but also in other epithelial adenocarcinomas (e.g. ovarian, lung, pancreas, gastrointestinal tract) and in some haematological malignancies (e.g. multiple myeloma, B-cell lymphoma and acute myeloid leukaemia)[124–129]. The gene encoding for MUC1 is located in chromosome 1 (long arm-q, position 21). Its expression is regulated both at the transcriptional and post-transcriptional level. Interestingly, the long arm in chromosome 1 has been reported to be commonly altered in breast cancer[130]. In accordance with this, overexpression of MUC1 has been related to gene amplification, leading to an increase in both mRNA and protein levels[131,132]. Additionally, the MUC1 gene promoter contains binding sites for multiple transcription factors[133]. An example is the

transcriptional regulation of MUC1 by IFN-γ and TNF-α as these cytokines signal through nuclear factor kappa B (NF-κB) and signal transducer and activator of transcription (STAT) transcription factors[134].

Post-transcriptional regulation of MUC1 can also result in its overexpression. One well-known post-transcriptional regulatory mechanism of gene expression involves microRNAs (miRNAs). These molecules decrease RNA expression by causing mRNA degradation or by inhibiting translation. Expression of miR-125b has been found to be decreased in breast cancers[135]. Additionally, miR-125b has been shown to have a binding site at the 3'UTR of MUC1[136]. Consequently, it was suggested that downregulation of miR-125b in breast cancer might contribute to MUC1 overexpression as a result of dysregulated translation of MUC1[136].

Epigenetic modifications have also been associated with regulation of MUC1 expression. It has been reported that demethylation of CpG islands and demethylation and acetylation of histone 3 lysine 9 (H3-K9) in the 5′ flanking region of the MUC1 promoter can lead to elevated MUC1 expression[137].

1.2.3.2 Aberrant glycosylation

A typical characteristic of tumour-associated MUC1 (TA-MUC1) is that it is aberrantly glycosylated and in particular is under-glycosylated[138]. This leads to the exposure of protein epitopes that are not normally accessible in normal, heavily glycosylated, MUC1 molecules.

The first step in the process of O-glycosylation is the addition of GalNAc to serine and threonine residues within the peptide chain by a GalNAc

transferase (Figure 1.7). This modification creates a classical tumour antigen known as the **Tn antigen**, which can have two fates. First, the chain may be further elongated through addition of galactose by core 1 β1,3-galactose transferase (core 1 β1,3-Gal T). This reaction generates the core 1 glycan, which is also referred to as the **T antigen**. Alternatively, chain elongation may be terminated by addition of sialic acid by the α6-sialyltransferase (ST6GalNAc I), to create the **STn antigen**. Similarly, the T antigen can either be sialylated (to give **ST antigen**) or glycosylated further in order to form the core 2 elongated glycans. Addition of sialic acid to T antigen is performed by α3-sialyltransferase (ST3Gal I). Core 2 glycans are created by adding N-acetyl glucosamine (GlcNAc) to core 1 glycan by core 2 β1,6-N-acetyl glucosamine transferase (β1,6-C2GnT I). The chain can be further elongated until a sialic acid is added to the last glycan.

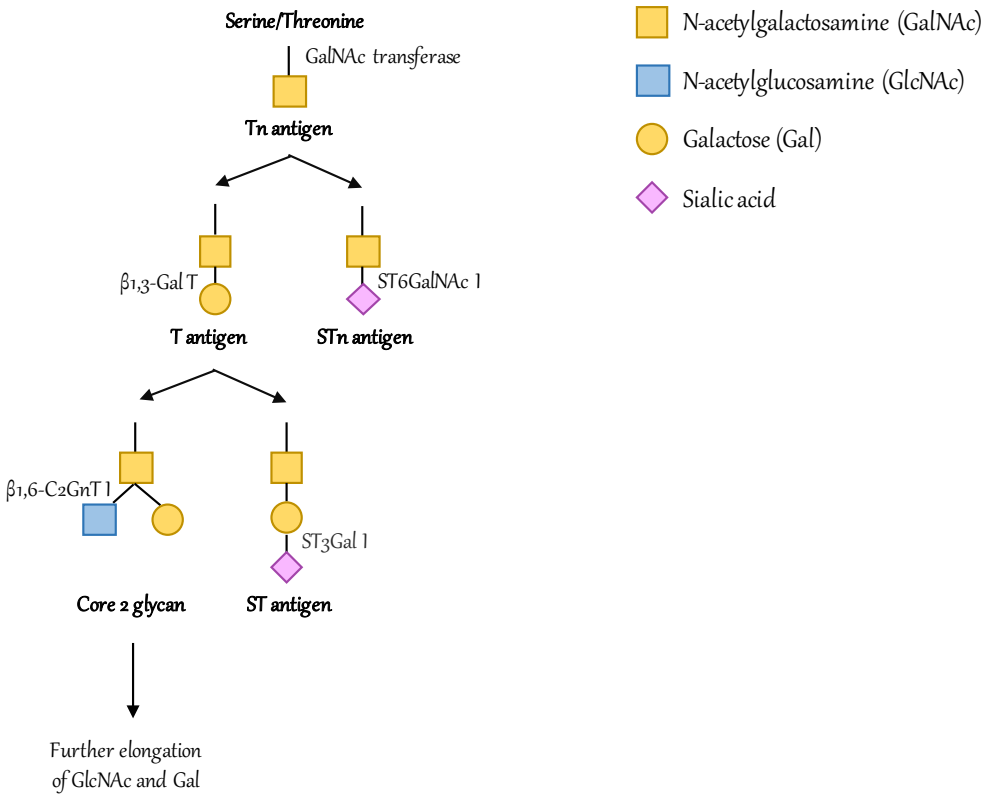

Figure 1.7: O-glycosylation. The process of O-glycosylation is initiated via the addition of the first monosaccharide, GalNAc, to serine and/or threonine residues of the peptide chain. The resulting glycan is known as Tn antigen and the addition of GalNAc is performed by the GalNAc trasnferases. The Tn antigen can be further glycosylated with the addition of galactose, a process that is mediated by the β1,3 Gal T enzyme. This reaction generates the T antigen. Alternatively, the elongation of Tn antigen can be terminated by the addition of sialic acid by the ST6GalNAC 1 sialic acid trasferase. The sialylated Tn antigen is known as STn antigen. In a similar manner, T antigen can be either further elongated or sialylated. In the case of chain elongation, GlcNAc is added to T antigen by C2GnT1 trasferase, which results in the formation of core 2 glycan. Alternatively, sialic acid can be added by ST3Gal1, thus forming the ST antigen. The core 2 glycan can be further elongation by the addtion of GlcNAc and Gal. GalNAc – N-acetylogalactosamine; GlcNAc – N-acetyloglucosamine; Gal – galactose; β1,3 Gal T – β1,3-galactose transferase; ST6GalNAc I – α6-sialyltransferase; ST3Gal I – α3-sialyltransferase; β1,6 C2GnT I - β1,6 N-acetyl glucosamine transferase.

Under normal conditions, MUC1 expressed by healthy cells is mainly covered with extensively elongated and branched core 2 glycans. By contrast, malignant cells are characterized by reduction of core 2 glycans and a predominance of core 1 glycans[139]. In breast cancer, this phenomenon is

associated with changes in the expression of a number of glycosyltransferases. One key change is the frequent downregulation in tumour cells of the core 2 transferase, β1,6 C2GnT1, which results in accumulation of core 1 glycans[139]. This is accompanied by early termination of chain elongation due to increased sialylation. Sialylation is mediated by enzymes such as ST3Gal-I, the expression of which is commonly increased in breast carcinomas[140]. It has been hypothesised that ST3Gal-I competes with β1,6 C2GnT1 for the same substrate (T antigen), thus resulting in increased expression of sialyl-T antigen by tumour cells[138,141].

In addition to the above, it has also been shown that under-glycosylated MUC1 demonstrates increased intracellular accumulation in comparison with heavily glycosylated MUC1[142]. It has been suggested that this increased accumulation is caused by enhanced clathrin-mediated endocytosis, not linked to increased MUC1 degradation[142].

1.2.3.3 Cell signalling and tumourigenesis

As previously mentioned, MUC1 is normally localised on the apical surface of epithelial cells[143]. By contrast, stressed or malignant cells demonstrate a loss of the apical-basal epithelial polarity (Figure 1.8). As a result, MUC1 and a number of growth factors and tyrosine kinase receptors (RTKs) which are normally positioned on the basal-lateral side of the epithelial cells become re-distributed across the entire surface of the cell[112]. The constitutive interaction between MUC1-C and a number of RTKs leads to MUC1-associated continuous activation of various signalling pathways that are involved in cell growth, proliferation and survival[102,112].

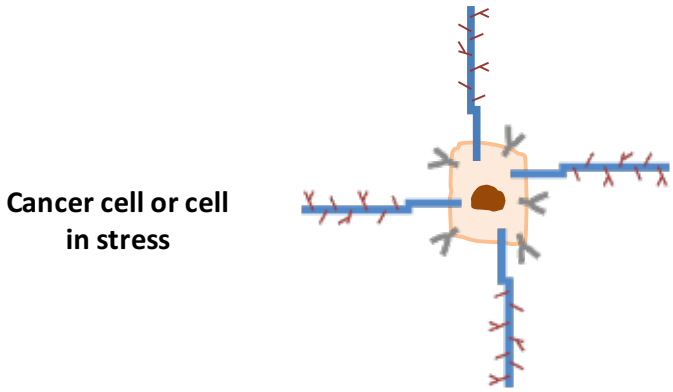

Figure 1.8: Distribution of MUC1 in cancer cells. In cancer or stressed cells, MUC1 is overexpressed and underglycosylated. In addition, a loss of cell polarity is observed that leads to the relocalisation of MUC1 and RTKs all over the cell surface. This results in constitutive interaction of the MUC1-C domain with these receptors, which in turn plays a critical role in cancer progression.

One typical example is the interaction of MUC1 with the epidermal growth factor receptor (EGFR). The N-glycosylation of an asparagine residue (Asn-36) present in the extracellular domain (ED) of MUC1 transforms the residue into a binding site for galectin-3. Galectin-3 will then function as an extracellular bridge between MUC1-C and EGFR thus allowing their interaction[144]. Interaction of MUC1 with EGFR has been reported to cause blockade of the EGFR degradation and increase in EGFR nuclear localization, thus resulting in enhanced activation of the cell cycle regulator cyclin D1 and myb-related protein B (MYBL2)[145,146].

Additionally, it has been reported that MUC1 mediates cell proliferation and enhances tumourigenesis via its interaction with the platelet-derived growth factor-A (PDGFA)[147]. According to the suggested mechanism, MUC1-CT interacts with hypoxia inducible factor-α (HIF1-α), leading to its translocation to the nucleus. HIF1-α then drives the expression and secretion of PDGFA[147]. PDGFA is associated with increased cell proliferation and

invasion through the activation Ras-Raf-MEK-ERK and phosphatidylinositol-3-kinase (PI3K) pathways respectively. In parallel, it has been shown that MUC1-CT interacts with β-catenin and the complex is then transported into the nucleus. This nuclear re-localisation appears to be dependent in part upon PDGFA secretion[147].

MUC1-C is further involved in the activation of the Ras-Raf-MEK-ERK pathway[148]. It has been suggested that MUC1-CT contains a YTPN site that becomes phosphorylated. Upon phosphorylation, growth factor receptor-bound protein 2 (Grb2) binds to phosphorylated MUC1-CT domain. The complex then binds to son of sevenless (Sos) protein through the SH3 domain of Grb2, which result in activation of the Ras-Raf-MEK-ERK signalling pathway[148].

Further work has demonstrated that hypoxia drives MUC1 overexpression which in turn promotes angiogenesis through formation of endothelial cell tubes[149]. In particular, it has been suggested that hypoxia-induced MUC1 overexpression leads to the translocation and accumulation of MUC1-CT into the nucleus. Nucleus-located MUC1-CT drives the expression of connective tissue growth factor (CTGF) by binding to the promoter of CTGF. Additionally, MUC1 induces the expression of other factors which promote angiogenesis, such as vascular endothelial growth factor-A (VEGFA) and platelet-derived growth factor B (PDGFB)[149].

Another suggested mechanism by which MUC1 may contribute to tumourigenesis is via its interaction with the Wnt signalling pathway[114]. Under normal conditions, the phosphorylation of β-catenin is promoted by glycogen synthase kinase 3β (GSK3β). Phosphorylated β-catenin is then recognised by

the β-TrCP (β-transducin repeat containing) domain of the E3 ubiquitin ligase, leading to its degradation. Increased accumulation of β-catenin has been reported upon downregulation of GSK3β. In malignant cells, the MUC1-CT domain interacts directly with β-catenin[114]. This interaction results in the blockage of GSK3β-mediated phosphorylation of β-catenin and thus to the stabilisation of β-catenin. Accumulation of β-catenin results in the transcription of Wnt target genes, such as cyclin-D1, thus promoting increased cell proliferation and tumourigenesis[114].

In another setting, Beatson *et al.* have reported that tumour-associated (TA)-MUC1 contributes to the formation of the tumour microenvironment[150]. In this study, it has been shown that a TA-MUC1 glycoform, MUC1-ST, binds to myeloid cells, such as macrophages and primary monocytes through Siglec-9[150]. Binding of MUC1-ST to primary monocytes induced the production of several factors related to promotion of inflammation and tumour progression. These include angiogenesis-promoting factors such as plasminogen-activator inhibitor (PAI-1) and interleukin (IL)-8, inflammatory cytokines such as IL-6 and monocyte- and neutrophil-recruiting factors such as C-X-C motif chemokine ligand 5 (CXCL5), CXCL1, chemokine (C-C motif) ligand 2 (CCL2) and CCL3. Additionally, the interaction of MUC1-ST with monocytes induced their differentiation to tumour-associated macrophages (TAM)[150]. This was accompanied by increased expression of indoleamine-pyrrole 2,3-dioxygenase (IDO) and programmed death-ligand 1 (PD-L1). Both molecules have been previously associated with inhibition of proliferation and functionality of T-cells. Binding of MUC1 to Siglec-9 induced increase in calcium flux and activation of the Ras-Raf-MEK-ERK signalling pathway[150].

1.2.4 MUC1 and clinical applications

Measurement of tumour-associated MUC1 has various clinical applications in diagnosis, the prediction of disease prognosis and in therapeutic intervention. Overexpression of MUC1 is associated with advanced tumours and poorer prognosis, particularly in colorectal and pancreatic carcinomas[151,152]. By contrast, in breast cancer, immune-histological studies have revealed that increased MUC1 expression is linked with more differentiated cells and better prognosis. Nevertheless, aberrantly localised MUC1 in the cytoplasm of malignant cells or in the non-apical surface is associated with worse prognosis[153]. In addition, MUC1 expression can inhibit the effects of tamoxifen in breast cancer patients. This is related to the fact that MUC1-C interacts with the oestrogen receptor and antagonises the binding of tamoxifen to the receptor[154].

MUC1 is also used as a disease biomarker for both breast and pancreatic cancer. As already mentioned, MUC1-N subunit is shed and released into the circulation of cancer patients. Different biomarker tests have been developed which are based on the detection of carbohydrate antigens 15-3 and 19-9 (CA 15-3, CA 19-9), both of which are glyco-epitopes of MUC1[155,156]. The CA 15-3 test was used for the detection of breast cancer metastasis and disease recurrences in breast cancer patients, even though it was not significantly successful in detecting early-stage disease[155]. The detection of CA 19-9 antigen is mainly used for the detection and management of pancreatic cancer[107]. In a study published in 2012, it was reported that MUC1 is a robust biomarker for predicting overall survival in pancreatic cancer

patients as MUC1 overexpression is associated with worse prognosis in these patients[157]. Nevertheless, the utility of these two biomarkers is generally confined to the monitoring of response to treatment[107]. As previously mentioned, release of MUC1-N domain is observed not only in malignant cells but also in stressed cells, a fact that could result in false-positive results.

1.2.5 MUC1-specific immunotherapy

The concept of immunotherapy is based on the idea of specifically targeting tumour-associated antigens in order to elicit antigen-specific immune responses. MUC1 has long been considered as an attractive immunotherapeutic target due to its overexpression and its aberrant glycosylation in malignant cells, in addition to its involvement in tumour pathogenesis[158].

In 1989, Barnd *et al*. were the first to show that tumour-associated (TA) MUC1 is immunogenic and capable of inducing specific immune responses[159]. Importantly, they were able to isolate MUC1-specific cytotoxic lymphocytes (CTLs) from breast and pancreatic cancer patients[159,160]. It should be noted however that despite the presence of TA-MUC1, antigen-specific cytotoxic T-cells (CTLs) fail to efficiently eliminate the tumour cells[161].

Different MUC1-specific immunotherapeutic strategies have been developed over the last three decades and have been investigated in the clinical setting in order to boost the cellular immune response against TA-MUC1. These include the development of MUC1-specific therapeutic peptide vaccines, monoclonal antibodies and chimeric antigen receptor (CAR) T-cells.

1.2.5.1 Therapeutic cancer vaccines

The mechanism of action of a cancer therapeutic vaccine is the generation of an antigen-specific immune response[162]. This includes the expansion of specific CTLs and the production of antigen-specific antibodies by B-cells[162]. Over the last few decades, a wide variety of MUC1 vaccines have been developed which have been recently reviewed by Hossain *et al*.[163]. The first developed MUC1 vaccines included peptide epitopes from the VNTR region of MUC1. These antigenic moieties were usually conjugated to a carrier molecule such as Keyhole Limpet Haemocyanin (KLH) or bovine serum albumin (BSA), and were co-delivered with adjuvants such as the attenuated mycobacteria, Bacille de Calmette et Guérin (BCG)[163]. These approaches aimed to increase the immunogenicity of the peptide vaccine, leading to more potent immune responses[164,165]. Another strong immunogenic carrier that has gained popularity is tetanus toxoid (TT)[166]. A number of studies have also shown that MUC1 vaccines conjugated with TT were able to produce strong immune response in mice[166,167].

Other interesting approaches have been developed in order to increase the efficacy of MUC1-peptide vaccines. Apostolopoulos *et al*. developed a MUC1-vaccine coupled with mannan in oxidized conditions (M-FP vaccine)[168]. The aim of this approach was to increase the efficacy of the vaccine by targeting mannose receptors that are expressed in antigen-presenting cells (APCs), such as macrophages and dendritic cells, resulting in increased antigen presentation and generation of more potent immune responses[169]. The efficacy of the M-FP vaccine was evaluated in a pilot Phase III clinical trial (ISRCTN71711835), in which 31 breast-cancer patients with early-stage

disease (stage II) were treated either with the M-FP vaccine (16 patients) or with placebo (15 patients). Based on the results obtained from long term (10-12 years) follow-up, the M-FP vaccine significantly decreased the disease recurrence rate. Specifically, only two out of 16 patients treated with M-FP presented recurrent disease while nine of 15 patients treated with placebo developed tumour recurrence[170,171]. However, others have further tested the efficacy of M-FP in clinical trials and no significant survival benefit was shown[172].

Another promising approach entailed the development of the L-BLP25 vaccine (Stimuvax®-Tecemotide)[173]. This vaccine consists of a 25-amino acid MUC1 peptide from the VNTR region, which is encapsulated in a liposomal formulation[173]. This approach could potentially facilitate the delivery of the peptide to APCs and thereby enhance MHC-peptide presentation. A Phase III clinical trial (START trial) was conducted in order to investigate if Stimuvax had any benefit for patients with stage III non-small cell lung cancer (NSCLC), when given as a maintenance treatment post chemoradiation[174]. No overall survival benefit was reported; nevertheless, it appeared that Stimuvax had notable benefit in Caucasian patients treated previously with concurrent chemoradiotherapy. The latter was not observed in patients treated with sequential chemoradiation. Merck decided to discontinue the further development of Stimuvax after the results of the EMR 63325-009 trial failed to show any benefit for any of the patients' subgroups[175]. This Phase I/II trial was conducted in Japanese patients with stage III unresectable NSCLC. The authors suggested that the differences in the outcome of the START and EMR 63325-009 trials could potentially be related to the fact that the latter trial was

underpowered (smaller number of patients) and due to genetic differences between Japanese and Caucasian patients[158,175].

More recently, another MUC1 vaccine named as TG4010 has shown promising efficacy in various clinical trials[176]. These data are summarised by Arriole *et al.* in a recent review publication[177]. TG4010 is a recombinant viral vector which carries the sequences of both full-length MUC1 and of the immune-stimulating cytokine, IL-2. The viral vector is derived from the modified virus of Ankara (MVA). This vaccinia viral strain is significantly attenuated, but nevertheless has retained its immunogenicity. Based on results from these clinical trials, TG4010 in combination with chemotherapy seems to significantly improve the progression free survival of NSCLC patients. Nevertheless, a robust biomarker is being actively sought in order to predict the subgroup of patients that could benefit the most from this treatment[177].

Another notable approach has been developed by the research group of O. Finn. In this approach, MUC1-specific antibodies were isolated from healthy individuals who were treated in a prophylactic setting with a MUC1-peptide vaccine[178]. The trial was the first in which a cancer vaccine specific for a tumour-associated antigen was administered to individuals that have not been diagnosed with malignancy. The vaccine proved to be highly immunogenic. Consequently, the authors suggest that the induced MUC1-specific antibodies could prove beneficial in antibody-based therapy approaches or for the development of chimeric antigen receptors[178].

1.2.5.2 MUC1-specific antibody-based therapy

Monoclonal antibody-based cancer therapy has shown exceptional promise in recent years, as best exemplified by trastuzumab, which is used for the treatment of HER-2-positive breast cancer and some other tumours. The efficacy of antibody-based therapy relies on the ability of monoclonal antibodies to block the targeted protein and to recruit immune effector functions, such as complement- and antibody-dependent cell-mediated cytotoxicity (ADCC)[179]. Numerous MUC1-specific antibodies have been developed in recent decades and a few of these have been tested clinically.

The efficacy of a fully humanized HMFG1 antibody, named as AS1402, was evaluated in Phase I and Phase II clinical trials. In the Phase II clinical trial, patients with locally advanced or metastatic breast cancer were treated with AS1402 alone or in combination with an aromatase inhibitor named letrozole[180]. However, the study was stopped early due to worsening of disease progression.

Additionally, MUC1-specific monoclonal antibody conjugates have been developed. In 1993, Hird *et al.* developed an HMFG1 antibody conjugated with the Yttrium-90 (^{90}Y) radio-isotope[181]. This conjugated antibody had the property to bind preferentially to MUC1-expressing tumour cells and eliminate them through the release of radiation from ^{90}Y[181]. Promising results led to a Phase III clinical trial in 447 women with epithelial ovarian cancer who had previously been treated with surgery and chemotherapy. Patients received a single intraperitoneal dose of ^{90}Y-HMFG1[182]. However, no improvement in the overall survival or in the disease-free survival rate was observed. Nevertheless, there were significantly lower

intraperitoneal recurrences in the patients treated with the ^{90}Y-HMFG1 and significantly higher appearance of extraperitoneal tumours[182,183].

Another conjugated MUC1-specific monoclonal antibody is clivatuzumab tetraxetan, which is derived from a humanised version of the PAM4 monoclonal antibody[184]. PAM4 specifically targets pancreatic cancer cells by binding to TA-MUC1 and is additionally labelled with ^{90}Y. The efficacy of this radiolabelled antibody was evaluated in a Phase I clinical trial in which untreated patients with stage III/IV pancreatic adenocarcinoma received a single or repeated cycles of ^{90}Y-PAM4 in combination with low-dose gemcitabine. The results showed modest anti-tumour activity with 16% of patients achieving partial response and 44% showing stable disease[184].

Over the course of these studies, it became apparent that the development of an effective MUC1-specific antibody therapy was potentially hindered by circulating MUC1 in the serum of cancer patients, thus preventing effective drug delivery to tumour cells and the generation of ADCC[185].

1.3 Cancer Immunotherapy

1.3.1 Overview

The immune system is a fundamental defence mechanism of the human body. In recent decades, there has been enormous progress in our understanding of the human immune system and its close inter-relationship to cancer. Although considerable evidence indicates that immune surveillance of cancer occurs, it is apparent that T-cells generally do not create immune responses potent enough to eliminate established tumours. Different mechanisms have been proposed which are responsible for this incapability. For example, it has been suggested that cancer cells can “hide” from immune cells by down-regulation of tumour-specific antigens or of MHC molecules[186–190]. In addition, tumours have an increased content of immunosuppressive cytokines (e.g. IL-10 and transforming growth factor (TGF)-β) as well as increased concentration of suppressive cell populations such as regulatory T-cells (Tregs), M2 polarised macrophages (TAM) and myeloid derived suppressor cells (MDSC) (reviewed by Hanahan and Weinberg[191])[192–195].

Three fundamentally different immunotherapeutic approaches have been developed that have in common the harnessing of the immune system against cancer. Examples of these different strategies have already been mentioned in previous sections. The first category includes the administration of cancer vaccines that aim to boost the immune responses against an immunogenic tumour antigen (e.g. MUC1 vaccines). Another category consists of the production and use of monoclonal antibodies (mAbs) which

block overexpressed proteins such as ErbB dimers. A major antibody application involves immune checkpoint blockade (ICB). The third category includes various adoptive T-cell immunotherapeutic strategies that have been developed (see section 1.3.3).

1.3.2 Immune checkpoint blockade

The concept of immune checkpoint blockade is based on the idea of counteracting tumour-mediated inhibition of immune responses. T-cell activation is positively or negatively regulated by the interaction of co-stimulatory or co-inhibitory ligands with their receptors. Co-inhibitory ligands are commonly expressed on tumour cells or immunosuppressive subtypes of dendritic cells or macrophages. A variety of monoclonal antibodies have been generated which inhibit the effect of these negative regulatory signals. Most clinically relevant immune checkpoint inhibitors are targeted against CTLA-4 and PD-1, which are expressed on T-cells, and PD-L1 which is expressed on tumour cells. Ipilimumab (Yervoy), an anti-CTLA-4 antibody has shown promising results in clinical trials for the treatment of patients with metastatic melanoma[196,197]. These positive results led to its approval by the FDA for the treatment of melanoma patients with metastatic or unresectable disease in 2011[198]. In 2015, FDA approved ipilimumab for the treatment of patients post-surgery that are in high-risk for disease recurrence[199]. Additionally, two anti-PD-1 antibodies, namely pembrolizumab (Keytruda) and nivolumab (Opdivo), have been approved for the treatment of different advanced malignancies, including melanoma, head and neck squamous cell carcinoma, non-small cell

lung cancer, classical Hodgkin's lymphoma, non-squamous non-small lung cancer and urothelial carcinoma[200,201]. In May 2017, pembrolizumab was also approved for the treatment of patients with any type of metastatic or unresectable solid malignancy which is characterized by microsatellite instability-high (MSI-H) or mismatch repair deficiency (dMMR)[202].

1.3.3 Adoptive T-cell therapy

Adoptive T-cell therapy (ACT) is the most recently developed immunotherapeutic strategy and it includes the adoptive transfer of either autologous or allogeneic T-cells into cancer patients. The pioneer of adoptive T-cell therapy is Steven Rosenberg who developed T-cell immunotherapy using tumour-infiltrating lymphocytes (TILs). In this approach, patient's TIL cells are isolated from an excised tumour mass, expanded *ex-vivo* in culture with IL-2 and then re-injected back to the patient after conditioning with either chemotherapy or radiotherapy. The first promising results came in 1988 when 60% of melanoma patients achieved tumour regression after injection of TILs[203]. Nevertheless, this approach is not applicable in many other tumour types as it is very difficult to detect tumour-specific T-cells or to expand TIL cells.

In an attempt to broaden the tumour types in which ACT is applicable, other strategies were developed which became feasible with improved efficiency of gene transfer technology. In these derivative approaches, patient-derived T-cells are re-directed against tumour cells by introduction of genetically encoded receptors. The redirection is achieved by expressing on

the T-cell surface either an antigen specific T-cell receptor (TCR) or chimeric antigen receptor (CAR). Conventional $\alpha\beta$ T-cell receptors recognise processed peptide antigen, presented in a HLA-dependent manner. By contrast, chimeric antigen receptors are artificial fusion molecules that recognise native cell surface targets in an antibody-like manner. Chimeric antigen receptor technology is described in further detail in section 1.3.4.

Exemplifying the former approach, a variety of TCRs with different antigenic specificities have been developed and tested in numerous clinical trials[204]. The efficacy results derived from some early-phase clinical trials are promising. In 2015, it was reported that NY-ESO-specific TCR engineered T-cells demonstrated promiscuous clinical responses, including 50% response rate in multiple myeloma patients and 91% in synovial sarcoma[205].

Despite the promising results, this approach may be complicated by occurrence of “on target, off tumour” toxicity. These toxicities result from the fact that the expression of the targeted antigen is not restricted to tumour cells but is also present in some normal tissues. In a trial in patients with metastatic melanoma, patients were treated either with engineered TCR T-cells specific for either the melanoma-associated antigen recognized by T cells (MART-1) or the glycoprotein 100 (gp100)[206]. Objective tumour regressions were observed in 30% and 19% of patients respectively. Responses were accompanied by on target off tumour toxicity to skin, ears and eyes, due to the presence of melanocytes in these tissues[206]. In another clinical trial, anti-MAGE (melanoma associated antigen) A3/A9/A12 TCR-engineered T-cells were administrated to nine patients with melanoma, synovial sarcoma or oesophageal cancer[207]. Five patients achieved tumour regression.

Nevertheless, three of the patients developed altered mental status which proved fatal in two cases. These neurological toxicities were associated with physiological expression of MAGE A12 in the brain which was recognised by the TCR engineered T-cells, leading to neuronal cell destruction[207].

1.3.4 Chimeric Antigen Receptors

In the last decade, CAR engineered T-cells have shown exceptional promise in the treatment of patients with refractory B-cell malignancy[208–211]. The concept of the chimeric antigen receptors was first introduced in 1989 by Eshhar and colleagues who created chimeric T-cell receptors[212,213]. These fusion molecules were combining the specificity of monoclonal antibodies with the cytolytic activity of T-cells. In this concept, they have replaced the TCR's antigen binding domain by that of a mAb; thus the T-cells attacked and destroyed the tumour cells as a result of recognition of surface antigens in an MHC independent manner[212,213]. The fact that the CAR T-cells can recognise tumour-antigen in non-MHC restricted manner is an important advantage over TCR engineered T-cells, since the latter are MHC-restricted.

1.3.4.1 CAR structure

A CAR molecule is comprised from three domains: the extracellular antigen-specific domain, a transmembrane element and the intracellular signalling domain (Figure 1.9). The extracellular domain is responsible for the recognition and binding to the target antigen of interest. The binder can be of different types; the most commonly used is a single chain variable fragment

(scFv) derived from an antibody. Alternatively, target binding may be achieved using a ligand specific for a receptor or an antigen-binding fragment (Fab). When compared to engineered TCR, CARs have the advantage that they recognize not only peptides but any type of macromolecules. Nevertheless, an important drawback of CARs, which is not characteristic of TCRs, is that they can only bind to cell surface antigens. The antigen-binding moiety is followed by the spacer which is connected with the transmembrane domain. The spacer should be flexible and of optimal length in order to allow the binder to reach the target of interest[214]. The CAR intracellular domain contains the signalling motifs necessary for the activation of the receptor and is connected with the extracellular domain via a transmembrane element. The simplest CAR signalling domain consists of the CD3ζ chain, adapted from the CD3 signalling complex (normally associated with the TCR). The CD3ζ chain contains three immune-receptor tyrosine-based activation motifs (ITAMs) which are phosphorylated upon the attachment of the binder to the antigen of interest. The phosphorylation events are followed by the activation of more downstream signalling pathways which are responsible for the production of antigen-specific immune response.

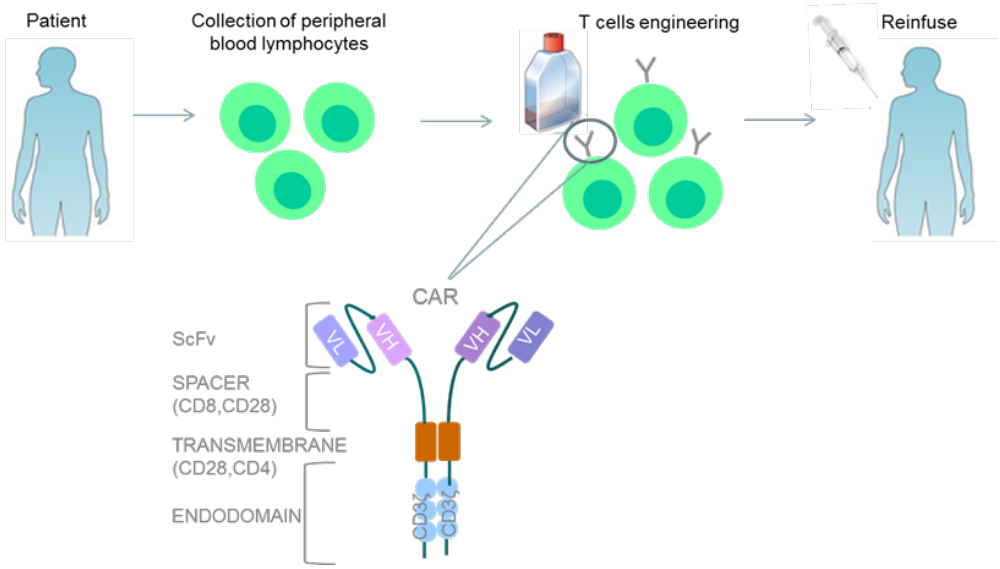

Figure 1.9: Adoptive CAR T-cell immunotherapy. Patient-derived T-lymphocytes are isolated by leukapheresis or blood sampling and are genetically engineered (for example with a retroviral or lentiviral vector) to express the desired cell surface chimeric antigen receptor (CAR). Subsequently the T-cells are expanded *ex-vivo* and then re-injected into the patient. Chimeric antigen receptors consist of three different parts: the extracellular domain, the transmembrane element and the endodomain. The extracellular region consists of the binding domain (which can be an scFv derived from a monoclonal antibody, a peptide or a receptor ligand) and a spacer of optimal length and flexibility (e.g. CD8, CD28). A transmembrane domain follows (e.g. CD28, CD4) and serves to connect the extracellular regions with the endodomain. The endodomain contains the CAR signalling domain. The simplest CAR endodomain generally contains the CD3ζ chain; nevertheless, most CARs that are being tested in clinical trials additionally include one or two co-stimulatory modules (e.g. CD28, 4-1BB, OX40).

The first *in vitro* experiments with CAR engineered T-cells, incorporating the CD3ζ signalling domain (1st generation CARs), showed that the CAR T-cells were able to mediate cytotoxic responses against antigen-expressing cancer cells; nevertheless these responses were not highly potent[215]. Further studies were focused on the improvement of the signalling domain in order to enhance the immune responses. This was achieved by the addition of either one (2nd generation CAR) or two co-stimulatory motifs (3rd

generation CAR) in the intracellular domain, such as CD28, OX40, 4-1BB etc (Figure 1.10)[216,217].

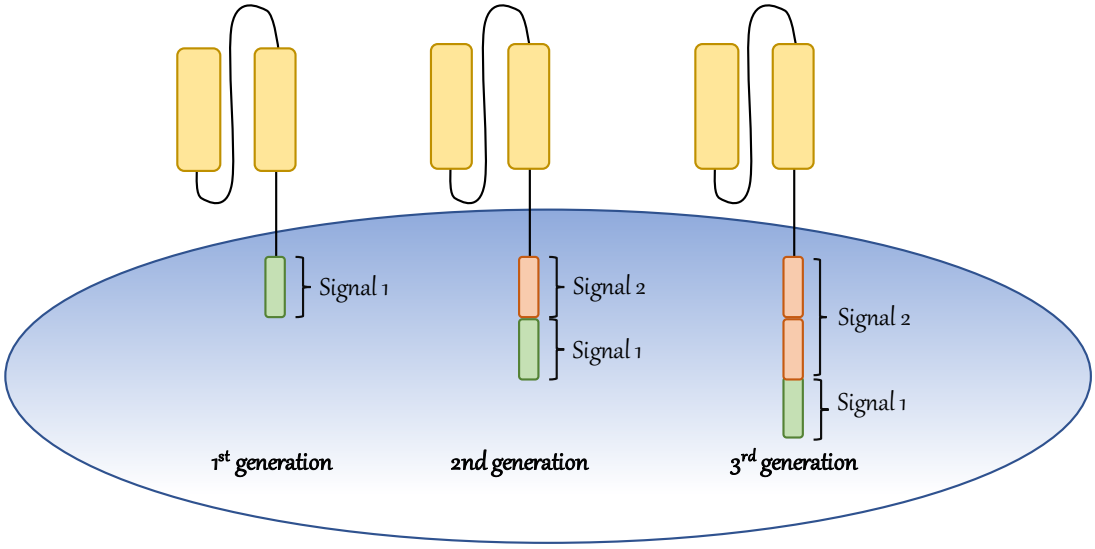

Figure 1.10: Schematic representation of first, second and third generation CARs. First generation CARs have incorporated the CD3ζ signalling chain (or another module that signals similarly), which provides signal 1 and thus results in T-cell activation upon antigen ligation to the CAR's binding domain. Second generation CARs utilise CD3ζ to provide signal 1 but they also have incorporated a co-stimulatory molecule upstream of CD3ζ, which provides signal 2. Delivery of both signal 1 and signal 2 is required for optimal T-cell activation. The signalling domain of third generation CARs contains the CD3ζ chain and two co-stimulatory modules. First – 1st; second – 2nd, third – 3rd.

1.3.4.2 CARs: from the bench to the clinic

As previously mentioned, CAR T-cells have shown remarkable responses in haematological malignancies in which CD19 proved to be a very attractive target. This success has been based upon the use of second generation CARs in which either CD28 or 4-1BB have been incorporated upstream of CD3ζ. In a historic moment, the first CAR T-cell therapy was recently approved by the FDA for the treatment of children and young adults with refractory acute lymphoblastic leukaemia (ALL)[202].

Several reports illustrate the clinical efficacy of CD19-targeted CAR T-cell immunotherapy of B-cell malignancy. In a trial conducted by Porter and colleagues in the University of Pennsylvania, 14 adults with refractory, relapsed chronic lymphocytic leukaemia (CLL) were treated with anti-CD19 CAR T-cells (CTL019 – comprising a 4-1BB based second generation CAR)[208]. Three patients achieved a complete response (CR), 5 patients had a partial response (PR) while 6 had no response. The overall response rate was 53%[208]. The same group has also treated 10 CLL patients in a Phase II dose optimisation trial, again using the CTL019 CAR approach. The results of this study indicated that 2 of the patients had CR and 2 of them PR with an overall response rate 40%[209].

In another trial, Kochenderfer *et al.* used anti-CD19 CAR T-cells for the treatment of 15 patients with either diffuse large B-cell lymphoma (DLBCL, n=9), indolent lymphoma (n=2) or CLL (n=4)[210]. Complete remissions were observed in eight patients. Four patients were partial responders, one had stable lymphoma and, in two cases, the results were not evaluable. Noticeably, four of the complete responders were DLBCL patients. Unfortunately, acute toxicities were observed, including neurological toxicities, while one patient died 16 days after injection for unknown reasons. Despite these toxicities, this was first study that showed complete responses in DLBCL patients and importantly the most durable CR was still ongoing at 23 months after treatment[210].

Remarkable results have also been seen in a trial where 25 patients aged 5-22 years old and five older patients with refractory or relapsed acute lymphoblastic leukaemia (ALL) were treated with CTL019 CAR T-cells[211].

Remarkably, CR were seen in 90% of patients (27/30 patients) while sustained remissions were observed in 15 out of 22 evaluable individuals (7 months average follow-up)[211]. Additionally, it has been reported that 63 ALL patients were treated with CTL019, with 83.2% overall response rate[218]. These impressing results led to the approval of the first CAR T-cell therapy (tisagenlecleucel, marketed by Novartis as Kymriah) in the USA and its release to the market. The product is administered in a single dose and is designated for patients with refractory and/or refractory ALL. According to the manufacture's dosing instructions, patients with body weight equal or less than 50kg will receive a single dose of 0.2-0.5x10^6 CAR-positive viable T-cells per kg while patients with body weight higher that 50kg will receive 0.1-2.5 x10^6 CAR-positive viable T-cells[219]. Tocilizumab, a monoclonal antibody directed against the receptor of interleukin-6 (IL6-R), was also approved together with Kymriah for the management of cytokine release syndrome[218,220].

1.3.4.3 The challenges of CAR T-cell immunotherapy

In contrast with these striking findings, CAR T-cell immunotherapy has progressed much more slowly in regard to the treatment of solid tumours. Nonetheless, various CAR T-cells have been engineered and tested against solid tumour cells in pre-clinical studies, while some of these experimental therapies are already in early phase clinical trials. Some examples include the administration of anti-mesothelin CAR T-cells in mesothelioma patients, anti-GD2 CAR T-cells for the treatment of patients with neuroblastoma[221,222] and ErbB-targeted CAR T-cells in patients with head and neck cancer[223].

Nonetheless, a variety of reasons account for the slower progress of CAR T-cell immunotherapy in patients with solid malignancies. Some of these challenges are considered in the section that follows.

1.3.4.3.1 Tumour microenvironment

One major obstacle that CAR T-cells have to overcome is the immunosuppressive microenvironment, which typifies solid tumours. Malignant cells require the support of the tumour microenvironment in order to proliferate, invade and metastasise. Different cell subsets are reported to contribute to tumourigenesis and modulate immune suppression. This include tumour-associated macrophages (TAM), cancer-associated fibroblasts (CAF), myeloid-derived suppressor cells (MDSC), tumour-associated neutrophils (TAN) and Tregs[193,224–227]. For example, M2 polarised macrophages secrete immunosuppressive cytokines, such as IL-10 and TGF-β which supress T-cell function[228,229]. Additionally, they produce cytokines, such as CCL20 and CCL22, that recruit Tregs[230,231]. Another mechanism by which TAMs suppress T-cell function is by the depletion of L-arginine, which results in downregulation of the CD3ζ chain in T-lymphocytes[232].

Different strategies have been designed which are focused on remodelling or re-educating the tumour microenvironment. Illustrating this, IL-12 secreting CARs have been engineered and are being investigated by multiple researchers. For example, Pegram *et al.* have constructed a CD19-specific CAR which constitutively secretes this cytokine and enabled the CAR T-cells to eradicate tumour in mice, even in the absence of chemotherapy

preconditioning[233]. Moreover, Yeku O. *et al.* reported that IL-12 "armoured CAR T-cells" can alter the tumour microenvironment and deplete tumour-associated macrophages[234]. Another strategy for overcoming the tumour immunosuppressive microenvironment is through combinatorial treatment of CAR T-cells with checkpoint inhibitors. Blocking of the inhibitory receptor PD-1 and its interaction with its ligand PD-L1 has emerged as a promising immunotherapeutic approach. John *et al.* were the first to show that combination of a HER-2 specific CAR treatment together a PD-1 blocking antibody significantly enhanced anti-tumour response in HER-2 transgenic mice[235]. In agreement with this study, a case report was recently published in which a patient with refractory DLBCL was treated with pembrolizumab, a PD-1 inhibitor, administered following treatment with CD19 CAR T-cells[236]. The authors have suggested that, although the patient did not initially respond to CAR T-cell treatment, enhanced proliferation of CD19 CAR T-cells was observed post treatment with pembrolizumab. This suggests a possible enhancement of CAR T-cell response due to PD-1 inhibition[236]. In another novel approach, CRISPR/Cas9 technology was used in order to knock out PD-1 in T-cells engineered with CAR molecules[237]. In the same study, the TCR gene was also disrupted simultaneously with PD-1 in order to produce "universal" allogeneic CAR T-cells[237].

1.3.4.3.2 Potency, persistence and proliferation

Second and third generation CARs have demonstrated significantly improved potency when compared to first generation CARs. The most

extensively used CARs have incorporated the CD3ζ signalling domain and endodomain sequences derived from either the CD28 or 4-1BB co-stimulatory molecule. These two distinct signalling domains have been reported to enhance efficacy and persistence of CAR T-cells. Notably however, CARs incorporating CD28 present a potent response characterized by shorter CAR T-cell persistence while CAR T-cells with 4-1BB show enhanced persistence in patients[238]. Kawalekar *et al.* have reported that the two distinct co-stimulatory molecules can affect significantly the differentiation status and metabolic profile of the T-cell populations[239]. CD28 CAR T-cells promoted the growth of effector memory T-cells with enhanced glycolysis. In contrast, 4-1BB CAR T-cells present central memory phenotype and increased fatty acid oxidation[239].

Another way of improving CAR T-cell potency, proliferation and persistence is by ameliorating the effects of T-cell exhaustion due to tonic signalling. In a novel approach, Eyquem *et al.* have engineered CAR T-cells in which the CAR is not randomly integrated into the T-cell genome[240]. In contrast, the gene encoding for this receptor was specifically integrated into the T-cell receptor α constant (TRAC) locus using CRISPR/Cas9 technology, rendering its expression subject to tight regulation by endogenous transcription factors. This new CAR design resulted in superior CAR T-cell activity when compared to a CD19-28z conventional CAR, with enhanced anti-tumour activity and reduced T-cell exhaustion[240]. In another study, Long *et al.* replaced the CD28 co-stimulatory molecule of constitutive activated (tonic signalling) CAR T-cells with 4-1BB. The incorporation of 4-1BB reduced T-cell exhaustion[241].

In another approach, IL-17 receptor was constitutively co-expressed with CAR T-cells[242]. The aim of this study was to provide signal 3 in CAR T-cells in order to improve their efficacy and persistence upon targeting solid tumours. The researchers suggest that co-expression of IL-17R can result in CAR T-cell stimulation without the need of exogenous addition of cytokines[242].

1.3.4.3.3 Trafficking

Trafficking of CAR T-cells to the site of tumours is a major challenge for targeting solid malignancies. Different reasons might be responsible for poor T-cell trafficking. These include the inability of T-cells to penetrate the tumour due to fibrotic phenotype and downregulation of chemo-attractive cytokines[238]. To overcome this, various groups have co-expressed a chemokine receptor in CAR T-cells that binds a cognate chemokine secreted by the tumour cells[243–245]. For example, K. Moon and colleagues have co-expressed a mesothelin-targeting CAR together with the CCR2 chemokine receptor[244]. The latter is specific for the C-C motif chemokine ligand 2 (CCL2). The co-expression of CCR2 resulted in increased T-cell infiltration within the tumour and improved therapeutic efficacy in mice with established mesothelioma tumours[244].

1.3.4.3.4 On-target off-tumour toxicities

One of the major obstacles to effective CAR T-cell immunotherapy is the lack of tumour specificity of the targeted antigen. It is highly desirable in this regard to target an antigen that allows discrimination between malignant

and normal cells. Expression of the cognate antigen in healthy tissues poses risk for significant toxicities due to “off-tumour” engagement of normal cells.

A number of factors have contributed to the success of CD19-targeted CAR T-cell immunotherapy for the treatment of B-cell malignancies. The CD19 glycoprotein is a hallmark of B-cells, and is also found on virtually all B-cell derived malignancies[246,247]. Its expression is minimal in cell types other than those of the B-lineage, a factor that makes it an ideal target for immunotherapy. It is now known that patients treated with anti-CD19 CAR T-cells commonly develop B-cell aplasia, since normal B-cells are also eliminated together with the malignant cells[248–250]. However, B-cell aplasia is considered a manageable on target off tumour toxicity as patients can be treated with intravenous or subcutaneous immunoglobulin replacement therapy (IVIg/ SCIg)[208,251].

Targeting solid tumours with CAR-engineered T-cells has proven challenging for various reasons. Severe cases of off-tumour toxicities have forced researchers to be extremely cautious in their choice of targeted antigen and in the design of clinical trials.

The efficacy of autologous T-cells modified to express an anti-CAIX CAR has been investigated in two different Phase I clinical trials for the treatment of patients with metastatic renal cell carcinoma[252,253]. Severe liver toxicity was observed in both clinical studies. Liver biopsies revealed expression of the CAIX antigen on bile duct epithelium, which resulted in CAR T-cell infiltration to these tissues[252,253].

A variety of solid malignancies - including breast, ovarian and colon cancer – exhibit overexpression of the receptor tyrosine-kinase protein ErbB2

(HER-2), which makes the latter an attractive immunotherapeutic target[254]. HER-2 is also found on normal epithelial cells such as in the gastrointestinal and respiratory tracts[255]. A HER-2-specific third generation CAR was developed which contained an scFv domain based on trastuzumab, a widely used anti-HER-2 monoclonal antibody[217]. The efficacy and safety of this CAR was investigated in a Phase I/II clinical trial of patients with metastatic cancer (NCT00924287). This study was terminated after treatment of the first patient who received $1x10^{10}$ anti-HER-2 CAR T-cells, administered intravenously over approximately 30 minutes. Unfortunately, she died within days of receiving CAR T-cell immunotherapy due to respiratory and multi-organ failure[256]. The authors speculated that the death of the patient resulted from the recognition of HER-2-positive lung cells (either parenchymal or endothelial) by the anti-HER-2 targeted CAR T-cells. This recognition caused the release of pro-inflammatory cytokines, leading to severe pulmonary toxicity and oedema[256]. Others have subsequently investigated the efficacy and safety of HER-2-directed CAR T-cells in clinical trials and have not reported any significant toxicities (NCT00902044)[257]. Differences in the scFv domain or endodomain of the CARs, injected CAR T-cell dose and pre-conditioning of the patients might be responsible for the different results obtained in these trials[217,256–258].

Carcinoembryonic antigen (CEA) is a large glycoprotein that is overexpressed in colorectal carcinoma and in other epithelial cancers. It is also expressed in normal epithelial cells throughout the gastrointestinal tract, such as in the intestinal epithelium[259]. In a distinct but related immunotherapeutic approach, T-cells have been engineered to express an

anti-CEA TCR[260]. The efficacy and safety of the engineered T-cells was tested in three patients with metastatic colorectal cancer[261]. Notably, all three patients developed severe inflammatory colitis, due to destruction of normal colon epithelial cells by the CEA-targeted T-cells. This was considered to be a dose-limiting toxicity which resulted in the termination of the clinical trial (NCT00923806).

A potential target for the treatment of multiple myeloma with CAR-engineered T-cells is the B-cell maturation antigen (BCMA). Similarly to CD19, the expression profile of BCMA is also lineage restricted in the sense that it is only found in plasma cells, both malignant and non-malignant[262]. Results published from an ongoing Phase I clinical trial showed that, as expected, multiple myeloma patients treated with anti-BCMA CAR T-cells also developed loss of normal plasma cells (NCT02215967)[263]. The authors suggested that, in some cases, this toxicity could also be manageable with immunoglobulin replacement therapy[263].

CD33 and CD123 are two targets that are over-expressed in myeloid malignancies. Consequently, CAR T-cells directed against these targets have been developed and are currently under investigation in clinical trials (NCT01864902, NCT02623582)[264–266]. Nevertheless, both antigens raise safety concerns as they are also expressed in normal haematopoietic cells and other healthy tissues. No evidence of on-target off-tumour toxicity due to treatment with autologous anti-CD33 or anti-CD123 CAR T-cells has been reported as yet in these studies[267]. The efficacy of allogeneic CD123-specific CAR T-cell immunotherapy is also being investigated in two other clinical trials for the treatment of patients with either AML or blastic plasmacytoid dendritic

cell neoplasm (BPDCN)[268]. These two trials were placed on hold by the FDA in September 2017 after the death of one BPDCN patient and the presentation of severe adverse events in a second AML patient post CAR T-cell treatment. These severe adverse events were reported to be related with CRS[268].

New strategies have been developed in order to improve tumour-specific antigen discrimination. Wilkie *et al.* were the first to co-express two CARs with different antigen specificity in primary human T-cells[269]. In this approach, one CAR incorporated a CD3ζ endodomain and the second receptor contained a co-stimulatory module. By this means, a complete T-cell activating signal is only delivered when both antigens are recognised[269–271].

In a similar way, a novel CAR T-cell circuit was designed where the presence of both antigens was required for CAR signalling. In this approach, a synthetic Notch (synNotch) receptor specific for antigen A is co-expressed with a CAR specific for antigen B[272]. Transcriptional activation of the CAR gene is allowed only upon recognition of antigen A by the Notch receptor. Thus, the tumour cells are eliminated only in the presence of both antigen A and B[272]. These synNotch receptors can be used for other purposes as they can be modified to activate the transcription of any desirable element upon antigen recognition[273,274]. For example, they can allow secretion of different cytokines, alter T-cell differentiation or deliver therapeutic agents such as monoclonal antibodies[273,274].

An additional way of regulating off-tumour toxicities is by co-expressing an inhibitory CAR receptor (iCAR), together with a signalling CAR, in order to restrain CAR T-cell activity upon antigen engagement. In this approach, the inhibitory CAR is specific for an antigen expressed in healthy tissues while the

signalling CAR has specificity for an antigen expressed on malignant cells. Thus, the signalling CAR is allowed to signal and eliminate the tumour cells only in the absence of the normal tissue-associated antigen. To achieve this, Fedorov *et al.* have designed two distinct iCARs which have incorporated either the PD-1 or CTLA-4 inhibitory domain[275].

1.3.4.3.5 Other safety concerns and control mechanisms

In addition to "on-target off-tumour toxicities", patients treated with CAR T-cell immunotherapy can present other severe adverse events such as cytokine release syndrome (CRS) and neurotoxicity. Cytokine release syndrome is characterized by elevated production of inflammatory cytokines, such as IL-6, IL-2, IL-10 and IFN-γ, due to uncontrolled *in vivo* CAR T-cell activation. Cytokine release syndrome can range in severity from mild to life threating and includes a range of features including fever, and major organ failure (e.g. cardiac dysfunction and respiratory failure).

Treatment of CRS is focussed on ameliorating these features without affecting the efficacy of CAR T-cells. Therapies directed against IL-2 and IFN-γ would probably affect the efficacy of CAR T-cell therapy. For this reason, Fitzgerald *et al.* selected tocilizumab for treatment of ALL paediatric patients with CRS post CD19 CAR T-cell infusion[276]. As previously mentioned, tocilizumab inhibits IL-6R, which blocks the interaction of IL-6 with its receptor. According to the authors of the study, blocking IL-6 interaction with IL-6R does not seem to influence the anti-tumour efficacy of CAR T-cells while it significantly improved clinical features of CRS[276].

Neurotoxicity has also been described in patients treated with CAR T-cells[277,278]. Patients with neurotoxicity present symptoms such as confusion, aphasia and seizures. In some cases, this toxicity can be lethal as five patients treated with CD19-specific CAR T-cells have died due to cerebral oedema[279]. The cause of this toxicity is not yet clearly understood. Nevertheless, there have been some suggestions that the neurotoxicity observed in patients treated with CAR T-cells might be caused due to intracerebral CRS or due to direct off-tumour toxicity[277,278].

In order to increase safety of CAR T-cell immunotherapy, different control mechanisms have been designed which allow regulation of CAR T-cell activity. These include suicide and elimination systems and drug-inducible CARs. Di Stasi *et al.* and Zhou *et al.* validated the efficacy of an inducible caspase 9 (iCasp9) suicide switch in patients who developed toxicity (eg graft versus host disease) following haploidentical stem-cell transplantation[280,281]. In this system, the pro-apoptotic protein caspase 9 undergoes dimerisation and is thus activated only upon administration of a small-molecule drug. In another approach, a drug-inducible CAR was designed[282]. The structure of this ON-switch CAR receptor is split into two separate polypeptides: the first consists of the scFv, the co-stimulatory molecules and one drug-inducible dimerisation domain, while the other polypeptide consists of the CD3ζ signalling domain of the CAR molecule and the second dimerisation motif. Upon addition of the drug, the two domains form heterodimers which allow the CAR to signal. The activity of the CAR can be tuned depending on the concentration of the administered drug[282].

In summary, the ability to reprogram T-cells to target tumour cells has revolutionised the way cancer patients are treated. The success of treating haematological malignancies with CAR T-cells is evident. Nevertheless, through clinical experience, some of the challenges of CAR T-cell immunotherapy have been revealed, especially for targeting solid tumours.

1.4 Overview of this PhD Project

1.4.1 Rationale

Breast cancer has the highest rate of cancer incidence in females worldwide. Despite many advances in treatment strategies and improvement in survival rates, breast cancer is still ranked as the 2nd most common cause of cancer death in women.

The field of immunotherapy has shown remarkable progress in the last decades and was characterized by the journal Science in 2013 as the "Breakthrough of the year". A very promising immunotherapeutic strategy entails adoptive T-cell therapy where T-cells are isolated from cancer patients, expanded *ex-vivo* and re-infused back to the patients. Based on this, the concept of CAR T-cell therapy was developed where T-cells are engineered to target antigen expressed on the cell surface of tumour cells. Engineered CAR T-cells have shown exceptional results in clinical trials for the treatment of patients with refractory leukaemia. One important drawback of this approach is the "on-target off-tumour toxicity" observed in many patients owing to engagement of target in normal tissues. Such toxic events have already caused the death of some patients, mandating the development of safer CAR T-cells approaches.

MUC1 is a large glycoprotein that is expressed in 90% of breast cancer patients, even in the individuals with triple negative breast cancer, a subtype with poorer outcome. MUC1 is considered as a very promising target for three reasons. First, MUC1 is transcriptionally upregulated in several tumour types,

including breast cancer. Second, MUC1 has the valuable characteristic of being aberrantly glycosylated in tumour cells in comparison with normal cells. This aberrant glycosylation exposes epitopes that are not seen in the normal tissues and is responsible for the immunogenic properties of the tumour-associated MUC1 (TA-MUC1). This has been exploited by the generation of antibodies, such as HMFG2 and TAB004, which are able to detect TA-MUC1. Third, MUC1 is normally expressed in a polarised manner on the luminal (e.g. inaccessible) surface of epithelial cells, but this polarity is lost in cancer cells, making the target accessible to immunotherapies such as CAR-engineered T-cells. A pilot project conducted by the National Cancer Institute (NCI) has ranked MUC1 as the second most attractive antigenic target for the development of immunotherapeutic approaches[283].

Based on the above, MUC1 seems to be a propitious target antigen for the development of CAR T-cell therapies, with less risk for the development of on-target off-tumour toxicity. Despite its unique characteristics, no significant advances have been made towards this direction. A reason for this might be the fact that MUC1 has a very large extracellular domain (200-500nm), which makes its targeting very challenging.

1.4.2 Aim of the PhD project

The aim of this PhD project was to develop a safe and effective MUC1-based CAR T-cell approach. In this approach, the anti-tumour capacity of a newly-developed MUC1 CAR named TAB28z has been evaluated in both the *in vitro* and *in vivo* setting. As previously mentioned, this CAR (named TAB28z) contains an scFv domain derived from TAB004 antibody (Figure 1.11). TAB004 has been generated by Curry *et al.* and has been shown to recognize TA-MUC1 on pancreatic cancer tumour cells[284]. TAB28z CAR is a second generation CAR which signals via CD3ζ and CD28. Throughout this project, TAB28z was compared with two other 2nd generation MUC1 CARs, namely H28z and HDF28z which have been previously developed in the lab by Wilkie *et al.*. Thus, I sought to investigate whether this newly developed MUC1 CAR demonstrates superior activity when compared to these two previously generated MUC1 CARs.

H28z and HDF28z CAR T-cells similarly signal via CD3ζ and CD28 (Figure 1.11). Both contain a scFv derived from another MUC1 antibody with specificity for TA-MUC1, named as HMFG2. The HDF28z CAR has incorporated a longer hinge (IgD), which provides enhanced flexibility and reach to the binding domain of the CAR. Throughout the project, I used three non-signalling (truncated) CARs as controls, which match each of the three signalling CARs (Figure 1.11). The six CAR constructs will be further explained in Chapter 3.

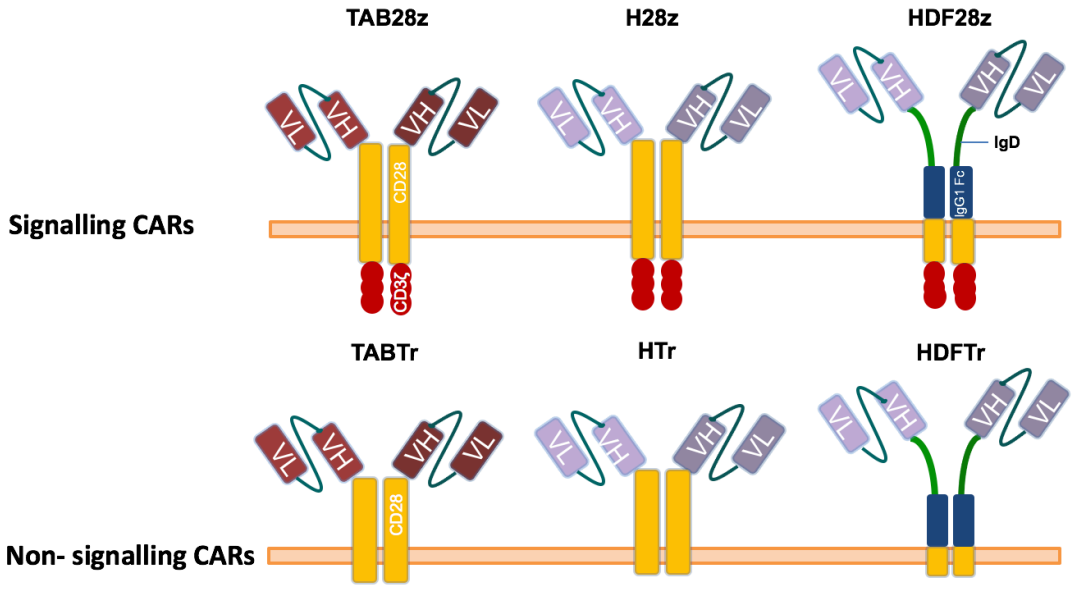

Figure 1.11: MUC1-specific CARs. Three signalling and three non-signalling CARs have been used throughout this project. All six CAR constructs have specificity for MUC1. TAB28z, H28z and HDF28z are second-generation CARs which signal via CD3ζ and CD28. TAB28z has a scFv derived from the TAB004 MUC1-specific antibody while H28z and HDF28z contain a scFv derived from the HMFG2 antibody. HDF28z has incorporated an IgG and IgD hinge, which provides length and flexibility to the binding domain of the CAR. Three non-signalling CARs, named as TABTr, HTr and HDFTr are additionally used throughtout this project as negative controls. Each of these match the relevant signalling CAR.

Of note, both HMFG2 and TAB004 antibodies bind to the VNTR region of MUC1[95,284]. Specifically, TAB004 has been reported to recognise the peptide epitope in position aa 950-958 while HMFG2 binds to a peptide sequence which is repeated in the MUC1 VNTR (UniProtKB #P15941) (Table 1.3) [95,284].

Table 1.3: Epitope binding sequence of TAB004 and HMFG2 anti-MUC1 antibodies.

Antibody	Epitope binding sequence	Position- Amino acids (aa)
TAB004	STAPPVHNV	950-958
HFMG2	PDTRPAPGSTAPPAHGVTSAPDTR	Repeated sequence

The TAB004 antibody has been generated by immunising Balb/c mice with MUC1-positive pancreatic tumours, previously generated i MUC1 transgenic mice. TAB004 has been reported to detect MUC1 in tumours isolated from stage 2-4 pancreatic cancer[284]. Additionally, TAB004 could bind to MUC1 in cancer stem cells (CSCs) isolated from pancreatic cancer patients[284]. Furthermore, the specificity of TAB004 was investigated in a breast cancer mouse model, where it showed detection of early and metastatic breast cancer[285]. Currently, TAB004 antibody is being commercially developed by OncoTAb Inc., a start-up company established by Professor Pinku Mukherjee[286]. The company has generated their first commercially-available product, named as Agkura™ Personal score. Agkura™ is a non-invasive blood test which is being offered for breast cancer detection, in supplementation to mammogram, for women with dense breast tissue. Its technology is based on detecting circulating MUC1 with the use of TAB004 antibody[286].

The HMFG2 antibody was produced by immunising Balb/c mice with delipidated human milk fat globule (HMFG) followed by milk epithelial cells[287]. HMFG protein is found to be expressed in the lactating mammary gland and in primary and metastatic breast cancer tumours. Burchell *et al.* have shown that HMFG2 detects MUC1 in serum of breast cancer patients[288]. It has also been shown to detect malignant epithelial cells in pleural and peritoneal effusions from patients with other epithelial-based malignancies, such as ovarian, prostate, pancreatic, lung and colon cancer[289,290]. Additionally, HMFG2-radiolabelled antibody (^{123}I) has been used in patients to localise ovarian, breast, and gastrointestinal tumours[291,292]. This antibody also detects

MUC1 expressed in some luminal epithelial cells such as in normal resting breast, albeit weakly[292].

As previously explained, on-target off-tumour toxicities pose a significant risk in CAR T-cells immunotherapy. For this reason, I explored the possibility of TA-MUC1 being recognised by CAR T-cells in an off-tumour setting.

1.4.3 Objectives of the PhD project

As described, the aim of this PhD project was to investigate the potential of TAB28z CAR for the treatment of MUC1-positive breast carcinoma. For this purpose, multiple objectives were set. These are:

1. *In vitro* characterization of TAB28z CAR T-cells:
    i) Generation of negative-control CAR constructs
    ii) Generation of stable packaging cell lines
    iii) Assessment of binding preference of MUC1-specific CAR T-cells to tumour-associated glycoforms
    iv) Validation of CAR expression in human primary T-cells
    v) Assessment of *in vitro* cytotoxic activity against a panel of breast cancer cell lines and
    vi) Target-dependent production of pro-inflammatory cytokines by CAR T-cells
2. MUC1 expression on activated T-cells and its effect on MUC1-specific CAR T-cell populations

3. Establishment of breast cancer xenograft model in NSG mice
4. Investigation of *in vivo* activity of TAB28z CAR T-cells and comparison with HMFG2-based CARs.

Chapter 2: Materials and Methods

2.1 Molecular Biology Techniques

2.1.1 SFG retroviral vector

Plasmid DNA encoding for the SFG retroviral vector was a gift of Dr Michel Sadelain (Memorial Sloan Kettering Cancer Center, New York, NY, USA) and contains the long terminal repeats (LTRs) of the Moloney murine leukaemia virus（MoMLV), responsible for driving the transcription of the inserted gene. The vector also contains the psi (ψ) packaging signal downstream of the 5'LTR. Psi packaging element is necessary for the encapsulation of the inserted genome into viral particles[293,294].

2.1.2 Engineering of CAR constructs

Six MUC1-specific CARs were used in this project, namely TAB28z, H28z, HDF28z and their matched negative-control CARs TABTr, HTr and HDFTr. The latter contain a truncated and signalling defective endodomain in which only the membrane proximal three amino acids of the CD28 endodomain are present. All constructs were expressed using the SFG retroviral expression vector[293].

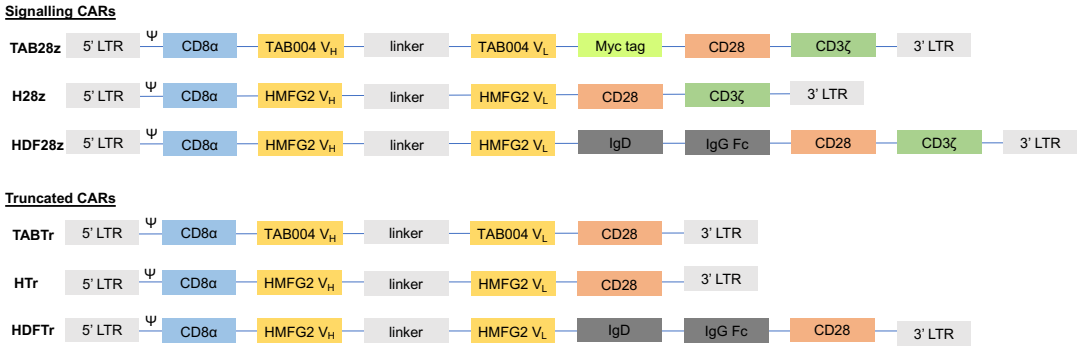

Figure 2.1: MUC1-specific CAR constructs. In total, six CAR constructs have been used throughout this project; three signalling intact CARs, TAB28z, H28z and HDF28z and three truncated CARs with a defective signalling domain. All six were cloned into SFG retroviral vector containing the 5' and 3' long terminal repeat (LTR) sequences and the psi (ψ) packaging signal. Additionally, they include the human CD8α leader sequence. TAB28z and TABTr constructs contain the heavy and light chains of the TAB004 antibody while H28z, HTr, HDF28z and HDFTr contain contain the heavy and light chains of the HMFG2 antibody. The three signalling intact CARs include CD28 (hinge/transmemberane/ endodomain – signal 2) and CD3ζ (endodomain - signal 1). HDF28z and HDFTr have an IgD hinge and IgG1 hinge plus Fc spacer while TAB28z contains a myc epitope tag which provides an alternative detection method. The three truncated CARs lack CD3ζ while only the membrane proximal three amino acids of the CD28 endodomain are present.

2.1.2.1 Construction of TAB28z, H28z, HDF28z and HDFTr

The TAB28z, H28z, HDF28z and HDFTr CARs were previously generated by colleagues and contain an scFv domain specific for MUC1[295]. The scFv domain of TAB28z is derived from the TAB004 MUC1-specific antibody while the scFv domain of H28z, HDF28z and HDFTr is derived from the HMFG2 MUC1-specific antibody[284,287]. TAB28z, H28z and HDF28z contain the CD3ζ signalling domain and the CD28 co-stimulatory endodomain. As mentioned previously, HDFTr contains a defective signalling domain.

The TAB28z CAR has not been previously tested and its activity has been evaluated in this project. The H28z and HDF28z CARs were used for comparative purposes while HDFTr was used as a negative control.

2.1.2.2 Construction of TABTr and HTr

2.1.2.2.1 Cloning Strategy

Plasmids encoding for the TABTr and HTr negative-control CARs were generated by sub-cloning, following restriction digestion of SFG containing plasmids. Two previously existing truncated CARs archived in the lab were used for this purpose, namely SFG V9-truncated (V9Tr) and SFG CT4-truncated (CT4Tr) (Dr Daniela Achkova)[296]. Initially, the scFv domains of TAB28z and H28z plasmids were isolated by Nco1-Not1 digestion. Similarly, the desired vector backbone sequences (SFG, spacer, transmembrane and truncated signalling domain) were isolated from V9-truncated and CT4-truncated, through Nco1-Not1 digestion. The TABTr construct was generated by ligating the TAB28z-derived scFv with the V9-truncated vector backbone while HTr was generated through ligation of the H28z-derived scFv with the CT4-derived vector backbone sequence.

2.1.2.2.2 Gel extraction of DNA fragments following restriction digestion of plasmids

Nco1 and Not1 restriction endonucleases (NEB, USA) were used to cleave the plasmids mentioned above and extract the DNA fragments of interest.

Table 2.1: Example of restriction digestion reaction prior to DNA extraction by agarose gel electrophoresis. Reagents and quantities used in the digestion reaction prior to gel extraction of the desired DNA fragments (insert and vector) are listed.

Reagent	Plasmid 1 (insert extraction)	Plasmid 2 (vector extraction)
Nuclease-free water	Up to 100 µl final volume	Up to 100 µl final volume
NEB Buffer (10x)	10 µl	10 µl
NEB enzyme 2	5 µl (50 units)	5 µl
NEB enzyme 1	5 µl (50 units)	5 µl
DNA	5 µg	5 µg

Table 2.2: Expected size of DNA fragments after restriction digestion with Nco1/ Not1. The fragments of interest are indicated in red.

1: V9Tr
1. 6582 bp (vector)
2. 141 bp

2: TAB28z
1. 7033 bp
2. 804 bp (insert)

3: CT4Tr
1. 6570 bp (vector)
2. 1710 bp
3. 528 bp

4: H28z
1. 7020 bp
2. 789 bp (insert)

The digested DNA products were subjected to electrophoretic separation on a 1% agarose gel containing ethidium bromide (see Section 2.1.2.2.3 for description of agarose gel electrophoresis). Bands of the desired size were extracted with the use of UV light (Table 2.2). The extracted bands were purified with a DNA purification kit (Promega, USA) and the DNA fragments were ready for ligation.

2.1.2.2.3 Agarose gel electrophoresis

In order to prepare the 1% agarose gel, 0.3 grams of UltraPure agarose (ThermoFisher Scientific, USA) were added to 30ml of 1x TBE solution contained in a microwavable flask. The solution was microwaved for 2 minutes until the agarose was completely dissolved. The mixture was allowed to cool down and, when the temperature reached 50˚C, ethidium bromide was added to a final concentration of 0.5μg/ml. The solution was then poured slowly into a gel tray containing well combs. The gel was allowed to sit at room temperature for 30 minutes and was then placed into the gel tank filled with 1x TBE, followed by the removal of the combs. The digested reactions together with the 1kb DNA ladder (NEB, USA) were prepared accordingly by adding 1x gel loading dye (NEB, USA) and were loaded carefully into the wells. The gel was run at 80V for approximately an hour. The gel was visualised using a UV light device and the DNA fragments were isolated using a sterile razor blade and were placed at 4˚C until further processing.

2.1.2.2.4 Ligation reactions

Restriction digestion led to the generation of DNA fragments with compatible sticky ends (Table 2.2) thus allowing their ligation. Fragment 1 obtained from SFG V9Tr was ligated with fragment 2 derived from TAB28z in order to generate TABTr. To generate SFG HTr, fragment 1 from CT4Tr was ligated with fragment 2 from H28z. The ligation was achieved by mixing the insert and vector of interest with QuickLigase (NEB, USA) for 5 minutes at room temperature (2.1.2.2.4). The ligated products were then validated by transforming *Escherichia* (*E.) coli* competent cells and by screening the DNA isolated from bacterial clones (See sections 2.1.3 - 2.1.6).

Table 2.3: Ligation reactions. Reagents and quantities used in ligation reactions are listed.

Reagent	Quantity
Nuclease-free water	Up to 20 µl
NEB Quick Ligase buffer	10 µl
Vector	50ng
Insert	37.5 ng
NEB Quick Ligase	1 µl

2.1.3 Plasmid transformation of *Escherichia coli*

The aforementioned DNA constructs were scaled-up by transforming DH5-alpha chemicaly competent *E. coli* (Life Technologies, USA). Plasmid DNA (1µl) was mixed with 50µl DH5-alpha cells and placed on ice for 30 minutes. The mixture was incubated in 42°C for 90 seconds (heat shock) and then placed back on ice for 5 minutes. Super optimal broth with catabolite

repression (SOC) medium (250µl) (Invitrogen, USA) was then added and the mixture was placed in a bacterial shaker for 1 hour (37°C, 220rpm). Finally, the bacteria-SOC medium mixture was spread onto pre-warmed Lysogeny broth (LB) agar plates containing ampicillin and incubated overnight at 37°C to allow the antibiotic-resistant bacterial clones to grow (see 2.1.4 for preparation of agar plates). All the plasmids have an ampicillin resistance gene. Consequently, only bacterial clones that contained the plasmid were expected to survive and grow on the ampicillin-containing agar plates.

On the day following plasmid transformation, several bacterial clones were picked from the agar plate. A yellow tip was used to pick individual colonies which were dropped in a Falcon tube containing 5ml LB medium with ampicillin (1ml of 50mg/ml ampicillin was added to 500ml of LB broth). Falcon tubes were then placed in the bacterial shaker (37°C, 220rpm) and left overnight.

2.1.4 Preparation of LB agar plates for bacterial growth

Initially, a bottle containing 500ml of LB agar was placed in the microwave and heated for 20 minutes at 40% power. The melted LB agar was allowed to cool down for 15 minutes at room temperature and ampicillin was then added (1ml of 50mg/ml ampicillin was added to 500ml of LB agar). After thorough mixing, the ampicillin-containing LB agar was poured into Petri dishes (10ml solution per Petri dish). The LB agar was allowed to set and the agar plates were stored afterwards at 4ºC.

2.1.5 Mini-plasmid preparation

On the following day, DNA was extracted from each of the bacterial clones that were picked. A low-yield “miniprep” plasmid extraction procedure was performed to determine if the bacterial clones contained the expected plasmid DNA. A QIAprep Miniprep Kit (Qiagen, Germany) was used to extract the DNA, according to the manufacturer’s protocol. The DNA was eluted in 50µl of nuclease-free water (Ambion, USA).

2.1.6 Validation of plasmid DNA with restriction enzyme digestion

Plasmid DNA digestion with the appropriate restriction endonucleases was performed in order to validate the purified plasmid. The miniprep DNA was incubated together with the reagents listed in Table 2.4 for one hour at 37°C. The digested products were separated on a 1% agarose gel containing ethidium bromide by electrophoresis (see Section 2.1.2.2.3).

Table 2.4: Screening digest of Miniprep DNA with restriction endonucleases. Enzymes and buffer were purchased from New England BioLabs (NEB, USA).

Reagent	Quantity (µl)
Nuclease-free-water	Up to 30
NEB buffer (10x)	3
NEB enzyme 1	0.5 (5 units)
NEB enzyme 2	0.5 (5 units)
Miniprep DNA	0.5-1µg

2.2 Cell culture

All cells were cultured in a humidified incubator at 37°C containing 5% CO_2 in air. All tumour cell lines and retroviral packaging cell lines were propagated in D10 medium while primary human T-cells were cultured in R5 medium.

D10 medium

- DMEM media (Lonza, Switzerland)
- 20mM L-Glutamine (Sigma-Aldrich, USA)
- 10% foetal bovine serum (FBS) (Sigma-Aldrich, USA)

R5 medium

- DMEM media (Lonza, Switzerland)
- 20mM L-Glutamine (Sigma-Aldrich, USA)
- 5% human AB serum (Sigma-Aldrich, USA)
- 50,000U penicillin/50mg streptomycin (Sigma-Aldrich, USA)

2.2.1 Culture of immortalised cell lines

2.2.1.1 Breast cancer cell lines

A panel of breast cancer cell lines was characterised for expression of MUC1 prior to investigating the target-dependent cytotoxic activity of the MUC1 CAR T-cells. These cell lines consisted of T-47D, MCF7, BT-20, MDA-

MB-468, ZR-75-1 and MDA-MB-231. The characteristics of these cell lines are listed in Table 2.5[297,298].

Table 2.5: Characteristics of the breast cancer cell lines used throughout this project. ER – oestrogen receptor; PR – progresterone receptor; HER-2 – ErbB2 receptor.

Cell line	Morphology	Origin of cells	ER/ PR/ HER-2
T-47D	Ductal carcinoma	Metastatic site; pleural effusion	ER+, PR+, HER-2 -
MCF-7	Luminal	Metastatic site; pleural effusion	ER+, PR-, HER-2 -
BT-20	Basal	Mammary gland	ER-, PR-, HER-2 -
MDA-MB-468	Basal	Metastatic site; pleural effusion	ER-, PR-, HER-2 -
ZR-75-1	Luminal	Metastatic site; ascites	ER+, PR-, HER-2 -
MDA-MB-231	Basal	Metastatic site; pleural effusion	ER+, PR+, HER-2 -

The cell lines listed above were propagated in D10 medium.

2.2.1.2 Retroviral packaging cell lines

A critical step in the generation o CAR T-cells is the genetic modification of T-lymphocytes to stably express the CAR construct of interest. This was achieved by delivering a retroviral vector that carries the CAR transgene into pre-activated T-cells. The retroviral vector is delivered to the cells by appropriately pseudotyped viral particles produced by retroviral packaging cell lines.

Retroviruses are considered a useful tool in the field of gene therapy as they have the ability to integrate their genome into the DNA of a host cell. Retroviral virions include two copies of singe-stranded RNA consisting of at least four genes, *gag*, *pol*, *pro* and *env*[299,300]. Each of these genes encode for

viral proteins with different function. *Gag* encodes for the structural proteins necessary for the viral core. *Pol* encodes for integrase, RNA H and reverse transcriptase. *Env* directs expression of the proteins related to the viral envelope and lastly, *pro* encodes for protease which is responsible for the processing of gag and pol proteins[300]. The structural features of a retroviral particle are shown schematically in Figure 2.2.

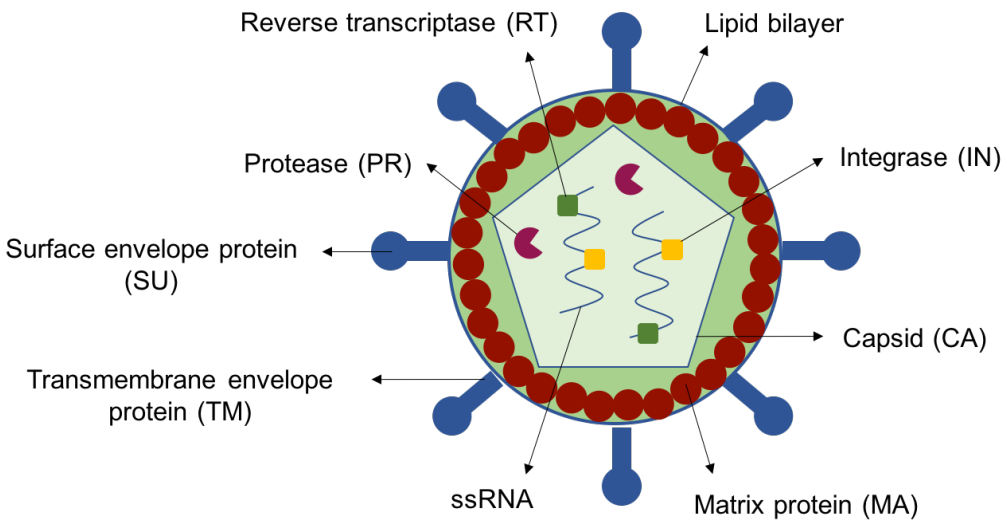

Figure 2.2: Schematic representation of the structure of a retroviral particle. Two-single stranded RNA (ssRNA) molecules are included inside the capsid (CA) together with the viral proteins, namely protease (PR), integrase (IN) and reverse transcriptase (RT). Capsid is surrounded by the matrix (MA) while the lipid bilayer forms the outer layer. Surface envelope protein (SU) and transmembrane envelope protein (TM) form the envelope of the viral particle.

The retroviral life cycle is summarised in Figure 2.3. Infection of the host cell by retroviruses is initiated when the glycoproteins of the viral envelope attach to their receptors expressed on the surface of the host cell. Upon recognition, the viral envelope is fused with the cell membrane and the viral RNA is released to the cytoplasm[301]. A viral protein, named reverse transcriptase, converts the viral RNA into double-stranded DNA which is then

transferred inside the host cell nucleus. Viral DNA is unable to entry the cell nucleus; nevertheless, it can enter the nucleus during mitosis after the dissolution of the nuclear membrane[302]. The next step is the integration of the double-stranded DNA (dsDNA) to the host cell genome in order to form the provirus. This process occurs in an almost random manner throughout the host cell genome. The integrated provirus is then transcribed to yield mRNA that encodes for viral proteins, a process mediated by RNA polymerase II. The mRNA is exported from the nucleus and is translated by the host-cell translation machinery. These translated proteins are further processed by a viral protease and are encapsulated into viral particles. The newly formed viral particles exit the infected cell through a process known as budding[303].

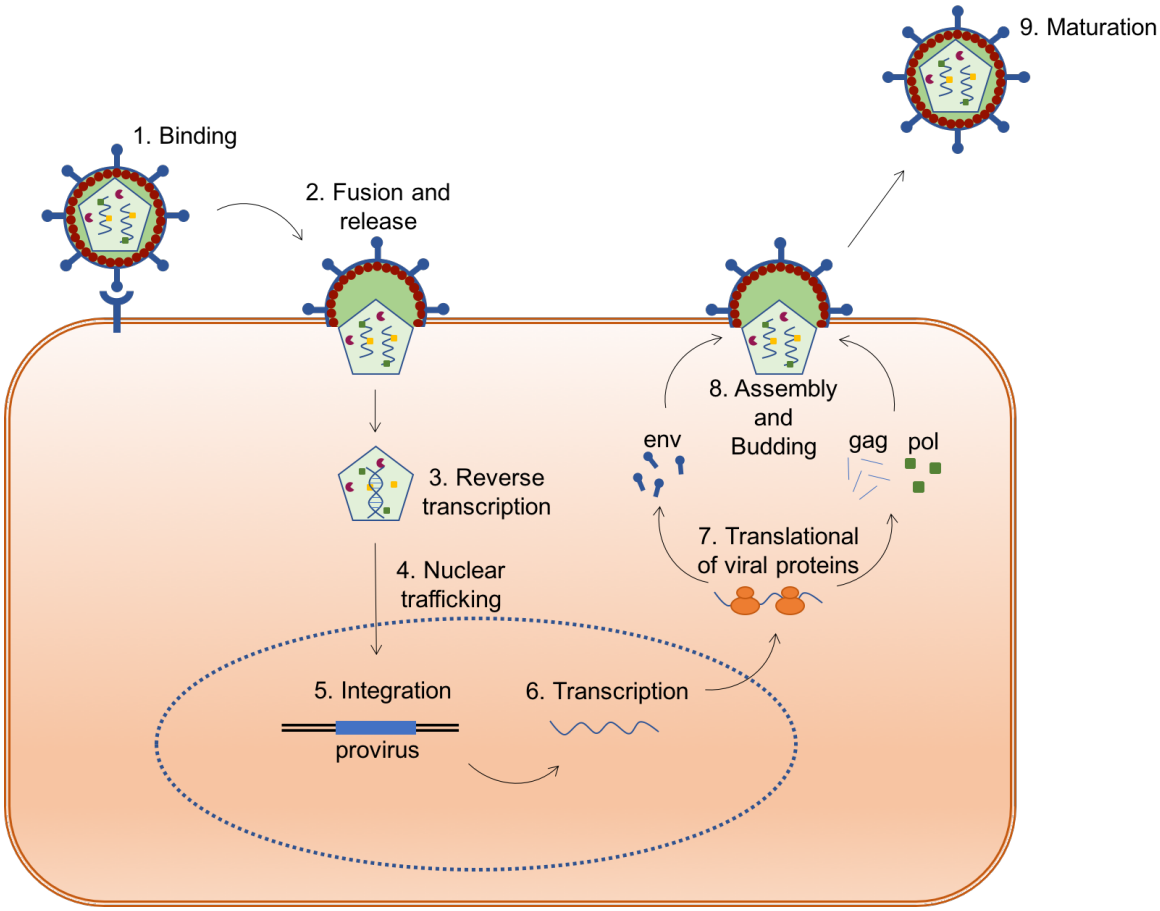

Figure 2.3: Life cycle of retrovirus. Infection of the host cell by the retrovirus begins when the viral envelope proteins bind to their receptors expressed on the cell membrane of the host cell (1). The viral and cell membranes are fused and the capsid including the ssRNA is released into the cytoplasm (2). ssRNA is reverse transcribed to cDNA (3) and is transported to the nucleus upon mitosis (4). Viral cDNA is integrated to the host cell DNA, thus forming the provirus (5). Provirus is transcriped to mRNA by the host cell's transcription machinery (6). The latter is translated, leading to the production of viral proteins (7). The latter are further processed by viral protease and subsequently are encapsulated together with new viral RNA in order to form new viral particles. The newly formed viral particles exit the host cell through budding (8) and they undergo maturation in order to initiate the infection of a host cell (9).

As mentioned above, retroviruses are often used in CAR T-cell immunotherapy to achieve stable expression of the gene of interest. Nevertheless, the ability of retrovirus to replicate is undesirable. For this reason, replication-defective retroviral vectors are used in which the four viral genes, *gag, pol, pro, env* are replaced by the gene of interest. Since these

viral proteins are necessary for the infection of the host cell, dedicated packaging cells that provide the missing proteins *in trans* are used to produce the retroviral vector for delivery to and integration within T-cells.

Four different retroviral packaging cell lines have been used throughout this PhD, namely H29, PG-13, HEK 293T VECs and HEK 293T cells.

2.2.1.2.1 H29 cells

The H29 packaging cell line is derived from human 293 cells which have been engineered to express the Moloney murine leukaemia virus (MoMLV) gag and pol proteins and the vesicular stomatitis virus (VSV)-G envelope protein[304]. VSV-G pseudotyped virus is produced in an inducible manner, under the control of tetracycline. Thus, the production of the pseudotyped viral particles is allowed only when the cells are not propagated in tetracycline. The regulation of the VSV-G expression from tetracycline is essential as the VSV-G protein is toxic to the 293T cells, owing to syncytialization[304]. H29 cells were obtained as a gift from Dr Michel Sadelain (Memorial Sloan Kettering Cancer Center, New York, NY, USA) and were cultured in D10 medium. The medium also contained 2μg/ml tetracycline (Calbiochem, USA) to suppress the expression of VSV-G protein, 0.3mg/ml G418 to maintain the expression of gag-pol and 2μg/ml puromycin to maintain the tetracycline-regulated expression of VSV-G.

2.2.1.2.2 PG-13 cells

PG-13 are retrovirus-packaging cells derived from TK-NIH/3T3 cells[305]. PG-13 cells contain the MoMLV gag-pol proteins and the envelope protein of gibbon ape leukaemia virus (GALV). Derived GALV pseudotyped retroviral particles can infect host cells of varying species origin, including human cells. Importantly however, it cannot be used to transduce murine cells. The virus that is produced is of high titre, generally $>10^6$ colony forming units (CFU)/ml[305]. PG-13 cells were obtained from the European Collection of Authenticated Cell Cultures (ECACC) and were cultured in D10 medium.

2.2.1.2.3 HEK 293T cells

HEK 293T (293T) cells are a subtype of the human embryonic kidney (HEK) cells, which have been transfected to express a mutant form of the SV40 T-antigen[306]. HEK 293T cells were propagated in D10 medium.

2.2.1.2.4 HEK 293T VEC cells

HEK 293T VEC packaging cells, pseudotyped with either RD114 or GALV envelope are derived from HEK 293T cells and were obtained as a gift from Dr Manuel Caruso (CHU de Québec Research Centre, Canada). The latter have been transfected to express the gag and pol proteins of the MoMLV virus together with the RD114 or the GALV envelope. These packaging cells are reported to produce viral titres of above $1x10^7$ CFU/ml[307]. HEK 293T VEC cells were propagated in D10 medium.

2.2.2 Generation of stable retroviral packaging cell lines expressing CAR constructs

2.2.2.1 Generation of TAB28z-expressing packaging cells

An overview of the method used in this project to generate stable retroviral packaging cells for SFG TAB28z is indicated in Figure 2.4. Initially, H29 cells were transfected with the plasmid vector of interest. The vector was then packaged into transiently produced viral particles that had the VSV-G envelope. The latter allows the viral particles to be delivered in the PG-13 packaging cell line for stable production of GALV pseudotyped retroviral vector that carries the transgene.

The transfection of H29 cells with TAB28z-encoding SFG plasmid DNA was achieved using the poly-ethylenimine (PEI) transfection reagent (Sigma-Aldrich, USA). The H29 cells were plated in tetracycline containing-medium in order to reach 90% confluence in a 6 well plate by the day of transfection. On the day of transfection, the tetracycline containing medium was replaced with 2ml of tetracycline-free D10 and cells were returned to the incubator for 2 hours. Subsequently, 1.5µl of 1mM PEI and 50µg of the vector of interest were mixed with 1.5ml of serum-free DMEM medium and incubated for 20 minutes. The H29 cells were washed three times with serum-free medium and the mixture was added to the cells. The cells were incubated in the incubator for 2 to 2.5 hours and the mixture was removed by replacing it with 3ml of D10.

To generate a stable retroviral packaging cell line, supernatant from the transfected H29 cells was harvested and transferred every day to a different

well of under-confluent PG-13 cells (approximately 30% confluent)[308]. The viral supernatant was filtered through a 0.45μm pore-size filter (Corning, USA) prior to its addition to the PG-13 cells.

As mentioned before, the virus produced by HEK 293T VEC packaging cells is of higher titre in comparison with that produced by the PG-13 cells. For that reason, HEK 293T VECs carrying the RD114 envelope were also engineered to express the CAR transgene, aiming to achieve high T-cell transduction efficiency. To achieve this, PG-13 cells that produce SFG TAB28z were trypsinized in order to reach 90% confluency by the next day. The viral supernatant was then harvested from these cells and was added to under-confluent HEK 293T VECs. The viral supernatant was filtered through a 0.45μm pore-size filter (Corning, USA) prior to its addition to the 293T VECs. The same process was repeated until over 80% of the 293T VECs expressed the CAR transgene, as determined by flow cytometry (see section 0).

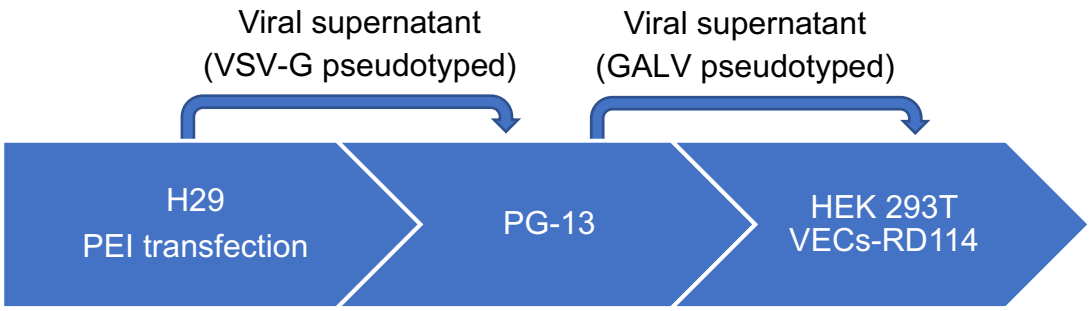

Figure 2.4: Schematic representation of the experimental process undertaken to generate TAB28z-expressing packaging cells. H29 cells were transfected to express TAB28z CAR plasmid with the use of poly-ethylenimine (PEI) agent. H29-produced viral supernatant (VSV-G envelope) was then used to transduce PG-13 cells. Subsequently, supernatant harvested from PG-13 packaging cells (GALV envelope) was transferred to HEK 293T VECs expressing the RD114 env.

2.2.2.2 Generation of H28z, HDF28z and HDFTr-expressing packaging cells

PG-13 packaging cells expressing individually the H28z, HDF28z and HDFTr CAR transgenes were made previously by colleagues. HEK 293T VECs expressing the RD114 envelope were furthered transduced to express the CARs following the method described in Section 2.2.2.1 (Figure 2.5).

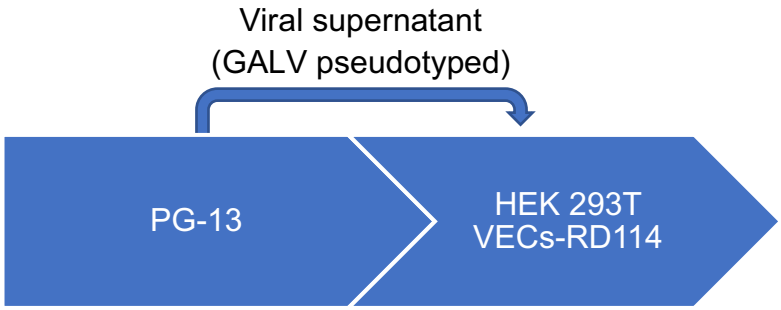

Figure 2.5: Schematic representation of the experimental process undertaken to generate H28z, HDF28z and HDFTr-expressing packaging cells. Supernatant harvested from PG-13 packaging cells (GALV envelope) expressing the CAR construct of interest was transferred to HEK 293T VECs expressing the RD114 envelope.

2.2.2.3 Generation of TABTr and HTr-expressing packaging cells

HEK 293T VECs expressing the GALV envelope were transduced to express the TABTr and HTr CAR through the method of simultaneous triple transfection of *gag-pol*, *env* and CAR-encoding plasmids (Figure 2.6). HEK 293T cells ($1.5x10^6$ cells) were plated in one 100mm plate per CAR construct, and were placed in the cell culture incubator. The cells were re-suspended in 10ml D10 medium. The HEK 293T cells were ready for transfection when they had confluency at 50-60%. For each plate, a mixture (A) of 470µl plain DMEM (Lonza, Switzerland) and 30µl of GeneJuice (Novagen, Germany) was

prepared and incubated for 5 min in the hood. Subsequently, a mixture (B) of 12.5µg DNA containing all three plasmids (Table 2.6) was added to mixture A and was incubated for 15 min in the hood. The mixture A+B was then added drop-wise into the plate. The plates were incubated in a cell incubator and at 48 hours post transfection the viral retroviral supernatant (10ml) was collected from each plate.

Table 2.6: Triple Transfection. Three different plasmids were used in total of 12.5µg per plate: 1.RD114 (envelope), 2.Gag-Pol, 3.CAR construct.

Plasmid	Quantity per plate (µg)
RD114	3.125
gag-pol	4.6875
CAR construct	4.6875
	Total = 12.5

Subsequently, 3ml of the collected supernatant was filtered (0.45µm-pore filter) and transferred to under-confluent HEK 293T VCs expressing the GALV envelope. D10 medium (10ml) was added to the 100mm cell plate which was incubated for additional 24 hours. The supernatant was harvested, filtered as before and 3ml was transferred to the HEK 293T VECs from the previous day.

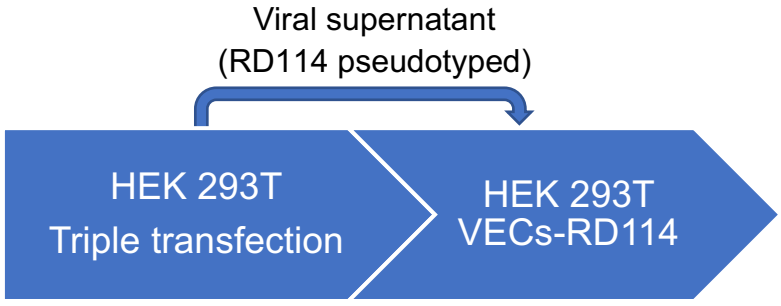

Figure 2.6: Schematic representation of the experimental process undertaken to generate TABTr and HTr-expressing packaging cells. HEK 293T cells were “triple transfected” to express the constructs of interest. Viral supernatant was harvested at 48 hours and 72 hours post-transfection and transferred to HEK 293T VECs expressing the GalV envelope.

2.2.3 Binding of MUC1-specific CARs to MUC1-IgG fusion proteins

The binding of TAB004 and HMFG2 scFv to different MUC1 glycoforms was investigated. Specifically, 2 x 10^5 TAB28z and H28z-expressing HEK 293T VEC cells were incubated with 200µg/ml MUC1 ectodomain-mouse IgG fusion proteins (decorated with T, ST, Tn or STn) on ice for 30 minutes[295]. Secondary goat anti-mouse IgG AlexaFluor 647-conjugated antibody was then added which allowed the detection of binding to each of the fusion proteins by flow cytometry. TAB28z and H28z HEK 293T VEC cells were stained with mouse IgG1 AlexaFluor 647-conjugated antibody as isotype controls. To correct for the difference in CAR expression on VEC cells, the mean fluorescence intensity (MFI) of binding was normalized to the MFI of CAR expression (MFI of bound glycoform/MFI of CAR-positive cells). The method of detection of CAR expression is described in Section 0).

The IgG fusion proteins decorated with T, ST, Tn or STn were provided as a gift by Dr Richard Beatson (King’s College London, UK) and were produced as described by Bäckström by using wild-type or ldlD-mutant[309] Chinese hamster ovary (CHO) cells[310–312].

2.2.4 Isolation of Peripheral Blood Mononuclear cells and activation of T-cells

Primary human peripheral blood mononuclear cells (PBMC) were isolated from healthy donors using Ficoll-Paque (GE Healthcare, UK)-based density gradient centrifugation. This protocol was approved by the Research Ethics Committee of Guy's Hospital (09/H0804 192; use of Donor Blood samples for pre-clinical development). Initially the blood was transferred into a Falcon tube that contained 5ml of citrate-dextrose anticoagulant (Sigma-Aldrich, USA). Ficoll-paque (15ml) was transferred into a 50ml Falcon tube and 25ml of anticoagulated blood was very slowly layered onto the ficoll, avoiding mixing between the two layers. The Falcon tube containing the layered blood was then centrifuged at 1150g for 25 minutes (acceleration and brake settings=0). The PBMC layer (buffy coat) was transferred into a new 50ml Falcon tube using a Pasteur pipette, diluted to a final volume of 50ml PBS and then centrifuged at 550g for 10 minutes. The supernatant was aspirated and the cells were re-suspended in 50ml of PBS and the centrifugation step was repeated. The cells were re-suspended in 10ml of R5 medium and counted. Following this step, the T-cells were activated with CD3/CD28 beads (Life Technologies, UK). After counting the cells, the required amount of beads was removed (3:1 or 1:1 PBMC:beads) and placed in a 15ml Falcon tube. The beads were washed three times with wash buffer consisting of 1 part R5 medium mixed with 9 parts PBS. After each wash, the beads were recovered by placing the Falcon tube on a magnet (Dynal magnet, ThermoFisher Scientific, UK). The waste was aspirated using a vacuum

pump. After the final wash, the beads were re-suspended in R5 medium in the required volume in order to achieve a PBMC density of $3x10^6$ cells/ml.

2.2.5 Retroviral transduction of T-cells

Twenty-four hours after activation of the T-cells, IL-2 (Novartis, Switzerland) was added (100units/ml). On the same day, the HEK 293T VEC retroviral packaging cells were passaged by trypsinisation in order to reach 90% confluency by the next day. On the following day, 3ml of retrovirus containing supernatant was collected from the packaging cells and transferred to a non-tissue culture treated 6 well plate that had been pre-coated with RetroNectin (RN, Takara, Japan). For the preparation of the RN- coated plates, 200µg of RN was re-suspended in 12ml PBS. Two ml of the resulting solution was transferred using a Pasteur pipette to each well of a non-tissue culture plate (Sigma-Aldrich, U.S) and allowed to coat the well for at least 2 hours at room temperature or overnight at 4°C. Activated T-cells (contained within $1x10^6$ activated PBMC) were added next, together with IL-2 (100units/ml). Usually, 2 x 10^6 T-cells were transduced for each CAR T-cell construct. Expression of the CAR of interest by transduced T-cells was determined on day 5 and day 10 post activation by flow cytometry (described in section 0).

2.2.6 Culture of activated and CAR transduced T-cells

Following activation and/ or retroviral transduction, T-cells were cultured in R5 medium with additional supplementation of IL-2 (100u/ml). Fresh R5 medium and IL-2 were added to cell cultures every second day.

2.2.7 Viable T-cell count using trypan blue exclusion test

Assessment of T-cell count was performed at day 10 post transduction with the use of trypan blue exclusion test[313]. T-cells were stained with trypan blue (GE Healthcare, USA) and the viable cell number was determined manually with a haemocytometer. The total cell number was calculated by multiplying the cell number/ml and the total volume (ml) of T-cells.

2.2.8 Measurement of cytotoxic activity of MUC1-specific CAR T-cells by MTT assay

The *in vitro* cytotoxic activity of MUC1-specific CAR T-cells was investigated by performing co-cultivation assays. In order to perform these experiments, CAR T-cells were expanded for 10 days post transduction and were then added to confluent breast cancer cell monolayers as per the scheme indicated in Table 2.7. The cytotoxic potential of the anti-MUC1 CAR T-cells was investigated against three breast cancer cell lines expressing different levels of MUC1. These consisted of T-47D (MUC+++), MDA-MB-468

(MUC1++) and ZR-75-1 (MUC1+) cell lines. All three signalling-intact MUC1 CARs (e.g. TAB28z, H28z and HDF28z) were included in these experiments, together with the matched truncated CARs (TABTr, HTr and HDFTr). Non-transduced cells were also added to the tumour monolayers in order to identify any non-specific T-cell activity. Each reaction was performed in triplicate in individual experiments.

Table 2.7: Co-cultivatation conditions used to examine cytotoxic activity of CAR T-cells against breast cancer cell lines. In both cases, the effector to target ratio was 4:1.

Size of cell-culture plate	Tumour cell number per well	T-cell number per well	Final volume per well
48-well	0.125×10^6	0.5×10^6	1ml
24-well	0.25×10^6	1×10^6	2ml

The cytotoxicity of CAR T-cells against individual breast cancer cell lines was measured using the MTT reduction assay. This asay allows for the measurement of cell viability based on cell metabolic activity and is based on the reduction of MTT[314]. MTT, or 3-(4,5-dimethylthiazol-2-yl)-2,5-diphenyltetrazolium bromide, is a tetrazolium salt and its reduction depends on the concentration of intracellular NADH and NADPH. Viable cells convert the yellow-coloured MTT dye into purple-coloured formazan crystals. Dead cells lose the ability to reduce MTT as they lack metabolic activity. Quantification of the formed formazan product is achieved by reading the absorbance, after its solubilisation[315].

Tumour cell destruction was measured at three different time points, namely 24 hours, 48 hours and 72 hours after the addition of CAR T-cells to the tumour monolayers. Triplicates of tumour cells alone (without the addition

of T-cells) served as control reactions. The results were analysed by normalizing the absorbance of each well to the mean of the absorbance of tumour cells alone.

At each of the time-points, the supernatant from the co-culture plates was aspirated and the wells were gently washed with PBS in order to remove residual T-cells from the tumour monolayers. Subsequently, 250µl (48-well plate) or 500µl (24-well plate) of 1/10 MTT dye (diluted in D10 medium) were added to each well and the plate was incubated in the cell incubator for 2 hours. The MTT dye (Sigma-Aldrich, USA) was aspirated and 300µl (48-well plate) or 500µl (24-well plate) of DMSO (VWR International, USA) was added to each well in order to re-suspend the formed formazan crystals. The absorbance was measured at a wavelength of 570nm with a FLUOstar Omega plate reader. Tumour cell viability was determined using the following formula:

$$\%\, cell\ viability = \left(\frac{average\ OD\ of\ co-culture\ reactions}{average\ OD\ of\ tumour\ cells\ alone}\right) * 100$$

2.2.9 Measurement of IFN-γ and IL-2 release by activated CAR T-cells

The production of IFN-γ and IL-2 by T-cells is an indication of whether they have undergone activation following contact with tumour cells. At 48 hours after establishment of the co-cultivation (described in Section 2.2.8), supernatant was harvested from each well in order to investigate the production of IFN-γ and IL-2 by sandwich enzyme-linked immunosorbent

assay (ELISA). The assays were performed by using the Human IFN-γ Ready-Set-Go kit (eBioscience, UK) and the Human IL-2 Ready-Set-Go kit (eBioscience, UK), according to the manufacturer's instructions. In summary, a 96-well plate was coated with the capture antibody and afterwards blocking buffer was added in order to prevent any non-specific binding. The samples were added to the plate, together with a series of dilutions of the IFN-γ or IL-2 standard, and any antigen present was bound by the capture antibody. An antigen-specific biotin-coated detection antibody was then added to the plate. Afterwards, avidin-conjugated horseradish peroxidase (HRP) was added to each well, which recognised the detection antibody. Finally, TMB (3,3',5,5'-Tetramethylbenzidine) substrate was added which was converted by HRP to a soluble blue product. The reaction was stopped by the addition of sulphuric acid and the absorbance was measured at 450nm with the FLUOstar Omega plate reader (BMG Labtech, UK). All optical density (OD) values were corrected by subtraction of background values generated using the medium alone control. A six-point standard curve was plotted using the serial two-fold diluted standard samples (top concentration 500pg/mL) and a line of best fit was generated by log transformation of the data, plotting concentration against OD. Cytokine concentrations contained within unknown samples were interpolated from the linear portion of the standard curve and were corrected for dilution as appropriate.

2.2.10 Flow-cytometry analysis

Flow cytometry analysis was performed as detailed below using the Becton Dickinson (BD) LSR Fortessa cytometer with DIVA software. The results were analysed using FlowJo software (version 10).

2.2.10.1 Investigation of expression of cell-surface molecules

2.2.10.1.1 Protocol

In order to investigate cell-surface expression of different molecules, a universal protocol was used. The amounts of antibodies/peptides that were used for staining reactions are specified in the sections below.

1. Cells (0.5-1 x 10^6) cells were added into FACS tubes (12x75mm round-bottom).
2. The cells were washed with 2ml PBS and were centrifuged at 400g for 5 minutes.
3. The cell pellet was re-suspended in 100µl PBS and the primary antibody or directly-conjugated antibody was added to each sample. In some cases, an isotype control was added instead of the primary antibody, which served as the negative-control in order to define the gate for the positively-stained populations.

   N.B: when Fc block was used, this was added 10 minutes prior to the addition of the primary antibody.
4. The samples were incubated for 30 minutes on ice.

5. Step 2 was repeated.
6. The cell pellet was either:
    a. Re-suspended in 100 µl and then the secondary antibody was added (in the case of non-conjugated primary antibodies).
    b. Re-suspended in 300 µl and the samples were analysed by flow cytometry (in the case of conjugated primary antibodies).
7. In the case of a., the cells were incubated for 30 minutes on ice in dark conditions.
8. The samples were washed with 2ml PBS and centrifuged for 5 minutes at 400g.
9. The cell pellet was re-suspended in 300µl and the samples were analysed using the flow cytometer.

2.2.10.1.2 Primary antibodies

The primary antibodies used in the flow-cytometry experiments are listed in the table below. The table also includes additional details, such as the reactivity, host species, isotype and the immunogen which was used for the production of the antibody.

Other details, such as which the secondary antibodies and isotype controls are used in each experiment, the amount of each antibody used and the catalogue number, are mentioned in the following sections.

Table 2.8: Primary antibodies used in the flow-cytometry assays.

Name	Specificity	Species reactivity	Immunogen	Recognised epitope	Clonality	Clone number	Host species	Isotype	Conjugation	References
MUC1 24mer peptide (APPAHGVTSAPDTRP APGSTAPP)		Human	-	-	-	-	-	-	biotin	[295]
HMFG1	MUC1	Human	Intact mucin from human milk fat globule (HMFG)	PDTR region of MUC1; strong reactivity with normal epithelial cells	Monoclonal	-	Mouse BALB/c	IgG1, κ'	-	[316–319]
HMFG2	MUC1	Human	Intact mucin from HMFG and mammary epithelial cells	PDTR region of MUC1; strong reactivity with tumour-associated MUC1; some reactivity with resting and strong reactivity with lactating breast	Monoclonal	-	Mouse BALB/c	IgG1, κ'	-	[316–319]
SM3	MUC1	Human	Stripped HMFG	PDTR region of MUC1; strong reactivity with tumour-associated MUC1; little to no reaction with benign or non-malignant cells	Monoclonal	-	Mouse BALB/c	IgG1, κ'	-	[320]
5E5	MUC1	Human	Fully glycosylated MUC1 Tn peptide (60-mer)	MUC1 Tn; GSTA region of MUC1 (HGVTSAPDTRPAPGS TAPPA). Minimal to no reactivity with benign or normal epithelial cells	Monoclonal	-	Mouse BALB/c	IgG1, κ'	-	[321]
CD3	CD3	Human	Human infant themocytes and peripheral blood lymphocytes from a Sezary syndrome donor	CD3 ε-chain (both extracellular and intracellular)	Monoclonal	UCHT1	Mouse BALB/c	IgG1, κ'	FITC	[322]
CD8	CD8	Human	Human peripheral blood lymphocytes	CD8 α-chain	Monoclonal	SK1	Mouse BALB/c	IgG1, κ'	PE-Cy7	[323]
CD45RO	CD45RO	Human	IL-2-dependent human T-cell line (CA1)	CD45 (180kDa isoform)	Monoclonal	UCHL1	Mouse BALB/c	IgG2α, κ'	PE	[324]
CCR7	CCR7	Human	CCR7-transfected human cell line	CCR7	Monoclonal	150503	Mouse	IgG2α	APC	-

PD-1 (CD279)	PD-1	Human	L-cells transfected with human CD279	PD-1	Monoclonal	MIH4	Mouse	IgG1, κ'	PE	-
TIM-3 (CD366)	TIM-3	Human	Recombinant human TIM-3	TIM-3	Monoclonal	F38-2E2	Mouse	IgG1, κ'	APC	-
CTLA-4 (CD152)	CTLA-4	Human	Human CTLA-4 extracellular domain fused with Fc portion of human IgG1	Extracellular domain of CTLA-4	Monoclonal	L3D10	Mouse BALB/c	IgG1, κ'	PE	[325]

2.2.10.1.3 Expression of MUC1-specific CARs

Cell surface expression of MUC1-specific test and control CARs in transduced human T-cells was determined at day 5 and day 10 post transduction. Cells were stained with a MUC1-derived 24mer peptide that contains the HMFG2 and TAB004 epitope and with the following sequence: biotinyl (TAPPAHGVTSAPDTRPAPGSTAPP). Bound MUC1 peptide was detected by the addition of streptavidin-PE (Life Technologies, UK) (Table 2.9)[295]. The CAR-positive population was defined by staining non-transduced T-cells in exactly the same way as the transduced T-cell populations.

The expression of MUC1-specific CARs in retroviral packaging cells was determined in a similar way. Parental (non-transduced) cells were used as negative control.

Table 2.9: Detection of cell surface expression of MUC1-specific CARs. This table lists the antibodies/peptides used for the detection of CAR expresion, the quantity used per sample and the catalogue number of each reagent.

Peptide/antibody	Amount per sample	Catalogue number	Company
Biotinylated MUC1 24mer peptide	7.5µg/ml	-	NeoMPS, US
Streptavidin-PE	5µg/ml	S866	Life Technologies, USA

2.2.10.1.4 MUC1 expression on breast cancer cell lines

Surface expression of MUC1 on breast cancer cell lines was determined by stainingthe cells with a biotinylated HMFG2 antibody followed by streptavidin-PE. Mouse IgG1-biotinylated (κ') antibody was used as an

isotype control (Table 2.10). Incubations were carried out in the dark and on ice for approximately 20 minutes. Samples were washed twice in PBS after each incubation step.

Table 2.10: Detection of expression of MUC1 on breast cancer cell lines. This table lists the antibodies used for the MUC1 detection, the amount of each of antibody added per sample and the catalogue number of each reagent. **As per manufacturer's protocol.*

Antibody	Amount per sample	Catalogue number	Company
HMFG2-biotinylated antibody	2µg/ml	-	-
Mouse IgG1-biotinylated (κ') isotype control	20µl*	555747	BD Pharmingen, USA
Streptavidin-PE	5µg/ml	S866	Life Technologies, USA

2.2.10.1.5 MUC1 expression on T-cells

Surface expression of MUC1 on T-cells was determined at different time points post-activation using HMFG2 biotinylated antibody followed by streptavidin-PE. Additionally, three other biotinylated MUC1-specific antibodies were used for comparison purposes, namely HMFG1, SM3 and 5E5, followed by streptavidin-PE. It should be noted that human Fc block was added to the samples prior the addition of the primary antibodies (Table 2.11). The MUC1-specific antibodies were kindly provided as a gift by Professor Joy Burchell (King's College London, UK). Cells stained with mouse IgG1-biotinylated isotype control followed by streptavidin-PE were used as negative control.

Table 2.11: Expression of MUC1 on T-cells. This table lists the antibodies used, the amount added per sample and the catalogue number. **As per manufacturer's protocol.*

Antibody	Amount per sample	Catalogue number	Company
FcR block (TruStain FcX)	5µl*	422302	BioLegend, UK
HMFG2-biotinylated antibody	2µg/ml	-	-
HMFG1-biotinylated antibody	2µg/ml	-	-
SM3-biotinylated antibody	2µg/ml	-	-
5E5-biotinylated antibody	2µg/ml	-	-
Mouse IgG1-biotinylated (κ') isotype control	20µl*	555747	BD Pharmingen, USA
Streptavidin-PE	5µg/ml	S866	Life Technologies, USA

2.2.10.1.6 MUC1 expression on $CD4^+$ and $CD8^+$ T-cells

Surface expression of MUC1 on $CD4^+$ and $CD8^+$ T-cell populations was investigated at day 5 post T-cell activation. In order to define the CD4 and CD8 T-cell populations, mouse anti-human CD3-FITC and CD8-PECy7 directly-conjugated antibodies were used (Table 2.12). To generate negative control samples, cells were stained with biotinylated mouse IgG1(κ') (isotype control) instead of HMFG2.

Anti-mouse IgG compensation beads (CompBeads, BD) were stained accordingly in order to set up the compensation.

Table 2.12: Surface expression of MUC1 on CD4 and CD8 T-cells. This table lists the antibodies used for the detection of MUC1 on CD4 and CD8 T-cells, the amount of each antibody added per sample and the catalogue number. **As per manufacturer's protocol.*

Antibody	Amount per sample	Catalogue number	Company
FcR block (TruStain FcX)	5µl*	422302	BioLegend, UK
HMFG2-biotinylated antibody	2µg/ml	-	-
Mouse IgG1-biotinylated (κ') isotype control	20µl*	555747	BD Pharmingen, USA
Streptavidin-PE	5µg/ml	S866	Life Technologies, USA
CD3-FITC	20µl*	555332	BD Pharmingen, USA
CD8-PECy7	5µl*	344712	BioLegend, UK

2.2.10.1.7 T-cell differentiation

Stage of differentiation of $CD4^+$ and $CD8^+$ CAR T-cells was determined at day 10 post T-cell transduction by staining the cells with anti-human CD3-FITC, CD8-PECy7, CD45RO-PE and CCR7-APC antibodies (Table 2.13).

Fluorescence minus one (FMO) controls were used to define positive and negative populations. Stained anti-mouse IgG compensation beads were also used to achieve correct compensation settings.

Table 2.13: Determining stage of differentation of CD4 and CD8 T-cells. This table lists the antibodies used, the amount added per sample and the catalogue number. **As per manufacturer's protocol.*

Antibody	Amount per sample	Catalogue number	Company
CD3-FITC	20µl*	555332	BD Pharmingen, USA
CD8-PECy7	5µl*	344712	BioLegend, UK
CD45RO-PE	20µl*	555493	BD Pharmingen, USA
CCR7-APC	10µl*	FAB197A	BD Pharmingen, USA

2.2.10.1.8 Expression of exhaustion markers

The expression of three exhaustion markers, PD-1, TIM-3 and CTLA-4 was investigated on CD4 and CD8 T-cells with the use of anti-human CD3-FITC, CD8-PECy7, PD-1-PE, TIM-3-APC and CTLA-4 PE antibodies.

Table 2.14: Expression of PD-1, TIM-3 and CTLA-4. This table lists the antibodies used, the amount added per sample and the catalogue number. **As per manufacturer's protocol.*

Antibody	Amount per sample	Catalogue number	Company
CD3-FITC	20µl*	555332	BD Pharmingen, USA
CD8-PECy7	5µl*	344712	BioLegend, UK
PD-1-PE	20µl*	557946	BD Pharmingen, USA
CTLA-4-PE	20µl*	L3D10	BioLegend, UK
TIM-3 APC	5µl*	345012	BioLegend, UK

As previously stated in section 2.2.10.1.7, FMO controls were used in order to deine the positive and negative-stained populations and compensation was set up using appropriately stained anti-mouse compensation beads.

2.2.10.1.9 Detection of viable human T-cells in mouse spleens and peritoneal fluid of mice treated with CAR T-cells

The percentage of human viable T-cells in peritoneal fluid and in spleen harvested by mice was investigated by staining the samples with mouse anti-human CD3-FITC conjugated antibody. The cells were incubated with mouse Fc block prior to staining. In order to define live cells, 7AA-D viability dye solution was added to the samples prior to the acquirement of data and

incubated in the dark for 5min. The samples were not washed after the addition of 7AA-D dye.

Cells incubated previously with DMSO and stained with 7AA-D were used as positive to control in order to define the gate of live/dead cells in the dot plots. Additionally, γδ T-cells stained with IgG1-FITC and 7AAD were used as negative control in order to define the gate for the CD3-positive population. γδ T-cells stained with both CD3-FITC and 7AA-D were used as positive control. Compensation was set up accordingly by using single stained samples.

Table 2.15: Detection of human viable T-cells in peritoneal fluid and in spleens post treatment of mice with CAR T-cells. This table lists the antibodies used, the amount added per sample and the catalogue number. **As per manufacturer's protocol.*

Antibody	Amount per sample	Catalogue number	Company
CD3-FITC	20µl*	555332	BD Pharmingen, USA
Mouse IgG1-FITC (κ') isotype control	20µl*	555909	BD Pharmingen, USA
7AA-D	5µl*	420404	BioLegend, UK

2.2.10.2 Maintenance and calibration of flow cytometer

The BD LSR Fortessa cytometer was cleaned thoroughly before and after each use with FACS Rinse maintenance solution (BD, USA), FACS Clean decontamination solution (BD, USA) and with distilled water in order to maintain the flow-cytometer's fluidic system.

A quality control procedure was applied daily to ensure that the flow cytometer's performance is optimal. For this purpose, BD FACSDiva™

Cytometer Setup and Tracking (CS&T) Research Beads were used (BD, USA)[326].

2.3 Breast cancer *in vivo* model

The animal studies were conducted under the Project Licence of Professor Joy Burchell (PPL No. 77/7794) and under my Personal Licence (PIL No. IA5692FB4). All experimental procedures were performed in accordance with the UK Home Office guidelines.

2.3.1 NOD *scid* gamma (NSG) mice

Female NOD.Cg-*Prkdc*^{scid} *IL-2rg*^{tm1Wjl}/SzJ mice, commonly known as NOD *scid* gamma (NSG), were used in all the *in vivo* experimental studies mentioned in this project[327]. These mice, originally developed at the Jackson Laboratory by Dr Leonard Shultz, carry two mutations which result in severe immunodeficiency. The first mutation is in the DNA repair complex named as Prkdc, which causes severe combined immunodeficiency (SCID) accompanied by lack of B and T-cell populations, owing to the failure of V(D)J recombination. The second mutation is in the IL-2 receptor common gamma chain, which results in deficient cytokine signalling and consequently in reduced NK cell numbers and impaired NK cell cytotoxic activity[327,328]. Owing to the NOD genetic background, macrophages and dendritic cells are also defective in these mice.

2.3.2 Generation of luciferase-positive breast cancer cells

Breast cancer tumour cells were injected either subcutaneously in close proximity to the mammary fat pad or in the peritoneal cavity (i.p) of NSG mice and the tumour growth was measured regularly with bioluminescence imaging (BLI) or with calliper measurements.

2.3.2.1 Retroviral transduction of breast cancer cell lines with ffluc_tdTomato

In order to allow for bioluminescence detection, T-47D and MDA-MB-468 cells were retrovirally transduced to express firefly luciferase (ffluc). Tandem dimer (td)Tomato fluorescent protein was co-expressed with firefly luciferase in order to be able to determine the transduction efficiency (Figure 2.7)[329]. PG-13 retroviral packaging cells expressing the SFG ffluc_tdTomato retroviral vector were used for this purpose. The ffluc-tdTomato-positive PG13 packaging cells were previously made by colleagues.

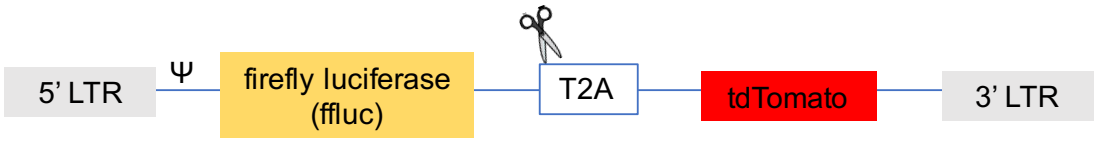

Figure 2.7: Schematic represantation of the SFG firefly luciferase_tdTomato retroviral vector. Firefly luciferase (ffluc) and tdTomato fluorescent protein were stoichiometrically co-expressed in an SFG retroviral vector, which contained the 5' and 3' long terminal repeats (LTR) and the psi (ψ) packaging signal. The *Thosea Asigna*-derived ribosomal skip 2A peptide (T2A) was inserted between the ffluc and tdTomato in order to achieve equimolar expression of the two proteins[330].

Fresh supernatant harvested from confluent PG-13 cells was filtered through a 0.45µm pore-size filter and was added to under-confluent tumour cells. This process was repeated daily until the tumour cells were highly positive for the ffluc_tdTomato construct (see section 2.2.2.1 for details of the protocol).

2.3.2.2 Validation of expression of ffluc and tdTomato in breast cancer cell lines

The transduction efficiency of the SFG ffluc_tdTomato construct was determined by flow-cytometry by detecting the tdTomato fluorescent protein (max. excitation 554nm).

In addition, the expression of ffluc was validated by performing an *in vitro* luciferase reporter assay. In this assay, $1x10^5$ cells were diluted 10-fold and 150µg/ml D-luciferin (Regis Technologies, USA) was added to each well. Emitted luminescence was measured with the FLUOstar Omega plate reader (BMG Labtech, UK).

2.3.3 Establishing breast cancer xenograft mouse model

As mentioned above, ffluc_tdTomato expressing tumour cells were injected either in the peritoneal cavity (i.p) of female NSG mice or subcutaneously in close proximity to mammary fat pad. The number of tumour cells injected in each experiment are specified in the sections below.

2.3.3.1 Subcutaneous administration of tumour cells

2.3.3.1.1 Preparation of the tumour-cells prior to subcutaneous injection

To establish tumour models, female NSG mice received a pre-specified tumour cell dose, as indicated in Table 2.16. The tumour cells were trypsinized, counted and the required number of tumour cells was acquired. The cells were re-suspended in 400µl cold PBS + matrigel (PBS: matrigel 1:1) per mouse. The mixture was kept on ice until it was injected into the mice.

Table 2.16: Tumour cell injection in the mammary fat pad of female NSG mice. The different cell doses of T-47D and MDA-MB-468 injected are listed in this table. Three mice per group were allocated in each cell dose group.

Cell line	Group A	Group B	Group C
T-47D	$0.5x10^6$	$2x10^6$	$5x10^6$
MDA-MB-468	$0.1x10^6$	$0.5x10^6$	$2x10^6$

2.3.3.1.2 Injection of tumour cells subcutaneously

The mouse was shaved and ethanol was spread across the right side of the abdomen in order to visualise the fatty tissue of the mammary gland. The mouse was immobilized by the scruff method and the cells (400µl PBS-matrigel) were injected subcutaneously in close proximity to the mammary fat pad. A 27G sterile needle (BD Microlance, USA) placed on a 0.5ml syringe (Terumo, Japan) was used for the injection. The cells were injected subcutaneously, proximal to the mammary fat pad.

Tumour growth was measured using a calliper tool and the tumour volume was calculated using the ellipsoid volume formula[331] as follows:

$$tumour\ volume = \left(\frac{width * width * length}{2}\right)$$

2.3.3.2 Intra-peritoneal injection of tumour cells

2.3.3.2.1 Preparation of the tumour-cells prior to i.p injection

As indicated previously, female NSG mice received a pre-specified tumour cell dose. The tumour cells were trypsinized, counted and the required number of tumour cells was acquired (Table 2.16). The cells were re-suspended in 200µl cold PBS (per mouse) and were kept on ice until their injection into the mice.

Table 2.17: Tumour cell injection in the peritoneal cavity of female NSG mice. The different cell doses of T-47D and MDA-MB-468 injected are listed in this table. Three mice per group were allocated in each cell dose group.

Cell line	Group A	Group B	Group C	Group D
T-47D	$0.5x10^6$	$2x10^6$	$5x10^6$	$10x10^6$
MDA-MB-468	$0.5x10^6$	$2x10^6$	$0.5x10^6$	-

2.3.3.2.2 Intraperitoneal injection of tumour cells

A sterile 27G needle was placed on a 1ml syringe (BD, USA) and 200µl of cells in PBS was drawn up, removing any air bubbles. The mouse was restrained by the scruff method and was held in a way that its head was tilted back. The needle was inserted either to the left or right lower quadrant of the animal's abdomen and the cells were injected.

2.3.4 Intraperitoneal injection of T-cells

In the two therapeutic experiments described in this thesis, mice with established tumours were treated either with MUC1-specific CAR T-cells or with non-transduced T-cells or PBS. The treatment was injected i.p, in a process similar to that described in Section 2.3.3.2. The cell dose injected is described for the individual experiments. Five to six mice were allocated to each treatment group.

2.3.5 Bio-luminescence (BLI) imaging

To quantify tumour growth using bio-luminescence imaging, mice were injected i.p with D-luciferin (150mg/kg; Regis Technologies, USA) and were imaged under 2% isoflurane anaesthesia, 12 minutes post injection. The image was acquired with the use of the IVIS Lumina platform (PerkinElmer, USA). Data were analysed using Living Image software (PerkinElmer, USA). The mice were imaged by using a 25cm field of view (FOV), with medium binning factor (=2) and auto-exposure.

2.3.6 Persistence of CAR T-cells in *in vivo* mouse model

2.3.6.1 Peritoneal lavage

In order to harvest the T-cells from the peritoneal cavity post euthanasia of the mice, the technique of peritoneal lavage was used. For this

purpose, 5ml of cold PBS was injected in the peritoneal cavity of each mouse. A 27G sterile needle (BD Microlance, USA) placed on a 5ml syringe (Terumo, Japan) was used for the injection. Post PBS injection, the peritoneum was gently massaged. The mouse was sprayed with ethanol and a small incision was made in the inner skin of the peritoneum. The fluid was collected in a 50ml cold Falcon tube using a Pasteur pipette and was placed on ice.

In order to prepare the samples for flow-cytometry analysis, 10ml of cold PBS was added in each sample and was centrifuged for 5min at 400g. The supernatant was aspirated and the pellet was re-suspended in 10ml cold PBS. This was followed by a centrifuge step (5 min, 400g). The supernatant was aspirated and the pellet was re-suspended in 500µl and placed on FACS tubes. These were kept on ice until the initiation of the staining protocol (2.2.10.1.9).

2.3.6.2 Harvesting of spleens

Upon euthanasia of the mouse, sterile scissors and forceps were used in order to make an incision across the peritoneum. The spleen was harvested and placed in a 5ml tube containing 3ml of cold PBS. The sample was placed on ice until further processing.

Prior to flow-cytometry analysis, the spleens were mechanically dissociated and single-cell suspensions were prepared. The cell suspension was transferred to a 15ml Falcon tube and 10ml of cold PBS was added. The cells were pelleted by centrifugation at 500g for 5min. The supernatant was aspirated and the pellet was re-suspended in 5ml of 1x red blood cell (RBC) lysis buffer (eBiosciences, USA). The cell suspension was incubated with the

lysis buffer for 5min. Post incubation, the cells were centrifuged at 500g for 5min and the supernatant was aspirated. The pellet was re-suspended in 5ml of PBS and centrifuged at 400g for 5 min. The supernatant was aspirated, the cells were re-suspended in 500µl and transferred to a FACS tube. The samples were kept on ice until initiation of the staining protocol (2.2.10.1.9).

Chapter 3: *In vitro* characterization of MUC1-specific CAR T-cells

3.1 Introduction

3.1.1 MUC1-adoptive T-cell therapy

In adoptive T-cell therapy, patient-derived PBMCs are isolated and different cell populations, such as T-cells or dendritic cells, are expanded. These can be further manipulated in distinct ways. One strategy includes the activation of CTLs or DCs by presenting to them tumour-associated peptides, such as those derived from MUC1[332]. The activated cell populations are expanded *ex vivo* and are then adoptively transferred back to the patient. These activated cells can either specifically eliminate tumour cells, in the case of CTLs, or enhance anti-tumour immune responses, in the case of antigen-loaded DCs[333].

Several clinical trials have been performed in which the effectiveness of CTLs or pulsed dendritic cells has been explored. In some cases, the combination of both approaches was shown to has some benefit in the patients' outcome[334]. In one combinatorial study, Kondo *et al*. treated 20 patients with unresectable or recurrent pancreatic cancer with both MUC1-pulsed dendritic cells and activated CTLs. Based on the results, one patient with metastatic disease showed complete response and four patients presented stable disease[334].

In another approach, patient-derived T-cells are isolated and engineered to express MUC1-specific CARs on their surface. Few research groups have engineered MUC1-specific CAR T-cells and have investigated their anti-tumour activity using pre-clinical *in vitro* and *in vivo* models. Wilkie *et al.*

developed various versions of a MUC1-specific CAR, as published in a study in 2008[295]. In this paper, a 3rd generation MUC1-specific CAR named HOX showed the most promising efficacy. This CAR consists of a binding domain based on the HMFG2 antibody and it signals via CD3ζ, CD28 and OX-40. Additionally, this CAR has incorporated a longer hinge (IgD), which provides enhanced flexibility to the binding domain of the CAR. Mice bearing MUC1-positive tumours showed delayed tumour growth after treatment with HOX-engineered CAR T-cells[295,335]. In a novel subsequent approach, Wilkie *et al.* co-expressed an anti-ErbB2 CAR (signals via CD3ζ alone) together with a MUC1-specific chimeric co-stimulatory receptor (containing CD28 alone). Their results showed that both antigens were required in order to achieve maximal tumour cell cytotoxicity and T-cell activation[269]. More recently, Posey *et al.* showed control of tumour growth in leukaemia and pancreatic cell xenograft models using a 2nd generation MUC1-specific CAR[336,337]. The latter contained an scFv based on 5E5 MUC1-Tn specific antibody (refer to section 1.2.3.2)[336,337].

Clinical testing of MUC1 specific CAR T-cells has been limited to date. The efficacy of two different SM3-based MUC1-specific CAR T-cells has been investigated in a Phase I clinical trial, although data from only a single patient has been reported as yet[338]. One set of CAR T-cells contained an SM3-based CAR co-expressed with IL-12. The second set contained a CAR with a modified SM3 scFv to achieve increased binding of the CAR to MUC1. The latter lacked co-expression of IL-12. In this trial, these two types of MUC1-specific CAR T-cells were injected using the intratumoral route in two different lesions in a patient with metastatic seminal vesicle malignancy. Based on a

published case report, the lesion treated with the modified-SM3 CAR T-cells showed significant tumour necrosis while no difference was observed in the lesion treated with the SM3-IL12 CAR[338].

Four other clinical trials are currently recruiting patients in order to test MUC1-specific CARs in patients with different types of malignancy. Distinct strategies are being evaluated. In two Phase I/II clinical trials (NCT02617134 and NCT02587689), the effectiveness and safety of MUC1-redirected CAR T-cells is being investigated in patients with solid malignancies[339,340]. In the NCT02839954 trial, the efficacy and safety of NK cells transduced with a MUC1 CAR is being evaluated[341]. Lastly, in a Phase I/II clinical trial (NCT03179007) patients with an advanced solid tumour burden are being treated with MUC1 CAR T-cells that are engineered to secrete PD-1 and CTLA-4 checkpoint inhibitors[342].

3.1.2 Aim

The aim of the work presented in this chapter was to undertake *in vitro* characterization of a newly developed MUC1-specific CAR, named TAB28z. Throughout this project, this CAR has been compared with two previously developed CARs, named H28z and HDF28z. The *in vitro* characterization of these CAR molecules included the investigation of (i) their binding properties to different TA-MUC1 glycans, (ii) their cytotoxic activity against a panel of breast cancer lines and (iii) measurement of their ability to produce pro-inflammatory cytokines (IFN-γ and IL-2), in a MUC1-dependent manner.

3.2 Results

3.2.1 Expression of MUC1 in human breast cancer cell lines

The first step undertaken was to investigate the expression of tumour-associated (TA) MUC1 in a panel of human breast cancer cell lines using flow-cytometry (see Table 2.5 for the characteristics of the breast cancer cell lines tested). Cells were stained with the HMFG2 antibody, which detects several tumour-associated MUC1 glycoforms, including those decorated with T, Tn, sialyl T and sialyl Tn. This analysis demonstrated a broad range of cell surface MUC1 expression in these cells lines. High MUC1 expression was detected on T-47D and BT-20 cells. By contrast, MDA-MB-468 and MCF7 showed intermediate levels of expression while ZR-75 had low levels of MUC1 (Figure 3.1). No MUC1 expression was detected on the surface of MDA-MB-231.

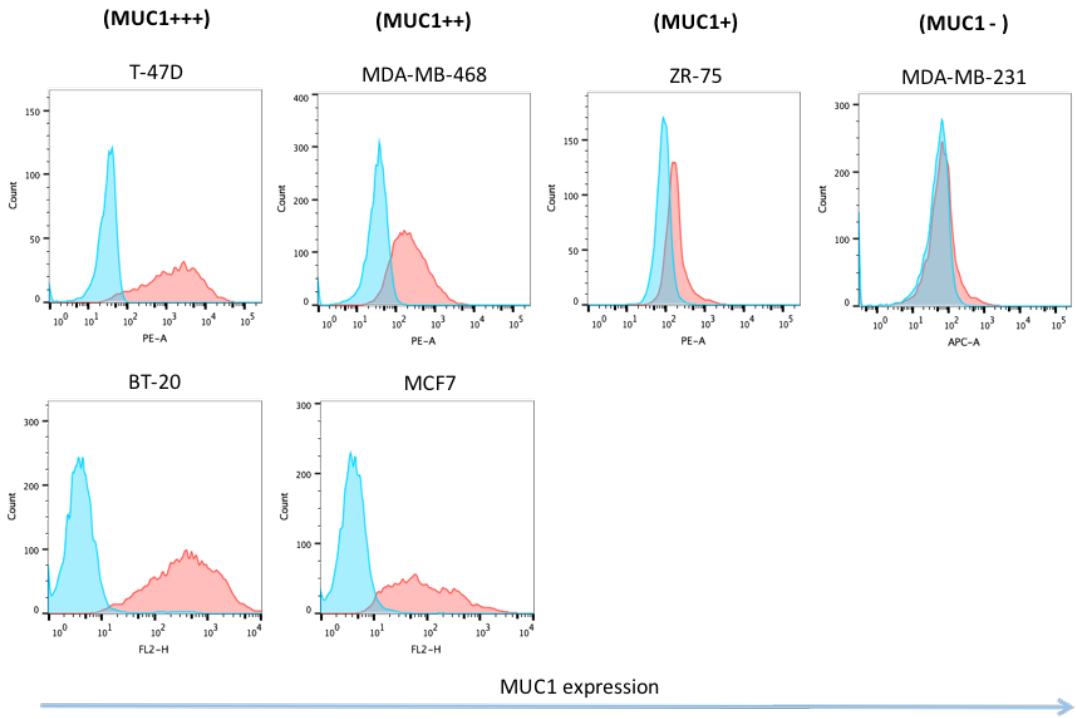

Figure 3.1: Expression of MUC1 in a panel of human breast cancer cell lines. Cell surface expression of the MUC1 mucin was determined in T-47D, BT-20, MDA-MB-468, MCF7, ZR-75 and MDA-MB-231 cell lines by flow cytometry. Herein histogram overlays are represented. The detection of MUC1 was achieved using HMFG2 biotinylated antibody followed by streptavidin PE (red histogram), while biotinylated IgG1, stained in the same way, was used as isotype control (blue histogram). Similar results were obtained in three independent replicate experiments.

3.2.2 Investigation of the activity of MUC1-specific CAR T-cells *in vitro*

As it has been stated in the Hypothesis of the Research Project, I set out to compare the anti-tumour activity of TAB28z CAR T-cells with that of T-cells engineered to express two other MUC1-specific CARs named H28z and HDF28z, which have been previously developed by colleagues in our research group. All three CARs are of second generation design since they contain a fused CD28 and CD3ζ endodomain[216]. Three additional non-

signalling anti-MUC1 CARs were included in the experiments mentioned below, as negative controls. In these control CARs, the endodomain contains only the membrane three proximal amino acids from CD28, thereby abrogating all signalling capacity. These control CARs, named TABTr, HTr and HDFTr respectively, contain an identical ecto- and transmembrane domain to that present in the corresponding signalling CARs (TAB28z, H28z and HDF28z respectively). The TABTr and HTr retroviral constructs were newly engineered for the purpose of this study, while HDFTr had previously been generated by a colleague[295].

3.2.2.1 Construction of TABTr and HTr retroviral plasmids

TABTr and HTr DNA plasmids were generated by molecular cloning as previously described (see section 2.1.2.2). Upon completion, the DNA plasmids were validated by diagnostic restriction digestion. Both TABTr and HTr DNA plasmids gave the expected pattern of fragments, confirming that the cloning was successful (Figure 3.2).

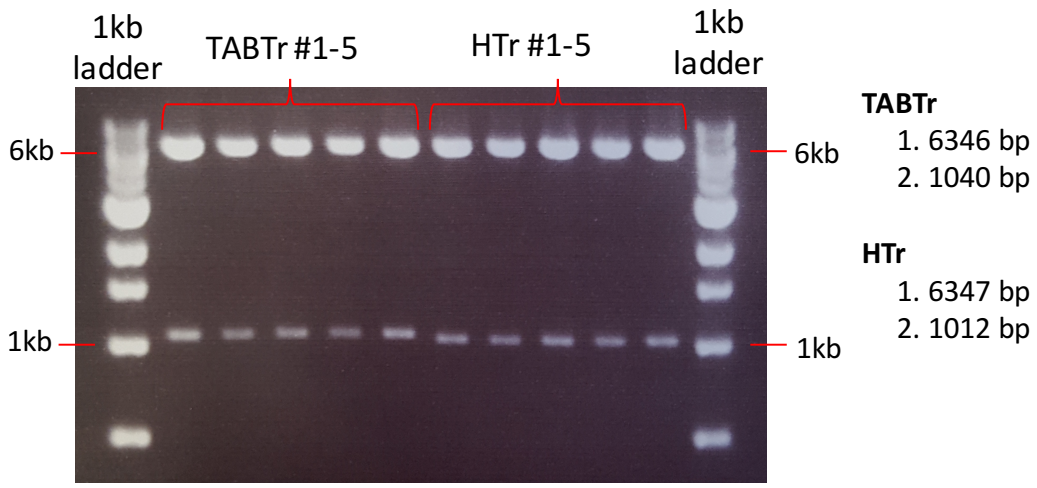

Figure 3.2: Screening digestion of TABTr and HTr plasmids. The TABTr and HTr retroviral plasmids were generated by molecular cloning. Plasmid DNA was extracted from five bacterial clones for each of the constructs and was digested with NcoI and XhoI endonucleases. The resultant DNA fragments were separated by electrophoresis on a 1% agarose gel. Digestion of plasmid DNA from all candidate TABTr bacterial clones (#1-5) resulted in the expected fragments, specifically a fragment of 6346kb (vector backbone) and a second smaller fragment of 1040kb (insert). Similarly, digestion of #1-5 candidate HTr plasmids revealed the expected two bands, the sizes of which were 6347kb (vector backbone) and 1012kb (insert).

3.2.2.2 Generation of stable retroviral packaging cell lines expressing the CAR transgenes

The next step undertaken before testing the functionality of these MUC1-specific CARs in primary T-cells was to generate stable retroviral packaging cell lines that could be used to deliver the CAR transgene to human T-cells. First, PG-13 retroviral packaging cells were transduced in order to produce retrovirus-containing supernatant encoding for the TAB28z CAR transgene. This was achieved by following a two-step procedure, described in Materials and Methods section (section 2.2.2.1). H28z, HDF28z and HDFTr PG-13 cells had been made by previous lab members. In each case, viral supernatant produced by the PG-13 cells was further used to transduce HEK

293T VEC packaging cells. Based on the literature, HEK 293T VEC are expected to produce high viral titres thus resulting in higher T-cell transduction efficiency (Appendix)[305,307]. TABTr and HTr HEK 293T VEC packaging cells were generated directly using the triple transfection method (section 2.2.2.3). All six MUC1-specific CARs/ truncated controls were highly expressed in the packaging cells, with expression levels ranging between 78% to 93.5% (Figure 3.3).

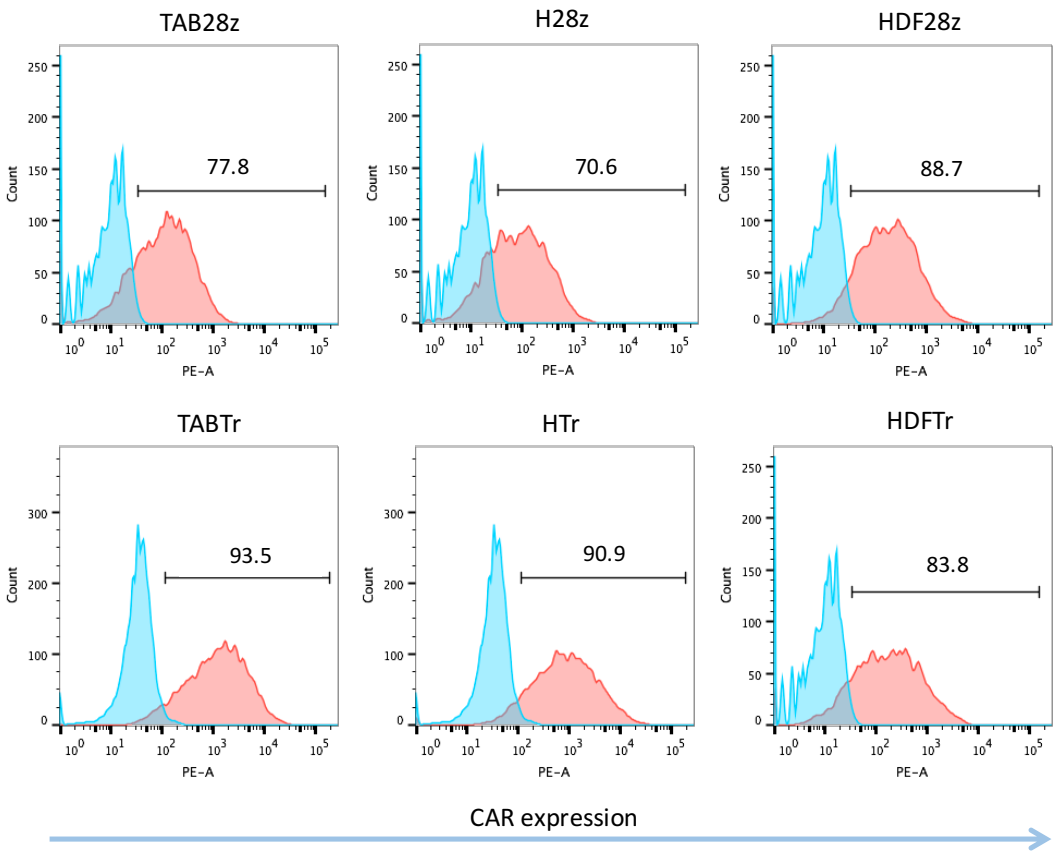

Figure 3.3: Expression of MUC1-specific CARs and matched truncated controls in HEK 293T VEC packaging cells. HEK 293T VEC packaging cells were transduced to express the MUC1-specific CARs, either using viral supernatant from PG-13 cells (TAB28z, H28z, HDF28z, HDFTr) or by triple transfection (TABTr, HTr). Retroviral particles produced by the HEK 293T VEC cells were pseudotyped with the RD114 envelope (TAB28z, H28z, HDF28z, HDFTr) or by the gibbon ape leukaemia virus envelope (GALV - TABTr, HTr). Representative histogram plots show the cell surface expression of CARs following flow cytometry analysis. Detection of the CARs was achieved using a human MUC1-derived 24mer biotinylated peptide (encompassing 1.2 MUC1 tandem repeats and containing the epitope recognised by all CARs), followed by streptavidin PE (red histograms). Non-transduced HEK 293T VEC cells were stained in the same way and were used as negative control (blue histograms). Data are representative of three independent replicate experiments, all of which yielded similar results.

3.2.2.3 Specificity of MUC1-specific CARs to tumour-associated MUC1-glycoforms

Tumour-associated MUC1 is characterized by aberrant glycosylation and specifically by the presentation of truncated O-glycan chains[343] (section

1.2). These core-1 or unglycosylated glycans are predominantly expressed on cancer cells and include the glycans T, Tn and their sialylated forms, ST and STn[343]. As previously stated, the TAB28z CAR contains an scFv binding domain derived from the TAB004 MUC1-specific antibody while the H28z and HDF28z CARs have an scFv derived from the HMFG2 antibody (also preferentially binds to tumour-associated glycoforms of MUC1)[284,295]. A binding assay was performed using HEK 293T VEC retroviral packaging cell lines for H28z and TAB28z to identify and characterize the binding preference of these CARs to MUC1 carrying the four tumour-associated glycans, T, ST, Tn and STn. Expression of these CARs by the retroviral packaging cells is shown in Figure 3.3. To undertake this study, recombinant human MUC1 ectodomain (containing 32 tandem repeats)-mouse IgG1 fusion proteins decorated with each of these glycans were used[310,312]. Binding was detected by the addition of PE-conjugated goat anti-mouse IgG. Owing to limited availability of these reagents, only a single experiment could be undertaken. While only limited conclusions can be drawn as a result, these data show that both TAB28z and H28z bound to all four tumour-associated MUC1 glycoforms (Figure 3.4). Differences in relative binding to MUC1-Tn and MUC1-ST and sialylated versus non-sialylated glycoforms would require further replicates to confirm.

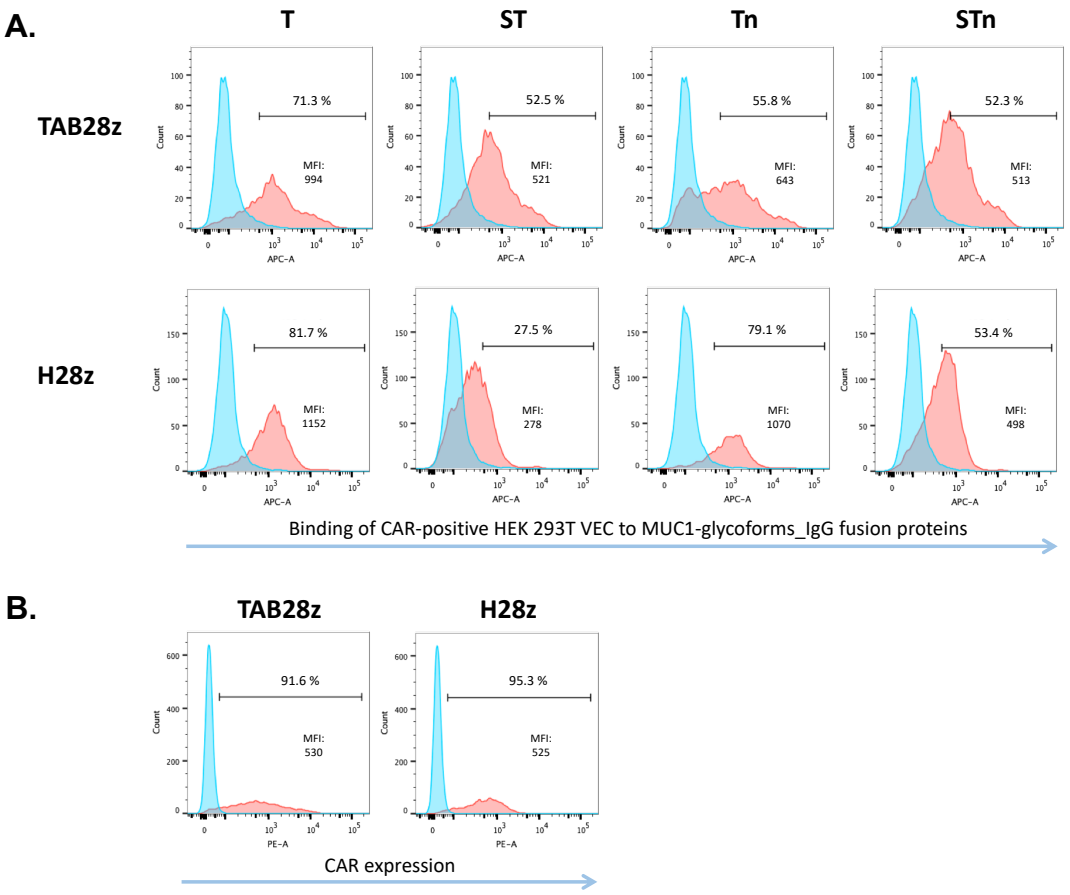

Figure 3.4: Binding of MUC-specific CARs to tumour-associated MUC1 glycoforms. A) The histograms demonstrate the binding of each CAR to the four different glycoforms. TAB28z and H28z-expressing HEK 293T VEC retroviral packaging cells were incubated for 30min with T, ST, Tn and STn-decorated MUC1 ectodomain-mouse IgG fusion proteins. The binding of the CARs to each of the fusion proteins was determined by flow-cytometry, after the incubation of cells with goat anti-mouse AlexaFluor 647-conjugated antibody (red histograms). TAB28z and H28z HEK 293T VEC cells were stained with mouse IgG1 AlexaFluor 647-conjugated antibody as isotype controls (blue histograms). The percentage of the binding, as well as the median fluorescence intensity (MFI), are mentioned within each histogram. B) The CAR expression was investigated by staining the cells with the 24mer-MUC1 peptide, followed by streptavidin PE (red histograms). Parental (untransduced) HEK 293T VEC cells were stained in the same way and were used as a negative control (blue histograms). The data shown here are derived from one experiment.

3.2.2.4 Detection of CAR expression by retrovirus-transduced T-cells

After validating the recognition of tumour-associated glycoforms by the MUC1-specific CARs, it was necessary to investigate whether these CARs

could be successfully expressed in human T-cells. Peripheral blood mononuclear cells (PBMCs) were isolated from healthy donors and activated T-cells were retrovirally transduced to individually express the three signalling-competent MUC1-specific CARs, TAB28z, H28z and HDF28z. The expression of the matched control-CARs, TABTr, HTr and HDFTr was also investigated. The surface expression of the CARs was validated using flow cytometry. As shown in representative histograms, all six different CARs were expressed at high levels on the surface of the transduced T-cells, allowing meaningful comparison of their cytotoxic activity against MUC1-positive breast cancer cell lines (Figure 3.5). Transduction efficiency ranged between 43% and 75%. Surface expression of TAB28z, H28z and HDF28z on day 11 post T-cell transduction was 68±11% (mean ± SD, n=8), 61±14% (n=8), 58±11% (n=8) respectively. Surface expression of TABTr, HTr and HFTr was 35±8% (mean ± SD, n=5), 37±12% (n=5) and 37±9%(n=9) respectively.

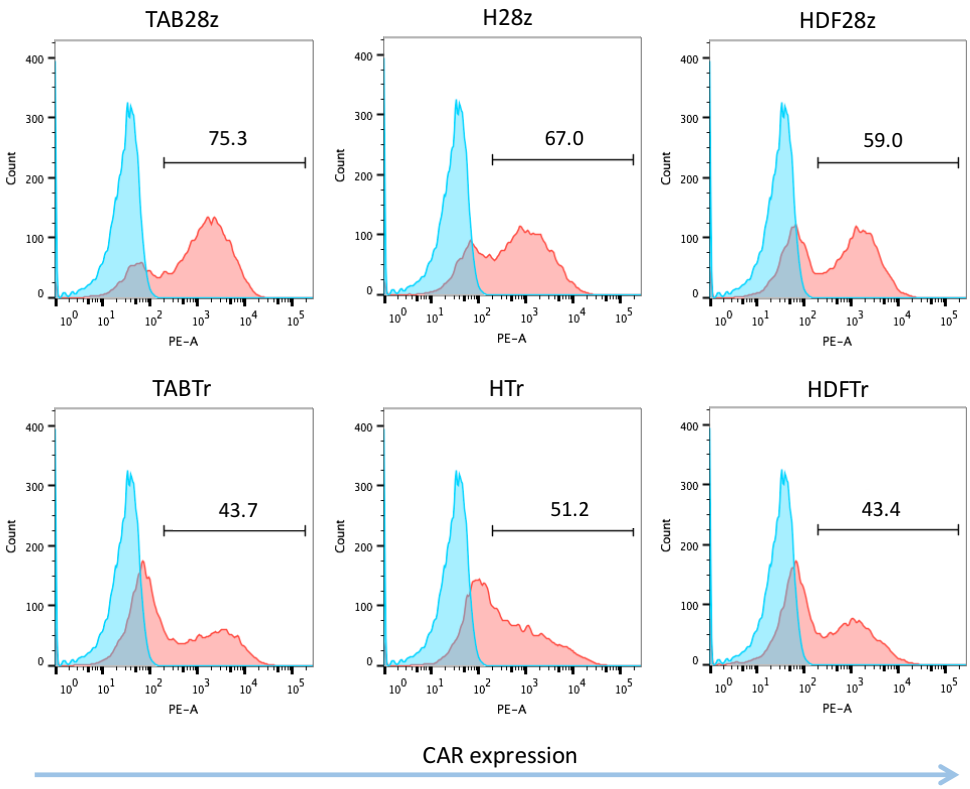

Figure 3.5: Expression of MUC1-specific CARs by retrovirus-transduced T-cells. Activated T-cells were engineered by retroviral transduction to express the indicated MUC1-specific CARs or truncated controls. Representative histogram plots showing cell surface CAR expression in retrovirus transduced healthy donor T-cells, as detected by flow cytometry. Eleven days after transduction, T-cells were stained with the biotinylated MUC1-24mer peptide, followed by streptavidin-PE. The CAR expression levels are represented by red histograms. Non-transduced T-cells were stained in the same way as previously described and were used as negative control (blue histograms). The percentage (%) of positive cells is indicated. Cytotoxic activity of MUC1-retargeted CAR T-cells against a panel of breast cancer cell lines

The anti-tumour activity of the signalling-competent CARs was investigated by performing co-cultivation experiments in which CAR T-cells were co-cultured with human breast cancer cell lines expressing various levels of MUC1. The breast cancer cells that have been used are T-47D (MUC1+++), MDA-MB-468 (MUC1++) and ZR-75 (MUC1+). Cytotoxicity was measured after 24h, 48h and 72h of co-culture. The three matched truncated CARs, TABTr, HTr and HDFTr were additionally used as negative controls,

together with non-transduced T-cells. Based on the results shown herein, all of the signalling-competent CARs exhibited significant cytotoxic activity against T-47D cells (Figure 3.6A). By 72h, the number of viable tumour cells was less than 20%. Similarly, these CAR T-cells achieved significant killing of MDA-MB-468 tumour cells, which was apparent even from the 24h time point (Figure 3.6B). By contrast, minimal cytotoxic activity was observed against the lowest MUC1-expressing cells, ZR-75 (Figure 3.6C). Neither the truncated CARs or the non-transduced cells caused any background cytotoxic activity. The three signalling-competent CAR T-cells, TAB28z, H28z and HDF28z, performed similarly and there was no statistical difference between their cytotoxic activity in these assays.

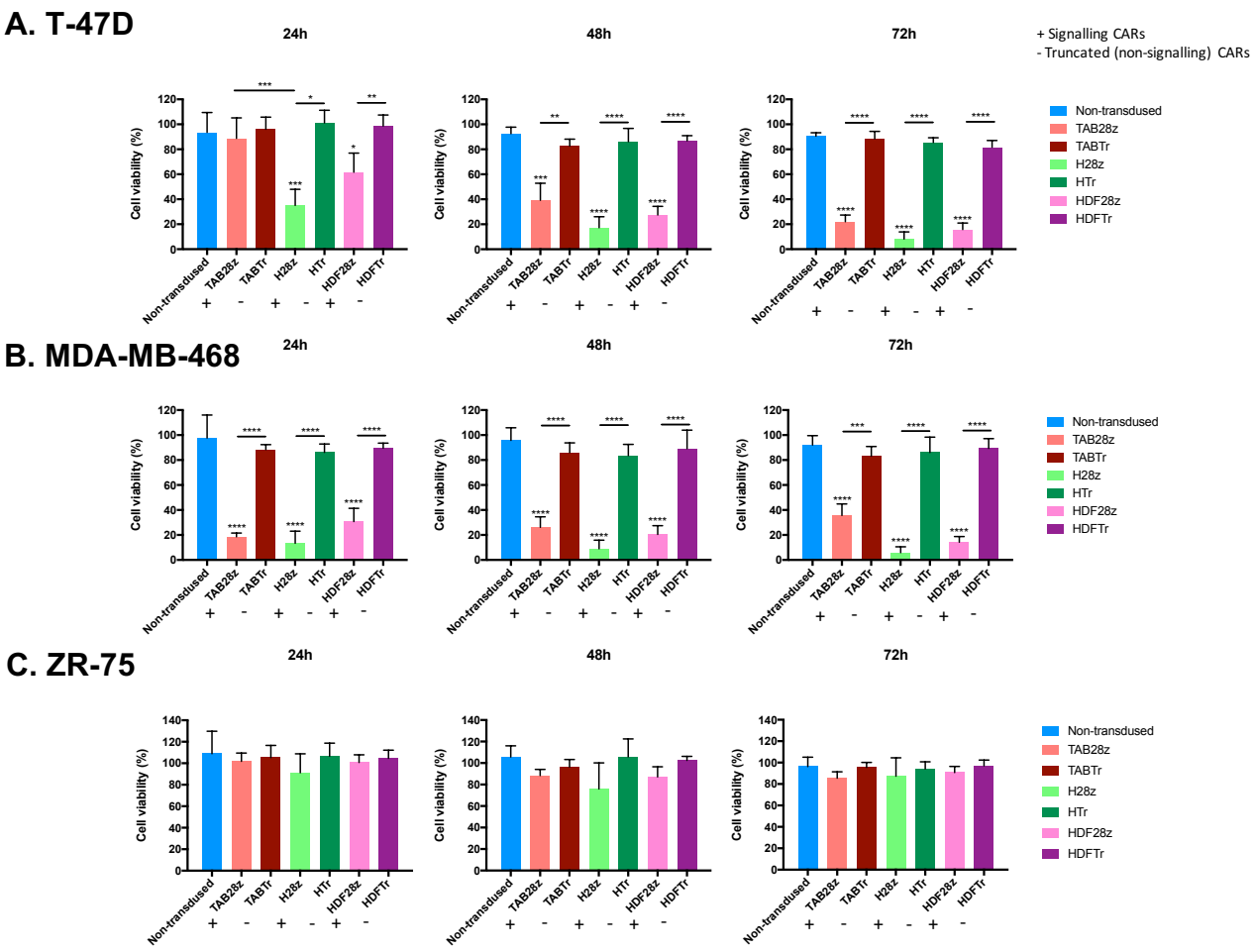

Figure 3.6: Cytotoxic activity of MUC1-specific CAR T-cells against a panel of breast cancer cell lines. T-cells were engineered to express the indicated test or control CARs and 5 x 10^5 T-cells were added to confluent tumour cell monolayers (A - T-47D; B- MDA-MB-468 and C - ZR-75), propagated in a 24-well plate. Non-transduced T-cells were additionally used to investigate any non-specific cytotoxic activity. Co-cultures were maintained for 24, 48h and 72h and tumour cell-viability was measured at each time-point using an MTT assay. In these graphs, the percentage of tumour cell viability has been expressed relative to a matched well containing tumour cells-only (% cell viability = ($OD_{co\text{-}culture\ reaction}$ / $OD_{tumor\text{-}cells\ only}$) x 100). Data show mean + SD of n=5 independent replicate experiments. Statistical analysis was performed by One-way ANOVA, followed by Tukey post hoc test. Asterisks above each bar represent the statistical significance when compared to non-transduced T-cells. The asterisks above each bar graph represent the significance of cytotoxic activity when compare to non-transduced T-cells. P value 0.01 to 0.05; ** → P value 0.001 to 0.01; *** → P value 0.0001 to 0.001; **** → P value < 0.0001, ns → not significant.

3.2.2.5 Quantification of Interferon (IFN)-γ production by MUC1 re-targeted CAR T-cells

The activation of MUC1-retargeted CAR T-cells upon recognition of target antigen was further investigated by quantification of IFN-γ release. Signalling competent MUC1-specific CAR T-cells produced significant amounts of IFN-γ upon recognition of MUC1 on the breast cancer cell lines (Figure 3.7A). Higher amounts were produced upon co-culture of the signalling competent CAR T-cells with T-47D. TAB28z-engineered T-cells released significantly more IFN-γ than H28z- or HDF28z-expressing T-cells when co-cultured with MDA-MB-468 cells.

In these experiments, T-cells that were cultured in the absence of tumour cells were used as a further negative control. Notably, background cytokine release was observed by the signalling competent CAR T-cells (Figure 3.7B), whereas non-transduced T-cells and truncated control CAR T-cells (e.g. expressing TABTr, HTr or HDFTr) did not demonstrate this pattern.

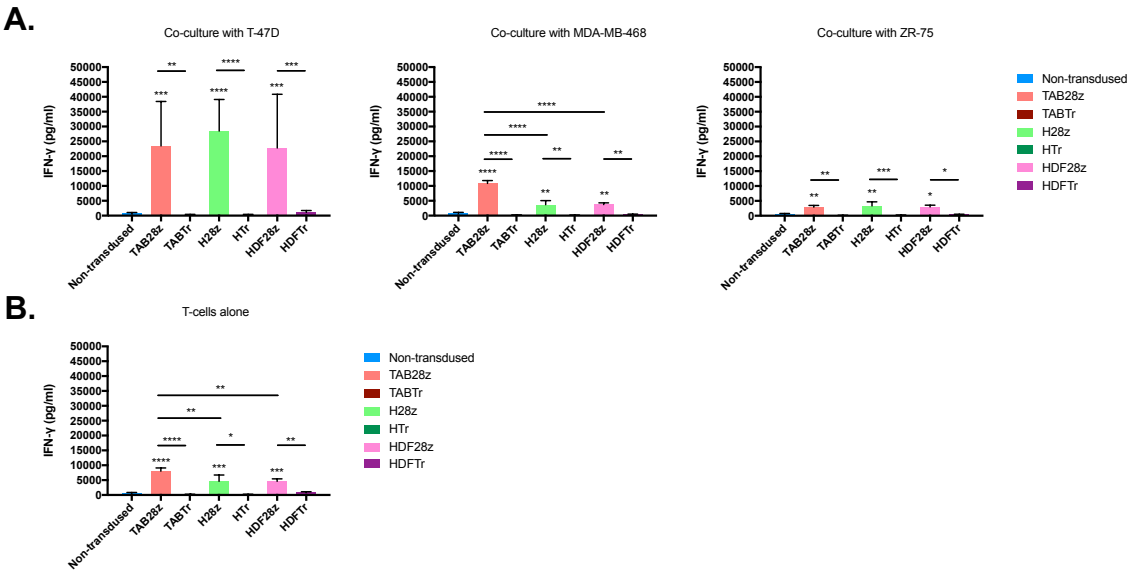

Figure 3.7: Quantification of IFN-γ production by MUC1-specific CAR T-cells. Supernatants were collected after 48h from the co-cultivation experiments described in Fig. 3.2.6 and were analysed for IFN-γ by sandwich ELISA. A) IFN-γ release was investigated upon co-cultivation of CAR T-cells together with the indicated breast cancer cell lines. B) IFN-γ production by T-cells alone. These negative-control reactions were kept in the same conditions as the T-cells which were co-cultured with the tumour cells. Data shown are mean + SD of n=5-9 independent replicates. Statistical analysis was performed with One-way ANOVA, followed by Tukey post hoc test. The asterisks above each bar graph represent the significance of cytotoxic activity when compare to non-transduced T-cells. P value 0.01 to 0.05; ** → P value 0.001 to 0.01; *** → P value 0.0001 to 0.001; **** → P value < 0.0001, ns → not significant.

3.2.2.6 Quantification of IL-2 release by MUC1-specific CAR T-cells

The ability of the MUC1 re-targeted CAR T-cells to produce cytokines in response to antigen-dependent stimulation was further investigated by quantifying the production of IL-2. All three signalling-intact MUC1-specific CAR T-cell populations produced significant levels of IL-2 when co-cultivated with MUC1^{+++} T-47D tumour cells. Notably, TAB28z-expressing, but neither H28z or HDF28z-expressing T-cells produced detectable levels of IL-2 when co-cultivated with MDA-MB-468 cells or ZR-75 cells. As expected, truncated control CAR-expressing T-cells did not produce IL-2 under any condition.

Additionally, T-cells that were cultured in the absence of tumour cells did not release IL-2.

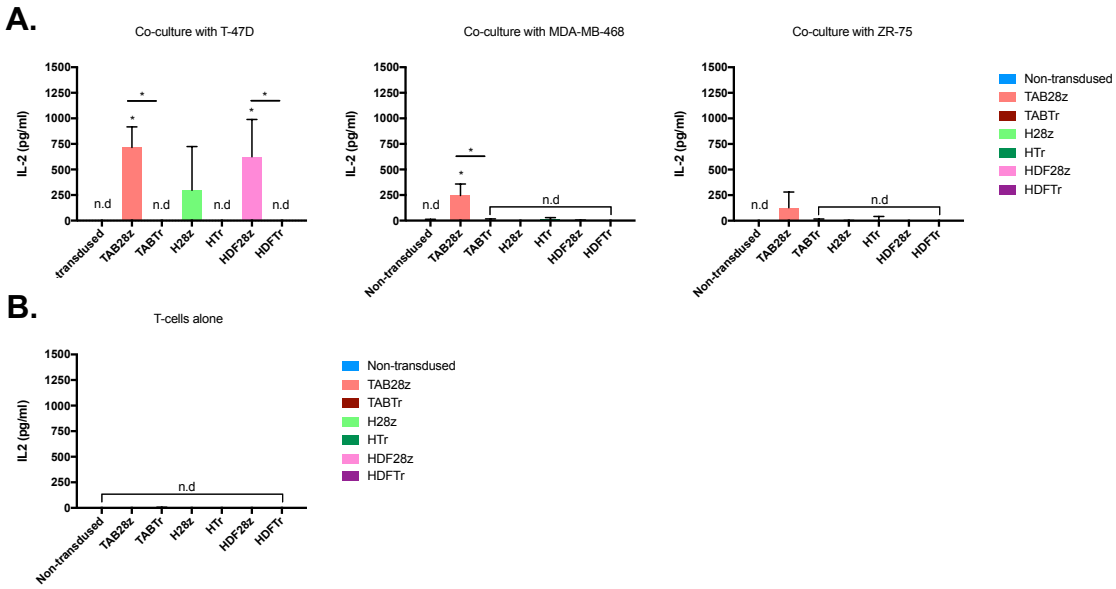

Figure 3.8: Quantification of IL-2 production by MUC1-specific CAR T-cells. A) Supernatants were collected 24h post co-culture of CAR T-cells with T-47D, MDA-MB-468 and ZR-75 tumour cells (as described in Figure 3.2.6) and were analysed for IL-2 content by sandwich-ELISA. B) IL-2 ELISA was also performed on supernatants collected from T-cells that were cultured under similar conditions, except that they were maintained in the absence of tumour cells. These served as an additional negative control. Data shown are mean + SD of n=3 independent replicates. Statistical analysis was performed with One-way ANOVA, followed by Tukey post hoc test. N.d – non detectable. It should be noted that supernatants were thawed in advance of analysis, which may have compromised stability of cytokine detected in this assay. P value 0.01 to 0.05; ** → P value 0.001 to 0.01; *** → P value 0.0001 to 0.001; **** → P value < 0.0001, ns → not significant.

3.3 Discussion

In this chapter, I have undertaken an initial assessment of the activity of a newly developed MUC1-specific CAR, named TAB28z. This CAR has been engineered in collaboration with Professor Pinku Mukherjee (University of North Carolina at Charlotte, NC, USA), who provided the scFv sequence from the TAB004 antibody. Here, I aimed to characterize the *in vitro* anti-tumour activity of this newly developed CAR using breast cancer cell lines that express a range of levels of MUC1. Comparison was made with two other MUC1-specific CARs that had previously been developed in our lab using the HMGF2 scFv sequence, named H28z and HDF28. In addition, a panel of endodomain-truncated control CARs were also included in this analysis.

The first step of this PhD project was to investigate the expression of TA-MUC1 in a panel of breast cancer cell lines. TA-MUC1 was detected on the surface of various tumour cell lines by flow cytometry analysis using the HMFG2 anti-MUC1 antibody. HMFG2 antibody was used for the detection of MUC1 for two main reasons: 1) it is known to react strongly with malignant cells and less well with normal epithelial cells[288,320], 2) H28z and HDF28z CARs contain a binding domain (scFv) derived from the HMFG2 antibody[295]. The surface expression of TA-MUC1 was investigated in a panel of six different breast cancer cell lines with different morphological and genotypical characteristics (Table 2.2). MUC1 was detected on five out of six tumour cell lines, a result that supports the frequent expression of TA-MUC1 in diverse molecular subtypes of breast cancer[124]. Other groups have investigated the expression of TA-MUC1 in various human breast carcinoma cell lines,

consistent with my results[344]. The sole inconsistency is related to the MUC1 expression on ZR-75. Specifically, Walsh *et al.* have reported high detection levels of MUC1 on the surface of these cells, while my results indicate low surface expression[344]. This inconsistency could be explained by the usage of a different anti-MUC1 antibody (BC2), the difference in the passage number of the cells, general differences in the handling of the cells, or other unknown technical reasons.

Before I proceeded to the *in vitro* characterization of the MUC1-specific CAR T-cells, I designed and cloned two negative control CARs, named TABTr and HTr. These matched the signalling-intact CARs, TAB28z and H28z. The matched negative-control CAR for HDF28z, named HDFTr, had already been developed in the lab previously. The generation of the full panel of signalling and defective-signalling CARs was necessary in order to ensure that the activity of the signalling CARs is dependent on antigen recognition and resultant signalling by the CAR endodomain. The cloning of TABTr and HTr was successful, as evident from the validation restriction digest of the DNA minipreps (Figure 3.2).

Gamma retroviral vectors, such as SFG, are commonly used for the genetic modification of T-cells (reviewed by S. Bear *et al.*)[345]. Stable packaging cell lines release virion particles which contain the CAR-expressing retroviral vectors and are widely used for T-cell transductions. This methodology provides a robust, safe and inexpensive way of CAR expression in human T-cells[346]. For the above reasons, HEK 293T VEC packaging cells, pseudotyped with either the RD114 or GALV envelope, have been used throughout this PhD project in order to achieve stable CAR expression by T-

cells. The expression levels of the CARs in these cells were high for all the CAR constructs (>70%, Figure 3.5).

It is known that HMFG2 and TAB004 MUC1 antibodies both bind to the VNTR region of MUC1[284,288]. The binding capacity of HMFG2-based CARs to different MUC1 glycoforms has already been reported by Wilkie *et. al*[295]*.* Nevertheless, no information has been available related to the binding preference of TAB004 to different TA-MUC1 glycoforms (patent #US-2011-0123442)[284,285,347]. For this reason, it was essential to characterize and compare the binding pattern of TAB004-based and the HMFG2-based CARs. A binding assay was performed in which the binding preference of TAB28z and H28z CARs to different under-glycosylated glycoforms was evaluated. Four different glycoforms were used, T, sialyl-T, Tn and sialyl-Tn. The binding profile of the H28z CAR agrees with the results published by Wilkie *et al.,* where they show that H28z CAR binds less well to the sialyl-T glycoform (49% ST binding, 85% T, 85% STn, 87% Tn)[295]. Overall, both TAB28z and H28z CARs showed similar binding preferences, although definitive conclusions cannot be drawn owing to lack of availability of glycosylated MUC1-Fc fusion proteins, which precluded repeat experimentation. One noted difference in the experiment that was performed is the ability of H28z to bind better to the Tn glycoform. This could potentially provide an advantage for the HMFG2-based CARs since the MUC1 Tn glycan is known to be overexpressed in the majority of breast cancers[312,337,348].

Next, it was essential to demonstrate that the TAB28z CAR can be successfully expressed in primary human T-cells. This was validated using flow cytometry (surface expression). High CAR surface expression is

desirable in CAR T-cell immunotherapy in order to achieve optimal CAR activity.

To investigate the *in vitro* anti-tumour activity, MUC1-specific CAR T-cells were co-cultivated with three different cell lines expressing various levels of MUC1. TAB28z CAR T-cells exhibited significant cytotoxic activity against T-47D and MDA-MB-468 tumour cells. Nevertheless, this activity did not prove superior when compared to H28z and HDF28z CAR T-cells. A notable observation was the fact that all three MUC1-specific CAR T-cells eliminated the MDA-MB-468 cells (MUC1++) more effectively in comparison with the T-47D cells (MUC1+++). This difference was most apparent at the 24h time-point post initiation of the co-culture. One possible explanation for this observation is that the MDA-MB-468 are more susceptible to T-cell-mediated cytotoxicity, in comparison with T-47D cells. Another surprising observation was that the number of viable MDA-MB-468 cells was progressively increased upon their co-culture with the TAB28z CAR T-cells. It could be hypothesized that TAB28z CAR T-cells could not control tumour growth due to high cell growth rate. This pattern was not observed in the co-cultures with H28z and HDF28z CAR T-cells. Potentially, this could reflect differences in affinity, recycling kinetics and/or tumour-associated glycoform preference of the CARs, a point that warrants further study using glycosylated MUC1-Fc fusion proteins.

As expected, non-transduced T-cells and signalling-defective anti-MUC1 CARs showed no background cytotoxic activity against the MUC1-positive breast cancer cell lines. Importantly, all three signalling-intact MUC1-specific CAR T-cells showed limited cytotoxic activity against ZR-75 cells,

which expressed low levels of MUC1. In the clinical setting, the latter has a double-edged significance. Minimal killing of low-antigen expressing cells could be advantageous as normal cells can potentially express low levels of TA-MUC1. In contrast, it could be considered a disadvantage as it might lead to tumour-escape where low-expressing MUC1 tumour cells will not be eliminated. The latter is emerging as a significant problem in CAR T-cell immunotherapy of CD19-expressing malignancy[349].

MTT assay gave a clear indication for the magnitude of CAR T-cell-mediated cytotoxicity against each of the cell lines. Nevertheless, this assay is not ideal for the comparison of the observed cytotoxicity *between* the different cell lines in different time-points as each of these cell lines has different growth rate. For this reason, no solid statements can be made in regards with the differences observed between T-47D and MDA-MB-468. Chromium (Cr^{51})-release assay is considered the gold standard for the measurement of cell-mediated cytotoxicity. In this assay, cell death is measured by quantifying the release of radioactivity from chromium-labelled cells[350]. The protocol requires a 4-hour incubation of the effector cells with the target cells, whilst MTT requires at least 24-hours of co-culture[351]. The latter gives an advantage to ^{51}Cr-release assay over MTT for the comparison of cell-mediated cytotoxicity observed between the different cell lines. Nevertheless, ^{51}Cr-release assay requires specific facilities for the handling and disposal of radioactive elements, which makes the use of this technique impractical. It was not possible to perform the ^{51}Cr-release assay during this PhD project as the lab facilities do not comply with these requirements. Additionally, high spontaneous release of ^{51}CR by some target cells can be observed. Other

assays have been developed as alternatives for the measurement of cell viability *in vitro*. Similar to MTT, the principle of some of these assays is dependent to the enzymatic activity of the target cells. Some examples are the lactate dehydrogenase (LDH) assay and the luciferase reporter assay[352]. LDH is released in the cell supernatant upon cell lysis. Cell death is quantified upon a colorimetric enzymatic reaction, which results to the conversion of tetrazolium salt (INT) into formazan crystals[353,354]. The luciferase reporter assay requires the transduction of the target cells with a luciferase reporter gene[355]. The produced bioluminescence is measured upon the addition of luciferin. Only live cells are able to produce luminescence due to the requirement of ATP. Both LDH and luciferase assay are easy and straightforward to perform. Additionally, cell cytotoxicity can be measured in multiple time points by using the co-cultured reactions that were initially set up. Direct comparison of ^{51}Cr-release and luciferase reporter assay has shown that luciferase assay is superior due to increased kinetics and reduced signal-to-noise ratio[356]. Nevertheless, similarly with MTT, both LDH and luciferase assay require longer incubation period of the effector cells with the target cells, thus making them inappropriate for the comparison of cell-cytotoxicity observed against various cell lines. Flow-cytometric assays are also being used for quantifying cell-mediated cytotoxicity. In these experiments, cells are labelled with a fluorescent dye, such as CFSE[357]. Additional staining of the cells allows for the differentiation between effector and target cells. The advantage of flow-cytometry-based experiments is that multiple fluorescent markers can be used.

The incorporation of the elongated hinge in the HDF28z CAR did not seem to improve its anti-tumour activity *in vitro*. Wilkie *et al.* have reported that the incorporation of a longer spacer resulted in increased secretion of IFN-γ and improved proliferation, nevertheless no such benefit was observed in my results (See Chapter 4 for total T-cell count)[295]. Qin *et al.* have also suggested that incorporation of a hinge resulted in better expansion of anti-mesothelin CAR T-cells. In parallel, and in agreement with my results, the hinge-incorporated CAR did not present improved anti-tumour activity when tested *in vitro*. Nevertheless, it showed improved anti-tumour activity when this was further investigated in tumour-bearing mice (See Chapter 5 for the investigation of the in vivo efficacy of MUC1-specific CAR T-cells)[358].

In support of the results showing the cytotoxic activity of MUC1 retargeted CAR T-cells, all three signalling-intact CARs produced significant levels of IFN-γ upon antigen recognition. Interestingly, lower levels of IFN-γ were produced by the MUC1-specific signalling intact CAR T-cells when cultured with the MDA-MB-468 cells, despite their significant cytotoxic activity. Differences in expression of inhibitory molecules by the three breast cancer cell lines under study might potentially have influenced the ability of T-cells to produce IFN-γ. As reported by Mittendorf *et al*., the T-cell inhibitory molecule PD-L1 is detected on high levels in the surface of MDA-MB-468 cells while T-47D cells showed lower PD-L1 surface expression[82]. Further experiments need to be conducted in order to explore this hypothesis and to investigate the levels of PD-L1 and other inhibitory molecules in these breast cancer cell lines.

Another interesting observation was that TAB28z CAR T-cells achieved significantly higher production of IFN-γ compared to H28z and HDF28z CAR T-cells, when co-cultured with the MDA-MB-468 cells. The expression pattern of TA-MUC1 glycoforms in MDA-MB-468s could potentially explain this result. Preliminary data presented here showed that the TAB28z CAR may bind the MUC1-ST glycan more efficiently, in comparison with the HMFG2-based CAR (Figure 3.4). The expression pattern of different glycans in MDA-MB-468 cells is not known and would be interesting to explore it in future experiments.

The most unexpected result obtained in this analysis was the demonstration of significant IFN-γ secretion by all three signalling-intact MUC1 CAR T-cell populations in the absence of MUC1-positive tumour cells. Importantly, this pattern was not observed with non-transduced T-cells or signalling-defective CAR T-cells. Additional experimental reactions are required to be included in this assay in order draw any conclusions. These would be: a) co-culture of MUC1-specific CAR T-cells with a MUC1-negative cell line in order to validate the pattern of IFN-γ production in the absence of MUC1 from tumour cells, and b) co-culture of MUC1-positive cell lines with a non-specific (irrelevant) CAR. The latter would indicate whether this background CAR T-cell activation is a phenomenon associated solely with the MUC1-specific CARs under investigation.

Others have reported activation of CAR T-cells independently of antigen engagement, for a variety of reasons. First, it has been widely reported that inclusion of the IgG1 Fc spacer in the extracellular domain of the CAR molecule can cause T-cell activation due its crosslinking by other Fc receptors that present in accompanying innate immune cells[359,360]. Although the

HDF28z CAR contains an IgG1 Fc spacer, this is not present in either the TAB28z or H28z. Consequently, this cannot be the explanation for the background IFN-γ production. Second, a number of studies have reported that the scFv domain of a CAR could mediate tonic signalling since certain elements within the scFvs could promote aggregation (and thus crosslinking) of the CAR receptors[241,361]. A third possible explanation for this tonic signalling is the expression of cognate antigen on activated T-cells[241]. This hypothesis has been further investigated in Chapter 4.

In addition to IFN-γ secretion, the production of IL-2 by the MUC1-specific CAR T-cells was also investigated. IL-2 was detected only in the supernatant derived from the TAB28z co-cultured T-cells. Nonetheless, issues with sample storage may mean that these levels represent an underestimate of IL-2 release by these cells.

3.4 Conclusions

In this chapter, I initially investigated the surface expression of MUC1 in various breast cancer cell lines. MUC1 was, as expected, detected in the majority of breast cancer cell lines. The next step undertaken was to create negative-control (signalling-defective) CARs, named as TABTr and HTr, which match the signalling CARs TAB28z and H28z respectively. The *in vitro* characterization of TAB28z included the validation of recognising distinct TA-MUC1-glycoforms. I then validated that TAB28z CAR can be successfully expressed on the surface of human primary PBMCs, activated with CD3/CD28 paramagnetic beads. TAB28z proved effective in eliminating MUC1-positive tumour cells. This activity was accompanied by significant production of IFN-γ upon antigen-stimulation. Nevertheless, the activity of TAB28z did not seem superior when compared to that of H28z and HDF28z CAR T-cells. An unexpected observation was the background production of IFN-γ by all three signalling CAR T-cells, in the absence of co-culture with tumour cells. This led to the hypothesis that these CAR T-cells might tonically signal. One suggested hypothesis for this observation is the detection of MUC1 on activated T-cells by the anti-MUC1 CARs during their *in vitro* expansion. This possibility has been explored in Chapter 4.

Chapter 4: MUC1 expression on activated T-cells and its effect on MUC1-specific CAR T-cell populations

4.1 Introduction

The fundamental role of the immune system is the protection of individuals from invading pathogens. To accomplish this, both the innate and adaptive arms of the immune system are required. Innate immunity is the first defence line against foreign antigens and it refers to non-specific defence mechanisms, such as macrophages and neutrophils, that take place in the site of infection[362]. On the other hand, adaptive immunity elicits antigen-specific responses. T-lymphocytes are the main defence mechanism of adaptive immunity. A broad variety of T-cell receptors are expressed on the T-cell surface. These receptors encompass specificity against the vast majority of pathogens in order to be able to provide protection upon antigen encounter. The T-cell receptor repertoire is generated in thymus via somatic recombination of TCR genes[362]. At this stage, elimination of self-reactive T-cells and establishment of self-tolerance is crucial in order to prevent autoimmunity (negative selection). Various mechanisms are in place in order to ensure that self-tolerance is established. These mechanisms are part either of central tolerance, which occur in primary lymphoid organs, or of peripheral tolerance, which take place in the lymphocytes once they have migrated outside thymus[362]. Both types of self-tolerance will be analysed further in the next section, with focus on the peripheral tolerance.

4.1.1 T-cell central and peripheral tolerance

As previously described, central tolerance occurs in the thymus. Medullary thymic epithelial cells (mTECs) play an important role in the process of negative selection. mTECs have the property to process and present various peripheral antigens which are not normally found in they thymus, a process that is controlled by the autoimmune regulator gene (*AIRE*)[363]. Auto-reactive T-cells with high affinity to self-peptide-MHC complexes get deleted, as they pose great risk autoimmunity. Alternatively, T-cells with high affinity to a self-antigen can undergo functional diversion to form T-regulatory cells, known as natural Tregs (nTregs)[364]. On the other hand, low-affinity self-peptide-MHC complexes get spared[365]. Natural Tregs are CD4-positive and are characterised by upregulation of FoxP3 and expression of CD25 and CTLA-4[362]. nTregs cells can escape to the peripery and contribute further to the establishment of tolerance by producing anti-inflammatory cytokines and by modulating the activation status of APCs. Despite the mechanisms of central tolerance in place, there is still the possibility that not all autoreactive T-cells will be eliminated due to the fact that not all self-antigens are expressed in the thymus[366]. Thus, tolerance mechanisms that operate in the periphery are additionally required. The mechanisms of peripheral tolerance include ignorance, suppression by Tregs (iTregs), deletion and anergy.

Naïve self-reactive T-cells with low affinity to self-antigen might never be activated as the threshold for T-cell activation in the periphery is higher than that for T-cell deletion in the thymus[366,367]. This phenomenon is named as peripheral ignorance. Ignorance is also achieved when activation of self-

reactive T-cells is physically prevented by the restriction of self-antigen into immune privileged sites[368].

Various environmental factors present in the periphery can influence naïve CD4 T-cells to differentiate into Tregs[362]. This subset of Tregs is known as induced Trges (iTregs) and it contributes further to the establishment of tolerence, together with the nTregs. The mechanisms by which Tregs promote immune tolerance include the production of anti-inflammatory cytokines and the influence of the maturation stage of the dendritic cells. iTregs, similar to nTregs, are characterised by expression of CD25 and CTLA-4[362]. Immature dendritic cells (also known as tolerogenic DCs), play also an important role in the establishment of peripheral tolerance. Immature DC are characterized by reduced expression of MHC molecules and of costimulatory ligands, such as CD80 and CD86. The latter results in impaired T-cell activation and proliferation. Lack of co-stimulation leads to tolerance either by inducing anergy or deletion of self-reactive T-cells[369–372]. The mechanism by which T-cells decide to undergo either anergy or deletion is still under investigation. Deletion of autoreactive T-cells is mediated by apoptosis upon activation of Fas-mediated and Bim-2-mediated apoptotic pathways[362].

As previously mentioned, lack of T-cell co-stimulation results in functional unresponsiveness (anergy). Anergic self-reactive T-cells do not undergo apoptosis. They remain viable, but at the same time they lose their responsiveness to antigen exposure. This functional unresponsiveness is accompanied by downregulation of self-reactive TCR and IL-2 expression. Importantly, removal of the recognised self-antigen restores the functionality of self-reactive T-cells. Inhibitory receptors, such as PD-1 and CTLA-4,

additionally contribute to the establishment of peripheral tolerance and the induction of T-cell anergy by inhibiting T-cell response with the attenuation of the PI3k and Akt signalling pathways. PD-L1 can also mediate the conversion of naïve CD4 T-cells to iTregs[373].

Some of the mechanisms of tolerance mentioned above can also be exploited by tumour cells in order to escape inhibition and killing by immune cells. Adoptive T-cell immunotherapy aims to break this tolerance established by tumour cells by introducing to them tumour-specific T-cell receptors, such as CARs and TCRs, with high affinity. Despite the enormous therapeutic potential that these strategies have, engineered T-cells can also present immune dysfunction.

Various distinct types of T-cell dysfunction have been described, one of them being anergy which has been mentioned in the previous section. Other types of T-cell dysfunction include exhaustion and senescence. Senescence is a permanent and irreversible phenomenon characterised by telomere shortening and cell cycle arrest upon extensive cell proliferation (Hayflick limit). Exhaustion occurs upon chronic exposure of a T-cell to an antigen, accompanied by continuous T-cell activation. T-cell exhaustion is observed in conditions such as chronic infection, chronic inflammation and cancer. Exhausted T-cells are characterised by dysfunction, decreased production or pro-inflammatory cytokines (such as IL-2, IFN-γ and TNF-α) and upregulation of inhibitory receptors (such as PD-1, Tim33 and Lag-3). Importantly, exhausted T-cells are unable to restore their function upon removal of the stimulus. Different studies have reported that adoptively transferred T-cells can also become exhausted, even in the absence of interaction with tumour

cells. This have been attributed to tonic CAR T-cell signalling and to the inhibitory effector of the tumour microenvironment[241,374].

4.1.2 Aim

In Chapter 3, I have presented results showing unexpected secretion of IFN-γ by all three signalling-intact MUC1 CAR T-cell populations, when cultured in the absence of MUC1-positive tumour cells. Background T-cell activation could potentially cause CAR T-cell dysfunction. Additionally, as discussed previously, expression of the targeted antigen by non-malignant cells raises significant concerns about the safety of an experimental CAR T-cell immunotherapeutic approach. For this reason, I sought to investigate if background CAR T-cell activation resulted from the expression of so called "tumour-associated" (TA) glycoforms of MUC1 by activated T-cells, leading to a form of on target off tumour toxicity. This hypothesis was explored by (i) further characterisation of the *in vitro* behaviour of the MUC1-specific CAR T-cell populations and (ii) investigation of the cell surface expression of MUC1 on T-cells.

4.2 Results

4.2.1 Expression of TA-MUC1 on peripheral blood mononuclear cells following T-cell activation

Previous investigators have demonstrated that MUC1 is expressed by activated T-cells[375–378]. However, Correa *et al.* reported that TA-glycoforms of MUC1 recognised by the HMFG2 antibody have been reported to be absent on T-cells[378]. Given the background production of IFN-γ by the experimental CAR T-cells under study, I wished to confirm that the HMFG2 antibody does not bind to MUC1 on these cells.

To test this, a time-course assay was performed in which non-transduced primary human T-cells were activated using paramagnetic beads coated with CD3 and CD28 antibodies. Serial expression of MUC1 was monitored by flow cytometry using the HMFG2 MUC1-specific antibody. Expression of CD69 was also investigated in these experiments as a marker of T-cell activation[379]. As expected, Figure 4.1 demonstrates that cell surface expression of CD69 became evident as early as three hours post T-cell activation, with peak expression at day 3, followed by a progressive decline thereafter. Minimal levels of MUC1 were detected on PBMCs prior to T-cell activation (indicated as '0' in the graph) and at the early time-points post activation (30min, 3h and 1 day). However, cell surface MUC1 expression progressively increased subsequently, with peak levels of HMFG2 binding found on days 5 to 7 post activation. Thereafter, cell surface MUC1 expression

progressively declined. Minimal co-expression of MUC1 and CD69 was observed.

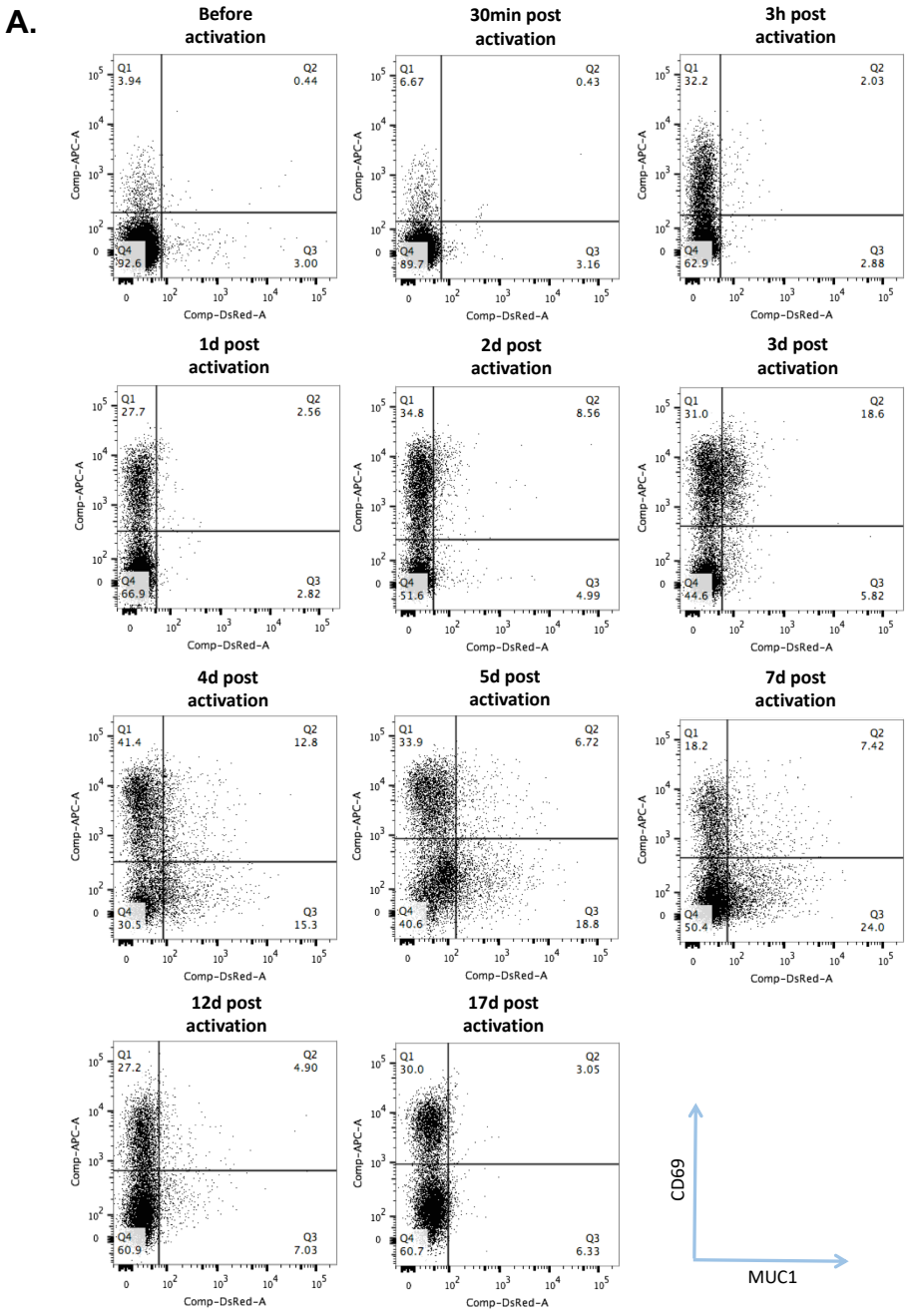
A.
Before activation
Q1 3.94
Q2 0.44
Q4 92.6
Q3 3.00
30min post activation
Q1 6.67
Q2 0.43
Q4 89.7
Q3 3.16
3h post activation
Q1 32.2
Q2 2.03
Q4 62.9
Q3 2.88
1d post activation
Q1 27.7
Q2 2.56
Q4 66.9
Q3 2.82
2d post activation
Q1 34.8
Q2 8.56
Q4 51.6
Q3 4.99
3d post activation
Q1 31.0
Q2 18.6
Q4 44.6
Q3 5.82
4d post activation
Q1 41.4
Q2 12.8
Q4 30.5
Q3 15.3
5d post activation
Q1 33.9
Q2 6.72
Q4 40.6
Q3 18.8
7d post activation
Q1 18.2
Q2 7.42
Q4 50.4
Q3 24.0
12d post activation
Q1 27.2
Q2 4.90
Q4 60.9
Q3 7.03
17d post activation
Q1 30.0
Q2 3.05
Q4 60.7
Q3 6.33
Comp-APC-A
Comp-DsRed-A
CD69
MUC1

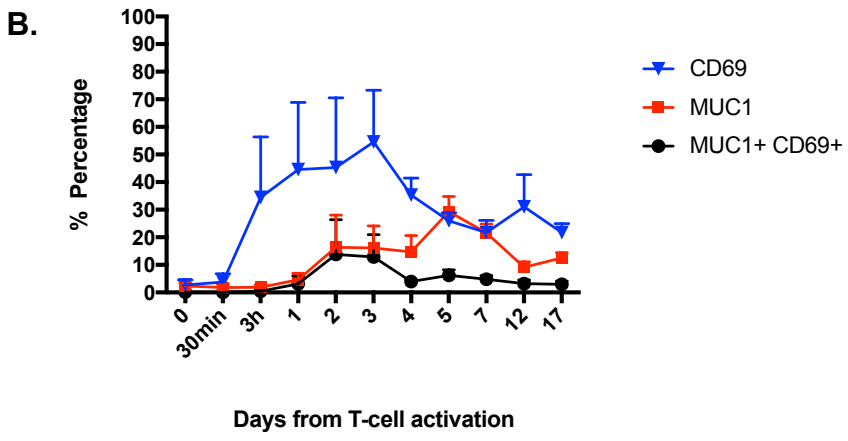
B.
% Percentage
100
90
80
70
60
50
40
30
20
10
0
0
30min
3h
1
2
3
4
5
7
12
17
Days from T-cell activation
CD69
MUC1
MUC1+ CD69+

Figure 4.1: Expression of TA-MUC1 on cells prior to and post T-cell activation. PBMCs were isolated from healthy volunteers and T-cells were activated with anti-CD3/anti-CD28 beads. T-cells were expanded as per usual (IL-2 and R5 medium supplementation every other day). Surface expression of MUC1 was investigated in different time-points, prior and post T-cell activation. Detection of TA-MUC1 was achieved by flow cytometry using the HMFG2 anti-MUC1 antibody followed by streptavidin-PE. In parallel, expression of CD69 (blue-triangle line) and co-expression of MUC1 and CD69 were investigated. Surface detection of MUC1, CD69 and MUC1+CD69+ is presented herein as percentage (%). Two different negative controls were used during the flow cytometry analysis for each of the time-points. These included cells stained with: 1) mouse IgG1-biotinylated isotype control followed by streptavidin-PE and CD69-APC, and 2) HMFG2-biotinylated followed by streptavidin-PE and mouse IgG1κ'-APC. A) Represenative results of n=3 are shown herein as dot plots. Each dot plot corresponds to a specific time-point as indicated. B) Data shown herein are mean + SEM of n=3 independent replicates from different donors; MUC1+ - red-square line; CD69+ - blue-triangle line; MUC1+ CD69+ – black-dot line.

4.2.2 Expression of TA-MUC1 on CD4 and CD8 T-cells

The data presented in section 4.2.1 indicate that TA-MUC1 can be detected on PBMC cultures following T-cell activation. To determine if this involved $CD4^+$ or $CD8^+$ T-cell subsets, I next investigated the expression of MUC1 on these two T-cell populations. This analysis was performed on day 5 post T-cell activation as it has been shown previously that, at this time-point, cell surface MUC1 is detected at maximum levels. Furthermore, a broader panel of donors was tested in order to assess the donor dependence of these findings. Figure 4.2 shows that MUC1 was expressed at significantly higher levels on the surface of activated $CD4^+$ T-cells in comparison with the $CD8^+$ cell subset (Figure 4.2). Mean expression of MUC1 on CD4 T-cells was 30% while on CD8 T-cells was 18.5%.

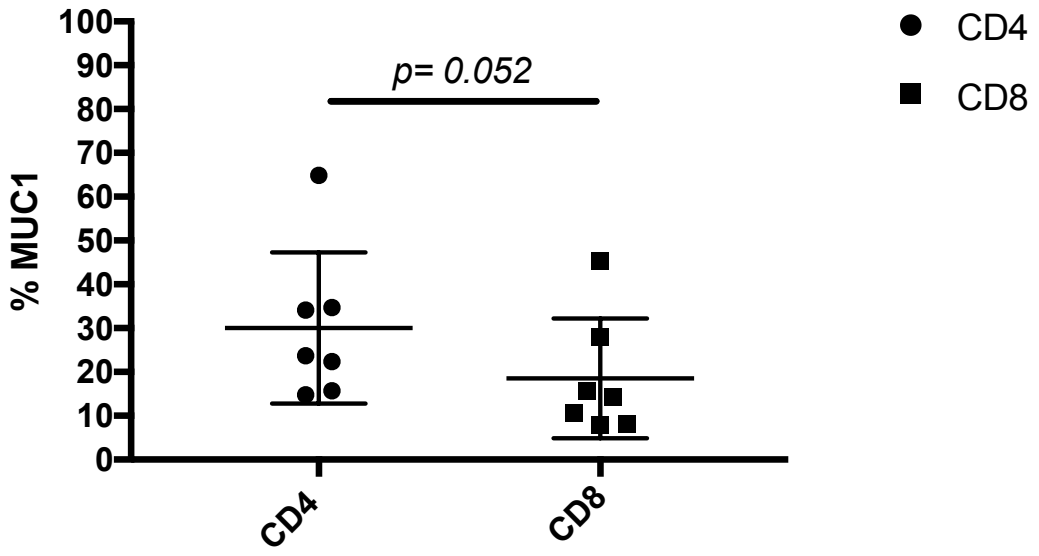

Figure 4.2: Expression of TA-MUC1 on CD4 and CD8 T-cells. Surface expression of TA-MUC1 on CD4 and CD8 T-cells was investigated using flow cytometry analysis at day 5 post T-cell activation. Detection of MUC1 was achieved by using the HMFG2 biotinylated antibody, followed by PE-conjugated streptavidin. T-cells stained with biotinylated mouse IgG1 isotype control, followed by streptavidin PE, were used as negative control. As previously mentioned, PBMCs were isolated from healthy volunteers and T-cells were activated with anti-CD3/anti-CD28 coated paramagnetic beads. T-cells were expanded as per usual (IL-2 and R5 supplementation every other day). Surface expression of MUC1 is presented herein as percentage. Data shown are mean $\pm$ SD of n=7 independent replicates from different donors. Statistical analysis was performed with a paired Student's *t*-test.

4.2.3 *In vitro* expansion of MUC1 re-targeted CAR T-cells

Given the fact that HMFG2 binding was found on activated $CD4^+$ and $CD8^+$ T-cells, I next characterised the possible effects of recognition of cell surface MUC1 on the *in vitro* expansion of the CAR-engineered T-cells under study. As previously described, CAR T-cells were expanded for 10 days post retroviral transduction. All three signalling anti-MUC1 CARs were used in these experiments (Figure 1.11), together with the matched signalling-

truncated CAR T-cells and non-transduced T-cells, both of which served as negative controls. It needs to be clarified that the non-transduced T-cells were treated and expanded in exact same conditions as the transduced T-cell populations. The only difference is that during the process of transduction, DMEM media was used for mock transduction, instead of viral supernatant. Assessment of cell count was performed by trypan exclusion (see section 2.2.7). Notably, unexpected differences were observed in the cell number of the distinct CAR T-cell populations. All three signalling-intact MUC1-specific CAR T-cell cultures presented significantly lower total cell numbers when compared to non-transduced T-cells or to their matched signalling-defective CAR T-cell populations.

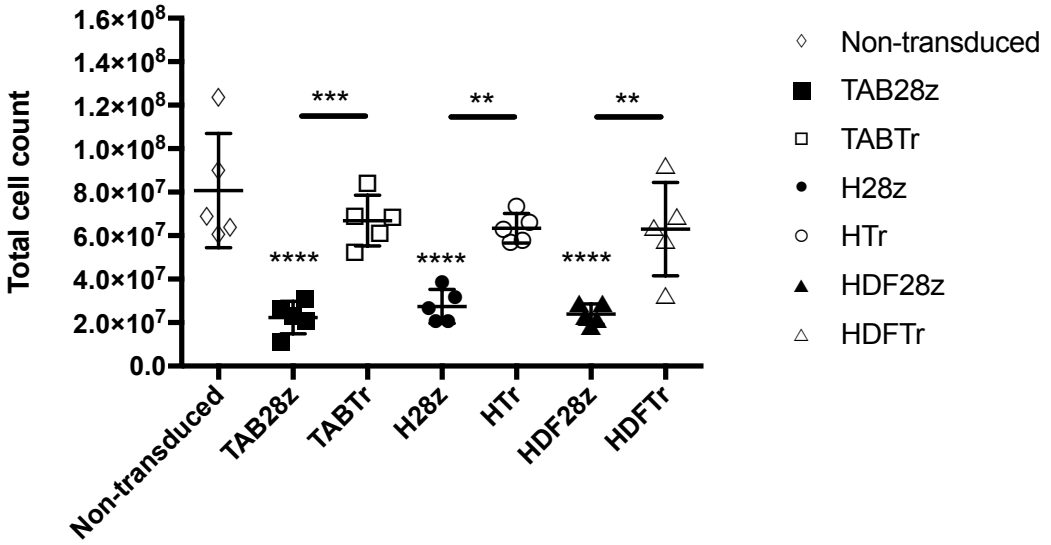

Figure 4.3: Total T-cell count following *in vitro* expansion of MUC1 re-targeted CAR T-cells. PBMCs were activated with anti-CD3/anti-CD28 beads and were transduced at 48h in order to express each of the CAR constructs. CAR T-cells were expanded for 10 days post transduction and were then counted using the trypan blue exclusion test. Data shown are mean ± SD of n=5 independent replicates. Statistical analysis was performed with One-way ANOVA, followed by Tukey post hoc test. The asterisks above each data set indicate the statistical significance of this data group in comparison with non-transduced activated T-cells (where no line is present) or between groups (where a line is present). * → P value 0.01 to 0.05; ** → P value 0.001 to 0.01; *** → P value 0.0001 to 0.001; **** → P value < 0.0001.

4.2.4 CAR T-cell enrichment

If MUC1 expressed on activated T-cells could engage MUC1 CARs, this might be expected to stimulate the CAR T-cells during their expansion, leading to their enrichment over time. To test this, CAR T-cell transduction efficiency was evaluated by flow cytometry on day 5 post transduction (see 2.2.11.1.2) and was re-evaluated on day 11. All three T-cell populations containing signalling-intact MUC1-specific CARs demonstrated a significant increase in the percentage of CAR-positive cells present on day 11, in comparison with day 5 (Figure 4.4A-C). T-cells engineered to express

TAB28z, H28z and HDF28z respectively demonstrated an average 24%, 20% and 31% increase in CAR expression over this period. By contrast, none of the signalling-defective anti-MUC1 CAR T-cell cultures presented a similar pattern of enrichment (Figure 4.4D-F).

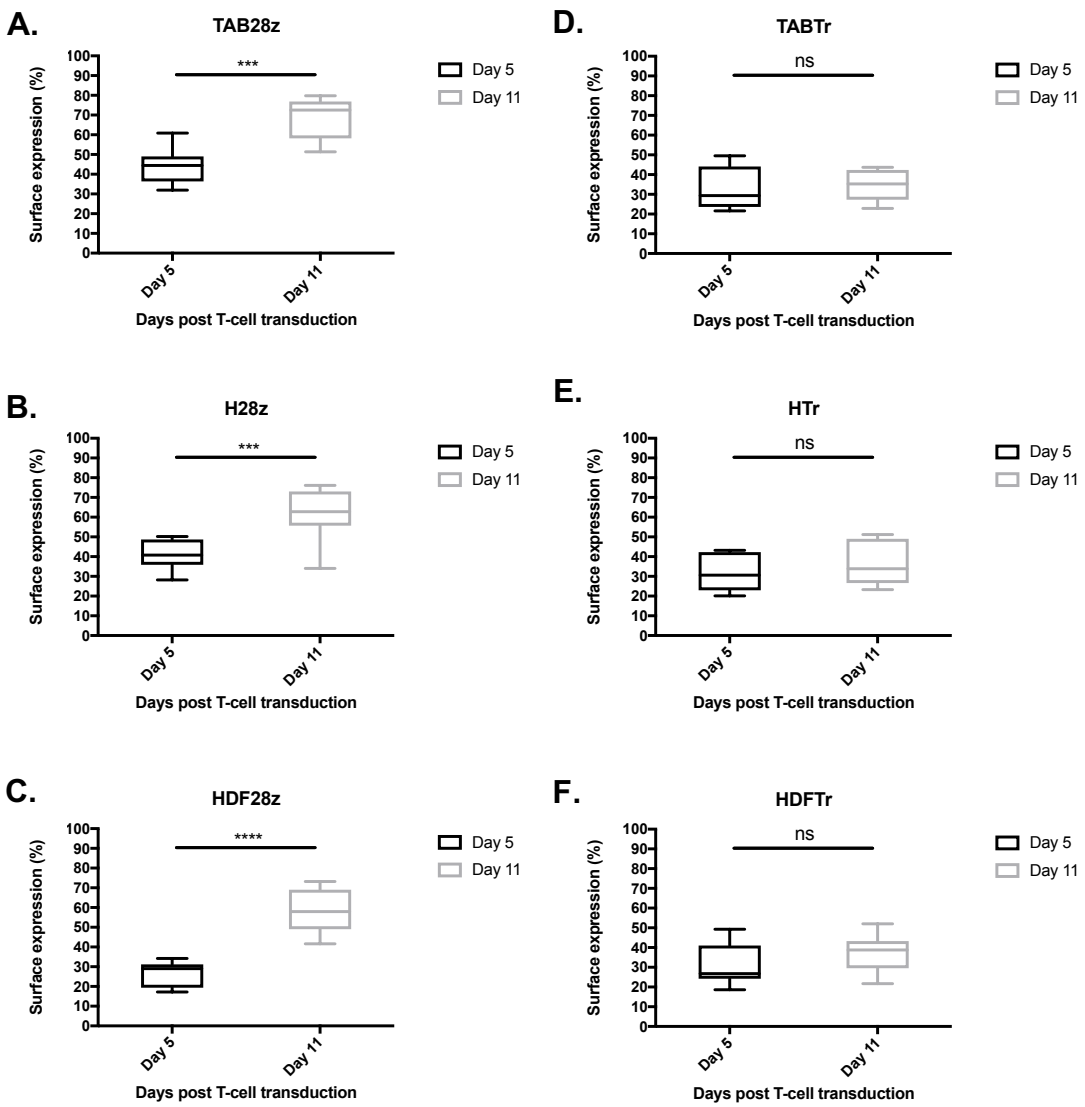

Figure 4.4: CAR T-cell enrichment during *in vitro* culture. Cell surface expression of the indicated CAR by human T-cells was investigated on day 5 and day 11 post T-cell transduction. The detection of CAR molecules on T-cells was evaluated using flow cytometry after addition of the MUC1 24mer peptide, followed by strepavidin-PE, as previously described in section 2.2.11.1.2. A-C) Signalling intact MUC1-specific CAR T-cells demonstrated a significant increase in the percentage of CAR-positive cells between day 5 and day 11 post T-cell transduction. Data are represented with box plots, showing minimum and maximum values, and are derived from n=9 independent replicates in the case of A-C,F and n=5 in the case of TABTr and HTr CAR T-cell populations. Statistical analysis was performed for each graph with a paired Student's *t*-test. * → P value 0.01 to 0.05; ** → P value 0.001 to 0.01; *** → P value 0.0001 to 0.001; **** → P value < 0.0001, ns → not significant.

4.2.5 Detection of MUC1 with different MUC1-specific antibodies

To establish the generality of these findings, three other anti-MUC1 antibodies were next used to detect MUC1 expressed on activated T-cells. As before, T-cells used herein were non-transduced and were activated with anti-CD3/anti-CD28 beads. The antibodies included in these experiments are HMFG1, SM3 and 5E5[287,320,380]. HMFG2 was additionally used for comparison purposes. Staining of activated T-cells was performed as described in section 2.2.10.1.5. In summary, different MUC1 levels were detected by each of these antibodies. Staining of T-cells with HMFG2 and HMFG1 antibodies showed broadly similar MUC1 surface expression, with mean expression levels of 16% and 13% respectively (Figure 4.5). By contrast, staining with the SM3 antibody demonstrated the highest levels of MUC1 (60%) while 5E5 showed minimal binding to the T-cells (2%).

As 5E5 showed no reactivity with MUC1 expressed on T-cells, I sought to investigate whether the 5E5 epitope might be suitable for a CAR T-cell-based immunotherapeutic approach for breast cancer. For this reason, detection of MUC1 by the 5E5 antibody was further investigated. In this experiment, five different breast cancer cell lines were stained with the 5E5 antibody and its reactivity was investigated with flow cytometry. The panel of breast cancer cell lines consisted of T-47, MDA-MB-468, ZR-75, SKBR3 and MCF7. Jurkat cells were additionally included as a positive control. MUC1 was detected on these cell lines at various levels, ranging from 0.5% to 50% (Figure 4.5B). As shown in the dot plots below, minimal MUC1 expression was

detected in the MDA-MB-468, ZR-75 and SKBR3 cell lines. Around 8% of T-47D cells were stained positively for MUC1 with the 5E5 antibody while MCF7 cells showed 50% surface expression.

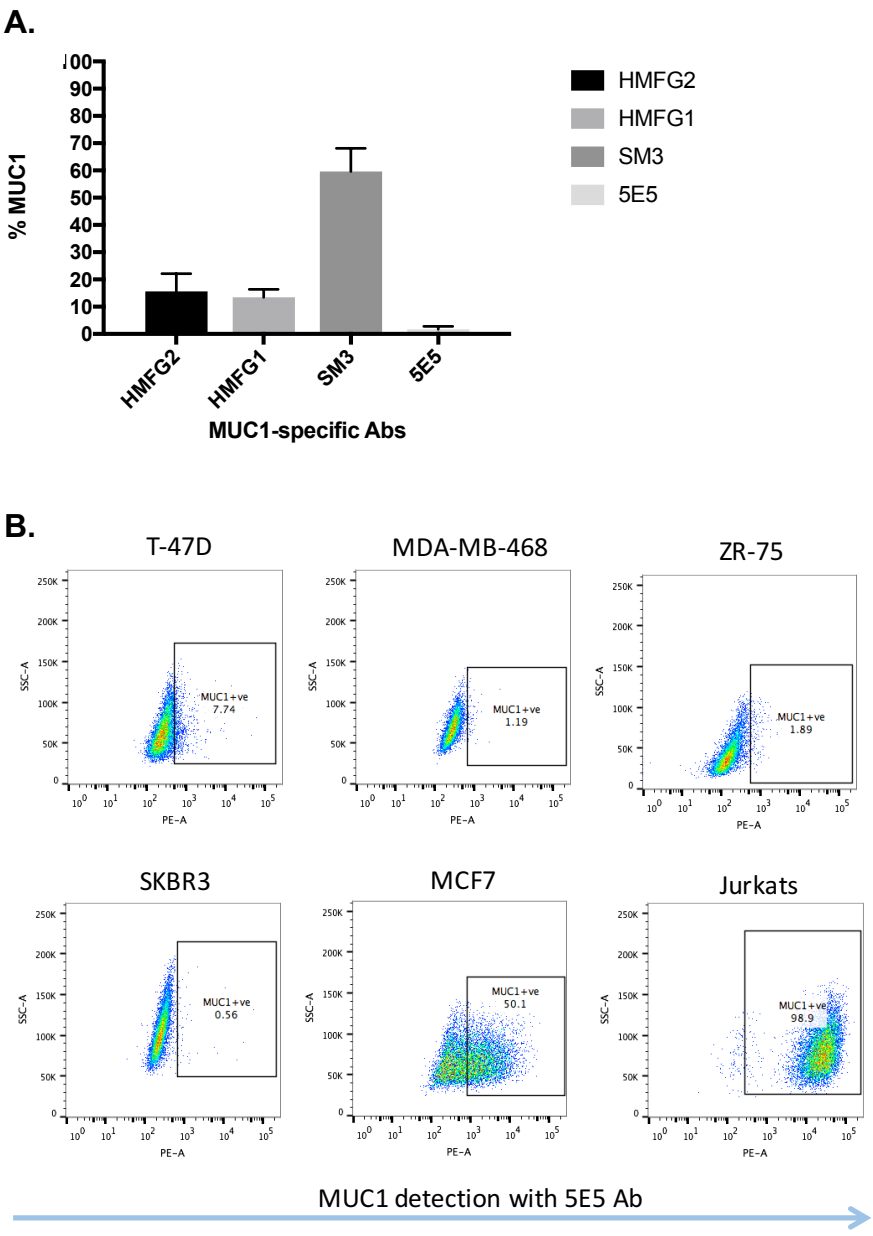

Figure 4.5: Detection of MUC1 with different MUC1-specific antibodies. A) The HMFG2, HMFG1, SM3 and 5E5 antibodies were used to detect MUC1 on the surface of activated human T-cells by flow cytometry (day 12 post T-cell activation). In each case, cells were stained with a biotinylated primary antibody followed by streptavidin-PE. Cells stained with biotinylated mouse IgG1 followed by streptavidin-PE were used as negative-control. Data shown are mean + SEM of n=7 independent replicates. B) The 5E5 antibody was used for the detection of MUC1 in a panel of five breast cancer cell lines, using flow cytometry analysis. The cells were stained with the biotinylated 5E5 antibody, followed by streptavidin PE. Jurkat cells stained in the same way were used as a positive control (known to express high levels of Tn – add a reference). Cells stained with biotinylated mouse IgG1 isotype control followed by streptavidin PE, were used as negative control. The results from this analysis are presented herein as dot plots and are representative of n=2 independent replicates.

4.2.6 MUC1 expression on MUC1-specific CAR T-cell populations

The data presented above indicate that TA-MUC1 was detected on the surface of human, non-transduced activated T-cells. Given these findings, I next investigated serial expression of MUC1 post T-cell activation by the CAR T-cells under study. This was achieved by staining all six CAR T-cells populations (signalling-intact and non-signalling control CARs) with the HMFG2 anti-MUC1 antibody. Non-transduced T-cells were also included in these experiments. It should be noted that T-cells were transduced to express the different CAR molecules on day 2 post activation.

In general, MUC1 was detected at the highest levels either on day 5 or day 7 post T-cell activation, while levels had declined by day 14 (Figure 4.6). Surprisingly, different levels of MUC1 were observed on each T-cell population, with this difference being most apparent at day 7. At this time-point, MUC1 expression was observed to be higher in the H28z$^+$ and HTr$^+$ CAR T-cells, with mean expression levels of 49% and 31% respectively (Figure 4.6). Non-transduced T-cells presented a mean of 24% MUC1 expression while HDF28z$^+$ and HDFTr$^+$ CAR T-cells showed 10% and 15% average expression respectively. Notably, MUC1 was detected at lower levels in the TAB28z$^+$ and TABTr$^+$ CAR T-cell populations with 6% and 3% average expression respectively (Figure 4.6). While differences were not statistically significant, these data confirm that TA-MUC1 could also be detected on these CAR T-cell populations.

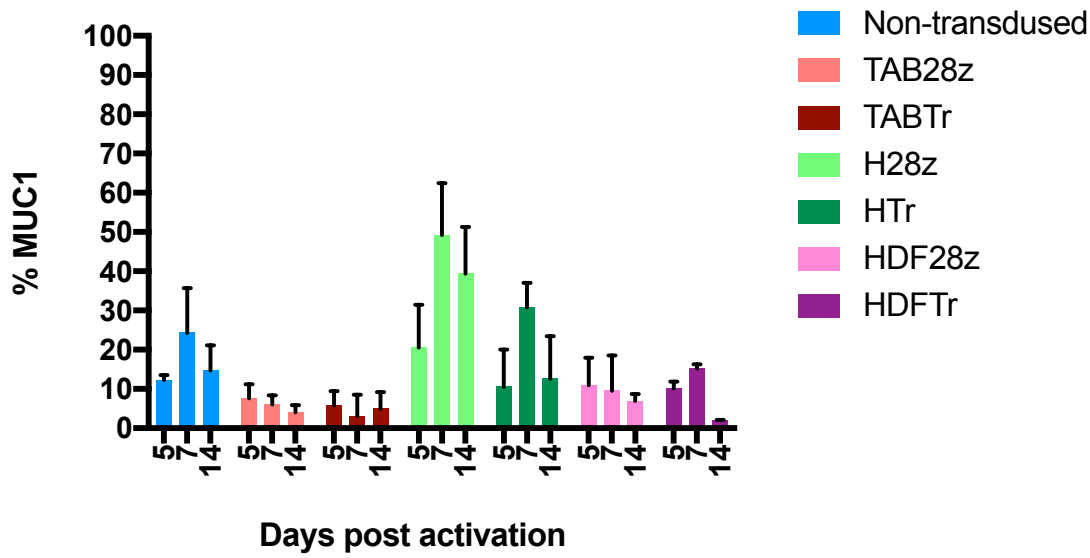

Figure 4.6: MUC1 expression on the indicated MUC1-specific CAR T-cell populations. Cell surface expression of MUC1 on the six different CAR T-cell populations was investigated using flow cytometry on day 5, day 7 and day 14 post T-cell activation. T-cells were stained with biotinylated HMFG2 antibody, followed by streptavidin PE. T-cells stained with biotinylated mouse IgG1 isotype control, followed by streptavidin PE, were used as negative control. As previously mentioned, PBMCs were isolated from healthy volunteers and T-cells were activated with CD3/CD28 beads. T-cells were expanded as per usual (IL-2 and R5 supplementation every other day) and they were retrovirally transduced to express the CAR molecules at day 2 post activation. Data shown are mean + SEM of n=3 independent replicates. Statistical analysis was performed with One-way ANOVA, followed by Tukey post hoc test. No statistically signifficant differences were observed.

4.2.7 CD4$^+$ and CD8$^+$ composition of MUC1-retargeted CAR T-cells

The percentage of CD4-positive and CD8-positive T-cells within each CAR T-cell population was defined by flow cytometry analysis. This analysis demonstrated that the CAR T-cell populations under study consisted of broadly similar proportions of CD4$^+$ and CD8$^+$ T-cells (Figure 4.7). None of the minor differences observed between populations reached statistical significance. In these experiments, non-transduced T-cells were also included

as an additional control. The latter contained a similar proportion of $CD4^+$ and $CD8^+$ cells to the CAR T-cell populations mentioned above (Figure 4.7).

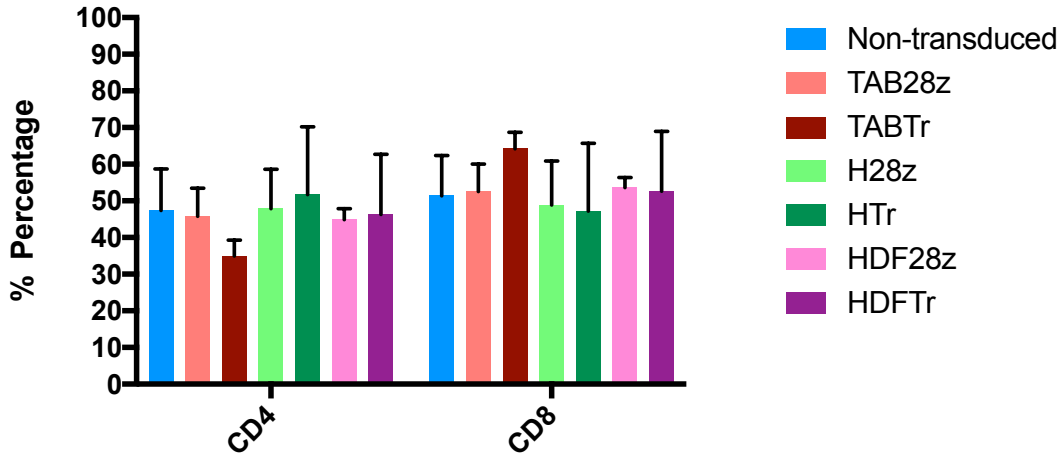

Figure 4.7: Proportion of $CD4^+$ and $CD8^+$ T-cells present in MUC1-specific CAR T-cell populations. The percentage of $CD4^+$ and $CD8^+$ T-cells in each CAR T-cell population was defined using flow cytometry, performed on day 11 post T-cell transduction. For this purpose, cells were stained with CD3-FITC and CD8-PECy7 conjugated antibodies. Non-transduced T-cells were also included in these assays. The positive and negative populations were defined by using fluorescence minus one (FMO) controls. Data shown are mean + SEM of n=2-3 independent replicates. Statistical analysis was performed with One-way ANOVA, followed by Tukey post hoc test. No statistically significant differences were observed between groups.

4.2.8 Investigation of activation status of MUC1-specific CAR T-cells

If MUC1 re-targeted CAR T-cells could engage TA-MUC1 expressed on cells within the culture, this would be expected to activate the cells, perhaps leading to cell loss via fratricide or activation-induced death, enrichment of transduced cells and release of IFN-γ. To test if the MUC1 re-targeted CAR T-cells were indeed more activated, expression of CD69 was compared

between the signalling-intact and signalling-defective CAR T-cell populations under study. Surface CD69 expression was measured by flow cytometry analysis which was performed at two distinct time-points, namely at day 5 and at day 11 post T-cell transduction. A similar tendency was observed at both time-points, although it was more apparent on day 11 post transduction (Figure 4.8). A trend was noted whereby all three MUC1-signalling CAR T-cell populations presented higher detectable levels of CD69 in comparison with the negative-control T-cell populations, although differences were not statistically significant. Additionally, all T-cell populations presented increased CD69 expression at day 11 in comparison with day 5 post-transduction (Figure 4.8).

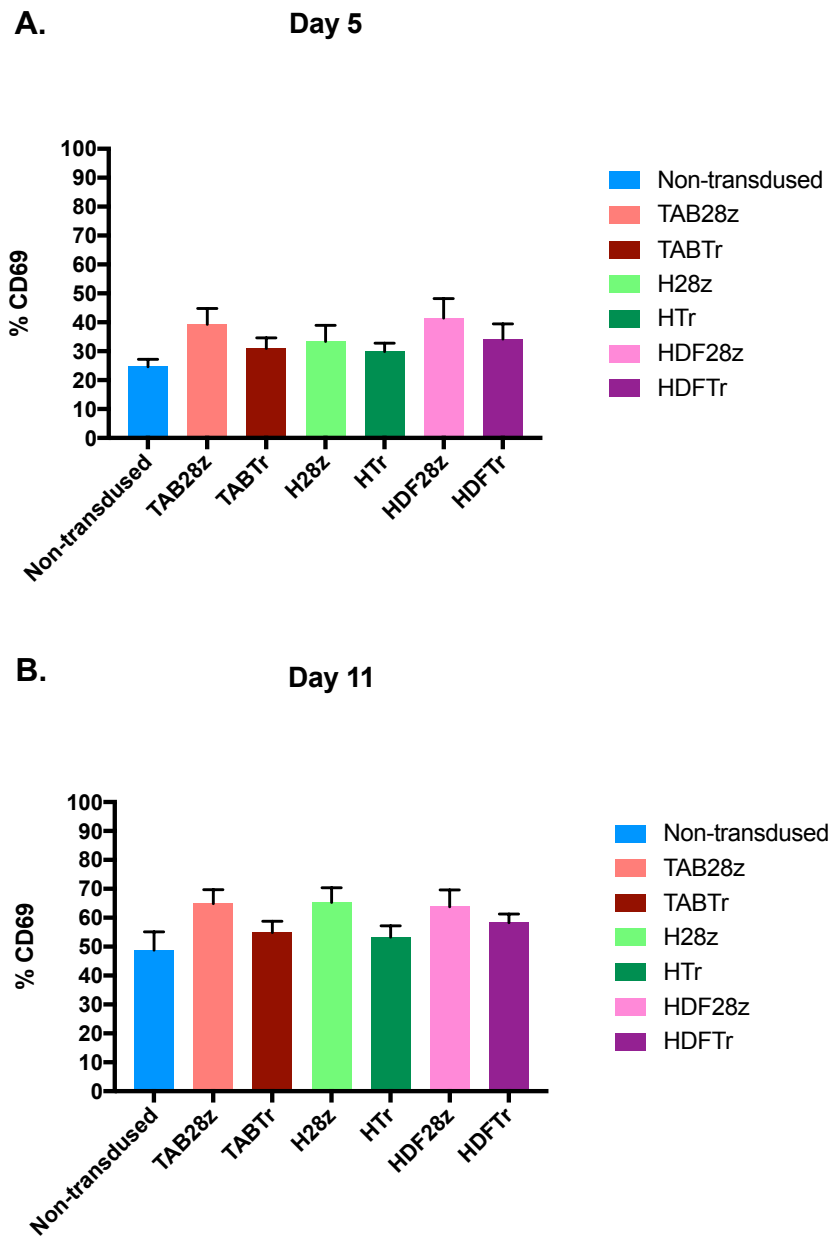

Figure 4.8: Expression of CD69 by the indicated CAR T-cell populations. Surface expression of CD69, a T-cell activation marker, was investigated in all six MUC1-specific CAR T-cell populations. Non-transduced T-cells were also included in these experiments for comparison purposes. Expression of CD69 was determined using flow cytometry analysis, performed on day 5 and day 11 post T-cell transduction. Data shown are mean + SEM of n=7 independent replicates for Day 5 post transduction and of n=6 for Day 11 post transduction. Statistical analysis was performed with One-way ANOVA, followed by Tukey post hoc test.

4.2.9 Expression of exhaustion markers on MUC1-specific CAR T-cells

Constitutive activation of MUC1 CAR T-cells by cell surface MUC1 would be expected to promote the exhaustion of these cells, owing to tonic signalling. To investigate this, I measured the expression of T-cell exhaustion markers in the distinct MUC1 re-targeted CAR T-cell populations. Cell surface expression of PD-1, TIM-3 and CTLA-4 was investigated in both $CD4^+$ and $CD8^+$ subsets in all cases. Non-transduced T-cells were also included in these experiments as an additional control. The assay was performed at day 11 post T-cell transduction.

As shown in the bar graph below, all three signalling-intact MUC1 CAR T-cells exhibited a trend towards higher expression of PD-1, in comparison with their matched-truncated control CAR T-cells (Figure 4.9A-B). This trend was more apparent in the $CD8^+$ cell subset (Figure 4.9, B). Similarly, TIM-3 presented increased surface expression in all three signalling CAR T-cell populations, in both $CD4^+$ and $CD8^+$ subsets (Figure 4.9C-D). Additionally, MUC1-signalling CARs presented increased expression of CTLA-4, nevertheless this was observed only in the $CD8^+$ T-cell subset (Figure 4.9E-F). As shown herein, all three-signalling MUC1-specific CARs presented similar expression levels of exhaustion markers to each other. It should be noted that despite the trend of upregulation of exhaustion markers by the three signalling CAR T-cells, the study was underpowered thus no strong statements can be made.

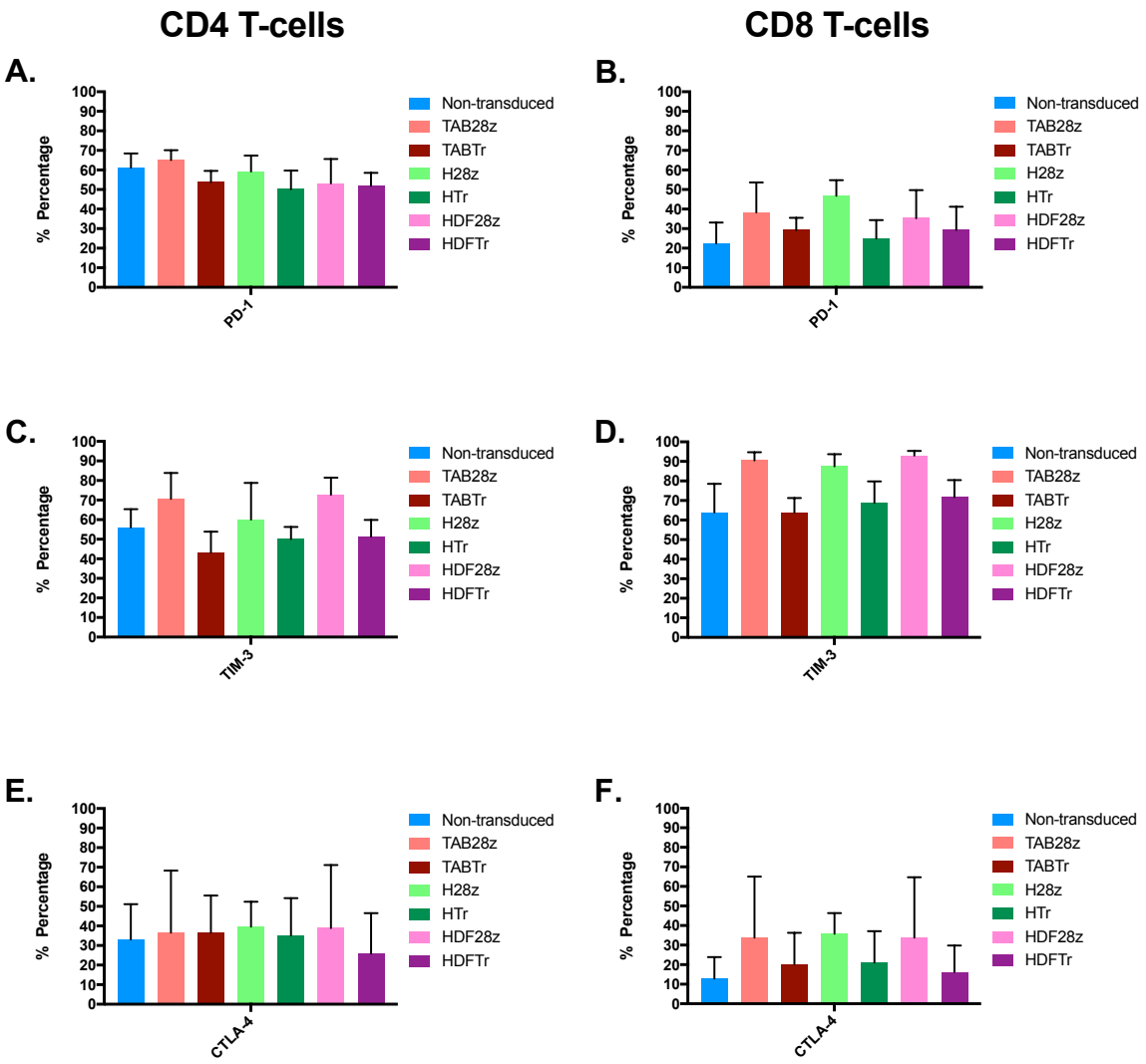

Figure 4.9: Expression of exhaustion markers on CAR T-cell populations. The surface expression of PD-1, TIM-3 and CTLA-4 was investigated in $CD4^+$ and $CD8^+$ CAR T-cell populations using flow cytometry analysis. The assay was performed at day 11 post T-cell transduction. A-B) expression of PD-1 in the six CAR T-cell populations and in non-transduced T-cells, C-D) expression of TIM-3 in the six CAR T-cell populations and in non-transduced T-cells, E-F) expression of CTLA-4 in the six CAR T-cell populations and in non-transduced T-cells. Data shown are mean + SEM of n=3 independent replicates for PD-1 and TIM-3 expression analysis and of n=2 independent replicates for CTLA-4. No statistical analysis was performed as the study was underpowered.

4.2.10 T-cell differentiation stage of MUC1-specific CAR T-cells

Next, I compared the state of differentiation of the distinct CAR T-cell populations, making comparison with signalling defective control CAR T-cells. This was investigated at day 11 post T-cell transduction using flow cytometry. As previously described (section 2.2.10.1.7), stage of differentiation of both $CD4^+$ and $CD8^+$ cell CAR T-cells was defined with the use of CD45RO and CCR7 markers.

In regard to $CD4^+$ T-cells, all three signalling-intact CAR T-cells showed a slightly increased central memory cell population ($CCR7^+$ $CD45RO^-$) (Figure 4.10). Additionally, a higher percentage of cells with an effector memory phenotype ($CCR7^+$ $CD45RO^+$) was observed in the negative control cell populations (non-transduced cells and signalling-defective CAR T-cells) (Figure 4.10).

In regard to $CD8^+$ T-cells, a trend towards a higher percentage of naïve cells was observed in the negative control T-cell populations (Figure 4.10). Additionally, a trend towards increased numbers of central memory T-cells was observed in the $CD8^+$ signalling CAR T-cell populations (Figure 4.10). Overall however, differences were minor and did not reach statistical significance.

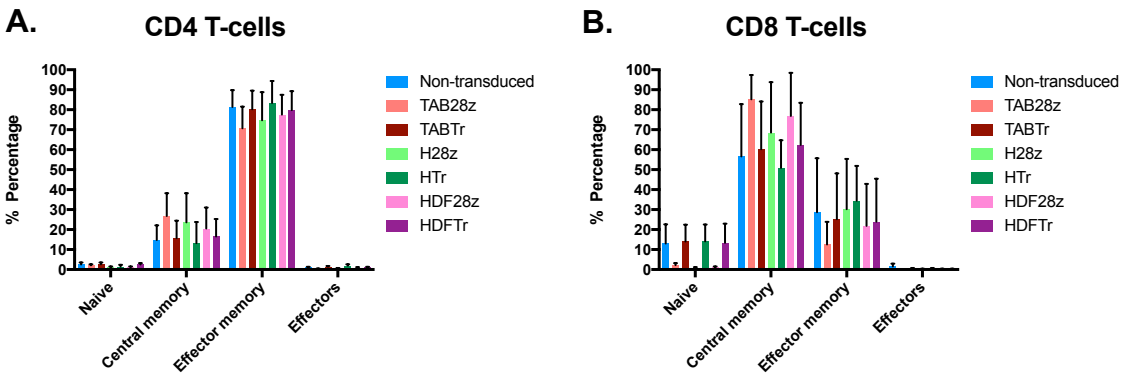

Figure 4.10: State of T-cell differentiation of MUC1 re-targeted CAR T-cells. Differentiation status of $CD4^+$ and $CD8^+$ T-cell subsets within the indicated the CAR T-cell populations was defined using flow cytometry analysis, performed at day 11 post-transduction. Non-transduced cells were included in this analysis for comparative purposes. The four distinct differentiation stages, naïve, central memory, effector memory and effectors were defined with the use of the CD45RO and CCR7 markers and FMO controls. A) differentiation of $CD4^+$ T-cells, B) differentiation of $CD8^+$ T-cells. Data shown are mean + SEM of n=2-3 independent replicates. Statistical analysis was performed with One-way ANOVA, followed by Tukey post hoc test. No statistical signifficances were observed.

4.3 Discussion

Results presented in Chapter 3 indicate that all of the MUC1-specific signalling intact CAR T-cells under study in this thesis release IFN-γ in the absence of co-culture with MUC1-positive tumour cells. This led to the hypothesis that MUC1 re-targeted CAR T-cells might recognise MUC1 expressed on activated T-cells, resulting in their activation during *in vitro* expansion. Herein, I present results that strongly support this hypothesis.

Based on the above, I sought to investigate if the HMFG2 antibody binds MUC1 on activated T-cells. HMFG2 antibody was used in these assays since two out of three signalling anti-MUC1 CARs contain an scFv derived from the HMFG2 antibody. Furthermore, this antibody has been reported to bind preferentially to tumour-associated glycoforms of this mucin[288,295]. As hypothesized previously, HMFG2 binding to the surface of activated T-cells was indeed detected, with peak levels observed at day 5 to day 7 post-activation. MUC1 surface expression on activated T-cells have been previously shown in numerous studies, using different MUC1-specific antibodies[375–378,381]. Results published by Agrawal *et al.* have shown similar findings to those presented here, whereby MUC1 surface expression decreased over time, upon removal of mitogen. The recognition of MUC1 by HMFG2 on T-cells was unpredicted as a previous study by Correa *et al.* has shown lack of binding of this antibody to activated T-cells[378]. Experimental differences, such as method of T-cell activation could potentially explain these differences. As shown in Figure 4.1, cell surface MUC1 was absent on resting PBMCs. The latter supports the results of three other studies, in which MUC1

was not detected on resting T-cells[377,378,381]. A study by Chang *et al.* has shown expression of MUC1 on resting T-cells, nevertheless this was not validated neither by my results or by the results of the studies mentioned previously[376].

To track the expression of MUC1 with T-cell activation status, expression of CD69 was quantified. As described in section 4.2.1, MUC1 was detected later on following T-cell activation than was the case with CD69. This finding is in agreement with results published by Agrawal *et al.* and by Correa *et al.* as both groups have reported that MUC1 appeared in the surface of activated T-cells later than CD69 or CD25[375,378]. Agrawal *et al.* have also shown co-expression of MUC1 and T-cell activation markers (CD69 and CD25), with the percentage of co-expression being higher in the later stages post T-cell activation[375]. This does not agree with my results, whereby minimal co-expression of MUC1 and CD69 was observed. These divergent findings could be attributed to the use of different methods to achieve T-cell activation, use of the different antibodies to detect MUC1 on T-cells or other differences in culture conditions. Agrawal *et al.* used phytohemagglutinin (PHA)-activated T-cells and cultured the cells in the continued presence of PHA[375]. By contrast, in my experiments I activated T-cells with anti-CD3 and anti-CD28 coated beads and supplemented the media with IL-2 every other day. It would be interesting to explore further if different stimuli used to achieve T-cell activation could potentially affect MUC1 expression levels and the co-expression of this mucin with other T-cell activation markers.

The effect of this background MUC1 recognition on T-cells on MUC1-specific CAR T-cells was further documented. All three signalling-intact

MUC1-specific CAR T-cell populations achieved a significantly lower total cell count after 10-days of expansion, in comparison with the untransduced or endodomain truncated control CAR T-cell populations. A possible explanation for this is that the CAR T-cells recognise MUC1 expressed on neighbouring T-cells, leading to elimination of these T-cells by fratricide. Others have observed reduced expansion of some CAR T-cell populations; nevertheless this was attributed to tonic signalling and T-cell exhaustion as no expression of the targeted-antigen was observed on T-cells[241]. Another study reported increased proliferation of continuously activated CAR T-cells[361]. Nonetheless, this was observed when T-cells were expanded in the absence of cytokines[361]. Consequently, it would be interesting to conduct a similar experiment in which expansion of MUC1-specific signalling intact and control CAR T-cells is compared in the absence of IL-2 support. Another explanation for the reduced cell count of the signalling MUC1-specific CAR T-cells could be that they underwent apoptosis due to activation-induced cell death (AICD). Under normal condition, T-cells might undergo AICD upon antigen encounter which leads to T-cell apoptosis via the Fas-FasL signalling pathway[382]. This phenomenon has also been documented in CAR T-cell studies. Künkele *et al.* have reported that CAR components can make the CAR T-cells more susceptible to FasL-mediated AICD upon prolonged antigen exposure[383]. A similar observation was made by Gargett and colleagues who reported that repeated antigen stimulation induced AICD to GD-2 CAR T-cells[384].

Another observation that supported the hypothesis that MUC1 CARs signal tonically due to target recognition on T-cells is the fact that MUC1-signalling intact CAR T-cells underwent enrichment during their expansion.

Importantly, T-cells engineered to express all three signalling-defective CARs did not present this pattern. A similar observation has been reported by Frigault *et al.,* whereby continuously activated CAR T-cells demonstrated enrichment during their *ex vivo* expansion[361].

An important question is whether the MUC1 detected on T-cells is decorated with core-1 (tumour-associated) or core-2 (normal) glycans. To explore this, I investigated MUC1 expression on T-cells using three other MUC1-specific antibodies (HMFG1, SM3, 5E5). Each of these antibodies has different reactivity with the various forms of MUC1 found in normal and tumour cells. SM3 specifically recognises tumour-associated glycoforms with little to no reaction to benign tumour cells or non-malignant cells[320]. HMFG1 and HMFG2 both react very strongly with tumour-associated MUC1[316]. Nevertheless, they have shown some reactivity with normal lactating breast, with HMFG1 showing stronger recognition of these tissues[288,317,320].

Notably, as shown in Figure 4.5, SM3 presented the strongest reactivity with T-cell-associated MUC1. This result supports the findings of Agrawal *et al.* where they have reported 54% binding of SM3 to MUC1 on activated T-cells[375]. This would suggest that MUC1 detected on T-cells is mainly decorated with “tumour-associated” glycans. Nevertheless, this does not agree with Correa *et al.* who reported an absence of binding by the SM3 antibody to activated or resting T-cells[378]. They suggested that MUC1 expressed on activated T-cells is decorated with core-2 and not core-1 glycans, indicated by the lack of binding of both SM3 and HMFG2 to MUC1 in their experiments[378]. The time-point at which the flow-cytometry assay is performed may be crucial in this regard and could potentially explain the

differences in results obtained in both of these studies. Correa *et al.* have shown that HMFG2 and SM3 antibodies did not recognise MUC1 on T-cells. Nevertheless, they do not specify in which time-point post activation the flow-cytometry analysis was performed[378]. As indicated by the results shown in Figure 4.1, timing is important as MUC1 was undetectable by HMFG2 in the early time-points post activation. Another explanation could be, as mentioned previously, use of different protocols to culture and activate T-cells in both studies. Further research needs be conducted in order to understand the glycosylation pattern of MUC1 expressed on T-cells and to investigate if the method of activation has any role in influencing this process.

Another interesting observation is that the 5E5 antibody showed minimal detection of MUC1 on T-cells. It is known that the 5E5 antibody recognises specifically the MUC1-Tn/STn glycoforms[380,385]. Posey *et al.* have recently generated a MUC1-specific CAR T-cell immunotherapy approach, where they have an engineered a CAR based on the 5E5 antibody[337]. In this approach, this MUC1-specific CAR has been used to target leukaemic and pancreatic tumours overexpressing MUC1-Tn[337].

As 5E5 did not show any reactivity with MUC1 expressed on T-cells, one could suggest that the approach developed by Posey *et al.* is advantageous. Based on this, I sought to investigate the potential of developing a 5E5-based CAR to target MUC1-positive breast cancer. Thus, I investigated the detection of MUC1 by the 5E5 antibody in various breast cancer cell lines. As shown in Figure 4.5, 5E5 did not show reactivity with the majority of breast cancer cell lines used in this assay, with the exception of T-47D, where minimal binding was observed and MCF7 with moderate binding

levels. Others have reported low surface expression of the MUC1 Tn/STn glycoforms in these two breast cancer cell lines[385]. The latter suggests that a 5E5-based immunotherapeutic approach for the treatment of breast cancer might not be broadly beneficial. Additionally, it highlights the challenge in CAR T-cell immunotherapy in finding the right balance between targeting a widely-expressed antigen and limiting the risk of on-target off-tumour toxicities.

Having demonstrated that “tumour associated” glycoforms of MUC1 are also found on activated T-cells, I explored the MUC1 expression levels on the different CAR T-cell populations. I hypothesized that lower MUC1 levels would be detected on the signalling intact CAR T-cell populations due to depletion of the MUC1-positive cells. Nevertheless, this was not confirmed in my study. An unexpected observation was that CAR T-cells engineered to express H28z exhibited higher levels of MUC1 in comparison with non-transduced T-cells. This higher expression did not seem to be dependent on the signalling activity of the CAR as HTr also presented increased MUC1 expression. Interestingly, the TAB004-transduced CAR T-cells demonstrated the lowest MUC1 surface expression. One explanation could be the different percentage of CD4 and CD8 subsets within each T-cell population examined herein. As previously indicated, $CD4^+$ T-cells tend to present higher levels of MUC1 when compared to the $CD8^+$ cell subset. Thus, a higher percentage of $CD4^+$ T-cells within the high MUC1-expressing cell populations could be an explanation for this result. This possibility was refuted by the results shown in Figure 4.7, as non-significant differences were observed in the percentage of $CD4^+$ and $CD8^+$ T-cells found in these populations. Further experiments need to be conducted in order to understand the differences in MUC1 levels

between the CAR T-cell populations under study. Published results suggest that MUC1 expression is strongly correlated with cell proliferation rate and mitotic division[381]. Thus, a labelling experiment using a dye such as carboxyfluorescein succinimidyl ester (CFSE) could be performed in order to explore if they are any differences in the proliferation rate of the distinct CAR T-cell populations.

It was also important to characterise the effect of prolonged recognition of MUC1 upon the anti-MUC1 re-targeted CAR T-cells. A trend towards increased T-cell activation was observed in all three signalling-intact CAR T-cell population, as indicated by the increased surface expression of CD69. This was expected and fits with the hypothesis described above, since continued recognition of MUC1 by the CAR T-cells could potentially sustain their activation. These results are in agreement with those of Frigault *et al.* and Long *et al.* who both reported that constitutive CAR signalling resulted in increased T-cell activation[241,361].

It is known that prolonged T-cell activation can result in T-cell exhaustion. For this reason, expression of three exhaustion markers, PD-1, TIM-3 and CTLA-4 was also investigated in all CAR T-cell populations, hypothesizing that the signalling-CARs would present increased levels. Indeed, a trend towards further upregulation of exhaustion markers was observed in all three signalling-intact CAR T-cell populations. Long *et al.* have published similar results whereby tonic CAR signalling led to T-cell exhaustion[241].

Lastly, I sought to characterise the differentiation stage of signalling intact MUC1 specific CAR T-cells. I hypothesized that prolonged MUC1

recognition could potentially lead to terminal differentiation of the MUC1-signalling CARs[361]. Surprisingly, a trend was observed where signalling CAR T-cells presented an increased central memory phenotype in comparison with their matched truncated controls. Nevertheless, no strong statements can be made due to lack of statistical significance of the data. More experimental repeats need to be performed in order to explore if the same trend is observed in a larger number of donors.

As shown previously, MUC1 expression on activated T-cells could significantly hinder T-cell expansion. Additionally, signalling-intact MUC1-specific CAR T-cells presented a trend of increased T-cell activation and up-regulation of exhaustion markers. A potential way to overcome these issues would be to isolate and transduce only MUC1-negative T-cell subsets. For this reason, it was of crucial importance to explore if MUC1 is expressed selectively in either CD4 or CD8 T-cell subsets. The results presented here indicate that MUC1 is upregulated on both activated $CD4^+$ and $CD8^+$ T-cells, with higher expression levels on the $CD4^+$ subset. Thus, this strategy could not be used in order to limit the consequences of background MUC1 recognition. My results are in agreement with Agrawal *et al*., who have reported higher MUC1 expression on CD4-positive PHA activated T-cells in comparison with CD8-positive cells[377]. However, these findings do not agree with the results of Correa *et al.*, who reported absence of reactivity with the HMFG2 antibody and similar levels of MUC1 expression on both $CD4^+$ and $CD8^+$ T-cells. Nevertheless, is impossible to comment further on the latter finding, since these data are not shown in their publication[378].

4.4 Conclusions

Different observations have led to the hypothesis that the MUC1-signalling CARs used herein recognise MUC1 expressed on T-cells. These observations include the i) production of IFN-γ by signalling-intact CAR T-cells in the absence of exposure to MUC1-positive tumour cells, ii) reduced cell expansion of signalling-intact CAR T-cells and iii) enrichment of MUC1 re-targeted CAR T-cells (but not T-cells containing matched control CARs) during *in vitro* expansion. Upon investigation, it was shown that HMFG2 bound to MUC1 expressed on activated T-cells. This result was unpredicted as previous studies have shown that the MUC1 found on T-cells carries predominantly “normal” extended glycan forms, which are not recognised by HMFG2.

The consequences of this finding for the behaviour of CAR T-cells was further investigated. As discussed previously, signalling intact CAR T-cells presented a trend towards a more activated and exhausted phenotype. Despite these observations, MUC1-specific CAR T-cells demonstrated significant cytotoxic activity against MUC1-positive breast cancer cell lines, as shown in chapter 2. Thus, I sought to explore further their activity *in vivo*. These results are presented in the next chapter (Chapter 5).

Chapter 5: *In vivo* efficacy of MUC1-specific CAR T-cells

5.1 Introduction

5.1.1 Assessment of efficacy and safety of CAR T-cells in pre-clinical models

Adoptive cell therapy is rapidly moving from bench to bed-side. In light of this, use of pre-clinical mouse models that recapitulate human malignancies is mandatory prior to the transition of a therapeutic strategy into the clinic.

One widely used mouse model for the pre-clinical assessment of efficacy and safety of CAR T-cell immunotherapy entails tumour xenograft implantation into immunodeficient mice. These models are often orthotopic, whereby immortalised human tumour cells are injected into the relevant anatomic side. An essential requirement for tolerance of cells of human origin (either CAR T-cells or tumour cells) is that the mice need to be immunodeficient. A number of commonly used immunocompromised mouse strains are athymic nude, NOD/SCID and SCID/Beige[296,386–391]. Nevertheless, residual mouse immune compartments in these models can potentially hinder the engraftment of human T-cells. In recent studies, NSG mice have increasingly been used for the assessment of *in vivo* efficacy of CAR T-cells[337,392,393]. This mouse strain is advantageous due to the presentation of extreme immunodeficiency, thus allowing for optimal T-cell engraftment[327]. In general, xenograft mouse models have predicted accurately the efficacy of some CAR T-cell approaches[278,394]. Nevertheless, due to absence of innate immune system-therapy interaction, they cannot often predict different type of

toxicities related to CAR T-cell therapy, such as cytokine release syndrome[211,395].

Another type of mouse model often used by investigators involves the administration of murine CAR T-cells, specific for the mouse homologue of a human antigen, into mice with an intact immune system. In this model, murine T-cells are transduced with a CAR construct which has been engineered using murine compartments. The latter minimises the immunogenicity of the CAR T-cells and provides the benefit of being able to better predict toxicities related to either cytokine release syndrome or on-target off-tumour reactivity[278,394,396,397]. Nevertheless, there are two essential parameters required for the use of this model. First, the human and murine proteins must have very high homology. Second, a similar expression pattern should be observed between the mouse and human homologues[398].

5.1.2 *In vivo* breast cancer models for evaluation of CAR T-cell immunotherapy

Various studies have evaluated the efficacy of CAR T-cells in breast cancer animal models. Xenograft mouse models are commonly used for this purpose. In these studies, different human breast cancer cell lines have been inoculated either subcutaneously or into the peritoneal cavity of immunocompromised mice. Tumour progression has been evaluated with either caliper measurements or bio-luminescence imaging (BLI), depending on the site of tumour injection. The route of administration of CAR T-cells

varies depending on the model, with the intravenous and intraperitoneal routes most commonly used.

Subcutaneous injection of breast cancer cells in the flank of mice is widely used to investigate the effect of novel therapies due to its simplicity. At least three studies investigating the efficacy of CAR T-cells have reported the use of immortalised breast cancer cell lines injected subcutaneously in immunocompromised mice[399–401]. The efficacy of folate receptor-alpha (FRα)-specific CAR T-cells was assessed in NSG mice established with MDA-MB-231 subcutaneous tumours[399]. In this study, CAR T-cells were injected intravenously and tumour growth was monitored with both caliper and BLI, as the tumour cells were engineered to express firefly luciferase[399]. In a similar manner, *in vivo* assessment of a HER-2-specifc second generation CAR was performed in NOD/SCID mice inoculated subcutaneously with SKBR3 tumour cells[400]. Other cell lines used in a similar manner include MDA-MB-453 and HCC1954[401].

Three other studies have reported the use of xenograft models where immortalised human breast cancer cells have been injected in the intra-peritoneal cavity of immunodeficient mice[269,295,296]. In all instances, CAR T-cells were administered locally in the peritoneal cavity. For example, Whilding *et. al* used a xenograft model for the assessment of efficacy of a CAR specific for αvβ6 integrin[296]. For this purpose, MDA-MB-468 cells were injected into the peritoneal cavity of NSG mice.

Xenograft breast cancer models, where tumour cells are engrafted subcutaneously or in the peritoneal cavity, provide a non-invasive, quick and convenient method for the evaluation of response to treatment[402]. Others have

used immunodeficient mice to orthotopically inject breast cancer cells in the mammary fat pad. The latter provides the advantage of more closely recapitulating the human disease in mice. Nevertheless, this usually requires mammary fat pad clearance through surgery, a fact that makes this method impractical. Only one study has reported the use of this method for the evaluation of CAR T-cell activity, where the investigators implanted MDA-MB-231 cells in the mammary fat pad[401].

5.1.3 Aim

Previous results presented in Chapter 2 have indicated significant *in vitro* cytotoxic activity of TAB28z CAR T-cells against MUC1-expressing breast cancer cell lines. This was observed despite the continuous activation of CAR T-cells due to recognition of MUC1 expressed on the surface of activated T-cells.

In this chapter, I present results related to the *in vivo* assessment of activity of TAB28z CAR T-cells. In parallel, its activity was compared with H28z and HDF28z-engineered CAR T-cells in order to investigate if this CAR performs in a superior manner. In detail, the data presented herein include the i) generation of firefly-luciferase –positive breast cancer cell lines to allow for bio-luminescence monitoring of tumour growth, ii) establishment of xenograft breast cancer mouse models, iii) *in vivo* evaluation of anti-tumour activity of MUC1-specific CAR T-cells.

5.2 Results

5.2.1 Engineering of firefly luciferase-expressing breast cancer cells

A robust way of monitoring tumour growth in mouse models entails the use of bio-luminescence imaging. The initial step undertaken, prior to designing a pilot study for the establishment of a xenograft model, was to generate firefly luciferase (ffluc)-expressing breast cancer cells. For this purpose, T-47D and MDA-MB-468 tumour cells were transduced with an SFG retroviral vector (Figure 5.1A, Figure 2.7) in which tandem dimer (td)Tomato (a red fluorescent protein), was co-expressed with ffluc. The presence of tdTomato allows easy assessment of transduction efficiency and flow sorting of cells where required. Both T-47D and MDA-MB-468 cell lines were highly transduced (>76%), as evaluated by detecting tdTomato with flow cytometry (Figure 5.1C). Furthermore, a luciferase assay was performed in order to validate ffluc expression by these cells. In this assay, different cell dilutions were used in order to define the range of detectable levels of bioluminescence. As depicted in Figure 5.1B, luminescence was detected in both cell lines upon addition of D-luciferin, with the lowest detectable levels produced by 10^4 cells. Surface expression of MUC1 was additionally validated in both cell lines post-transduction with ffluc_tdTomato (Figure 5.1 D).

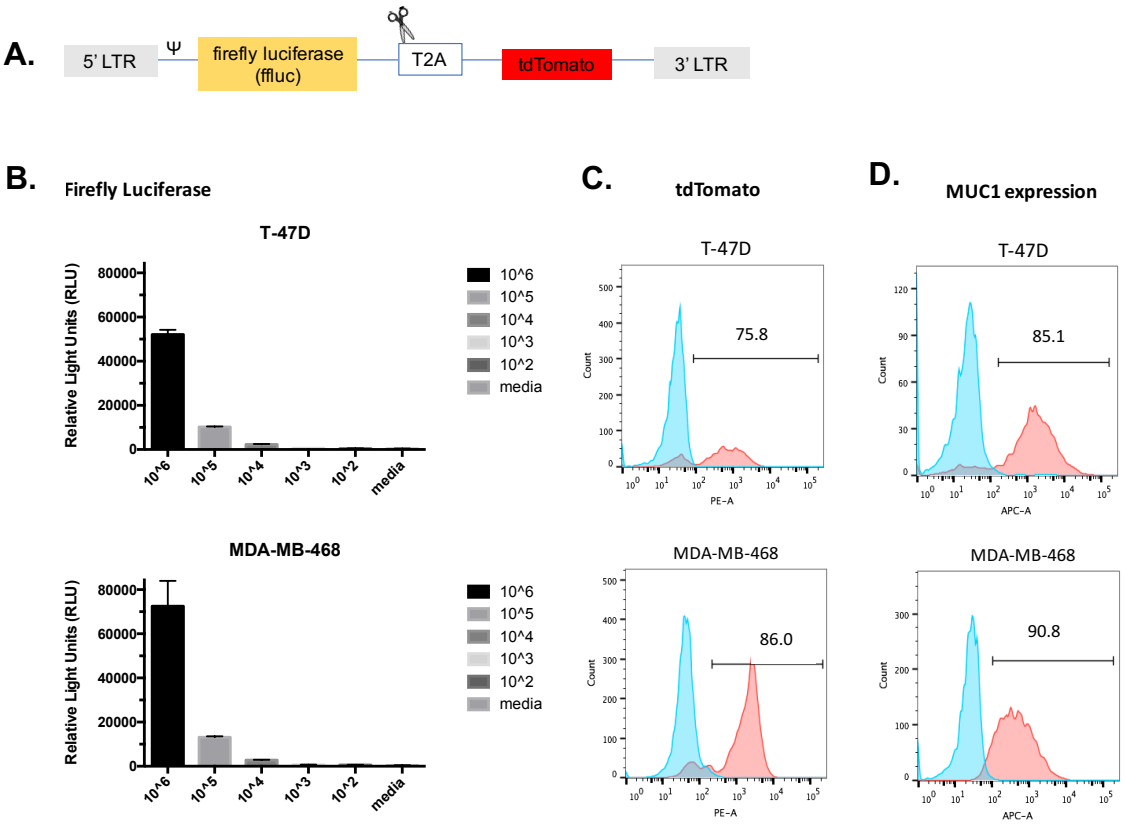

Figure 5.1: Generation of firefly luciferase-expressing breast cancer cells. T-47D and MDA-MB-468 cells were retrovirally transduced to express ffluc_tdTomato. A) Schematic illustration of ffluc_tdTomato retroviral construct. An SFG retroviral vector carrying the ffluc and tdTomato has been used for the expression of the two proteins in breast cancer cells. B) Expression of ffluc in breast cancer cells was validated with luciferase assay. $1x10^6$ cells were serially diluted 10-fold and 150µg/ml D-luciferin was added to each well. D10 medium alone was used as negative control. Emitted luminescence was measured with a FLUOstar Omega plate reader. Data shown are mean + SD of n=3 independent replicates. C) Transduction efficiency of ffluc_tdTomato was evaluated using flow cytometry, by detecting the tdTomato protein (red histogram). Parental (non-transduced) cells were used as negative control (blue histograms). The histograms overlays are representative of n=5 independent replicates. D) Surface MUC1 expression was evaluated with flow cytometry, using the biotinylated HMFG2 antibody, followed by streptavidin-APC (red histograms). Cells stained with biotinylated IgG1, followed by streptavidin-APC, were used as isotype control (blue histograms). The histograms overlays are representative of n=5 independent replicates.

5.2.2 Pilot study for establishing a breast cancer xenograft model. Site of injection: subcutaneous

In order to establish a breast cancer xenograft model, a pilot study was performed where T-47D_ffluc and MDA-MB-468_ffluc cells were injected subcutaneously in the vicinity of mammary fat pad. In this study, individual female NSG were inoculated with different cell doses in order to evaluate which cell number is required for optimal tumour growth (Figure 5.2). Each cell-dose group included four mice. The cell doses of T-47D_ffluc investigated herein were $5x10^6$, $2x10^6$ and $0.5x10^6$ while doses of MDA-MB-468_ffluc were $2x10^6$, $0.5x10^6$ and $0.1x10^6$ cells. Tumour growth was monitored with BLI imaging and expression of ffluc by tumour cells was validated once again prior to initiation of the study.

Mice injected with T-47D_ffluc cells presented a progressive decrease in BLI signal over time (Figure 5.2C). Nevertheless, this did not correspond to tumour volume as tumours were observed to grow over time by caliper measurement (Figure 5.2A). All mice injected with T-47D_ffluc cells had to be euthanized at three weeks post injection due to tumour ulceration. All three cell doses presented a similar growth pattern without differences in the levels of detectable BLI signal.

Inconsistencies were observed in the BLI signal derived from mice injected with MDA-MB-468_ffluc cells. Increase in bioluminescence was observed in mice injected with $0.1x10^6$ cells after day 21 while decrease of detected signal was observed in mice injected with $2x10^6$ cells after day 21 (Figure 5.2D). Unstable bioluminescence pattern was observed in mice

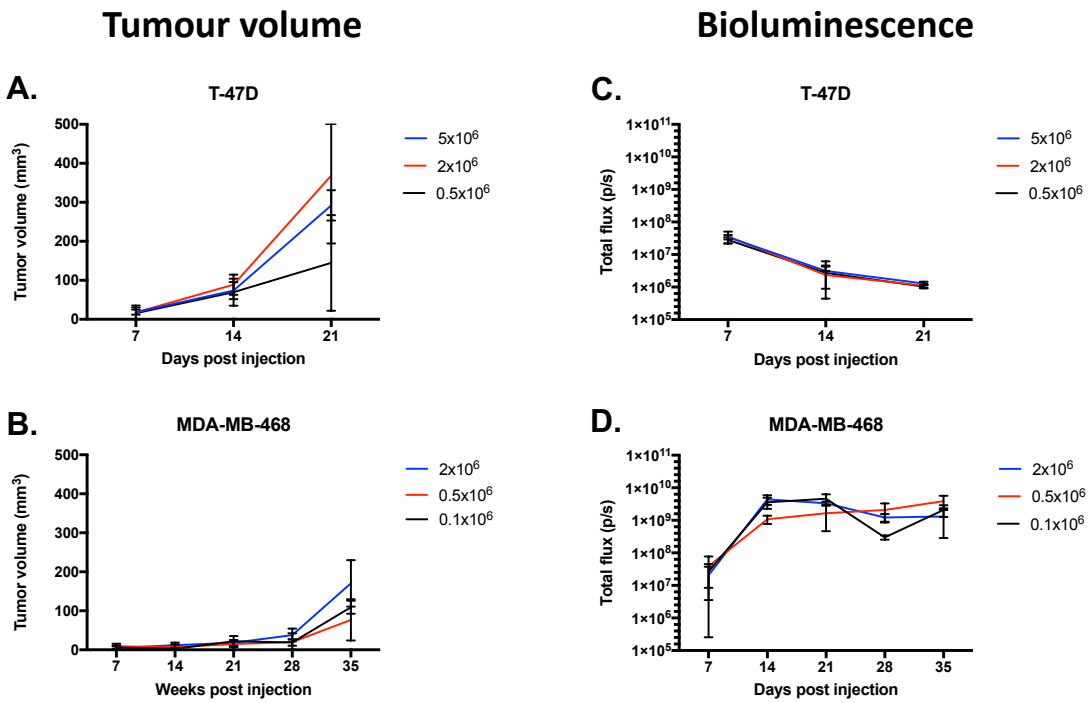

Figure 5.2: Establishment of breast cancer xenograft mouse model (subcutaneous flank injection). Female NSG mice were injected subcutaneously with either T-47D_ffluc or MDA-MB-468_ffluc tumour cells. T-47D cells were injected with $5x10^6$ (blue), $2x10^6$ (red) and $0.5x10^6$ cells (black). MDA-MB-468 cells were injected with $2x10^6$ (blue), $0.5x10^6$ (red) and $0.1x10^6$ cells (black). Tumour cells were injected together with matrigel. The tumour growth was monitored weekly by using both caliper measurements and BLI. A-B) Tumour volume as measured with the use calipers. C-D) Bioluminesce recorded with BLI. Data shown are mean ± SD (n=4 mice per group).

injected with $0.1x10^6$ (Figure 5.2D). Additionally, these mice developed ulcerating tumours (data not shown). The study was terminated five weeks post injection due to un-related issues present in the animal facility.

5.2.3 Pilot study for establishing a breast cancer xenograft model. Site of injection: peritoneal cavity

As the models described in sections 5.2.2 proved unsatisfactory, I next sought to establish a xenograft model where the breast cancer cells would be injected in the peritoneal cavity. Both ffluc-positive T-47D and MDA-MB-468 cells were used in this pilot experiment. Similar to the previous study, different cell doses were used in each mouse group. For T-47D, cell doses investigated were $10x10^6$, $5x10^6$, $2x10^6$ and $0.5x10^6$ cells. In the case of MDA-MB-468, mice received $5x10^6$, $2x10^6$ and $0.5x10^6$ cells. Tumour growth was monitored with BLI imaging until day 62 where the experiment terminated. Expression of ffluc_tdTomato in each cell line was again validated prior to the initiation of the study (data not shown).

Mice inoculated with T-47D_ffluc presented no increase in BLI signal over-time (Figure 5.3A). This was observed with all four cell doses. Mice in the three groups which received the highest tumour cell doses showed a slight decrease in the detectable levels of luminescence until day 21, after which signal appeared to plateau. Upon termination of the experiment, few mice of each cell-dose group were dissected and no palpable tumour nodules were observed within the peritoneal cavity, suggesting that the tumour cells were dispersed (data not shown).

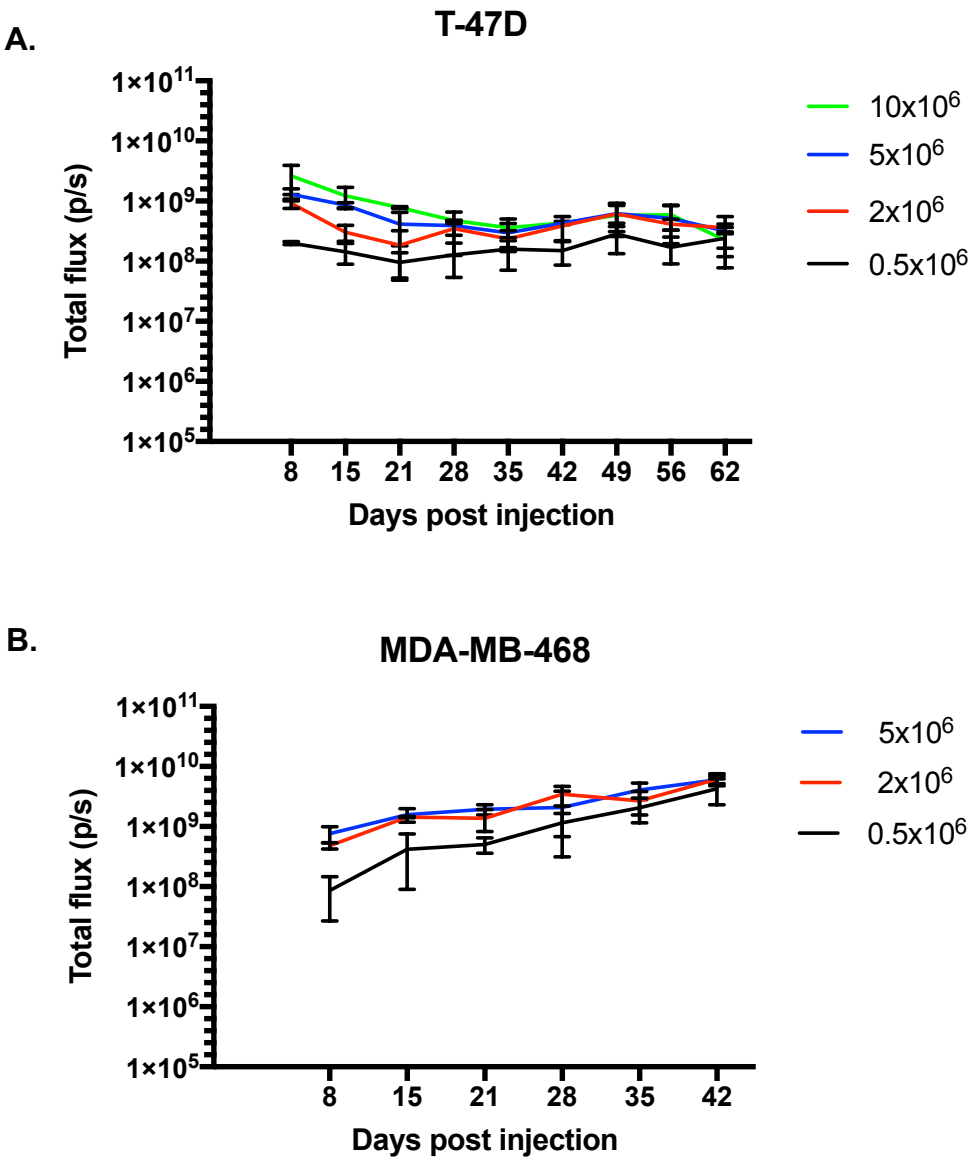

Figure 5.3: Establishment of breast cancer xenograft mouse model (site of injection peritoneal cavity). Groups of three female NSG mice were injected in the peritoneal cavity with the indicated doses of (A) T-47D_ffluc and (B) MDA-MB-468_ffluc tumour cells. Tumour growth was monitored approximately weekly with BLI imaging, upon injection of D-luciferin. Data shown are mean ± SD (n=3).

By contrast, mice inoculated with MDA-MB-468_ffluc cells presented progressive tumour growth, as indicated by an increasing BLI signal (Figure 5.3B). All three doses presented a similar tumour growth pattern. The study was terminated at day 49 as the mice presented distress symptoms, probably

due to high tumour burden. Upon termination, mice from each cell-dose group were dissected and large palpable tumours were observed in the site of cell injection or in the peritoneal cavity. Mice from both $2x10^6$ and $5x10^6$ cell-dose groups appeared to have additional tumour nodules throughout the peritoneal cavity, although these were more apparent in mice that had received the higher tumour cell inoculum.

5.2.4 Assessment of *in vivo* activity of MUC1-specific CAR T-cells in MDA-MB-468 xenograft model

Assessment of the *in vivo* efficacy of TAB28z, H28z and HDF28z MUC1-specific CAR T-cells was investigated in NSG mice with established MDA-MB-468_ffluc peritoneal tumours. The experimental design of the study is depicted in Figure 5.4. Tumour growth was monitored regularly with BLI imaging. In parallel, weight measurements were acquired to monitor for toxicity.

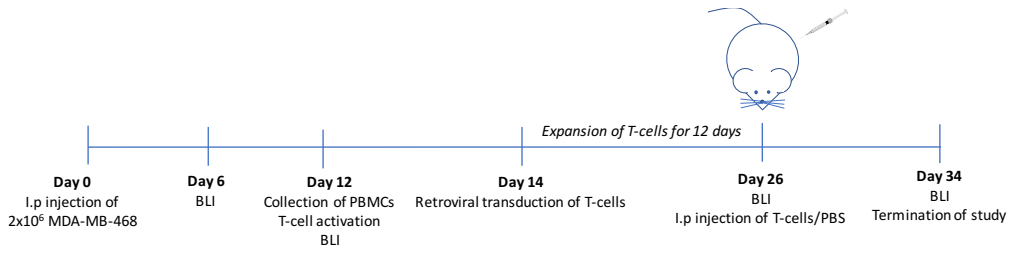

Figure 5.4: Experimental design of therapeutic study using MDA-MB-468 xenograft model.

Thirty female NSG mice were inoculated i.p. with $2x10^6$ MDA-MB-468_ffluc cells. In parallel, PBMCs from a healthy donor were isolated, activated with anti-CD3 and anti-CD28-coated beads and engineered by

retroviral transduction to express either TAB28z, H28z and HDF28z CAR molecules. Tumour engraftment was evaluated at day 26, prior to the infusion of CAR T-cells, and mice were then assigned into groups with similar average bioluminescence. Non-transduced cells were included in the experimental study as an indicator of non-specific anti-tumour activity. Additionally, some mice were treated with PBS in order to be able to evaluate tumour progression without any therapeutic intervention. T-cells were expanded for 12 days, assessed for transduction efficiency (Figure 5.5) and injected into the peritoneal cavity. Each group included six mice. CAR T-cells were injected at a dose of $8x10^6$ CAR-positive cells (corrected for transduction efficiency). The injected dose of non-transduced T-cells was equal to the highest number of total CAR T-cells given.

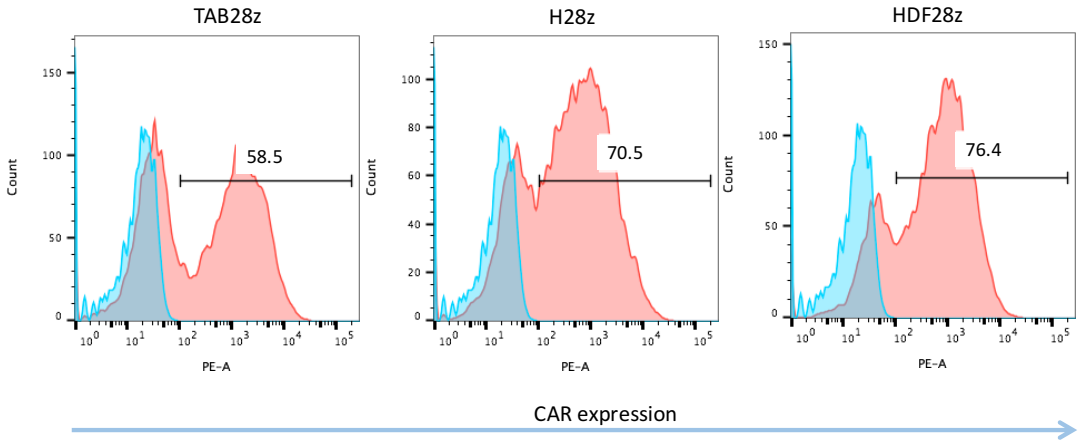

Figure 5.5: Transduction efficiency of CAR T-cells infused in the mice with established MDA-MB-468_ffluc tumours. Histograms show cell expression of the TAB28z, H28z and HDF28-CARs in tranduced T-cells. This was investigated with flow cytometry analysis, performed prior to CAR T-cell infusion. In order to evaluate the CAR surface expression, T-cells were stained with biotinylated MUC1-24mer peptide, followed by streptavidin PE (red histograms). Non-transduced (negative control) T-cells were stained in the same way (blue histograms).

Disappointingly, none of the CAR T-cell populations elicited significant tumour reduction (

A). A hint of anti-tumour activity was observed in animal 2 (A2) treated with TAB28z and in animals 1 (A1) and 2 (A2) treated with HDF28z (

B). Nevertheless, this effect was not followed further as the experiment had to be terminated due to mice presenting distress symptoms. Based upon post-mortem examination, this appeared to be related to high tumour burden (data not shown).

Body weight of each individual mouse was also monitored throughout the study, as indicated above. Weight either progressively increased or stabilised over time (Figure 5.7) and no other clinical indicators of toxicity were

A.

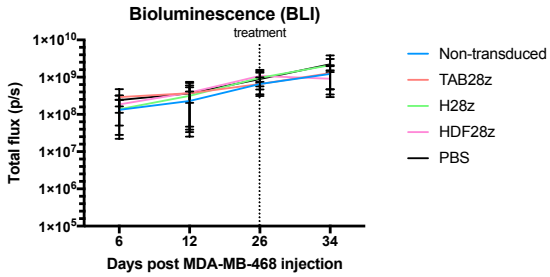
Bioluminescence (BLI)
treatment
Total flux (p/s)
1×10^10
1×10^9
1×10^8
1×10^7
1×10^6
1×10^5
6
12
26
34
Days post MDA-MB-468 injection
Non-transduced
TAB28z
H28z
HDF28z
PBS

B.

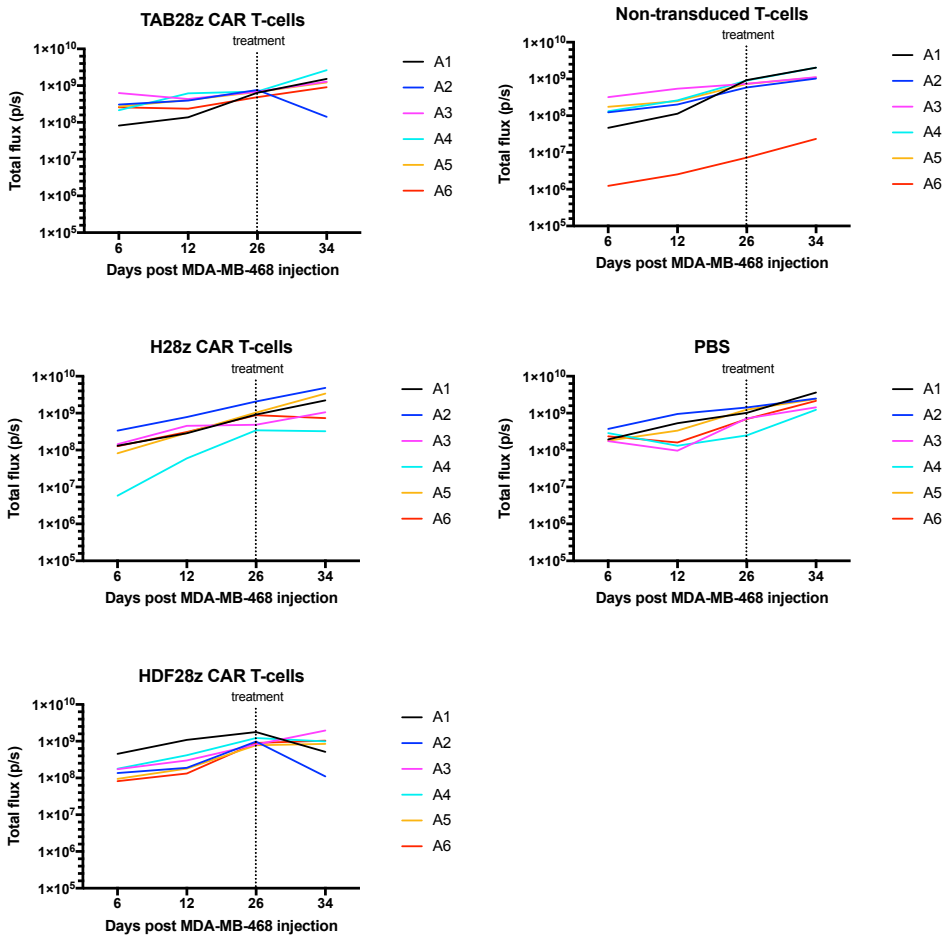
TAB28z CAR T-cells
Non-transduced T-cells
H28z CAR T-cells
PBS
HDF28z CAR T-cells
treatment
Total flux (p/s)
1×10^10
1×10^9
1×10^8
1×10^7
1×10^6
1×10^5
6
12
26
34
Days post MDA-MB-468 injection
A1
A2
A3
A4
A5
A6

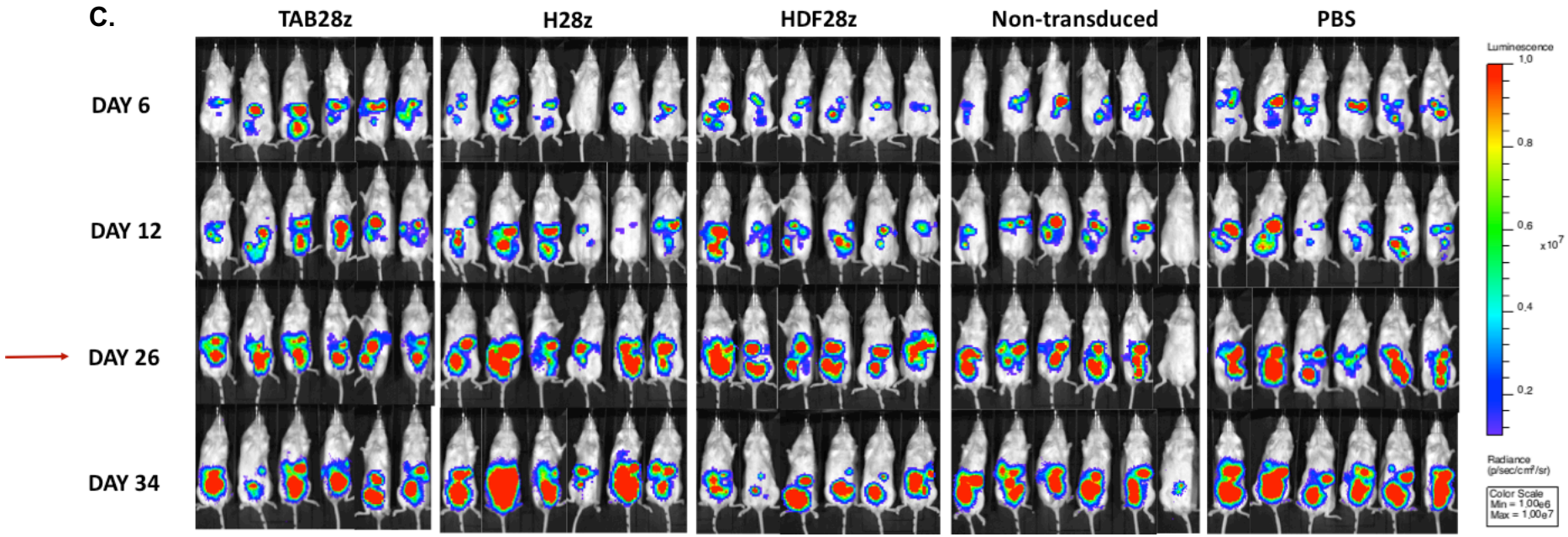

Figure 5.6: *In vivo* assessment of MUC1-specific CAR T-cells in MDA-MB-468 xenograft model. Female NSG mice were injected i.p. with $2x10^6$ MDA-MB-468 cells. Tumour growth was evaluated regularly with BLI imaging and quantified as total flux (photons/second). On day 26, indicated mice received either $8x10^6$– positive CAR T-cells, non-transduced T-cells or PBS, all administered i.p. A) Mean ± SD of BLI signal prior to and post treatment (n=6 mice per group). B-C) Serial BLI emission from the individual animals (A1-6) within each group. Data were analyzed using Living Image software (PerkinElmer).

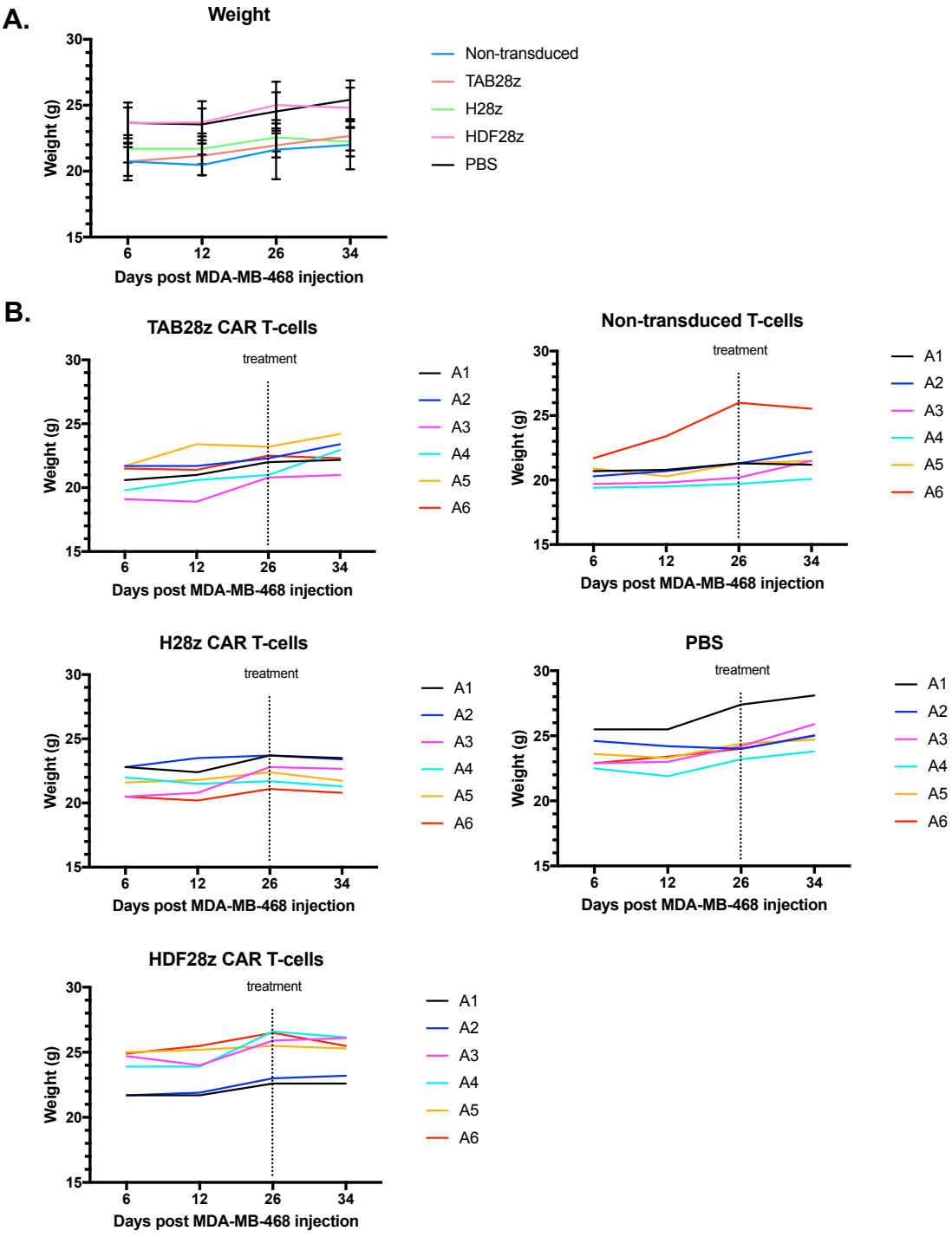

Figure 5.7: Weight measurements of mice used in the therapeutic study shown in Figure 5.6. A) Mean ± SD body weight of all five mice groups (n=6 mice per group). B) Body weight of individual mice. Each graph represents a treament group. A1 to A6 – animal 1 to animal 6.

observed in CAR T-cell treated mice. A few mice presented minimal weight decrease post-treatment, a point that could have been attributable to high tumour burden.

5.2.5 Assessment of *in vivo* activity of MUC1-specific CAR T-cells in T-47D xenograft model

Next, I sought to investigate the *in vivo* activity of MUC1-specific CAR T-cells in a less aggressive tumour model. The experimental design of the study is shown in Figure 5.8.

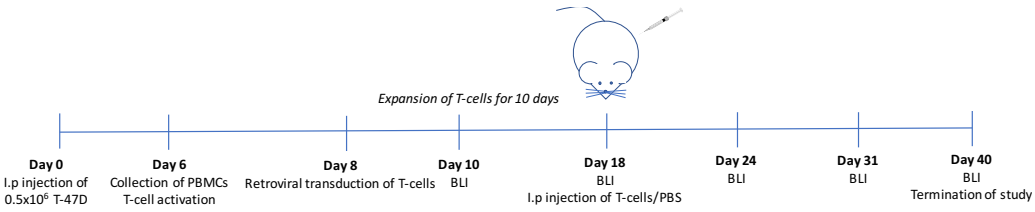

Figure 5.8: Experimental design of therapeutic study using T-47D xenograft model.

In brief, NSG mice were inoculated i.p with $0.5x10^6$ T-47D_ffluc cells. PBMCs were harvested from a healthy volunteer, were activated with PHA and were subjected to retroviral transduction. As previously described in section 5.2.4, five groups of mice were treated with T-cells that had been engineered to express TAB28z, H28z or the HDF28z CAR, making comparison with control groups that received non-transduced T-cells or PBS. On day 18 post tumour cell injection, mice were assigned into groups with similar average tumour-derived bioluminescence and were treated i.p with $12x10^6$ CAR-positive T-cells (corrected for transduction efficiency). Control

animals received PBS to indicate tumour growth without the presence of any therapeutic intervention. In addition, non-transduced T-cells were infused at a number equal to the highest total T-cell dose injected in the CAR T-cell groups.

Transduction efficiency of CAR T-cells was investigated on the day prior to T-cell infusion. Based on these data, $12x10^6$ CAR-expressing T-cells were infused in each group. As shown in Figure 5.9, all three CAR T-cell populations presented similar CAR surface expression.

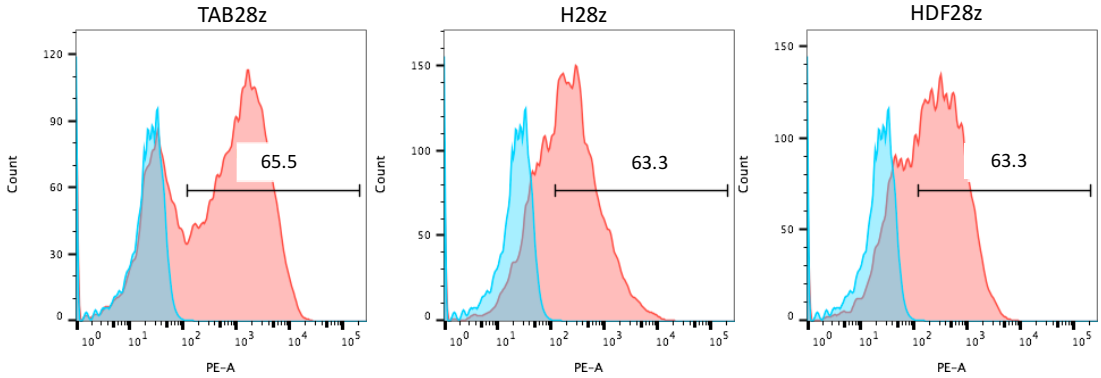

Figure 5.9: Transduction efficiency of CAR T-cells infused in mice with established T-47D_ffluc tumours. CAR surface expression was investigated using flow cytometry, performed on the day prior to CAR T-cell administration. T-cells were stained with biotinylated MUC1-24mer peptide, followed by streptavidin PE (red histograms), making comparison with non-transduced T-cells as negative control (blue histograms). Histograms depict transduction efficiency of TAB28z, H28z and HDF28 CAR T-cell populations.

No significant tumour response was observed in the TAB28z, H28z and HDF28z treatment groups (A). Nevertheless, data obtained from individual mice suggested that tumour regression had occurred in some cases (B). Notably, A6 treated with TAB28z CAR T-cells, A3 with H28z and A1, A2 and A6 treated with HDF28z presented prolonged response to treatment until day 31 post study initiation. At this time-point, bioluminescence signal increased

once again in most of the responding mice. No similar pattern was observed in any of the mice treated with non-transduced cells or with PBS, indicating that response was probably due to the activity of CAR T-cells. Animal 6 (A6) treated with non-transduced T-cells presented a decrease in BLI signal at day 40, nevertheless this could be attributed to technical fault during BLI imaging. Animal 1 (A1) treated with HDF28z CAR T-cells had to be culled at day 31 due to unrelated health issues (suspected ear infection).

Body weight of mice increased or stabilised over-time, indicating absence of toxicity upon treatment with MUC1-specific CAR T-cells (Figure 5.11).

A.

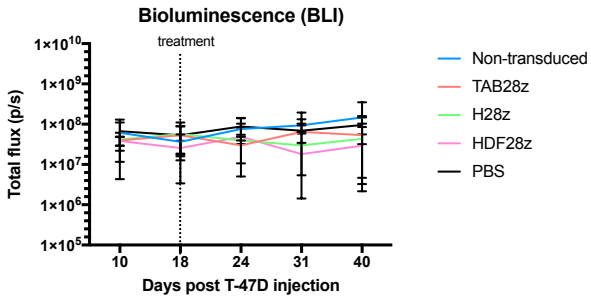
Bioluminescence (BLI)
treatment
Total flux (p/s)
1×10^10
1×10^9
1×10^8
1×10^7
1×10^6
1×10^5
10
18
24
31
40
Days post T-47D injection
Non-transduced
TAB28z
H28z
HDF28z
PBS

B.

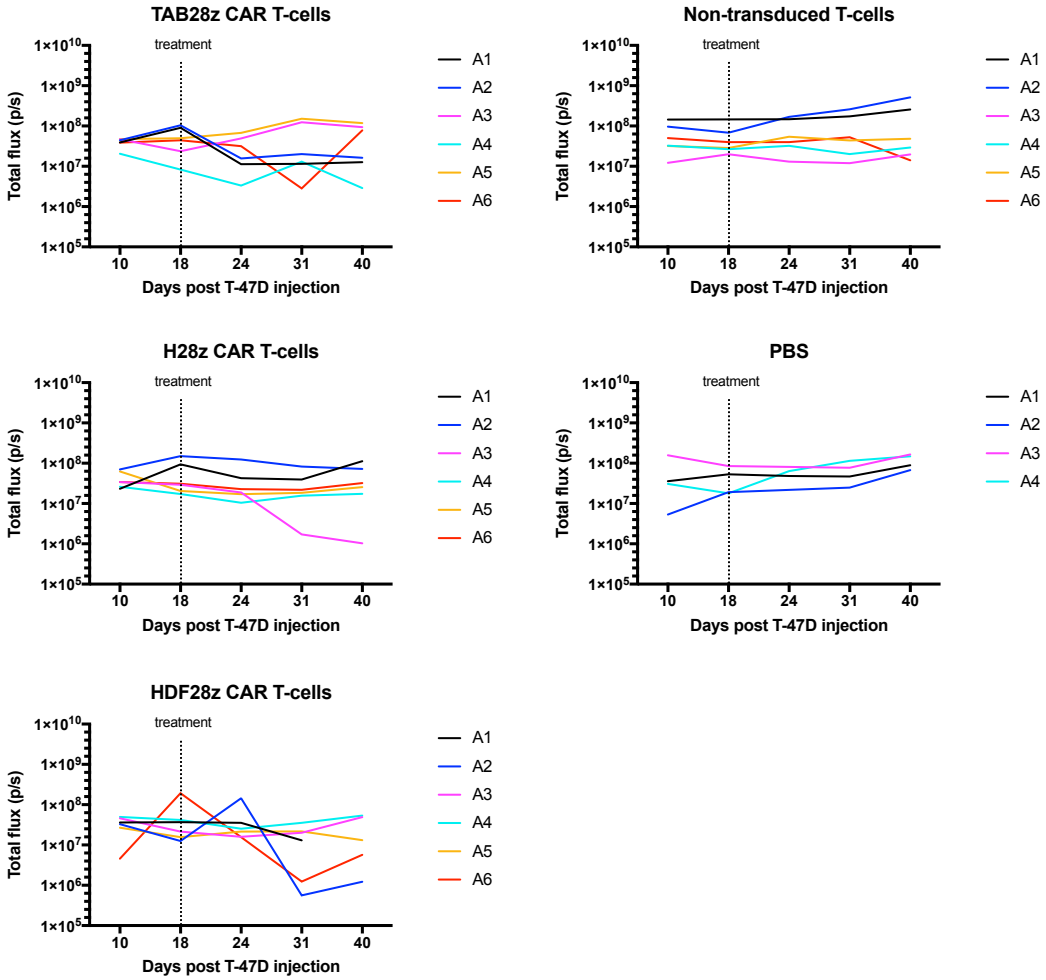
TAB28z CAR T-cells
Non-transduced T-cells
H28z CAR T-cells
PBS
HDF28z CAR T-cells
treatment
Total flux (p/s)
Days post T-47D injection
A1
A2
A3
A4
A5
A6

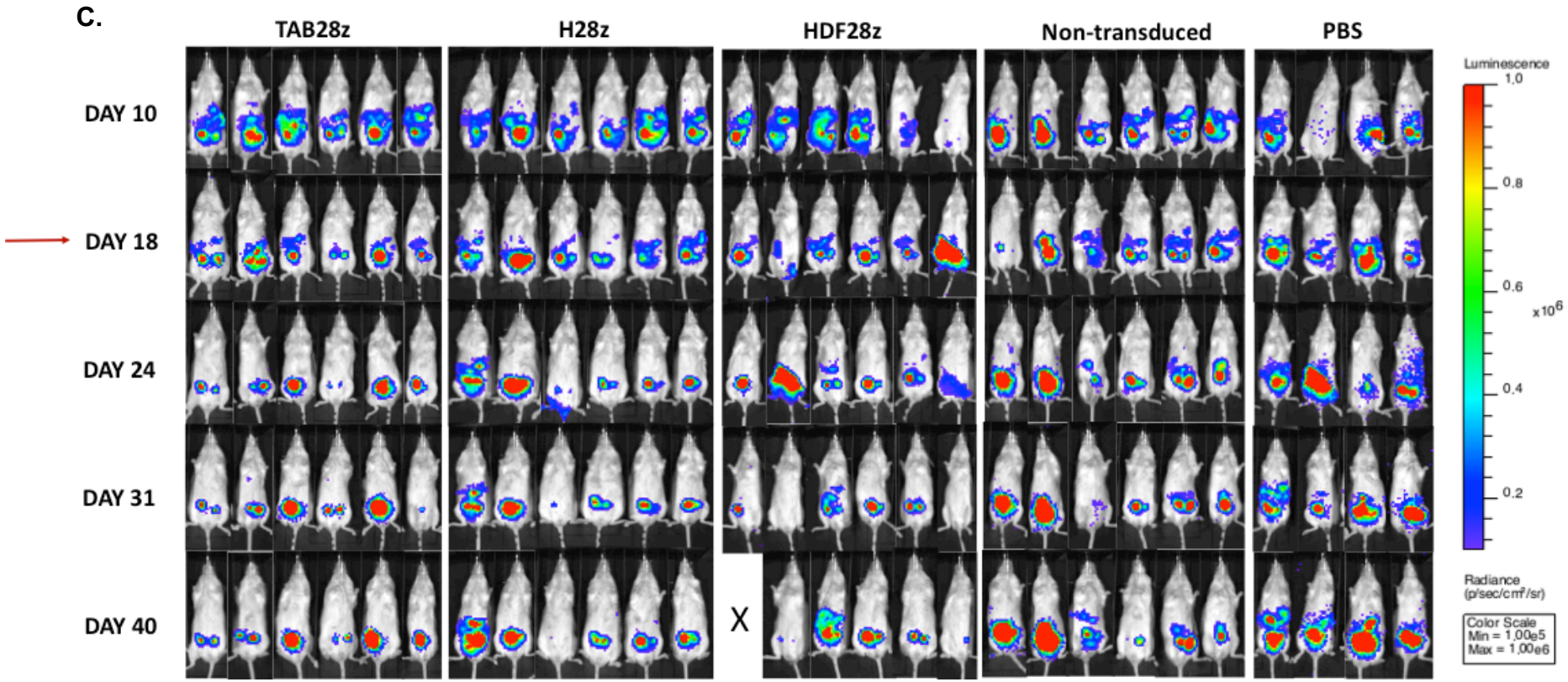

Figure 5.10: Assessment of in vivo efficacy of MUC1-specific CAR T-cells in T-47D xenograft model. Female NSG mice were inoculated i.p. with 0.5x106 T-47D_ffluc tumour cells. Tumour growth was monitored regularly with BLI imaging. On day 18 post-tumour cell injection, 12x106 CAR-positive T-cells were infused i.p. Additionally, mice injected with non-transduced cells and with PBS were used as controls. A) Tumour growth was evaluated regularly with BLI imaging, and quantified as total flux (photons/second). The graph depicts the mean ± SD of bioluminescence emission (n=6 mice per T-cell group and n=4 for the PBS group). B-C) Serial BLI emission from the individual animals (A1-6) within each group. Data were analyzed using Living Image software (PerkinElmer).

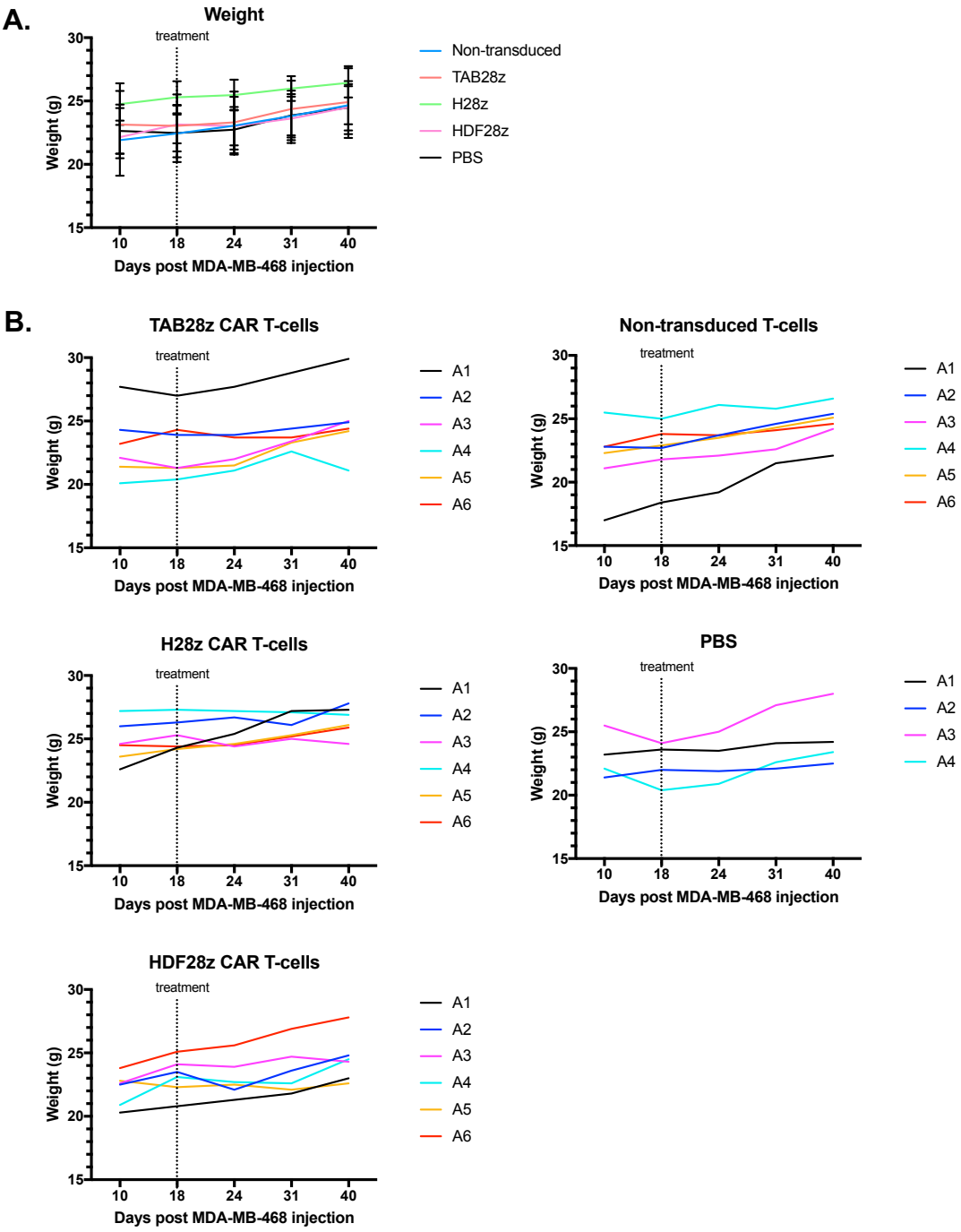

Figure 5.11: Weight measurements of mice used in the therapeutic study shown in Figure 5.10. A) Mean ± SD of body weight of treatment groups (n=6 mice per T-cell treatment group and n=4 for the PBS group). B) Body weight of individual mice. Each graph represents a treament group. A1 to A6 – animal 1 to animal 6.

5.2.6 Persistence of MUC1 specific CAR T-cells *in vivo*

As shown in , anti-tumour efficacy of MUC1-specific CAR T-cells was inadequate. For this reason, I sought to investigate if infused T-cells were still present *in vivo*, 22 days after their infusion. Upon termination of the study, samples of peritoneal fluid and spleen were randomly collected from two mice in each intervention group (TAB28z, H28z, HDF28z, non-transduced T-cells). Additionally, samples from one mouse injected with PBS were collected as negative controls. It should be mentioned that although peritoneal fluid was collected from two mice treated with HDF28z CAR T-cells, one sample had to be excluded from further analysis due to technical issues. Detection of viable cells was performed with flow cytometry.

Viable human T-cells were detected in most of the peritoneal lavage samples collected, ranging from 0.35% to 69% (Figure 5.12B). Notably, viable T-cells were also observed in both samples acquired from mice treated with non-transduced T-cells. This suggests that persistence could be related to the immune compromised nature of the host and/or alloreactivity, rather than an anti-MUC1 CAR T-cell response. Additionally, persistence did not seem to be an indicator of tumour response (Table 5.1). For example, no decrease in tumour burden was observed in mice treated with non-transduced T-cells. Nevertheless, a higher percentage of viable T-cells was detected in these two samples in comparison with a sample acquired from a mouse treated with HDF28z.

Table 5.1: Response to treatment and detection of viable human T-cell in peritoneal fluid. In this table are listed i) the treatment group from which each peritoneal fluid was collected, ii) the percentage (%) of viable human T-cells detected and iii) response to treatment.

Intervention	Animal	Response	% Viable human T-cells in peritoneal fluid
Non-transduced T-cells	A1	No response	36.5
Non-transduced T-cells	A2	No response	25.8
TAB28z	A1	Initial response	2.09
TAB28z	A2	Initial response	27.9
H28z	A2	Minimal prolonged response	67.9
H28z	A4	Minimal initial response	37.4
HDF28z	A5	Minimal prolonged response	0.35

Minimal numbers of viable T-cells were detected in any of the processed spleens (Figure 5.12C). The only exception is A2 treated with TAB28z CAR T-cells, where 1.52% viable T-cells were detected.

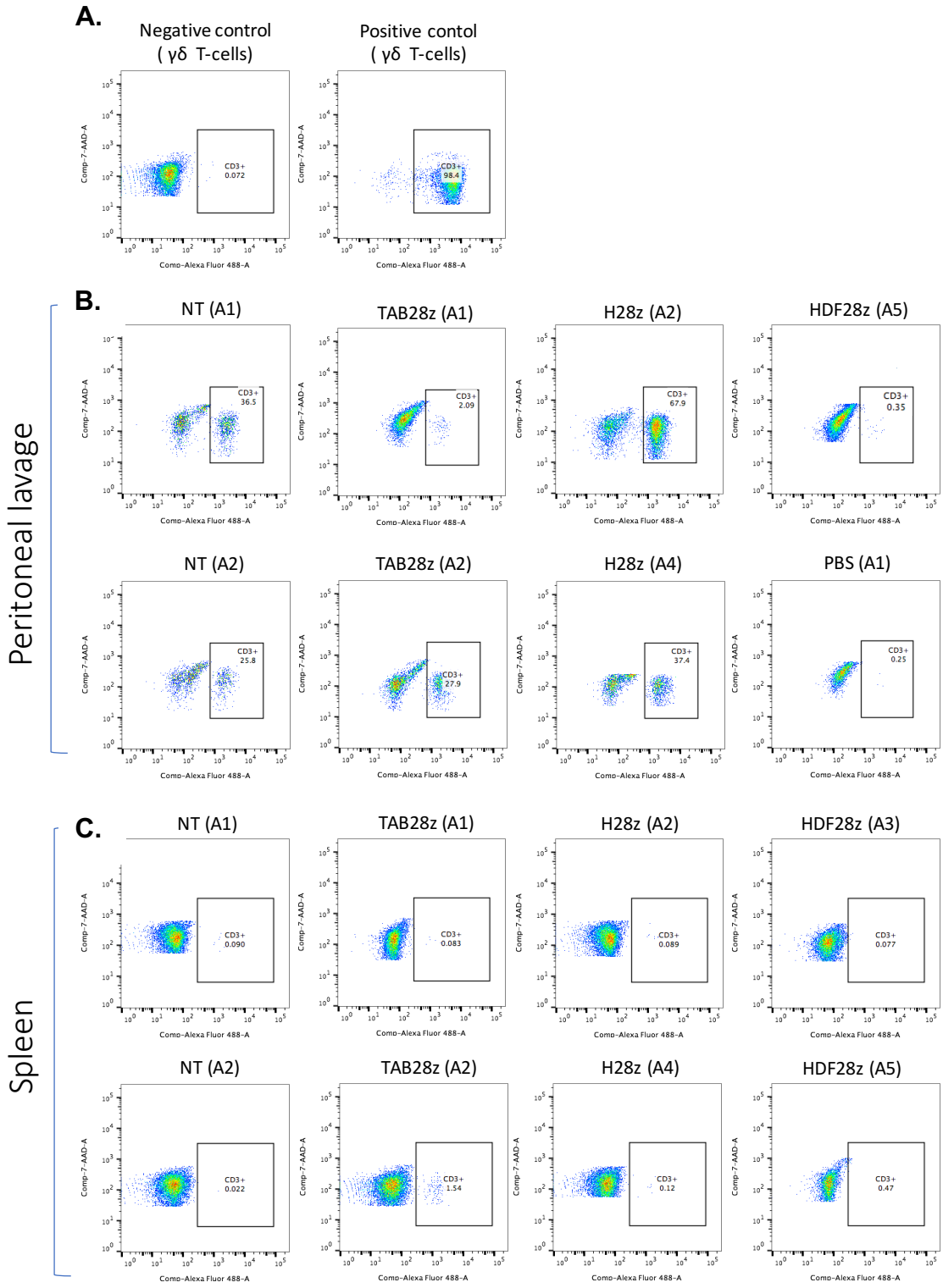
A.
Negative control
(γδ T-cells)
Positive contol
(γδ T-cells)
CD3+
0.072
CD3+
98.4
B.
Peritoneal lavage
NT (A1)
TAB28z (A1)
H28z (A2)
HDF28z (A5)
CD3+
36.5
CD3+
2.09
CD3+
67.9
CD3+
0.35
NT (A2)
TAB28z (A2)
H28z (A4)
PBS (A1)
CD3+
25.8
CD3+
27.9
CD3+
37.4
CD3+
0.25
C.
Spleen
NT (A1)
TAB28z (A1)
H28z (A2)
HDF28z (A3)
CD3+
0.090
CD3+
0.083
CD3+
0.089
CD3+
0.077
NT (A2)
TAB28z (A2)
H28z (A4)
HDF28z (A5)
CD3+
0.022
CD3+
1.54
CD3+
0.12
CD3+
0.47
Comp-7-AAD-A
Comp-Alexa Fluor 488-A

Figure 5.12: Persistence of MUC1 re-targeted T-cells *in vivo*. The presence of viable human T-cells was investigated in the peritoneal fluid and in spleen acquired from mice of each intervention group, upon termination of the study indicated in Figure 5.10. This was investigated by flow cytometry analysis using the 7-AAD viability dye and human anti-CD3 FITC antibody. A) γδ T-cells were used, for convenience, as positive and negative staining controls. In particular, γδ T-cells were stained with either 7-AAD and anti-CD3 FITC (positive control) or with 7-AAD and IgG1-FITC (isotype) (negative control). B) Dot plots showing the percentage (%) of viable human T-cells detected in each peritoneal fluid sample. Two samples per intervention group were acquired, with the exceptions of PBS and HDF28z where only one sample has been analysed. C) Dot plots represent the percentage (%) of viable human T-cells detected in each spleen sample. Two samples per intervention group were acquired, with the exception of PBS where only one sample has been analysed.

5.3 Discussion

In this chapter, I present results related to the evaluation of the *in vivo* efficacy of MUC1-specific CAR T-cells. Two different breast cancer xenograft models were used for this purpose; the MDA-MB-468 and T-47D mouse model in which the tumour cells have been inoculated i.p.

Prior to the initiation of the study, I decided to establish a breast cancer xenograft model where assessment of tumour growth and response to treatment could be performed with BLI imaging. This imaging system provides a quantitative, objective, non-invasive and high throughput method for monitoring tumour growth[403]. Additionally, it can detect microscopic tumours with accuracy and high sensitivity, even before the tumours are palpable using caliper measurements[404,405]. Bioluminescence imaging requires the expression of a luciferase reporter gene in the cells under investigation, in order to achieve light emission upon interaction with its substrate. For this purpose, T-47D and MDA-MB-468 cells were engineered to express firefly luciferase. These two breast cancer cell lines were selected as MUC1 was detected at high levels on the cell surface.

Breast cancer subcutaneous models are being extensively used for the evaluation of efficacy of various therapeutic agents. Consequently, I sought initially to establish a similar model. Varied doses of T-47D_ffluc and MDA-MB-468_ffluc cells were injected subcutaneously in female NSG mice. However, these models proved to be inappropriate for further use for various reasons. Firstly, BLI signal appeared to decrease or stabilise over time (Figure 5.2). Nevertheless, this did not correspond to actual tumour volume as these

xenografts increased significantly in size over time (Figure 5.2). Secondly, tumours in both models presented ulceration which is not desirable for animal welfare. Tumour ulceration is commonly observed in tumours developing subcutaneously and it is characterized by necrotic phenotype as a result of poor vascularization and lack of nutrients[406,407]. Others have reported reduction in BLI signal due to the development of necrotic and hypoxic tumours[408–410]. Similar to my observations, even though the intensity of bioluminescence emission decreased, tumour volume increased when measured by other means[408–410]. This is explained by the fact that light emission is produced upon interaction of luciferase with luciferin, in the presence of oxygen. As previously mentioned, ulcerating tumours are necrotic and often hypoxic, resulting in reduced availability of oxygen and poor localisation of luciferin into the tumour due to poor blood supply. Measurement of subcutaneous tumours in mouse models with the usage of caliper is a widely used technique. It has the benefits of being low-cost and there is no requirement for anaesthetising the mice. Nevertheless, caliper measurements can be inaccurate due to a variety of reasons, including i) subjectivity; ii) inability to measure tumours of very small size, iii) difficulty of detecting small differences in tumour volume post treatment, iv) variability in tumour shape, v) thickness of the skin and vi) variability in measurements between different investigators[411,412]. For these reasons, I decided that it was necessary to establish a breast cancer xenograft model in which the tumour growth would be assessed with BLI imaging.

For the above reasons, alternative xenografts models were established whereby T-47D and MDA-MB-468 cells were inoculated i.p., prior to treatment

with i.p. delivered T-cells. Although these models do not recapitulate the manner in which metastatic human breast cancer might be treated with CAR T-cell immunotherapy, they were used as convenient proof-of-concept models for the assessment of the *in vivo* efficacy of MUC1-specific CAR T-cells. While intravenous injection of CAR T-cells might be deemed more clinically relevant, previous members of our lab have reported that CAR T-cells administered using this route traffic poorly to the peritoneal cavity[413].

In the two *in vivo* therapeutic studies, NSG mice were inoculated i.p. with either $2x10^6$ MDA-MB-468_ffluc cells or $0.5x10^6$ T-47D_ffluc cells. As indicated by the results of the pilot study shown in section 5.2.3, mice injected with $2x10^6$ and $5x10^6$ MDA-MB-468_ffluc cells presented a similar pattern of tumour growth. Additionally, they presented better tumour distribution in comparison with mice inoculated with $0.5x10^6$ cells, since tumour nodules were observed throughout the peritoneal cavity (data not shown). Given their similar behaviour, a cell dose of $2x10^6$ MDA-MB-468_ffluc cells was selected to be used in the therapeutic study (rather than $5x10^6$ cells) to reduce total tumour cell number that needed to be expanded for this study. In regard to T-47D cells, the dose of $0.5x10^6$ cells was chosen since a more stable BLI signal was observed over-time, when compared with the other three doses included in that pilot study.

In the first therapeutic study, mice with established MDA-MB-468_ffluc tumours received $8x10^6$ MUC1-specific CAR T-cells or non-transduced T-cells. However, no tumour response was observed in any of the treated groups. This may be accounted for by the fact that mice already had high tumour burden when they received the treatment (day 32). This is indicated

by the fact that the study had to be terminated only 10 days post CAR T-cell injection, due to progressive disease. It should be noted that in the initial study design, it was planned to inject the CAR T-cells at day 12 post tumour inoculation. Nevertheless, technical issues led to a delay in the timing of treatment. It would be interesting to repeat the same experiment but, on this occasion, inject the MUC1-specific CAR T-cells in an earlier time point. Lack of response has been attributed to various reasons in other similar studies, one of them being poor localization of CAR T-cells[243,414]. This explanation seems unlikely in this case as MUC1-specific CAR T-cells were injected in the same locus (peritoneal cavity) as the engrafted tumour cells. Another possible explanation could be lack of T-cell persistence. This was not further investigated as the study had to be terminated urgently.

In the second therapeutic study, mice inoculated with T-47D_ffluc received $12x10^6$ MUC1-specific CAR T-cells or non-transduced cells. This model was chosen as it was important to investigate if the MUC1-specific CAR T-cells could demonstrate tumour regression in a less aggressive tumour model. Although no significant tumour regression was observed in any of the treatment groups, at least seven mice across the individual groups presented at least some degree of tumour regression post treatment with CAR T-cells. Notably, this was not observed in mice treated with non-transduced T-cells, indicating that the response was specific to treatment with MUC1 re-targeted CAR T-cells. T-cell persistence was evaluated upon termination of the study for two reasons. First, few mice showed long-term response post-treatment. Second, poor activity of CAR T-cells *in vivo* and in the clinical setting has been attributed in other studies to poor CAR T-cell persistence[415–418]. As shown in

Figure 5.12, viable human T-cells were detected in the peritoneal fluid obtained from most of the mice. This raises the possibility that the lack of response to CAR T-cells treatment was not due to poor CAR T-cell persistence. Notably, persistence did not seem to correlate with recognition of MUC1 by MUC1-specific CAR T-cells, as T-cells were also detected in the peritoneal cavity of mice treated with non-transduced T-cells. Non-specific persistence could be possibly attributed to alloreactivity and/or the profoundly immune compromised nature of the host mice. In support of this, it has been widely documented that NSG mice injected with human PBMCs commonly develop xenogeneic graft-versus-host disease (GvHD)[419–421]. Xenogeneic GvHD has been reported to develop upon recognition of host MHC class I/II by injected human PBMCs[422]. A limitation of the experiment presented in Figure 5.12 is that it is uncertain whether the T-cells detected in the peritoneal fluid are CAR-positive or non-transduced T-cells. Additionally, the absolute number of T-cells was not quantified. Therefore, no conclusive statement can be made regarding the possibility that lack of persistence of MUC1 re-targeted T-cells accounted for limited efficacy in this model.

Another notable observation was the fact that no T-cells were detected in the spleens isolated from treated mice. This finding is in agreement with the results published by Pereira *et al*. who showed that CAR T-cells injected i.p. in SCID/Beige mice did not appear to migrate outside the peritoneal cavity[413]. However, these results do not agree with those published by Adusumilli *et al.*[423]. In this study, NSG mice bearing orthotopic mesothelioma tumours were treated with intra-pleural delivery of mesothelin-specific CAR T-cells (M28z).

After treatment, human T-cells were detected within the spleens of treated mice[423].

One other study has explored the *in vivo* cytotoxic activity of MUC1-specific CAR T-cells in a breast cancer mouse model. Wilkie *et al.* reported significant delay in tumour progression using a MUC1-engineered MDA-MB-435 xenograft model, following i.p. administration of a 3rd generation CAR with elongated hinge (HOX)[295]. It needs to be noted that MDA-MB-435 is now considered to be of melanoma origin[424]. Similar to the two therapeutic experiments undertaken in this PhD project, both tumour cells and CAR T-cells were injected intraperitoneally. Furthermore, the tumour cells were engineered to over-express MUC1 by gene transfer, contrasting with the models used here in which endogenous TA-MUC1 was targeted. Importantly, Wilkie *et al.* did not investigate further whether the hinge is responsible for the anti-tumour activity of the CAR observed in the *in vivo* experiment. For this reason, is unclear whether the hinge or the presence of two costimulatory molecules were responsible for tumour regression. In my study, HDF28z CAR T-cells did not present superior activity than TAB28z in neither of the two therapeutic experiments, suggesting that the incorporation of the hinge was not particularly beneficial. Thus, it would be interesting to investigate if addition of a second co-stimulatory domain in the TAB28z could potentially improve its anti-tumour activity.

Finally, as indicated earlier, it is of great importance to be able to predict on-target off-tumour toxicities in pre-clinical *in vivo* studies. It has been reported by Spicer *et al.* that the murine protein of MUC1 presents 85% homology in the cytoplasmic and transmembrane regions with human MUC1

protein[425]. Nevertheless, the homology in the tandem repeat domain is only 34%, a fact that makes impossible the prediction of off-tumour toxicity using CAR T-cells that target immunodominant epitopes in this location[425]. A possible way to predict off-tumour toxicity would be to re-design the CAR molecule by replacement its components with the ones of murine origin and investigate activity in mice with an intact immune system. Another possible way of exploring the risk for of on-target off-tumour toxicity is by administrating CAR T-cells in a MUC1-transgenic model. Others have previously used transgenic mice for the same purpose[235,426]. For example, Wang *et al.* investigated the anti-tumour activity and the risk of off-tumour toxicity of HER-specific CAR T-cells in a HER-2 transgenic mice.

5.4 Conclusions

The *in vivo* efficacy of TAB28z, H28z and HDF28z CAR T-cells was assessed in two individual mice models. MUC1-specific CAR T-cells failed to control tumour growth in NSG mice inoculated with MDA-MB-468 breast cancer cells. Nevertheless, the tumour burden was too high at the time-point of CAR T-cell injection which might have underestimated the therapeutic potential of anti-MUC1 CAR T-cells in this study. Assessment of *in vivo* activity of CAR T-cells was further performed using NSG mice engrafted with T-47D cells. Although no significant tumour reduction was observed, a few mice presented tumour reduction following treatment. This response was mostly observed in mice treated with either TAB28z and HDF28z CAR T-cells. Lack of overall response was not attribute to lack of T-cell persistence as T-cells were detected in the peritoneal fluid. Further *in vivo* studies should be performed in order to evaluate the therapeutic potential of CAR T-cells. Additionally, inclusion of an additional co-stimulatory molecule in the intracellular signalling domain of the CAR receptor might potentially improve its activity.

Chapter 6: Discussion

6.1 Overview

The aim of this PhD project was to develop a CAR T-cell immunotherapy approach for breast cancer. For this purpose, MUC1 was chosen as the target antigen due its overexpression in 90% of breast cancers[124]. Another special characteristic of MUC1 that enhances its attractiveness as a CAR T-cell target is the fact that it is aberrantly glycosylated in tumour cells[138]. In this project, the anti-tumour potential of a novel second generation MUC1-specific CAR named TAB28z was investigated in both the *in vitro* and *in vivo* setting. I also investigated whether the anti-tumour activity of TAB28z was superior when compared to two previously generated MUC1-specific CARs, named H28z and HDF28z[295]. As previously stated, these three MUC1-specific CARs contain a binding domain derived either from TAB004 or HMFG2. Previous studies have shown that both antibodies recognise tumour-associated MUC1[284,287,320].

A fundamental initial step in this project was to characterize this newly developed MUC1-specific CAR *in vitro*. While TAB004 and HMFG2 antibodies both recognise tumour-associated glycoforms of MUC1, the binding preference of TAB004 in this regard was not known. According to the results presented in Chapter 3, both TAB004-based and HMFG2-based CARs recognise all four TA glycoforms: e.g. MUC1 that is decorated with the T, ST, Tn or STn antigens.

Another significant step was to investigate whether TAB28z could be successfully expressed on the surface of activated human T-cells, isolated from healthy donors. This was validated using flow cytometry. The *in vitro* anti-tumour activity of TAB28z was investigated using a panel of breast cancer cell lines that express a broad range of levels of cell surface MUC1. TAB28z-engineered T-cells demonstrated significant anti-tumour activity against MUC1+++ and MUC1++ breast cancer cell lines, while minimal activity was observed against the cell line with low MUC1 surface expression. The anti-tumour activity of MUC1-specific CAR T-cells was accompanied by significant production of IFN-γ.

In the course of these experiments, I observed that MUC1-specific CAR T-cells released IFN-γ constitutively, in the absence of interaction with tumour cells. This finding was unexpected and led to the hypothesis that MUC1 expressed by activated T-cells could promote the activation of the CARs under study in this project. In support of this, I found that MUC1 expressed by activated T-cells was detectable using the HMFG2 antibody. This finding contrasts with previously published data which showed that T-cell associated MUC1 carried predominantly normal-associated glycoforms which were not detected using this antibody[378].

The effects of the continuous recognition of MUC1 during the *in vitro* CAR T-cell expansion period was further evidenced by the demonstration that all three signalling-intact MUC1-specific CAR T-cells underwent enrichment in culture, accompanied by a trend towards increased activation and exhaustion. Another significant effect of this background recognition was the reduced

number of cells present in these cultures, which may have resulted from fratricide or from activation-induced cell death.

Despite these unexpected findings, I proceeded to investigate the efficacy of TAB28z in two distinct breast cancer xenograft models. A hint of anti-tumour activity was observed in mice with non-aggressive T-47D tumours. Nevertheless, neither TAB28z or the other two signalling signalling anti-MUC1 CARs were able to generate a potent anti-tumour response. This could be possibly partly attributed to the T-cell exhaustion phenotype that these CAR T-cell presented due to tonic signalling.

6.2 Future directions

6.2.1 Ameliorating the effects of tonic signalling

Different strategies could be designed in order to attempt to overcome the effects of tonic signalling. In a previous study by Long *et al.* it has been shown that the detrimental effects of continuous signalling of CAR T-cells could be abrogated by replacing the CD28 co-stimulatory molecule of the CAR signalling domain with that of 4-1BB[241].

Another possible solution in order to restore T-cell function is the use of checkpoint inhibitors. As evident by the results presented in Chapter 4, signalling-intact MUC1-CAR T-cells presented a trend of upregulation of various exhaustion markers, such as PD-1. As previously mentioned in Section 1.3.4.3.1, the combination of CAR T-cells with checkpoint inhibitors have already been investigated in both the pre-clinical and clinical settings[235,236,427]. Two different types of experiments could be designed: 1) simultaneous treatment of breast cancer xenograft mice with both CAR T-cells and a checkpoint inhibitor such as pembrolizumab, and 2) *in vitro* treatment of CAR T-cells with a checkpoint inhibitor in order to reverse T-cell exhaustion, prior to their administration in mice with established breast cancer tumours. In support of the 2nd suggestion, K. Moon et *al.* have shown that mesothelin-targeted CAR T-cells failed to result in tumour regression in mice due to T-cell exhaustion caused by the tumour microenvironment[374]. They further suggested that this effect is reversible as they managed to restore the activity of CAR TILs *ex vivo* by treating them with a PD-L1 inhibitor[374].

6.2.2 Prevention of recognition of MUC1 expressed on activated T-cells by MUC1-specific CAR T-cells

The above suggestions are focused on managing T-cell exhaustion due to tonic signalling. Alternative strategies that warrant consideration entail the prevention of background recognition of MUC1 by the CAR T-cells during their *in vitro* expansion. One such approach would involve the prevention of binding of the scFv domain of the CAR to MUC1. This could be achieved in two distinct ways. One option entails the culture the CAR T-cells in the presence of the MUC1 24mer peptide. This would be expected to occupy the CAR's binding domain, thus preventing to bind to MUC1 without cross-linking the CAR. Alternatively, the CAR T-cells could be cultured in the presence of either HMFG2 or TAB004. The added antibody would be expected to bind to MUC1 expressed on T-cells, thus competing with the binding of the scFv.

The latter approach could also be applied in the clinical setting in order to prevent on-target off-tumour toxicities. This idea suggests the pre-treatment of patients with a MUC1 antibody, in order to pre-occupy MUC1 expressed on activated T-cells. A similar strategy was followed in a phase I clinical trial for RCC patients where the efficacy of an anti-CAIX CAR was investigated. Previously, patients treated with CAIX-specific CAR T-cells presented severe liver tumour toxicity due to off-tumour recognition of CAIX-positive cells in the bile duct[252]. In an attempt to prevent this on-target off-tumour toxicity, Lamers and colleagues pre-treated a small number patients with an anti-CAIX monoclonal antibody, prior to the administration of CAIX-specific CAR T-cells[253]. According to the results of the study, the pre-treatment prevented the

on-target toxicity, thus allowing for administration of higher CAR T-cell dose. It is noteworthy that, in this approach, the dose of administered antibody needs to be optimized in order to allow for blocking of the antigen expressed in normal tissues without shielding its detection in tumour cells.

As previously mentioned, blocking the interaction of the anti-MUC1 CAR with MUC1 expressed on T-cells could be achieved by culturing the T-cells in the presence of either the MUC1 24mer peptide or a MUC1-specific antibody. Each of these strategies poses some limitations. The binding of MUC1 peptide to the scFv domain of the CAR could cause activation and in turn downregulation of the CAR receptor[428]. On the other hand, “masking” MUC1 on activated T-cells by culturing the T-cells in the presence of MUC1 antibodies has been previously reported to affect T-cell proliferation. Various studies have examined the role of MUC1 expressed on T-cells by culturing them in the presence of distinct MUC1 antibodies[375,377,429]. The results derived from these studies suggest the addition of antibody resulted in crosslinking of MUC1 and subsequently in inhibition of T-cell proliferation[375,377,429].

Another potential strategy of inhibiting the MUC1-CAR T-cell interaction during the *in vitro* T-cell expansion period is the ablation of MUC1 genes, for example using CRISPR/Cas9 technology. As previously mentioned in Chapter 1, this approach has already been used for the genetic engineering of CAR T-cells[237,240]. Additionally, this technology could be used in order to investigate further the role of MUC1 expressed on activated T-cells, since this remains unclear. As mentioned above, there is some evidence that MUC1 regulates T-cell function by inhibiting T-cell proliferation and promoting T-cell

depletion[430]. Others have suggested that MUC1 might play a role in T-cell migration through its interaction with endothelial cells[378].

Expression of MUC1 in other immune subsets such as in γδ T-cells, natural killer (NK) cells or NK T-cells remains unknown. All three cell populations have been previously used as carriers of CAR molecules instead of using αβ T-cells[431–434]. Thus, it would be interesting to investigate whether MUC1 is detectable by HMFG2 or TAB004 in these cell populations and if not then they could be transduced with the MUC1-specific CARs.

6.2.3 Prevention of severe adverse events in the clinical setting

The recognition of MUC1 on activated T-cells does not only affect the functionality of the anti-MUC1 CAR T-cells but also poses a significant risk for on-target off-tumour toxicities. The effects of administrating these MUC1-specific CAR T-cells into patients with an infection or an autoimmune disease could be detrimental. Additionally, it has been reported that HMFG2 reacts strongly with lactating breast and to a lesser extent with some other epithelial tissues such as normal resting breast tissue[317,318,320]. If this was going to be tested in a clinical trial, the necessity of integrating a control system within the MUC1-specific CAR T-cells is undeniable. As previously explained in Chapter 1, different suicide systems and elimination switches could be applied and used in CAR T-cell immunotherapy in order to prevent or mitigate serious adverse events[281,282,435].

6.2.4 Considerations regarding potency of MUC1-specific CAR T-cells

The lack of *in vivo* tumour regression following adoptive transfer of MUC1 re-targeted CAR T-cells could not only be attributable to tonic signalling but also to lack of CAR T-cell potency. As previously mentioned, it is difficult to target MUC1 with CAR T-cells due to its large extracellular domain which results in steric hindrance. The MUC1 extracellular domain is 200-500nm long, largely accounted for by the polymorphic VNTR region[436]. The recognition of an antigen/MHC by a T-cell receptor (TCR) leads to the immune synapse formation which subsequently results to T-cell activation[437]. The length of the immunological synapse (i.e the distance between the plasma membrane of T-cell and the antigen presenting cell (APC)) is approximately 15 nm (Figure 6.1)[438].

According to the kinetic segregation model, some non-specific kinase phosphorylation events are observed in resting T-cells which would result in low levels of T-cell activation[437,439]. CD148 and CD45 are large phosphatases that regulate immune responses. These non-specific phosphorylation events are inhibited by the CD148 and CD45 as they block kinase activation by causing de-phosphorylation[440]. Upon specific T-cell-antigen (APC) interaction the immunological synapse is formed. At this point, CD45 and CD148 are excluded from the synapse due to their large extracellular domain and thus there is no inhibition of the specific immune response[440]. Nevertheless, the large extracellular domain of MUC1 could hinder the formation of close-contact regions, when engaged by a CAR. This could subsequently permit

access to inhibitory phosphatases, leading to sub-optimal T-cell activation and preventing the formation of a close contact between T-cell and target cell. Based on this concept, one could consider that MUC1 may be too large to be targeted efficiently using a CAR-engineered T-cells (Figure 6.1).

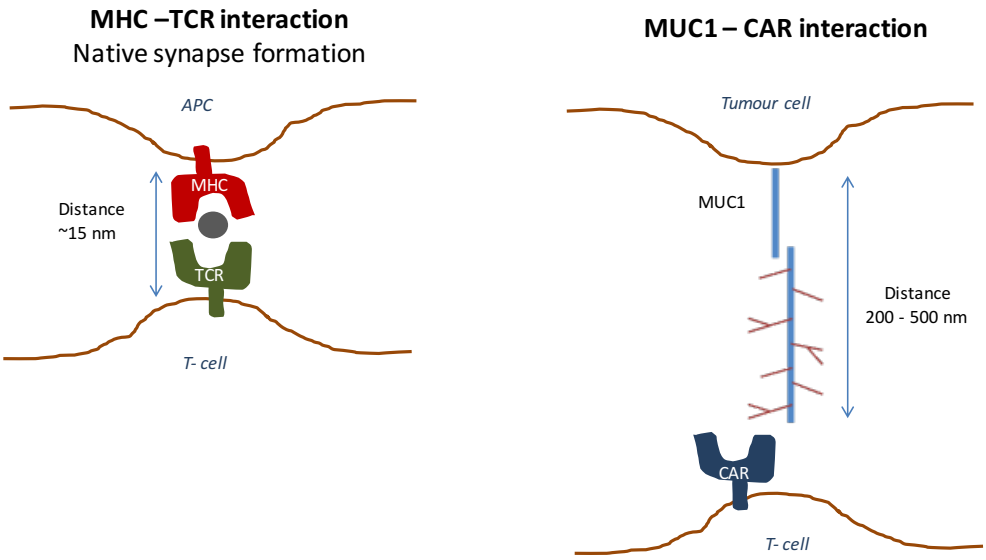

Figure 6.1: Steric hindrance due to the large extracellular MUC1 domain. In a normal MHC-interaction, the distance between a T-cell and an APC is ~15nm long. In the case where MUC1 is targeted by a CAR this distance is much bigger due to the large MUC1 extracellular domain.

Despite these considerations, others have shown that targeting MUC1 is possible with CAR T-cells. Nevertheless, in none of these studies the researchers suggested similar issues with tonic signalling. In the study by Wilkie *et al.,* the HMFG2-based CAR T-cells were expanded *in vitro* for a much shorter period of time (personal communication), thus making it impossible to make these observations[295]. Posey *et al.* used a scFv derived from the 5E5 antibody[337]. As previously shown in chapter 4, this antibody did not detect MUC1 on activated T-cells.

The low potency due to MUC1 steric inhabitation in combination with the effects of tonic signalling could have resulted to the lack of anti-tumour activity *in vivo* (Chapter 5).

Throughout this project, a CAR with an elongated spacer (HDF28z) was used in order to investigate if this will improve accessibility of the CAR to the MUC1 ectodomain[295]. Nevertheless, this did not result in improved T-cell activity such neither *in the vitro* or *in vivo* experiments presented. Other researchers have designed strategies in order to improve the anti-tumour activity of CAR T-cells. These include the targeted integration of the CAR transgene to the TRAC locus and co-expression of a CAR with the IL-17R cytokine receptor and they could be combined with the MUC1-immunotherapeutic approach presented herein[240,242].

6.2.5 Further comments

An important limitation of this study is that the surface expression of MUC1, in breast cancer cell lines and activated T-cells was only investigated using the HMFG2 antibody. Further studies need to be conducted whereby surface expression MUC1 in both settings is also investigated using the TAB004 antibody, allowing comparison with HMFG2. This was not done during this PhD project due to restricted access to TAB004. Nevertheless, the two antibodies seem to have similar binding preferences as indicated by their broadly similar binding profile to distinct TA glycoforms of MUC1. Additionally, both TAB004-based and HMFG2-based CARs are readily detectable by flow cytometry following incubation with a biotinylated VNTR-derived 24mer MUC1

peptide[284,441]. Both the TAB004-based and HMFG2-based CAR T-cells used in this project presented a similar pattern of background production of IFN-γ, CAR T-cell enrichment, reduced T-cell expansion and a trend towards increased T-cell activation and exhaustion. These observations strongly suggest that MUC1 expressed on T-cells is detectable by the TAB004 antibody in addition to HMFG2.

Another concern related to a MUC1-specific immunotherapeutic approach is the potential ability of the infused CAR T-cells to bind circulating (tumour-derived) MUC1. This could prevent the CAR T-cells from engaging MUC1 in the tumour site. Nevertheless, it has been previously shown that radiolabelled MUC1 antibodies effectively trafficked into the tumour site in patients with MUC1-expressing malignancies such as breast, ovarian and gastrointestinal cancer[291,292].

6.3 Conclusions

In summary, TAB28z CAR T-cells presented significant anti-tumour activity *in vitro*, which unfortunately was not maintained when evaluated in the *in vivo* setting. This novel CAR did not present superior functionality when compared to H28z and HDF28z CAR T-cells. An important finding of this PhD project is that MUC1 expressed on T-cells was detectable using the HMFG2 antibody, suggesting that is decorated with core-1 glycans. Recognition of MUC1 by MUC1-specific CAR T-cells during the *in vitro* expansion period led to tonic signalling which could have possibly contributed to the lack of efficacy in the breast cancer xenograft models used here. Different strategies could be designed in order to augment the results of this background recognition of MUC1 or to prevent it happening in the first place. Nevertheless, even if we prevent T-cell exhaustion, the risk of depletion of MUC1-positive T-cells by CAR T-cells administered to patients still exists. One possible solution would be to pre-treat patients with HMFG2 or TAB004 antibody in order to mask MUC1 epitopes expressed on T-cells. As it is unclear if this is going to be successful, administration of MUC1-specific CAR T-cells into patients should only take place only in combination with a CAR T-cell suicide system/ elimination switch. The results presented in this PhD project highlight one of the major obstacles which characterises CAR T-cell immunotherapy, namely the development of a safe and yet potent CAR T-cell immunotherapeutic approach directed against a tumour selective target found in solid tumours such as breast cancer.

Appendix

DNA sequences of MUC1-specific CAR constructs

TAB28z

ggatccGGATTAGTCCAATTTGTTAAAGACAGGATATCAGTGGTCCAGGCT
CTAGTTTTGACTCAACAATATCACCAGCTGAAGCCTATAGAGTACGAGC
CATAGATAAAATAAAAGATTTTATTTAGTCTCCAGAAAAAGGGGGGAAT
GAAAGACCCCACCTGTAGGTTTGGCAAGCTAGCTTAAGTAACGCCATTT
TGCAAGGCATGGAAAAATACATAACTGAGAATAGAGAAGTTCAGATCAA
GGTCAGGAACAGATGGAACAGCTGAATATGGGCCAAACAGGATATCTG
TGGTAAGCAGTTCCTGCCCCGGCTCAGGGCCAAGAACAGATGGAACA
GCTGAATATGGGCCAAACAGGATATCTGTGGTAAGCAGTTCCTGCCCC
GGCTCAGGGCCAAGAACAGATGGTCCCCAGATGCGGTCCAGCCCTCA
GCAGTTTCTAGAGAACCATCAGATGTTTCCAGGGTGCCCCAAGGACCT
GAAATGACCCTGTGCCTTATTTGAACTAACCAATCAGTTCGCTTCTCGC
TTCTGTTCGCGCGCTTCTGCTCCCCGAGCTCAATAAAAGAGCCCACAA
CCCCTCACTCGGGGCGCCAGTCCTCCGATTGACTGAGTCGCCCGGGT
ACCCGTGTATCCAATAAACCCTCTTGCAGTTGCATCCGACTTGTGGTCT
CGCTGTTCCTTGGGAGGGTCTCCTCTGAGTGATTGACTACCCGTCAGC
GGGGGTCTTTCACACATGCAGCATGTATCAAAATTAATTTGGTTTTTTTT
CTTAAGTATTTACATTAAATGGCCATAGTACTTAAAGTTACATTGGCTTC
CTTGAAATAAACATGGAGTATTCAGAATGTGTCATAAATATTTCTAATTTT
AAGATAGTATCTCCATTGGCTTTCTACTTTTTCTTTTATTTTTTTTTGTCC
TCTGTCTTCCATTTGTTGTTGTTGTTTGTTTGTTTGTTTGTTGGTTG
GTTGGTTAATTTTTTTTTAAAGATCCTACACTATAGTTCAAGCTAGACTAT
TAGCTACTCTGTAACCCAGGGTGACCTTGAAGTCATGGGTAGCCTGCT
GTTTTAGCCTTCCCACATCTAAGATTACAGGTATGAGCTATCATTTTTGG
TATATTGATTGATTGATTGATTGATGTGTGTGTGTGTGATTGTGTTTGTG
TGTGTGACTGTGAAAATGTGTGTATGGGTGTGTGTGAATGTGTGTATGT
ATGTGTGTGTGTGAGTGTGTGTGTGTGTGTGTGCATGTGTGTGTGTGT
GACTGTGTCTATGTGTATGACTGTGTGTGTGTGTGTGTGTGTGTGTGTG
TGTGTGTGTGTGTGTGTGTTGTGAAAAAATATTCTATGGTAGTGAGAGC
CAACGCTCCGGCTCAGGTGTCAGGTTGGTTTTTGAGACAGAGTCTTTC
ACTTAGCTTGGAATTCactggccgtcgttttacaacgtcgtgactgggaaaaccctggcgttacc
caacttaatcgccttgcagcacatccccctttcgccagctggcgtaatagcgaagaggcccgcaccgatc
gcccttcccaacagttgcgcagcctgaatggcgaatggcgcctgatgcggtattttctccttacgcatctgtg
cggtatttcacaccgcatatggtgcactctcagtacaatctgctctgatgccgcatagttaagccagccccg
acacccgccaacacccgctgacgcgccctgacgggcttgtctgctcccggcatccgcttacagacaagc
tgtgaccgtctccgggagctgcatgtgtcagaggttttcaccgtcatcaccgaaacgcgcgatgacgaaa
gggcctcgtgatacgcctatttttataggttaatgtcatgataataatggtttcttagacgtcaggtggcacttttt
cggggaaatgtgcgcggaacccctatttgtttatttttctaaatacattcaaatatgtatccgctcatgagaca
ataaccctgataaatgcttcaataatattgaaaaaggaagagtatgagtattcaacatttccgtgtcgcccttt
attcccttttttgcggcattttgccttcctgtttttgctcacccagaaacgctggtgaaagtaaaagatgctgaa
gatcagttgggtgcacgagtgggttacatcgaactggatctcaacagcggtaagatccttgagagttttcgc
cccgaagaacgttttccaatgatgagcacttttaaagttctgctatgtggcgcggtattatcccgtattgacgc
cgggcaagagcaactcggtcgccgcatacactattctcagaatgacttggttgagtactcaccagtcaca

gaaaagcatcttacggatggcatgacagtaagagaattatgcagtgctgccataaccatgagtgataac
actgcggccaacttacttctgacaacgatcggaggaccgaaggagctaaccgcttttttgcacaacatgg
gggatcatgtaactcgccttgatcgttgggaaccggagctgaatgaagccataccaaacgacgagcgtg
acaccacgatgcctgtagcaatggcaacaacgttgcgcaaactattaactggcgaactacttactctagct
tcccggcaacaattaatagactggatggaggcggataaagttgcaggaccacttctgcgctcggcccttc
cggctggctggtttattgctgataaatctggagccggtgagcgtgggtctcgcggtatcattgcagcactgg
ggccagatggtaagccctcccgtatcgtagttatctacacgacggggagtcaggcaactatggatgaac
gaaatagacagatcgctgagataggtgcctcactgattaagcattggtaactgtcagaccaagtttactcat
atatactttagattgatttaaaacttcatttttaatttaaaaggatctaggtgaagatccttttgataatctcatga
ccaaaatcccttaacgtgagttttcgttccactgagcgtcagaccccgtagaaaagatcaaaggatcttctt
gagatccttttttctgcgcgtaatctgctgcttgcaaacaaaaaaaccaccgctaccagcggtggtttgtttg
ccggatcaagagctaccaactctttttccgaaggtaactggcttcagcagagcgcagataccaaatactgt
ccttctagtgtagccgtagttaggccaccacttcaagaactctgtagcaccgcctacatacctcgctctgcta
atcctgttaccagtggctgctgccagtggcgataagtcgtgtcttaccgggttggactcaagacgatagtta
ccggataaggcgcagcggtcgggctgaacgggggggttcgtgcacacagcccagcttggagcgaacg
acctacaccgaactgagatacctacagcgtgagcattgagaaagcgccacgcttcccgaagggagaa
aggcggacaggtatccggtaagcggcagggtcggaacaggagagcgcacgagggagcttccaggg
ggaaacgcctggtatctttatagtcctgtcgggtttcgccacctctgacttgagcgtcgatttttgtgatgctcgt
caggggggcggagcctatggaaaaacgccagcaacgcggccttttacggttcctggccttttgctggcct
tttgctcacatgttctttcctgcgttatcccctgattctgtggataaccgtattaccgcctttgagtgagctgatac
cgctcgccgcagccgaacgaccgagcgcagcgagtcagtgagcgaggaagcggaagagcgccca
atacgcaaaccgcctctccccgcgcgttggccgattcattaatgcagctggcacgacaggtttcccgactg
gaaagcgggcagtgagcgcaacgcaattaatgtgagttagctcactcattaggcaccccaggctttaca
ctttatgcttccggctcgtatgttgtgtggaattgtgagcggataacaatttcacacaggaaacagctatgac
catgattacgccAAGCTTTGCTCTTAGGAGTTTCCTAATACATCCCAAACTCA
AATATATAAAGCATTTGACTTGTTCTATGCCCTAGGGGGCGGGGGGAA
GCTAAGCCAGCTTTTTTTAACATTTAAAATGTTAATTCCATTTTAAATGCA
CAGATGTTTTTATTTCATAAGGGTTTCAATGTGCATGAATGCTGCAATAT
TCCTGTTACCAAAGCTAGTATAAATAAAAATAGATAAACGTGGAAATTAC
TTAGAGTTTCTGTCATTAACGTTTCCTTCCTCAGTTGACAACATAAATGC
GCTGCTGAGCAAGCCAGTTTGCATCTGTCAGGATCAATTTCCCATTATG
CCAGTCATATTAATTACTAGTCAATTAGTTGATTTTTATTTTTGACATATA
CATGTGAATGAAAGACCCCACCTGTAGGTTTGGCAAGCTAGCTTAAGTA
ACGCCATTTTGCAAGGCATGGAAAAATACATAACTGAGAATAGAAAAGT
TCAGATCAAGGTCAGGAACAGATGGAACAGCTGAATATGGGCCAAACA
GGATATCTGTGGTAAGCAGTTCCTGCCCCGGCTCAGGGCCAAGAACAG
ATGGAACAGCTGAATATGGGCCAAACAGGATATCTGTGGTAAGCAGTT
CCTGCCCCGGCTCAGGGCCAAGAACAGATGGTCCCCAGATGCGGTCC
AGCCCTCAGCAGTTTCTAGAGAACCATCAGATGTTTCCAGGGTGCCCC
AAGGACCTGAAATGACCCTGTGCCTTATTTGAACTAACCAATCAGTTCG
CTTCTCGCTTCTGTTCGCGCGCTTATGCTCCCCGAGCTCAATAAAAGAG
CCCACAACCCCTCACTCGGGGCGCCAGTCCTCCGATTGACTGAGTCGC
CCGGGTACCCGTGTATCCAATAAACCCTCTTGCAGTTGCATCCGACTTG
TGGTCTCGCTGTTCCTTGGGAGGGTCTCCTCTGAGTGATTGACTACCC
GTCAGCGGGGGTCTTTCATTTGGGGGCTCGTCCGGGATCGGGAGACC
CCTGCCCAGGGACCACCGACCCACCACCGGGAGGTAAGCTGGCCAGC
AACTTATCTGTGTCTGTCCGATTGTCTAGTGTCTATGACTGATTTTATGC
GCCTGCGTCGGTACTAGTTAGCTAACTAGCTCTGTATCTGGCGGACCC
GTGGTGGAACTGACGAGTTCGGAACACCCGGCCGCAACCCTGGGAGA

CGTCCCAGGGACTTCGGGGGCCGTTTTTGTGGCCCGACCTGAGTCCTA
AAATCCCGATCGTTTAGGACTCTTTGGTGCACCCCCCTTAGAGGAGGG
ATATGTGGTTCTGGTAGGAGACGAGAACCTAAAACAGTTCCCGCCTCC
GTCTGAATTTTTGCTTTCGGTTTGGGACCGAAGCCGCGCCGCGCGTCT
TGTCTGCTGCAGCATCGTTCTGTGTTGTCTCTGTCTGACTGTGTTTCTG
TATTTGTCTGAAAATATGGGCCCGGGCTAGactgttaccactCCCTTAAGTTT
GACCTTAGGTCACTGGAAAGATGTCGAGCGGATCGCTCACAACCAGTC
GGTAGATGTCAAGAAGAGACGTTGGGTTACCTTCTGCTCTGCAGAATG
GCCAACCTTTAACGTCGGATGGCCGCGAGACGGCACCTTTAACCGAGA
CCTCATCACCCAGGTTAAGATCAAGGTCTTTTCACCTGGCCCGCATGG
ACACCCAGACCAGGTccccTACATCGTGACCTGGGAAGCCTTGGCTTTT
GACCCCCCTCCCTGGGTCAAGCCCTTTGTACACCCTAAGCCTCCGCCT
CCTCTTCCTCCATCCGCCCCGTCTCTCCCCCTTGAACCTCCTCGTTCGA
CCCCGCCTCGATCCTCCCTTTATCCAGCCCTCACTCCTTCTCTAGGCG
CCCCCATATGGCCATATGAGATCTTATATGGGGCACCCCCGCCCCTTG
TAAACTTCCCTGACCCTGACATGACAAGAGTTACTAACAGCCCCTCTCT
CCAAGCTCACTTACAGGCTCTCTACTTAGTCCAGCACGAAGTCTGGAG
ACCTCTGGCGGCAGCCTACCAAGAACAACTGGACCGACCGGTGGTAC
CTCACCCTTACCGAGTCGGCGACACAGTGTGGGTCCGCCGACACCAG
ACTAAGAACCTAGAACCTCGCTGGAAAGGACCTTACACAGTCCTGCTG
ACCACCCCCACCGCCCTCAAAGTAGACGGCATCGCAGCTTGGATACAC
GCCGCCCACGTGAAGGCTGCCGACCCCGGGGGTGGACCATCCTCTAG
ACTGCcATGGCCCTGCCCGTGACCGCCCTGCTCTTGCCCCTGGCCCTT
CTGCTCCACGCCGCCAGACCCGAGGTGCAGCTGCAGCAGAGCGGAGG
CGAGAGAGCCACCCCTGGCGCCAGCGTGAAGATGAGCTGCAAGACCA
GCGGCTACACCTTCACCAACTACTGGATGCACTGGGTGAAGCAGAGAC
CCGGCCAGGGCCTGGAGTGGATCGGCTACATCAACCCTAGCTCCGGC
TACACCCAGTACAACCAGAAGTTCAAGGACAAGGCCACCCTGACCGCC
GACAAGAGCTCCAGCACCGCCTACATCCAGCTGAGCTCCCTGACCAGC
GAGGACTCCGCCGTGTACTATTGCAGCACCTACTACGGCGACTACCTG
TTCCCCTACTGGGGCCAGGGCACCCTGGTGACCGTGAGCGCCGGCGG
AGGCGGAAGCGGAGGCGGCGGATCCGGAGGAGGCGGCAGCGACGTG
CTGATGACCCAGACCCCTCTGAGCCTGCCCGTGAGCCTGGGCGACCA
GGCCAGCATCAGCTGCAGAAGCTCCCAGGACATCGTGTACGGCAACG
GAAACACCTACCTGGAGTGGTACCTCCAGAAGCCCGGCCAGAGCCCC
AAGCTGCTGATCTACAAGGTGAGCAACAGATTCAGCGGCGTGCCCGAC
AGATTCAGCGGCTCCGGAAGCGGAACCGACTTCACCCTGAAGATCAGC
AGAGTGGAGGCCGAGGACCTGGGCGTGTACTATTGCTTCCAGGGCAG
CCACGTGCCCTACACCTTCGGCGGAGGCACCAAGCTGGAGATCAAGA
GAGCGGCCGCTATCGAGGTGGAGCAGAAGCTGATCAGCGAGGAGGAC
CTGCTAGACAATGAGAAGAGCAATGGAACCATTATCCATGTGAAAGGG
AAACACCTTTGTCCAAGTCCCCTATTTCCCGGACCTTCTAAGCCCTTTT
GGGTGCTGGTGGTGGTTGGTGGAGTCCTGGCTTGCTATAGCTTGCTAG
TAACAGTGGCCTTTATTATTTTCTGGGTGAGGAGTAAGAGGAGCAGGCT
CCTGCACAGTGACTACATGAACATGACTCCCCGCCGCCCCGGGCCCA
CCCGCAAGCATTACCAGCCCTATGCCCCACCACGCGACTTCGCAGCCT
ATCGCTCCAGAGTGAAGTTCAGCAGGAGCGCAGACGCCCCCGCGTAC
CAGCAGGGCCAGAACCAGCTCTATAACGAGCTCAATCTAGGACGAAGA
GAGGAGTACGATGTTTTGGACAAGAGACGTGGCCGGGACCCTGAGAT

GGGGGGAAAGCCGAGAAGGAAGAACCCTCAGGAAGGCCTGTACAATG
AACTGCAGAAAGATAAGATGGCGGAGGCCTACAGTGAGATTGGGATGA
AAGGCGAGCGCCGGAGGGGCAAGGGGCACGATGGCCTTTACCAGGG
TCTCAGTACAGCCACCAAGGACACCTACGACGCCCTTCACATGCAGGC
CCTGCCCCCTCGCTAACAGCCACTCGAG

H28z
ATGGCTCTCCCAGTGACTGCCCTACTGCTTCCCCTAGCGCTTCTCCTG
CATGCAGAGGTGCAGCTGCAGCAGTCTGGAGGAGGCTTGGTGCAACC
TGGAGGATCCATGAAACTCTCCTGTGTTGCCTCTGGATTCACTTTCAGT
AACTACTGGATGAACTGGGTCCGCCAGTCTCCAGAGAAGGGGCTTGAG
TGGGTTGCTGAAATTAGATTGAAATCTAATAATTATGCAACACATTATGC
GGAGTCTGTGAAAGGGAGGTTCACCATCTCAAGAGATGATTCCAAAAG
TAGTGTCTACCTGCAAATGAACAACTTAAGAGCTGAAGACACTGGCATT
TATTACTGTACCTTTGGTAACTCCTTTGCTTACTGGGGCCAAGGGACCA
CGGTCACCGTCTCCTCAGGTGGAGGTGGATCAGGTGGAGGTGGATCT
GGTGGAGGTGGATCTGACATTGTGCTCACTCAGGAATCTGCACTCACC
ACATCACCTGGTGAAACAGTCACACTCACTTGTCGCTCAAGTACTGGG
GCTGTTACAACTAGTAACTATGCCAACTGGGTCCAAGAAAAACCAGATC
ATTTATTCACTGGTCTAATAGGTGGTACCAACAACCGAGCACCAGGTGT
TCCTGCCAGATTCTCAGGCTCCCTGATTGGAGACAAGGCTGCCCTCAC
CATCACAGGGGCACAGACTGAGGATGAGGCAATATATTTCTGTGCTCT
ATGGTACAGCAACCATTGGGTGTTCGGTGGAGGAACCAAACTGACTGT
CCTAGGATCAGAGGCGGCCGCAATTGAAGTTATGTATCCTCCTCCTTAC
CTAGACAATGAGAAGAGCAATGGAACCATTATCCATGTGAAAGGGAAA
CACCTTTGTCCAAGTCCCCTATTTCCCGGACCTTCTAAGCCCTTTTGGG
TGCTGGTGGTGGTTGGTGGAGTCCTGGCTTGCTATAGCTTGCTAGTAA
CAGTGGCCTTTATTATTTTCTGGGTGAGGAGTAAGAGGAGCAGGCTCC
TGCACAGTGACTACATGAACATGACTCCCCGCCGCCCCGGGCCCACC
CGCAAGCATTACCAGCCCTATGCCCCACCACGCGACTTCGCAGCCTAT
CGCTCCAGAGTGAAGTTCAGCAGGAGCGCAGACGCCCCCGCGTACCA
GCAGGGCCAGAACCAGCTCTATAACGAGCTCAATCTAGGACGAAGAGA
GGAGTACGATGTTTTGGACAAGAGACGTGGCCGGGACCCTGAGATGG
GGGGAAAGCCGAGAAGGAAGAACCCTCAGGAAGGCCTGTACAATGAA
CTGCAGAAAGATAAGATGGCGGAGGCCTACAGTGAGATTGGGATGAAA
GGCGAGCGCCGGAGGGGCAAGGGGCACGATGGCCTTTACCAGGGTC
TCAGTACAGCCACCAAGGACACCTACGACGCCCTTCACATGCAGGCCC
TGCCCCCTCGCTAACAGCCACTCGAGGATCCGGATTAGTCCAATTTGTT
AAAGACAGGATATCAGTGGTCCAGGCTCTAGTTTTGACTCAACAATATC
ACCAGCTGAAGCCTATAGAGTACGAGCCATAGATAAAATAAAAGATTTT
ATTTAGTCTCCAGAAAAAGGGGGGAATGAAAGACCCCACCTGTAGGTT
TGGCAAGCTAGCTTAAGTAACGCCATTTTGCAAGGCATGGAAAAATACA
TAACTGAGAATAGAGAAGTTCAGATCAAGGTCAGGAACAGATGGAACA
GCTGAATATGGGCCAAACAGGATATCTGTGGTAAGCAGTTCCTGCCCC
GGCTCAGGGCCAAGAACAGATGGAACAGCTGAATATGGGCCAAACAG
GATATCTGTGGTAAGCAGTTCCTGCCCCGGCTCAGGGCCAAGAACAGA
TGGTCCCCAGATGCGGTCCAGCCCTCAGCAGTTTCTAGAGAACCATCA
GATGTTTCCAGGGTGCCCCAAGGACCTGAAATGACCCTGTGCCTTATTT
GAACTAACCAATCAGTTCGCTTCTCGCTTCTGTTCGCGCGCTTCTGCTC

CCCGAGCTCAATAAAAGAGCCCACAACCCCTCACTCGGGGCGCCAGTC
CTCCGATTGACTGAGTCGCCCGGGTACCCGTGTATCCAATAAACCCTC
TTGCAGTTGCATCCGACTTGTGGTCTCGCTGTTCCTTGGGAGGGTCTC
CTCTGAGTGATTGACTACCCGTCAGCGGGGGTCTTTCACACATGCAGC
ATGTATCAAAATTAATTTGGTTTTTTTTCTTAAGTATTTACATTAAATGGC
CATAGTACTTAAAGTTACATTGGCTTCCTTGAAATAAACATGGAGTATTC
AGAATGTGTCATAAATATTTCTAATTTTAAGATAGTATCTCCATTGGCTTT
CTACTTTTTCTTTTATTTTTTTTTGTCCTCTGTCTTCCATTTGTTGTTGTTG
TTGTTTGTTTGTTTGTTTGTTGGTTGGTTGGTTAATTTTTTTTTAAAGATC
CTACACTATAGTTCAAGCTAGACTATTAGCTACTCTGTAACCCAGGGTG
ACCTTGAAGTCATGGGTAGCCTGCTGTTTTAGCCTTCCCACATCTAAGA
TTACAGGTATGAGCTATCATTTTTGGTATATTGATTGATTGATTGATTGA
TGTGTGTGTGTGTGATTGTGTTTGTGTGTGTGACTGTGAAAATGTGTGT
ATGGGTGTGTGTGAATGTGTGTATGTATGTGTGTGTGTGAGTGTGTGTG
TGTGTGTGTGCATGTGTGTGTGTGTGACTGTGTCTATGTGTATGACTGT
GTGTGTGTGTGTGTGTGTGTGTGTGTGTGTGTGTGTGTGTGTGTTGTG
AAAAAATATTCTATGGTAGTGAGAGCCAACGCTCCGGCTCAGGTGTCA
GGTTGGTTTTTGAGACAGAGTCTTTCACTTAGCTTGGAATTCACTGGCC
GTCGTTTTACAACGTCGTGACTGGGAAAACCCTGGCGTTACCCAACTTA
ATCGCCTTGCAGCACATCCCCCTTTCGCCAGCTGGCGTAATAGCGAAG
AGGCCCGCACCGATCGCCCTTCCCAACAGTTGCGCAGCCTGAATGGC
GAATGGCGCCTGATGCGGTATTTTCTCCTTACGCATCTGTGCGGTATTT
CACACCGCATATGGTGCACTCTCAGTACAATCTGCTCTGATGCCGCATA
GTTAAGCCAGCCCCGACACCCGCCAACACCCGCTGACGCGCCCTGAC
GGGCTTGTCTGCTCCCGGCATCCGCTTACAGACAAGCTGTGACCGTCT
CCGGGAGCTGCATGTGTCAGAGGTTTTCACCGTCATCACCGAAACGCG
CGATGACGAAAGGGCCTCGTGATACGCCTATTTTTATAGGTTAATGTCA
TGATAATAATGGTTTCTTAGACGTCAGGTGGCACTTTTCGGGGAAATGT
GCGCGGAACCCCTATTTGTTTATTTTTCTAAATACATTCAAATATGTATC
CGCTCATGAGACAATAACCCTGATAAATGCTTCAATAATATTGAAAAAG
GAAGAGTATGAGTATTCAACATTTCCGTGTCGCCCTTATTCCCTTTTTTG
CGGCATTTTGCCTTCCTGTTTTTGCTCACCCAGAAACGCTGGTGAAAGT
AAAAGATGCTGAAGATCAGTTGGGTGCACGAGTGGGTTACATCGAACT
GGATCTCAACAGCGGTAAGATCCTTGAGAGTTTTCGCCCCGAAGAACG
TTTTCCAATGATGAGCACTTTTAAAGTTCTGCTATGTGGCGCGGTATTAT
CCCGTATTGACGCCGGGCAAGAGCAACTCGGTCGCCGCATACACTATT
CTCAGAATGACTTGGTTGAGTACTCACCAGTCACAGAAAAGCATCTTAC
GGATGGCATGACAGTAAGAGAATTATGCAGTGCTGCCATAACCATGAG
TGATAACACTGCGGCCAACTTACTTCTGACAACGATCGGAGGACCGAA
GGAGCTAACCGCTTTTTTGCACAACATGGGGGATCATGTAACTCGCCTT
GATCGTTGGGAACCGGAGCTGAATGAAGCCATACCAAACGACGAGCGT
GACACCACGATGCCTGTAGCAATGGCAACAACGTTGCGCAAACTATTA
ACTGGCGAACTACTTACTCTAGCTTCCCGGCAACAATTAATAGACTGGA
TGGAGGCGGATAAAGTTGCAGGACCACTTCTGCGCTCGGCCCTTCCG
GCTGGCTGGTTTATTGCTGATAAATCTGGAGCCGGTGAGCGTGGGTCT
CGCGGTATCATTGCAGCACTGGGGCCAGATGGTAAGCCCTCCCGTATC
GTAGTTATCTACACGACGGGGAGTCAGGCAACTATGGATGAACGAAAT
AGACAGATCGCTGAGATAGGTGCCTCACTGATTAAGCATTGGTAACTGT
CAGACCAAGTTTACTCATATATACTTTAGATTGATTTAAAACTTCATTTTT

AATTTAAAAGGATCTAGGTGAAGATCCTTTTTGATAATCTCATGACCAAA
ATCCCTTAACGTGAGTTTTCGTTCCACTGAGCGTCAGACCCCGTAGAAA
AGATCAAAGGATCTTCTTGAGATCCTTTTTTTCTGCGCGTAATCTGCTG
CTTGCAAACAAAAAAACCACCGCTACCAGCGGTGGTTTGTTTGCCGGA
TCAAGAGCTACCAACTCTTTTTCCGAAGGTAACTGGCTTCAGCAGAGCG
CAGATACCAAATACTGTCCTTCTAGTGTAGCCGTAGTTAGGCCACCACT
TCAAGAACTCTGTAGCACCGCCTACATACCTCGCTCTGCTAATCCTGTT
ACCAGTGGCTGCTGCCAGTGGCGATAAGTCGTGTCTTACCGGGTTGGA
CTCAAGACGATAGTTACCGGATAAGGCGCAGCGGTCGGGCTGAACGG
GGGGTTCGTGCACACAGCCCAGCTTGGAGCGAACGACCTACACCGAA
CTGAGATACCTACAGCGTGAGCATTGAGAAAGCGCCACGCTTCCCGAA
GGGAGAAAGGCGGACAGGTATCCGGTAAGCGGCAGGGTCGGAACAG
GAGAGCGCACGAGGGAGCTTCCAGGGGGAAACGCCTGGTATCTTTATA
GTCCTGTCGGGTTTCGCCACCTCTGACTTGAGCGTCGATTTTTGTGATG
CTCGTCAGGGGGGCGGAGCCTATGGAAAAACGCCAGCAACGCGGCCT
TTTTACGGTTCCTGGCCTTTTGCTGGCCTTTTGCTCACATGTTCTTTCCT
GCGTTATCCCCTGATTCTGTGGATAACCGTATTACCGCCTTTGAGTGAG
CTGATACCGCTCGCCGCAGCCGAACGACCGAGCGCAGCGAGTCAGTG
AGCGAGGAAGCGGAAGAGCGCCCAATACGCAAACCGCCTCTCCCCGC
GCGTTGGCCGATTCATTAATGCAGCTGGCACGACAGGTTTCCCGACTG
GAAAGCGGGCAGTGAGCGCAACGCAATTAATGTGAGTTAGCTCACTCA
TTAGGCACCCCAGGCTTTACACTTTATGCTTCCGGCTCGTATGTTGTGT
GGAATTGTGAGCGGATAACAATTTCACACAGGAAACAGCTATGACCATG
ATTACGCCAAGCTTTGCTCTTAGGAGTTTCCTAATACATCCCAAACTCAA
ATATATAAAGCATTTGACTTGTTCTATGCCCTAGGGGGCGGGGGGAAG
CTAAGCCAGCTTTTTTTAACATTTAAAATGTTAATTCCATTTTAAATGCAC
AGATGTTTTTATTTCATAAGGGTTTCAATGTGCATGAATGCTGCAATATT
CCTGTTACCAAAGCTAGTATAAATAAAAATAGATAAACGTGGAAATTACT
TAGAGTTTCTGTCATTAACGTTTCCTTCCTCAGTTGACAACATAAATGCG
CTGCTGAGCAAGCCAGTTTGCATCTGTCAGGATCAATTTCCCATTATGC
CAGTCATATTAATTACTAGTCAATTAGTTGATTTTTATTTTTGACATATAC
ATGTGAATGAAAGACCCCACCTGTAGGTTTGGCAAGCTAGCTTAAGTAA
CGCCATTTTGCAAGGCATGGAAAAATACATAACTGAGAATAGAAAAGTT
CAGATCAAGGTCAGGAACAGATGGAACAGCTGAATATGGGCCAAACAG
GATATCTGTGGTAAGCAGTTCCTGCCCCGGCTCAGGGCCAAGAACAGA
TGGAACAGCTGAATATGGGCCAAACAGGATATCTGTGGTAAGCAGTTC
CTGCCCCGGCTCAGGGCCAAGAACAGATGGTCCCCAGATGCGGTCCA
GCCCTCAGCAGTTTCTAGAGAACCATCAGATGTTTCCAGGGTGCCCCA
AGGACCTGAAATGACCCTGTGCCTTATTTGAACTAACCAATCAGTTCGC
TTCTCGCTTCTGTTCGCGCGCTTATGCTCCCCGAGCTCAATAAAAGAGC
CCACAACCCCTCACTCGGGGCGCCAGTCCTCCGATTGACTGAGTCGCC
CGGGTACCCGTGTATCCAATAAACCCTCTTGCAGTTGCATCCGACTTGT
GGTCTCGCTGTTCCTTGGGAGGGTCTCCTCTGAGTGATTGACTACCCG
TCAGCGGGGGTCTTTCATTTGGGGGCTCGTCCGGGATCGGGAGACCC
CTGCCCAGGGACCACCGACCCACCACCGGGAGGTAAGCTGGCCAGCA
ACTTATCTGTGTCTGTCCGATTGTCTAGTGTCTATGACTGATTTTATGCG
CCTGCGTCGGTACTAGTTAGCTAACTAGCTCTGTATCTGGCGGACCCG
TGGTGGAACTGACGAGTTCGGAACACCCGGCCGCAACCCTGGGAGAC
GTCCCAGGGACTTCGGGGGCCGTTTTTGTGGCCCGACCTGAGTCCTAA

AATCCCGATCGTTTAGGACTCTTTGGTGCACCCCCCTTAGAGGAGGGA
TATGTGGTTCTGGTAGGAGACGAGAACCTAAAACAGTTCCCGCCTCCG
TCTGAATTTTTGCTTTCGGTTTGGGACCGAAGCCGCGCCGCGCGTCTT
GTCTGCTGCAGCATCGTTCTGTGTTGTCTCTGTCTGACTGTGTTTCTGT
ATTTGTCTGAAAATATGGGCCCGGGCTAGACTGTTACCACTCCCTTAAG
TTTGACCTTAGGTCACTGGAAAGATGTCGAGCGGATCGCTCACAACCA
GTCGGTAGATGTCAAGAAGAGACGTTGGGTTACCTTCTGCTCTGCAGA
ATGGCCAACCTTTAACGTCGGATGGCCGCGAGACGGCACCTTTAACCG
AGACCTCATCACCCAGGTTAAGATCAAGGTCTTTTCACCTGGCCCGCAT
GGACACCCAGACCAGGTCCCCTACATCGTGACCTGGGAAGCCTTGGCT
TTTGACCCCCCTCCCTGGGTCAAGCCCTTTGTACACCCTAAGCCTCCG
CCTCCTCTTCCTCCATCCGCCCCGTCTCTCCCCCTTGAACCTCCTCGTT
CGACCCCGCCTCGATCCTCCCTTTATCCAGCCCTCACTCCTTCTCTAGG
CGCCCCCATATGGCCATATGAGATCTTATATGGGGCACCCCCGCCCCT
TGTAAACTTCCCTGACCCTGACATGACAAGAGTTACTAACAGCCCCTCT
CTCCAAGCTCACTTACAGGCTCTCTACTTAGTCCAGCACGAAGTCTGGA
GACCTCTGGCGGCAGCCTACCAAGAACAACTGGACCGACCGGTGGTA
CCTCACCCTTACCGAGTCGGCGACACAGTGTGGGTCCGCCGACACCA
GACTAAGAACCTAGAACCTCGCTGGAAAGGACCTTACACAGTCCTGCT
GACCACCCCCACCGCCCTCAAAGTAGACGGCATCGCAGCTTGGATACA
CGCCGCCCACGTGAAGGCTGCCGACCCCGGGGGTGGACCATCCTCTA
GACTGCC

HDF28z
ggatccGGATTAGTCCAATTTGTTAAAGACAGGATATCAGTGGTCCAGGCT
CTAGTTTTGACTCAACAATATCACCAGCTGAAGCCTATAGAGTACGAGC
CATAGATAAAATAAAAGATTTTATTTAGTCTCCAGAAAAAGGGGGGAAT
GAAAGACCCCACCTGTAGGTTTGGCAAGCTAGCTTAAGTAACGCCATTT
TGCAAGGCATGGAAAAATACATAACTGAGAATAGAGAAGTTCAGATCAA
GGTCAGGAACAGATGGAACAGCTGAATATGGGCCAAACAGGATATCTG
TGGTAAGCAGTTCCTGCCCCGGCTCAGGGCCAAGAACAGATGGAACA
GCTGAATATGGGCCAAACAGGATATCTGTGGTAAGCAGTTCCTGCCCC
GGCTCAGGGCCAAGAACAGATGGTCCCCAGATGCGGTCCAGCCCTCA
GCAGTTTCTAGAGAACCATCAGATGTTTCCAGGGTGCCCCAAGGACCT
GAAATGACCCTGTGCCTTATTTGAACTAACCAATCAGTTCGCTTCTCGC
TTCTGTTCGCGCGCTTCTGCTCCCCGAGCTCAATAAAAGAGCCCACAA
CCCCTCACTCGGGGCGCCAGTCCTCCGATTGACTGAGTCGCCCGGGT
ACCCGTGTATCCAATAAACCCTCTTGCAGTTGCATCCGACTTGTGGTCT
CGCTGTTCCTTGGGAGGGTCTCCTCTGAGTGATTGACTACCCGTCAGC
GGGGGTCTTTCACACATGCAGCATGTATCAAAATTAATTTGGTTTTTTTT
CTTAAGTATTTACATTAAATGGCCATAGTACTTAAAGTTACATTGGCTTC
CTTGAAATAAACATGGAGTATTCAGAATGTGTCATAAATATTTCTAATTTT
AAGATAGTATCTCCATTGGCTTTCTACTTTTTCTTTTATTTTTTTTTGTCC
TCTGTCTTCCATTTGTTGTTGTTGTTTGTTTGTTTGTTTGTTGGTTG
GTTGGTTAATTTTTTTTTAAAGATCCTACACTATAGTTCAAGCTAGACTAT
TAGCTACTCTGTAACCCAGGGTGACCTTGAAGTCATGGGTAGCCTGCT
GTTTTAGCCTTCCCACATCTAAGATTACAGGTATGAGCTATCATTTTTGG
TATATTGATTGATTGATTGATTGATGTGTGTGTGTGTGATTGTGTTTGTG
TGTGTGACTGTGAAAATGTGTGTATGGGTGTGTGTGAATGTGTGTATGT

ATGTGTGTGTGTGAGTGTGTGTGTGTGTGTGTGCATGTGTGTGTGTGT
GACTGTGTCTATGTGTATGACTGTGTGTGTGTGTGTGTGTGTGTGTG
TGTGTGTGTGTGTGTGTGTTGTGAAAAAATATTCTATGGTAGTGAGAGC
CAACGCTCCGGCTCAGGTGTCAGGTTGGTTTTTGAGACAGAGTCTTTC
ACTTAGCTTGGAATTCactggccgtcgttttacaacgtcgtgactgggaaaaccctggcgttacc
caacttaatcgccttgcagcacatccccctttcgccagctggcgtaatagcgaagaggcccgcaccgatc
gcccttcccaacagttgcgcagcctgaatggcgaatggcgcctgatgcggtattttctccttacgcatctgtg
cggtatttcacaccgcatatggtgcactctcagtacaatctgctctgatgccgcatagttaagccagccccg
acacccgccaacacccgctgacgcgccctgacgggcttgtctgctcccggcatccgcttacagacaagc
tgtgaccgtctccgggagctgcatgtgtcagaggttttcaccgtcatcaccgaaacgcgcgatgacgaaa
gggcctcgtgatacgcctatttttataggttaatgtcatgataataatggtttcttagacgtcaggtggcacttttt
cggggaaatgtgcgcggaacccctatttgtttatttttctaaatacattcaaatatgtatccgctcatgagaca
ataaccctgataaatgcttcaataatattgaaaaaggaagagtatgagtattcaacatttccgtgtcgcccttt
attcccttttttgcggcattttgccttcctgtttttgctcacccagaaacgctggtgaaagtaaaagatgctgaa
gatcagttgggtgcacgagtgggttacatcgaactggatctcaacagcggtaagatccttgagagttttcgc
cccgaagaacgttttccaatgatgagcacttttaaagttctgctatgtggcgcggtattatcccgtattgacgc
cgggcaagagcaactcggtcgccgcatacactattctcagaatgacttggttgagtactcaccagtcaca
gaaaagcatcttacggatggcatgacagtaagagaattatgcagtgctgccataaccatgagtgataac
actgcggccaacttacttctgacaacgatcggaggaccgaaggagctaaccgcttttttgcacaacatgg
gggatcatgtaactcgccttgatcgttgggaaccggagctgaatgaagccataccaaacgacgagcgtg
acaccacgatgcctgtagcaatggcaacaacgttgcgcaaactattaactggcgaactacttactctagct
tcccggcaacaattaatagactggatggaggcggataaagttgcaggaccacttctgcgctcggcccttc
cggctggctggtttattgctgataaatctggagccggtgagcgtgggtctcgcggtatcattgcagcactgg
ggccagatggtaagccctcccgtatcgtagttatctacacgacggggagtcaggcaactatggatgaac
gaaatagacagatcgctgagataggtgcctcactgattaagcattggtaactgtcagaccaagtttactcat
atatactttagattgatttaaaacttcatttttaatttaaaaggatctaggtgaagatccttttttgataatctcatga
ccaaaatcccttaacgtgagttttcgttccactgagcgtcagaccccgtagaaaagatcaaaggatcttctt
gagatccttttttttctgcgcgtaatctgctgcttgcaaacaaaaaaaccaccgctaccagcggtggtttgtttg
ccggatcaagagctaccaactctttttccgaaggtaactggcttcagcagagcgcagataccaaatactgt
ccttctagtgtagccgtagttaggccaccacttcaagaactctgtagcaccgcctacatacctcgctctgcta
atcctgttaccagtggctgctgccagtggcgataagtcgtgtcttaccgggttggactcaagacgatagtta
ccggataaggcgcagcggtcgggctgaacgggggggttcgtgcacacagcccagcttggagcgaacg
acctacaccgaactgagatacctacagcgtgagcattgagaaagcgccacgcttcccgaagggagaaa
aggcggacaggtatccggtaagcggcagggtcggaacaggagagcgcacgagggagcttccaggg
ggaaacgcctggtatctttatagtcctgtcgggtttcgccacctctgacttgagcgtcgatttttgtgatgctcgt
caggggggcggagcctatggaaaaacgccagcaacgcggccttttacggttcctggccttttgctggcct
tttgctcacatgttctttcctgcgttatcccctgattctgtggataaccgtattaccgcctttgagtgagctgatac
cgctcgccgcagccgaacgaccgagcgcagcgagtcagtgagcgaggaagcggaagagcgccca
atacgcaaaccgcctctccccgcgcgttggccgattcattaatgcagctggcacgacaggtttcccgactg
gaaagcgggcagtgagcgcaacgcaattaatgtgagttagctcactcattaggcaccccaggctttaca
ctttatgcttccggctcgtatgttgtgtggaattgtgagcggataacaatttcacacaggaaacagctatgac
catgattacgccAAGCTTTGCTCTTAGGAGTTTCCTAATACATCCCAAACTCA
AATATATAAAGCATTTGACTTGTTCTATGCCCTAGGGGGCGGGGGGAA
GCTAAGCCAGCTTTTTTTAACATTTAAAATGTTAATTCCATTTTAAATGCA
CAGATGTTTTTATTTCATAAGGGTTTCAATGTGCATGAATGCTGCAATAT
TCCTGTTACCAAAGCTAGTATAAATAAAAATAGATAAACGTGGAAATTAC
TTAGAGTTTCTGTCATTAACGTTTCCTTCCTCAGTTGACAACATAAATGC
GCTGCTGAGCAAGCCAGTTTGCATCTGTCAGGATCAATTTCCCATTATG
CCAGTCATATTAATTACTAGTCAATTAGTTGATTTTTATTTTTGACATATA

CATGTGAATGAAAGACCCCACCTGTAGGTTTGGCAAGCTAGCTTAAGTA
ACGCCATTTTGCAAGGCATGGAAAAATACATAACTGAGAATAGAAAAGT
TCAGATCAAGGTCAGGAACAGATGGAACAGCTGAATATGGGCCAAACA
GGATATCTGTGGTAAGCAGTTCCTGCCCCGGCTCAGGGCCAAGAACAG
ATGGAACAGCTGAATATGGGCCAAACAGGATATCTGTGGTAAGCAGTT
CCTGCCCCGGCTCAGGGCCAAGAACAGATGGTCCCCAGATGCGGTCC
AGCCCTCAGCAGTTTCTAGAGAACCATCAGATGTTTCCAGGGTGCCCC
AAGGACCTGAAATGACCCTGTGCCTTATTTGAACTAACCAATCAGTTCG
CTTCTCGCTTCTGTTCGCGCGCTTATGCTCCCCGAGCTCAATAAAAGAG
CCCACAACCCCTCACTCGGGGCGCCAGTCCTCCGATTGACTGAGTCGC
CCGGGTACCCGTGTATCCAATAAACCCTCTTGCAGTTGCATCCGACTTG
TGGTCTCGCTGTTCCTTGGGAGGGTCTCCTCTGAGTGATTGACTACCC
GTCAGCGGGGGTCTTTCATTTGGGGGCTCGTCCGGGATCGGGAGACC
CCTGCCCAGGGACCACCGACCCACCACCGGGAGGTAAGCTGGCCAGC
AACTTATCTGTGTCTGTCCGATTGTCTAGTGTCTATGACTGATTTTATGC
GCCTGCGTCGGTACTAGTTAGCTAACTAGCTCTGTATCTGGCGGACCC
GTGGTGGAACTGACGAGTTCGGAACACCCGGCCGCAACCCTGGGAGA
CGTCCCAGGGACTTCGGGGGCCGTTTTTGTGGCCCGACCTGAGTCCTA
AAATCCCGATCGTTTAGGACTCTTTGGTGCACCCCCCTTAGAGGAGGG
ATATGTGGTTCTGGTAGGAGACGAGAACCTAAAACAGTTCCCGCCTCC
GTCTGAATTTTTGCTTTCGGTTTGGGACCGAAGCCGCGCCGCGCGTCT
TGTCTGCTGCAGCATCGTTCTGTGTTGTCTCTGTCTGACTGTGTTTCTG
TATTTGTCTGAAAATATGGGCCCGGGCTAGactgttaccactCCCTTAAGTTT
GACCTTAGGTCACTGGAAAGATGTCGAGCGGATCGCTCACAACCAGTC
GGTAGATGTCAAGAAGAGACGTTGGGTTACCTTCTGCTCTGCAGAATG
GCCAACCTTTAACGTCGGATGGCCGCGAGACGGCACCTTTAACCGAGA
CCTCATCACCCAGGTTAAGATCAAGGTCTTTTCACCTGGCCCGCATGG
ACACCCAGACCAGGTccccTACATCGTGACCTGGGAAGCCTTGGCTTTT
GACCCCCCTCCCTGGGTCAAGCCCTTTGTACACCCTAAGCCTCCGCCT
CCTCTTCCTCCATCCGCCCCGTCTCTCCCCCTTGAACCTCCTCGTTCGA
CCCCGCCTCGATCCTCCCTTTATCCAGCCCTCACTCCTTCTCTAGGCG
CCCCCATATGGCCATATGAGATCTTATATGGGGCACCCCCGCCCCTTG
TAAACTTCCCTGACCCTGACATGACAAGAGTTACTAACAGCCCCTCTCT
CCAAGCTCACTTACAGGCTCTCTACTTAGTCCAGCACGAAGTCTGGAG
ACCTCTGGCGGCAGCCTACCAAGAACAACTGGACCGACCGGTGGTAC
CTCACCCTTACCGAGTCGGCGACACAGTGTGGGTCCGCCGACACCAG
ACTAAGAACCTAGAACCTCGCTGGAAAGGACCTTACACAGTCCTGCTG
ACCACCCCCACCGCCCTCAAAGTAGACGGCATCGCAGCTTGGATACAC
GCCGCCCACGTGAAGGCTGCCGACCCCGGGGGTGGACCATCCTCTAG
ACTGccATGGCTCTCCCagTgactgccCTaCTgCttCcccTAGCGCTTCTCCTG
CATGCAGAGGTGCAGCTGCAGcAGTCTGGAGGAGGCTTGGTGCAACCT
GGAGGATCCATGAAACTCTCCTGTGTTGCCTCTGGATTCACTTTCAGTA
ACTACTGGATGAACTGGGTCCGCCAGTCTCCAGAGAAGGGGCTTGAGT
GGGTTGCTGAAATTAGATTGAAATCTAATAATTATGCAACACATTATGCG
GAGTCTGTGAAAGGGAGGTTCACCATCTCAAGAGATGATTCCAAAAGTA
GTGTCTACCTGCAAATGAACAACTTAAGAGCTGAAGACACTGGCATTTA
TTACTGTACctttGgtaactccTTTGCTTACTGGGGCCAAGGGACCACGGTCA
CCGTCTCCTCAGGTGGAGGCGGTTCAGGCGGAGGTGGCTCTGGCGGT
GGCGGATCGcAggcCGtGgTCACTCAGGAATCTGCACTCACCACATCACC

TGGTGAAACAGTCACACTCACTTGTCGCTCAAGTACTGGGGCTGTTACA
ACTAGTAACTATGCCAACTGGGTCCAAGAAAAACCAGATCATTTATTCA
CTGGTCTAATAGGTGGTACCAACAACCGAGCACCAGGTGTTCCTGCCA
GATTCTCAGGCTCCCTGATTGGAGACAAGGCTGCCCTCACCATCACAG
GGGCACAGACTGAGGATGAGGCAATATATTTCTGTGCTCTATGGTACA
GCAACCATTGGGTGTTCGGTGGAGGAACCAAACTGACTGTCCTAGGAT
CAGAGGCGGCCGCtttccgatggccagAgtctccaaaggcacaggcctcctcagtgcccactg
cacaaccccaagcagagggcagcctcgccaaggcaaccacagccccagccaccacccgtaacaca
ggtggaagaggaggagaagagaagaagaaggagaaggagaaagaggaacaagaagagagag
agacaaagacaccTgaAGCGGCCGCaGTTGAGCCCAAATCTTGTGACAAAAC
TCACACATGCCCACCGTGCCCAGCACCTGAACTCCTGGGGGGACCGT
CAGTCTTCCTCTTCCCCCCAAAACCCAAGGACACCCTCATGATCTCCCG
GACCCCTGAGGTCACATGCGTGGTGGTGGACGTGAGCCACGAAGACC
CTGAGGTCAAGTTCAACTGGTACGTGGACGGCGTGGAGGTGCATAATG
CCAAGACAAAGCCGCGGGAGGAGCAGTACAACAGCACGTACCGTGTG
GTCAGCGTCCTCACCGTCCTGCACCAGGACTGGCTGAATGGCAAGGA
GTACAAGTGCAAGGTCTCCAACAAAGCCCTCCCAGCCCCCATCGAGAA
AACCATCTCCAAAGCCAAAGGGCAGCCCCGAGAACCACAGGTGTACAC
CCTGCCCCCATCCCGGGATGAGCTGACCAAGAACCAGGTCAGCCTGA
CCTGCCTGGTCAAAGGCTTCTATCCCAGCGACATCGCCGTGGAGTGGG
AGAGCAATGGGCAGCCGGAGAACAACTACAAGACCACGCCTCCCGTG
CTGGACTCCGACGGCTCCTTCTTCCTCTACAGCAAGCTCACCGTGGAC
AAGAGCAGGTGGCAGCAGGGGAACGTCTTCTCATGCTCCGTGATGCAT
GAGGCTCTGCACAACCACTACACGCAGAAGAGCCTCTCCCTGTCTCCG
GGTAAATTTTGGGTGCTGGTGGTGGTTGGTGGAGTCCTGGCTTGCTAT
AGCTTGCTAGTAACAGTGGCCTTTATTATTTTCTGGGTGAGGAGTAAGA
GGAGCAGGCTCCTGCACAGTGACTACATGAACATGACTCCCCGCCGCC
CCGGGCCCACCCGCAAGCATTACCAGCCCTATGCCCCACCACGCGAC
TTCGCAGCCTATCGCTCCAGAGTGAAGTTCAGCAGGAGCGCAGAGCCC
CCCGCGTACCAGCAGGGCCAGAACCAGCTCTATAACGAGCTCAATCTA
GGACGAAGAGAGGAGTACGATGTTTTGGACAAGAGACGTGGCCGGGA
CCCTGAGATGGGGGGAAAGCCGAGAAGGAAGAACCCTCAGGAAGGCC
TGTACAATGAACTGCAGAAAGATAAGATGGCGGAGGCCTACAGTGAGA
TTGGGATGAAAGGCGAGCGCCGGAGGGGCAAGGGGCACGATGGCCTT
TACCAGGGTCTCAGTACAGCCACCAAGGACACCTACGACGCCCTTCAC
ATGCAGGCCCTGCCCCCTCGCTAA

TABTr
ggatccGGATTAGTCCAATTTGTTAAAGACAGGATATCAGTGGTCCAGGCT
gCTAGTTTTGACTCAACAATATCACCAGCTGAAGCCTATAGAGTACGAG
CCATAGATAAAATAAAAGATTTTATTTAGTCTCCAGAAAAAGGGGGGAA
TGAAAGACCCCACCTGTAGGTTTGGCAAGCTAGCTTAAGTAACGCCATT
TTGCAAGGCATGGAAAAATACATAACTGAGAATAGAGAAGTTCAGATCA
AGGTCAGGAACAGATGGAACAGCTGAATATGGGCCAAACAGGATATCT
GTGGTAAGCAGTTCCTGCCCCGGCTCAGGGCCAAGAACAGATGGAAC
AGCTGAATATGGGCCAAACAGGATATCTGTGGTAAGCAGTTCCTGCCC
CGGCTCAGGGCCAAGAACAGATGGTCCCCAGATGCGGTCCAGCCCTC
AGCAGTTTCTAGAGAACCATCAGATGTTTCCAGGGTGCCCCAAGGACC
TGAAATGACCCTGTGCCTTATTTGAACTAACCAATCAGTTCGCTTCTCG

CTTCTGTTCGCGCGCTTCTGCTCCCCGAGCTCAATAAAAGAGCCCACA
ACCCCTCACTCGGGGCGCCAGTCCTCCGATTGACTGAGTCGCCCGGG
TACCCGTGTATCCAATAAACCCTCTTGCAGTTGCATCCGACTTGTGGTC
TCGCTGTTCCTTGGGAGGGTCTCCTCTGAGTGATTGACTACCCGTCAG
CGGGGGTCTTTCACACATGCAGCATGTATCAAAATTAATTTGGTTTTTTT
TCTTAAGTATTTACATTAAATGGCCATAGTACTTAAAGTTACATTGGCTT
CCTTGAAATAAACATGGAGTATTCAGAATGTGTCATAAATATTTCTAATT
TTAAGATAGTATCTCCATTGGCTTTCTACTTTTTCTTTTATTTTTTTTTGTC
CTCTGTCTTCCATTTGTTGTTGTTGTTTGTTTGTTTGTTTGTTGGTTG
GTTGGTTAATTTTTTTTTAAAGATCCTACACTATAGTTCAAGCTAGACTAT
TAGCTACTCTGTAACCCAGGGTGACCTTGAAGTCATGGGTAGCCTGCT
GTTTTAGCCTTCCCACATCTAAGATTACAGGTATGAGCTATCATTTTTGG
TATATTGATTGATTGATTGATTGATGTGTGTGTGTGTGATTGTGTTTGTG
TGTGTGACTGTGAAAATGTGTGTATGGGTGTGTGTGAATGTGTGTATGT
ATGTGTGTGTGTGAGTGTGTGTGTGTGTGTGTGCATGTGTGTGTGTGT
GACTGTGTCTATGTGTATGACTGTGTGTGTGTGTGTGTGTGTGTGTGTG
TGTGTGTGTGTGTGTGTGTTGTGAAAAAATATTCTATGGTAGTGAGAGC
CAACGCTCCGGCTCAGGTGTCAGGTTGGTTTTTGAGACAGAGTCTTTC
ACTTAGCTTGGAATTCactggccgtcgttttacaacgtcgtgactgggaaaaccctggcgttacc
caacttaatcgccttgcagcacatccccctttcgccagctggcgtaatagcgaagaggcccgcaccgatc
gcccttcccaacagttgcgcagcctgaatggcgaatggcgcctgatgcggtattttctccttacgcatctgtg
cggtatttcacaccgcatatggtgcactctcagtacaatctgctctgatgccgcatagttaagccagccccg
acacccgccaacacccgctgacgcgccctgacgggcttgtctgctcccggcatccgcttacagacaagc
tgtgaccgtctccgggagctgcatgtgtcagaggttttcaccgtcatcaccgaaacgcgcgatgacgaaa
gggcctcgtgatacgcctatttttataggttaatgtcatgataataatggtttcttagacgtcaggtggcacttttt
cggggaaatgtgcgcggaacccctatttgtttatttttctaaatacattcaaatatgtatccgctcatgagaca
ataaccctgataaatgcttcaataatattgaaaaaggaagagtatgagtattcaacatttccgtgtcgcccctt
attcccttttttgcggcattttgccttcctgtttttgctcacccagaaacgctggtgaaagtaaaagatgctgaa
gatcagttgggtgcacgagtgggttacatcgaactggatctcaacagcggtaagatccttgagagttttcgc
cccgaagaacgttttccaatgatgagcacttttaaagttctgctatgtggcgcggtattatcccgtattgacgc
cgggcaagagcaactcggtcgccgcatacactattctcagaatgacttggttgagtactcaccagtcaca
gaaaagcatcttacggatggcatgacagtaagagaattatgcagtgctgccataaccatgagtgataac
actgcggccaacttacttctgacaacgatcggaggaccgaaggagctaaccgcttttttgcacaacatgg
gggatcatgtaactcgccttgatcgttgggaaccggagctgaatgaagccataccaaacgacgagcgtg
acaccacgatgcctgtagcaatggcaacaacgttgcgcaaactattaactggcgaactacttactctagct
tcccggcaacaattaatagactggatggaggcggataaagttgcaggaccacttctgcgctcggcccttc
cggctggctggtttattgctgataaatctggagccggtgagcgtgggtctcgcggtatcattgcagcactgg
ggccagatggtaagccctcccgtatcgtagttatctacacgacggggagtcaggcaactatggatgaac
gaaatagacagatcgctgagataggtgcctcactgattaagcattggtaactgtcagaccaagtttactcat
atatactttagattgatttaaaacttcatttttaatttaaaaggatctaggtgaagatccttttttgataatctcatga
ccaaaatcccttaacgtgagttttcgttccactgagcgtcagaccccgtagaaaagatcaaaggatcttctt
gagatcctttttttctgcgcgtaatctgctgcttgcaaacaaaaaaaccaccgctaccagcggtggtttgtttg
ccggatcaagagctaccaactctttttccgaaggtaactggcttcagcagagcgcagataccaaatactgt
ccttctagtgtagccgtagttaggccaccacttcaagaactctgtagcaccgcctacatacctcgctctgcta
atcctgttaccagtggctgctgccagtggcgataagtcgtgtcttaccgggttggactcaagacgatagtta
ccggataaggcgcagcggtcgggctgaacgggggttcgtgcacacagcccagcttggagcgaacg
acctacaccgaactgagatacctacagcgtgagcattgagaaagcgccacgcttcccgaagggagaa
aggcggacaggtatccggtaagcggcagggtcggaacaggagagcgcacgagggagcttccaggg
ggaaacgcctggtatctttatagtcctgtcgggtttcgccacctctgacttgagcgtcgatttttgtgatgctcgt

caggggggcggagcctatggaaaaacgccagcaacgcggccttttacggttcctggccttttgctggcct
tttgctcacatgttctttcctgcgttatcccctgattctgtggataaccgtattaccgcctttgagtgagctgatac
cgctcgccgcagccgaacgaccgagcgcagcgagtcagtgagcgaggaagcggaagagcgccca
atacgcaaaccgcctctccccgcgcgttggccgattcattaatgcagctggcacgacaggtttcccgactg
gaaagcgggcagtgagcgcaacgcaattaatgtgagttagctcactcattaggcaccccaggctttaca
ctttatgcttccggctcgtatgttgtgtggaattgtgagcggataacaatttcacacaggaaacagctatgac
catgattacgccAAGCTTTGCTCTTAGGAGTTTCCTAATACATCCCAAACTCA
AATATATAAAGCATTTGACTTGTTCTATGCCCTAGGGGGCGGGGGGAA
GCTAAGCCAGCTTTTTTTAACATTTAAAATGTTAATTCCATTTTAAATGCA
CAGATGTTTTTATTTCATAAGGGTTTCAATGTGCATGAATGCTGCAATAT
TCCTGTTACCAAAGCTAGTATAAATAAAAATAGATAAACGTGGAAATTAC
TTAGAGTTTCTGTCATTAACGTTTCCTTCCTCAGTTGACAACATAAATGC
GCTGCTGAGCAAGCCAGTTTGCATCTGTCAGGATCAATTTCCCATTATG
CCAGTCATATTAATTACTAGTCAATTAGTTGATTTTTATTTTTGACATATA
CATGTGAATGAAAGACCCCACCTGTAGGTTTGGCAAGCTAGCTTAAGTA
ACGCCATTTTGCAAGGCATGGAAAAATACATAACTGAGAATAGAAAAGT
TCAGATCAAGGTCAGGAACAGATGGAACAGCTGAATATGGGCCAAACA
GGATATCTGTGGTAAGCAGTTCCTGCCCCGGCTCAGGGCCAAGAACAG
ATGGAACAGCTGAATATGGGCCAAACAGGATATCTGTGGTAAGCAGTT
CCTGCCCCGGCTCAGGGCCAAGAACAGATGGTCCCCAGATGCGGTCC
AGCCCTCAGCAGTTTCTAGAGAACCATCAGATGTTTCCAGGGTGCCCC
AAGGACCTGAAATGACCCTGTGCCTTATTTGAACTAACCAATCAGTTCG
CTTCTCGCTTCTGTTCGCGCGCTTATGCTCCCCGAGCTCAATAAAAGAG
CCCACAACCCCTCACTCGGGGCGCCAGTCCTCCGATTGACTGAGTCGC
CCGGGTACCCGTGTATCCAATAAACCCTCTTGCAGTTGCATCCGACTTG
TGGTCTCGCTGTTCCTTGGGAGGGTCTCCTCTGAGTGATTGACTACCC
GTCAGCGGGGGTCTTTCATTTGGGGGCTCGTCCGGGATCGGGAGACC
CCTGCCCAGGGACCACCGACCCACCACCGGGAGGTAAGCTGGCCAGC
AACTTATCTGTGTCTGTCCGATTGTCTAGTGTCTATGACTGATTTTATGC
GCCTGCGTCGGTACTAGTTAGCTAACTAGCTCTGTATCTGGCGGACCC
GTGGTGGAACTGACGAGTTCGGAACACCCGGCCGCAACCCTGGGAGA
CGTCCCAGGGACTTCGGGGGCCGTTTTTGTGGCCCGACCTGAGTCCTA
AAATCCCGATCGTTTAGGACTCTTTGGTGCACCCCCCTTAGAGGAGGG
ATATGTGGTTCTGGTAGGAGACGAGAACCTAAAACAGTTCCCGCCTCC
GTCTGAATTTTTGCTTTCGGTTTGGGACCGAAGCCGCGCCGCGCGTCT
TGTCTGCTGCAGCATCGTTCTGTGTTGTCTCTGTCTGACTGTGTTTCTG
TATTTGTCTGAAAATATGGGCCCGGGCTAGactgttaccactCCCTTAAGTTT
GACCTTAGGTCACTGGAAAGATGTCGAGCGGATCGCTCACAACCAGTC
GGTAGATGTCAAGAAGAGACGTTGGGTTACCTTCTGCTCTGCAGAATG
GCCAACCTTTAACGTCGGATGGCCGCGAGACGGCACCTTTAACCGAGA
CCTCATCACCCAGGTTAAGATCAAGGTCTTTTCACCTGGCCCGCATGG
ACACCCAGACCAGGTccccTACATCGTGACCTGGGAAGCCTTGGCTTTT
GACCCCCCTCCCTGGGTCAAGCCCTTTGTACACCCTAAGCCTCCGCCT
CCTCTTCCTCCATCCGCCCCGTCTCTCCCCCTTGAACCTCCTCGTTCGA
CCCCGCCTCGATCCTCCCTTTATCCAGCCCTCACTCCTTCTCTAGGCG
CCCCCATATGGCCATATGAGATCTTATATGGGGCACCCCCGCCCCTTG
TAAACTTCCCTGACCCTGACATGACAAGAGTTACTAACAGCCCCTCTCT
CCAAGCTCACTTACAGGCTCTCTACTTAGTCCAGCACGAAGTCTGGAG
ACCTCTGGCGGCAGCCTACCAAGAACAACTGGACCGACCGGTGGTAC

CTCACCCTTACCGAGTCGGCGACACAGTGTGGGTCCGCCGACACCAG
ACTAAGAACCTAGAACCTCGCTGGAAAGGACCTTACACAGTCCTGCTG
ACCACCCCCACCGCCCTCAAAGTAGACGGCATCGCAGCTTGGATACAC
GCCGCCCACGTGAAGGCTGCCGACCCCGGGGGTGGACCATCCTCTAG
ACTGCcATGGCCCTGCCCGTGACCGCCCTGCTCTTGCCCCTGGCCCTT
CTGCTCCACGCCGCCAGACCCGAGGTGCAGCTGCAGCAGAGCGGAGG
CGAGAGAGCCACCCCTGGCGCCAGCGTGAAGATGAGCTGCAAGACCA
GCGGCTACACCTTCACCAACTACTGGATGCACTGGGTGAAGCAGAGAC
CCGGCCAGGGCCTGGAGTGGATCGGCTACATCAACCCTAGCTCCGGC
TACACCCAGTACAACCAGAAGTTCAAGGACAAGGCCACCCTGACCGCC
GACAAGAGCTCCAGCACCGCCTACATCCAGCTGAGCTCCCTGACCAGC
GAGGACTCCGCCGTGTACTATTGCAGCACCTACTACGGCGACTACCTG
TTCCCCTACTGGGGCCAGGGCACCCTGGTGACCGTGAGCGCCGGCGG
AGGCGGAAGCGGAGGCGGCGGATCCGGAGGAGGCGGCAGCGACGTG
CTGATGACCCAGACCCCTCTGAGCCTGCCCGTGAGCCTGGGCGACCA
GGCCAGCATCAGCTGCAGAAGCTCCCAGGACATCGTGTACGGCAACG
GAAACACCTACCTGGAGTGGTACCTCCAGAAGCCCGGCCAGAGCCCC
AAGCTGCTGATCTACAAGGTGAGCAACAGATTCAGCGGCGTGCCCGAC
AGATTCAGCGGCTCCGGAAGCGGAACCGACTTCACCCTGAAGATCAGC
AGAGTGGAGGCCGAGGACCTGGGCGTGTACTATTGCTTCCAGGGCAG
CCACGTGCCCTACACCTTCGGCGGAGGCACCAAGCTGGAGATCAAGA
GAGCGGCCGCTATCGAGGTGCTAGACAATGAGAAGAGCAATGGAACC
ATTATCCATGTGAAAGGGAAACACCTTTGTCCAAGTCCCCTATTTCCCG
GACCTTCTAAGCCCTTTTGGGTGCTGGTGGTGGTTGGTGGAGTCCTGG
CTTGCTATAGCTTGCTAGTAACAGTGGCCTTTATTATTTTCTGGGTGAG
GAGTAAGTAACAGCCACTCGAG

HTr
ggatccGGATTAGTCCAATTTGTTAAAGACAGGATATCAGTGGTCCAGGCT
CTAGTTTTGACTCAACAATATCACCAGCTGAAGCCTATAGAGTACGAGC
CATAGATAAAATAAAAGATTTTATTTAGTCTCCAGAAAAAGGGGGGAAT
GAAAGACCCCACCTGTAGGTTTGGCAAGCTAGCTTAAGTAACGCCATTT
TGCAAGGCATGGAAAAATACATAACTGAGAATAGAGAAGTTCAGATCAA
GGTCAGGAACAGATGGAACAGCTGAATATGGGCCAAACAGGATATCTG
TGGTAAGCAGTTCCTGCCCCGGCTCAGGGCCAAGAACAGATGGAACA
GCTGAATATGGGCCAAACAGGATATCTGTGGTAAGCAGTTCCTGCCCC
GGCTCAGGGCCAAGAACAGATGGTCCCCAGATGCGGTCCAGCCCTCA
GCAGTTTCTAGAGAACCATCAGATGTTTCCAGGGTGCCCCAAGGACCT
GAAATGACCCTGTGCCTTATTTGAACTAACCAATCAGTTCGCTTCTCGC
TTCTGTTCGCGCGCTTCTGCTCCCCGAGCTCAATAAAAGAGCCCACAA
CCCCTCACTCGGGGCGCCAGTCCTCCGATTGACTGAGTCGCCCGGGT
ACCCGTGTATCCAATAAACCCTCTTGCAGTTGCATCCGACTTGTGGTCT
CGCTGTTCCTTGGGAGGGTCTCCTCTGAGTGATTGACTACCCGTCAGC
GGGGGTCTTTCACACATGCAGCATGTATCAAAATTAATTTGGTTTTTTTT
CTTAAGTATTTACATTAAATGGCCATAGTACTTAAAGTTACATTGGCTTC
CTTGAAATAAACATGGAGTATTCAGAATGTGTCATAAATATTTCTAATTTT
AAGATAGTATCTCCATTGGCTTTCTACTTTTTCTTTTATTTTTTTTTGTCC
TCTGTCTTCCATTTGTTGTTGTTGTTTGTTTGTTTGTTTGTTGGTTG
GTTGGTTAATTTTTTTTTAAAGATCCTACACTATAGTTCAAGCTAGACTAT

TAGCTACTCTGTAACCCAGGGTGACCTTGAAGTCATGGGTAGCCTGCT
GTTTTAGCCTTCCCACATCTAAGATTACAGGTATGAGCTATCATTTTTGG
TATATTGATTGATTGATTGATTGATGTGTGTGTGTGTGATTGTGTTTGTG
TGTGTGACTGTGAAAATGTGTGTATGGGTGTGTGTGAATGTGTGTATGT
ATGTGTGTGTGTGAGTGTGTGTGTGTGTGTGTGCATGTGTGTGTGTGT
GACTGTGTCTATGTGTATGACTGTGTGTGTGTGTGTGTGTGTGTGTGTG
TGTGTGTGTGTGTGTGTGTTGTGAAAAAATATTCTATGGTAGTGAGAGC
CAACGCTCCGGCTCAGGTGTCAGGTTGGTTTTTGAGACAGAGTCTTTC
ACTTAGCTTGGAATTCactggccgtcgttttacaacgtcgtgactgggaaaaccctggcgttacc
caacttaatcgccttgcagcacatccccctttcgccagctggcgtaatagcgaagaggcccgcaccgatc
gcccttcccaacagttgcgcagcctgaatggcgaatggcgcctgatgcggtattttctccttacgcatctgtg
cggtatttcacaccgcatatggtgcactctcagtacaatctgctctgatgccgcatagttaagccagccccg
acacccgccaacacccgctgacgcgccctgacgggcttgtctgctcccggcatccgcttacagacaagc
tgtgaccgtctccgggagctgcatgtgtcagaggttttcaccgtcatcaccgaaacgcgcgatgacgaaa
gggcctcgtgatacgcctatttttataggttaatgtcatgataataatggtttcttagacgtcaggtggcacttttt
cggggaaatgtgcgcggaacccctatttgtttatttttctaaatacattcaaatatgtatccgctcatgagaca
ataaccctgataaatgcttcaataatattgaaaaaggaagagtatgagtattcaacatttccgtgtcgcccctt
attccctttttgcggcattttgccttcctgtttttgctcacccagaaacgctggtgaaagtaaaagatgctgaa
gatcagttgggtgcacgagtgggttacatcgaactggatctcaacagcggtaagatccttgagagttttcgc
cccgaagaacgttttccaatgatgagcacttttaaagttctgctatgtggcgcggtattatcccgtattgacgc
cgggcaagagcaactcggtcgccgcatacactattctcagaatgacttggttgagtactcaccagtcaca
gaaaagcatcttacggatggcatgacagtaagagaattatgcagtgctgccataaccatgagtgataac
actgcggccaacttacttctgacaacgatcggaggaccgaaggagctaaccgcttttttgcacaacatgg
gggatcatgtaactcgccttgatcgttgggaaccggagctgaatgaagccataccaaacgacgagcgtg
acaccacgatgcctgtagcaatggcaacaacgttgcgcaaactattaactggcgaactacttactctagct
tcccggcaacaattaatagactggatggaggcggataaagttgcaggaccacttctgcgctcggcccttc
cggctggctggtttattgctgataaatctggagccggtgagcgtgggtctcgcggtatcattgcagcactgg
ggccagatggtaagccctcccgtatcgtagttatctacacgacggggagtcaggcaactatggatgaac
gaaatagacagatcgctgagataggtgcctcactgattaagcattggtaactgtcagaccaagtttactcat
atatactttagattgatttaaaacttcatttttaatttaaaaggatctaggtgaagatccttttttgataatctcatga
ccaaaatcccttaacgtgagttttcgttccactgagcgtcagaccccgtagaaaagatcaaaggatcttctt
gagatccttttttttctgcgcgtaatctgctgcttgcaaacaaaaaaaccaccgctaccagcggtggtttgtttg
ccggatcaagagctaccaactctttttccgaaggtaactggcttcagcagagcgcagataccaaatactgt
ccttctagtgtagccgtagttaggccaccacttcaagaactctgtagcaccgcctacatacctcgctctgcta
atcctgttaccagtggctgctgccagtggcgataagtcgtgtcttaccgggttggactcaagacgatagtta
ccggataaggcgcagcggtcgggctgaacgggggggttcgtgcacacagcccagcttggagcgaacg
acctacaccgaactgagatacctacagcgtgagcattgagaaagcgccacgcttcccgaagggagaa
aggcggacaggtatccggtaagcggcagggtcggaacaggagagcgcacgagggagcttccaggg
ggaaacgcctggtatctttatagtcctgtcgggtttcgccacctctgacttgagcgtcgatttttgtgatgctcgt
caggggggcggagcctatggaaaaacgccagcaacgcggccttttacggttcctggccttttgctggcct
tttgctcacatgttctttcctgcgttatcccctgattctgtggataaccgtattaccgcctttgagtgagctgatac
cgctcgccgcagccgaacgaccgagcgcagcgagtcagtgagcgaggaagcggaagagcgccca
atacgcaaaccgcctctccccgcgcgttggccgattcattaatgcagctggcacgacaggtttcccgactg
gaaagcgggcagtgagcgcaacgcaattaatgtgagttagctcactcattaggcaccccaggctttaca
ctttatgcttccggctcgtatgttgtgtggaattgtgagcggataacaatttcacacaggaaacagctatgac
catgattacgccAAGCTTTGCTCTTAGGAGTTTCCTAATACATCCCAAACTCA
AATATATAAAGCATTTGACTTGTTCTATGCCCTAGGGGGCGGGGGGAA
GCTAAGCCAGCTTTTTTTAACATTTAAAATGTTAATTCCATTTTAAATGCA
CAGATGTTTTTATTTCATAAGGGTTTCAATGTGCATGAATGCTGCAATAT

TCCTGTTACCAAAGCTAGTATAAATAAAAATAGATAAACGTGGAAATTAC
TTAGAGTTTCTGTCATTAACGTTTCCTTCCTCAGTTGACAACATAAATGC
GCTGCTGAGCAAGCCAGTTTGCATCTGTCAGGATCAATTTCCCATTATG
CCAGTCATATTAATTACTAGTCAATTAGTTGATTTTTATTTTTGACATATA
CATGTGAATGAAAGACCCCACCTGTAGGTTTGGCAAGCTAGCTTAAGTA
ACGCCATTTTGCAAGGCATGGAAAAATACATAACTGAGAATAGAAAAGT
TCAGATCAAGGTCAGGAACAGATGGAACAGCTGAATATGGGCCAAACA
GGATATCTGTGGTAAGCAGTTCCTGCCCCGGCTCAGGGCCAAGAACAG
ATGGAACAGCTGAATATGGGCCAAACAGGATATCTGTGGTAAGCAGTT
CCTGCCCCGGCTCAGGGCCAAGAACAGATGGTCCCCAGATGCGGTCC
AGCCCTCAGCAGTTTCTAGAGAACCATCAGATGTTTCCAGGGTGCCCC
AAGGACCTGAAATGACCCTGTGCCTTATTTGAACTAACCAATCAGTTCG
CTTCTCGCTTCTGTTCGCGCGCTTATGCTCCCCGAGCTCAATAAAAGAG
CCCACAACCCCTCACTCGGGGCGCCAGTCCTCCGATTGACTGAGTCGC
CCGGGTACCCGTGTATCCAATAAACCCTCTTGCAGTTGCATCCGACTTG
TGGTCTCGCTGTTCCTTGGGAGGGTCTCCTCTGAGTGATTGACTACCC
GTCAGCGGGGGTCTTTCATTTGGGGGCTCGTCCGGGATCGGGAGACC
CCTGCCCAGGGACCACCGACCCACCACCGGGAGGTAAGCTGGCCAGC
AACTTATCTGTGTCTGTCCGATTGTCTAGTGTCTATGACTGATTTTATGC
GCCTGCGTCGGTACTAGTTAGCTAACTAGCTCTGTATCTGGCGGACCC
GTGGTGGAACTGACGAGTTCGGAACACCCGGCCGCAACCCTGGGAGA
CGTCCCAGGGACTTCGGGGGCCGTTTTTGTGGCCCGACCTGAGTCCTA
AAATCCCGATCGTTTAGGACTCTTTGGTGCACCCCCCTTAGAGGAGGG
ATATGTGGTTCTGGTAGGAGACGAGAACCTAAAACAGTTCCCGCCTCC
GTCTGAATTTTTGCTTTCGGTTTGGGACCGAAGCCGCGCCGCGCGTCT
TGTCTGCTGCAGCATCGTTCTGTGTTGTCTCTGTCTGACTGTGTTTCTG
TATTTGTCTGAAAATATGGGCCCGGGCTAGactgttaccactCCCTTAAGTTT
GACCTTAGGTCACTGGAAAGATGTCGAGCGGATCGCTCACAACCAGTC
GGTAGATGTCAAGAAGAGACGTTGGGTTACCTTCTGCTCTGCAGAATG
GCCAACCTTTAACGTCGGATGGCCGCGAGACGGCACCTTTAACCGAGA
CCTCATCACCCAGGTTAAGATCAAGGTCTTTTCACCTGGCCCGCATGG
ACACCCAGACCAGGTccccTACATCGTGACCTGGGAAGCCTTGGCTTTT
GACCCCCCTCCCTGGGTCAAGCCCTTTGTACACCCTAAGCCTCCGCCT
CCTCTTCCTCCATCCGCCCCGTCTCTCCCCCTTGAACCTCCTCGTTCGA
CCCCGCCTCGATCCTCCCTTTATCCAGCCCTCACTCCTTCTCTAGGCG
CCCCCATATGGCCATATGAGATCTTATATGGGGCACCCCCGCCCCTTG
TAAACTTCCCTGACCCTGACATGACAAGAGTTACTAACAGCCCCTCTCT
CCAAGCTCACTTACAGGCTCTCTACTTAGTCCAGCACGAAGTCTGGAG
ACCTCTGGCGGCAGCCTACCAAGAACAACTGGACCGACCGGTGGTAC
CTCACCCTTACCGAGTCGGCGACACAGTGTGGGTCCGCCGACACCAG
ACTAAGAACCTAGAACCTCGCTGGAAAGGACCTTACACAGTCCTGCTG
ACCACCCCCACCGCCCTCAAAGTAGACGGCATCGCAGCTTGGATACAC
GCCGCCCACGTGAAGGCTGCCGACCCCGGGGGTGGACCATCCTCTAG
ACTGcCATGGCTCTCCCAGTGACTGCCCTACTGCTTCCCCTAGCGCTTC
TCCTGCATGCAGAGGTGCAGCTGCAGCAGTCTGGAGGAGGCTTGGTG
CAACCTGGAGGATCCATGAAACTCTCCTGTGTTGCCTCTGGATTCACTT
TCAGTAACTACTGGATGAACTGGGTCCGCCAGTCTCCAGAGAAGGGGC
TTGAGTGGGTTGCTGAAATTAGATTGAAATCTAATAATTATGCAACACAT
TATGCGGAGTCTGTGAAAGGGAGGTTCACCATCTCAAGAGATGATTCC

AAAAGTAGTGTCTACCTGCAAATGAACAACTTAAGAGCTGAAGACACTG
GCATTTATTACTGTACCTTTGGTAACTCCTTTGCTTACTGGGGCCAAGG
GACCACGGTCACCGTCTCCTCAGGTGGAGGTGGATCAGGTGGAGGTG
GATCTGGTGGAGGTGGATCTGACATTGTGCTCACTCAGGAATCTGCAC
TCACCACATCACCTGGTGAAACAGTCACACTCACTTGTCGCTCAAGTAC
TGGGGCTGTTACAACTAGTAACTATGCCAACTGGGTCCAAGAAAAACCA
GATCATTTATTCACTGGTCTAATAGGTGGTACCAACAACCGAGCACCAG
GTGTTCCTGCCAGATTCTCAGGCTCCCTGATTGGAGACAAGGCTGCCC
TCACCATCACAGGGGCACAGACTGAGGATGAGGCAATATATTTCTGTG
CTCTATGGTACAGCAACCATTGGGTGTTCGGTGGAGGAACCAAACTGA
CTGTCCTAGGATCAGAGGCggccgcaattgaagttatgtatcctcctccttacctagacaatg
agaagagcaatggaaccattatccatgtgaaagggaaacacctttgtccaagtcccctatttcccggacct
tctaagccctttgggtgctggtggtggttggtggagtcctggcttgctatagcttgctagtaacagtggcctta
ttattttctgggtgaggagtAAGTAA

HDFTr
ggatccGGATTAGTCCAATTTGTTAAAGACAGGATATCAGTGGTCCAGGCT
CTAGTTTTGACTCAACAATATCACCAGCTGAAGCCTATAGAGTACGAGC
CATAGATAAAATAAAAGATTTTATTTAGTCTCCAGAAAAAGGGGGGAAT
GAAAGACCCCACCTGTAGGTTTGGCAAGCTAGCTTAAGTAACGCCATTT
TGCAAGGCATGGAAAAATACATAACTGAGAATAGAGAAGTTCAGATCAA
GGTCAGGAACAGATGGAACAGCTGAATATGGGCCAAACAGGATATCTG
TGGTAAGCAGTTCCTGCCCCGGCTCAGGGCCAAGAACAGATGGAACA
GCTGAATATGGGCCAAACAGGATATCTGTGGTAAGCAGTTCCTGCCCC
GGCTCAGGGCCAAGAACAGATGGTCCCCAGATGCGGTCCAGCCCTCA
GCAGTTTCTAGAGAACCATCAGATGTTTCCAGGGTGCCCCAAGGACCT
GAAATGACCCTGTGCCTTATTTGAACTAACCAATCAGTTCGCTTCTCGC
TTCTGTTCGCGCGCTTCTGCTCCCCGAGCTCAATAAAAGAGCCCACAA
CCCCTCACTCGGGGCGCCAGTCCTCCGATTGACTGAGTCGCCCGGGT
ACCCGTGTATCCAATAAACCCTCTTGCAGTTGCATCCGACTTGTGGTCT
CGCTGTTCCTTGGGAGGGTCTCCTCTGAGTGATTGACTACCCGTCAGC
GGGGGTCTTTCACACATGCAGCATGTATCAAAATTAATTTGGTTTTTTTT
CTTAAGTATTTACATTAAATGGCCATAGTACTTAAAGTTACATTGGCTTC
CTTGAAATAAACATGGAGTATTCAGAATGTGTCATAAATATTTCTAATTTT
AAGATAGTATCTCCATTGGCTTTCTACTTTTTCTTTTATTTTTTTTTGTCC
TCTGTCTTCCATTTGTTGTTGTTGTTTGTTTGTTTGTTTGTTGGTTG
GTTGGTTAATTTTTTTTTAAAGATCCTACACTATAGTTCAAGCTAGACTAT
TAGCTACTCTGTAACCCAGGGTGACCTTGAAGTCATGGGTAGCCTGCT
GTTTTAGCCTTCCCACATCTAAGATTACAGGTATGAGCTATCATTTTTGG
TATATTGATTGATTGATTGATTGATGTGTGTGTGTGTGATTGTGTTTGTG
TGTGTGACTGTGAAAATGTGTGTATGGGTGTGTGTGAATGTGTGTATGT
ATGTGTGTGTGTGAGTGTGTGTGTGTGTGTGTGCATGTGTGTGTGTGT
GACTGTGTCTATGTGTATGACTGTGTGTGTGTGTGTGTGTGTGTGTGTG
TGTGTGTGTGTGTGTGTGTTGTGAAAAAATATTCTATGGTAGTGAGAGC
CAACGCTCCGGCTCAGGTGTCAGGTTGGTTTTTGAGACAGAGTCTTTC
ACTTAGCTTGGAATTCactggccgtcgttttacaacgtcgtgactgggaaaaccctggcgttacc
caacttaatcgccttgcagcacatccccctttcgccagctggcgtaatagcgaagaggcccgcaccgatc
gcccttcccaacagttgcgcagcctgaatggcgaatggcgcctgatgcggtattttctccttacgcatctgtg
cggtatttcacaccgcatatggtgcactctcagtacaatctgctctgatgccgcatagttaagccagccccg

acacccgccaacacccgctgacgcgccctgacgggcttgtctgctcccggcatccgcttacagacaagc
tgtgaccgtctccgggagctgcatgtgtcagaggttttcaccgtcatcaccgaaacgcgcgatgacgaaa
gggcctcgtgatacgcctatttttataggttaatgtcatgataataatggtttcttagacgtcaggtggcacttttt
cggggaaatgtgcgcggaacccctatttgtttatttttctaaatacattcaaatatgtatccgctcatgagaca
ataaccctgataaatgcttcaataatattgaaaaaggaagagtatgagtattcaacatttccgtgtcgcccctt
attcccttttttgcggcattttgccttcctgtttttgctcacccagaaacgctggtgaaagtaaaagatgctgaa
gatcagttgggtgcacgagtgggttacatcgaactggatctcaacagcggtaagatccttgagagttttcgc
cccgaagaacgttttccaatgatgagcacttttaaagttctgctatgtggcgcggtattatcccgtattgacgc
cgggcaagagcaactcggtcgccgcatacactattctcagaatgacttggttgagtactcaccagtcaca
gaaaagcatcttacggatggcatgacagtaagagaattatgcagtgctgccataaccatgagtgataac
actgcggccaacttacttctgacaacgatcggaggaccgaaggagctaaccgcttttttgcacaacatgg
gggatcatgtaactcgccttgatcgttgggaaccggagctgaatgaagccataccaaacgacgagcgtg
acaccacgatgcctgtagcaatggcaacaacgttgcgcaaactattaactggcgaactacttactctagct
tcccggcaacaattaatagactggatggaggcggataaagttgcaggaccacttctgcgctcggcccttc
cggctggctggtttattgctgataaatctggagccggtgagcgtgggtctcgcggtatcattgcagcactgg
ggccagatggtaagccctcccgtatcgtagttatctacacgacggggagtcaggcaactatggatgaac
gaaatagacagatcgctgagataggtgcctcactgattaagcattggtaactgtcagaccaagtttactcat
atatactttagattgatttaaaacttcatttttaatttaaaaggatctaggtgaagatccttttttgataatctcatga
ccaaaatcccttaacgtgagttttcgttccactgagcgtcagaccccgtagaaaagatcaaaggatcttctt
gagatccttttttctgcgcgtaatctgctgcttgcaaacaaaaaaaccaccgctaccagcggtggtttgtttg
ccggatcaagagctaccaactctttttccgaaggtaactggcttcagcagagcgcagataccaaatactgt
ccttctagtgtagccgtagttaggccaccacttcaagaactctgtagcaccgcctacatacctcgctctgcta
atcctgttaccagtggctgctgccagtggcgataagtcgtgtcttaccgggttggactcaagacgatagtta
ccggataaggcgcagcggtcgggctgaacgggggttcgtgcacacagcccagcttggagcgaacg
acctacaccgaactgagatacctacagcgtgagcattgagaaagcgccacgcttcccgaagggagaa
aggcggacaggtatccggtaagcggcagggtcggaacaggagagcgcacgagggagcttccaggg
ggaaacgcctggtatctttatagtcctgtcgggtttcgccacctctgacttgagcgtcgatttttgtgatgctcgt
caggggggcggagcctatggaaaaacgccagcaacgcggccttttacggttcctggccttttgctggcct
tttgctcacatgttctttcctgcgttatcccctgattctgtggataaccgtattaccgcctttgagtgagctgatac
cgctcgccgcagccgaacgaccgagcgcagcgagtcagtgagcgaggaagcggaagagcgccca
atacgcaaaccgcctctccccgcgcgttggccgattcattaatgcagctggcacgacaggtttcccgactg
gaaagcgggcagtgagcgcaacgcaattaatgtgagttagctcactcattaggcaccccaggctttaca
ctttatgcttccggctcgtatgttgtgtggaattgtgagcggataacaatttcacacaggaaacagctatgac
catgattacgccAAGCTTTGCTCTTAGGAGTTTCCTAATACATCCCAAACTCA
AATATATAAAGCATTTGACTTGTTCTATGCCCTAGGGGGCGGGGGGAA
GCTAAGCCAGCTTTTTTTAACATTTAAAATGTTAATTCCATTTTAAATGCA
CAGATGTTTTTATTTCATAAGGGTTTCAATGTGCATGAATGCTGCAATAT
TCCTGTTACCAAAGCTAGTATAAATAAAAATAGATAAACGTGGAAATTAC
TTAGAGTTTCTGTCATTAACGTTTCCTTCCTCAGTTGACAACATAAATGC
GCTGCTGAGCAAGCCAGTTTGCATCTGTCAGGATCAATTTCCCATTATG
CCAGTCATATTAATTACTAGTCAATTAGTTGATTTTTATTTTTGACATATA
CATGTGAATGAAAGACCCCACCTGTAGGTTTGGCAAGCTAGCTTAAGTA
ACGCCATTTTGCAAGGCATGGAAAAATACATAACTGAGAATAGAAAAGT
TCAGATCAAGGTCAGGAACAGATGGAACAGCTGAATATGGGCCAAACA
GGATATCTGTGGTAAGCAGTTCCTGCCCCGGCTCAGGGCCAAGAACAG
ATGGAACAGCTGAATATGGGCCAAACAGGATATCTGTGGTAAGCAGTT
CCTGCCCCGGCTCAGGGCCAAGAACAGATGGTCCCCAGATGCGGTCC
AGCCCTCAGCAGTTTCTAGAGAACCATCAGATGTTTCCAGGGTGCCCC
AAGGACCTGAAATGACCCTGTGCCTTATTTGAACTAACCAATCAGTTCG

CTTCTCGCTTCTGTTCGCGCGCTTATGCTCCCCGAGCTCAATAAAAGAG
CCCACAACCCCTCACTCGGGGCGCCAGTCCTCCGATTGACTGAGTCGC
CCGGGTACCCGTGTATCCAATAAACCCTCTTGCAGTTGCATCCGACTTG
TGGTCTCGCTGTTCCTTGGGAGGGTCTCCTCTGAGTGATTGACTACCC
GTCAGCGGGGGTCTTTCATTTGGGGGCTCGTCCGGGATCGGGAGACC
CCTGCCCAGGGACCACCGACCCACCACCGGGAGGTAAGCTGGCCAGC
AACTTATCTGTGTCTGTCCGATTGTCTAGTGTCTATGACTGATTTTATGC
GCCTGCGTCGGTACTAGTTAGCTAACTAGCTCTGTATCTGGCGGACCC
GTGGTGGAACTGACGAGTTCGGAACACCCGGCCGCAACCCTGGGAGA
CGTCCCAGGGACTTCGGGGGCCGTTTTTGTGGCCCGACCTGAGTCCTA
AAATCCCGATCGTTTAGGACTCTTTGGTGCACCCCCCTTAGAGGAGGG
ATATGTGGTTCTGGTAGGAGACGAGAACCTAAAACAGTTCCCGCCTCC
GTCTGAATTTTTGCTTTCGGTTTGGGACCGAAGCCGCGCCGCGCGTCT
TGTCTGCTGCAGCATCGTTCTGTGTTGTCTCTGTCTGACTGTGTTTCTG
TATTTGTCTGAAAATATGGGCCCGGGCTAGactgttaccactCCCTTAAGTTT
GACCTTAGGTCACTGGAAAGATGTCGAGCGGATCGCTCACAACCAGTC
GGTAGATGTCAAGAAGAGACGTTGGGTTACCTTCTGCTCTGCAGAATG
GCCAACCTTTAACGTCGGATGGCCGCGAGACGGCACCTTTAACCGAGA
CCTCATCACCCAGGTTAAGATCAAGGTCTTTTCACCTGGCCCGCATGG
ACACCCAGACCAGGTccccTACATCGTGACCTGGGAAGCCTTGGCTTTT
GACCCCCCTCCCTGGGTCAAGCCCTTTGTACACCCTAAGCCTCCGCCT
CCTCTTCCTCCATCCGCCCCGTCTCTCCCCCTTGAACCTCCTCGTTCGA
CCCCGCCTCGATCCTCCCTTTATCCAGCCCTCACTCCTTCTCTAGGCG
CCCCCATATGGCCATATGAGATCTTATATGGGGCACCCCCGCCCCTTG
TAAACTTCCCTGACCCTGACATGACAAGAGTTACTAACAGCCCCTCTCT
CCAAGCTCACTTACAGGCTCTCTACTTAGTCCAGCACGAAGTCTGGAG
ACCTCTGGCGGCAGCCTACCAAGAACAACTGGACCGACCGGTGGTAC
CTCACCCTTACCGAGTCGGCGACACAGTGTGGGTCCGCCGACACCAG
ACTAAGAACCTAGAACCTCGCTGGAAAGGACCTTACACAGTCCTGCTG
ACCACCCCCACCGCCCTCAAAGTAGACGGCATCGCAGCTTGGATACAC
GCCGCCCACGTGAAGGCTGCCGACCCCGGGGGTGGACCATCCTCTAG
ACTGccATGGCTCTCCCagTgactgccCTaCTgCttCcccTAGCGCTTCTCCTG
CATGCAGAGGTGCAGCTGCAGcAGTCTGGAGGAGGCTTGGTGCAACCT
GGAGGATCCATGAAACTCTCCTGTGTTGCCTCTGGATTCACTTTCAGTA
ACTACTGGATGAACTGGGTCCGCCAGTCTCCAGAGAAGGGGCTTGAGT
GGGTTGCTGAAATTAGATTGAAATCTAATAATTATGCAACACATTATGCG
GAGTCTGTGAAAGGGAGGTTCACCATCTCAAGAGATGATTCCAAAAGTA
GTGTCTACCTGCAAATGAACAACTTAAGAGCTGAAGACACTGGCATTTA
TTACTGTACctttGgtaactccTTTGCTTACTGGGGCCAAGGGACCACGGTCA
CCGTCTCCTCAGGTGGAGGCGGTTCAGGCGGAGGTGGCTCTGGCGGT
GGCGGATCGcAggcCGtGgTCACTCAGGAATCTGCACTCACCACATCACC
TGGTGAAACAGTCACACTCACTTGTCGCTCAAGTACTGGGGCTGTTACA
ACTAGTAACTATGCCAACTGGGTCCAAGAAAAACCAGATCATTTATTCA
CTGGTCTAATAGGTGGTACCAACAACCGAGCACCAGGTGTTCCTGCCA
GATTCTCAGGCTCCCTGATTGGAGACAAGGCTGCCCTCACCATCACAG
GGGCACAGACTGAGGATGAGGCAATATATTTCTGTGCTCTATGGTACA
GCAACCATTGGGTGTTCGGTGGAGGAACCAAACTGACTGTCCTAGGAT
CAGAGGCGGCCGCtttccgatggccagAgtctccaaaggcacaggcctcctcagtgcccactg
cacaaccccaagcagagggcagcctcgccaaggcaaccacagccccagccaccacccgtaacaca

ggtggaagaggaggagaagagaagaagaaggagaaggagaaagaggaacaagaagagagag
agacaaagacaccTgaAGCGGCCGCaGTTGAGCCCAAATCTTGTGACAAAAC
TCACACATGCCCACCGTGCCCAGCACCTGAACTCCTGGGGGGACCGT
CAGTCTTCCTCTTCCCCCCAAAACCCAAGGACACCCTCATGATCTCCCG
GACCCCTGAGGTCACATGCGTGGTGGTGGACGTGAGCCACGAAGACC
CTGAGGTCAAGTTCAACTGGTACGTGGACGGCGTGGAGGTGCATAATG
CCAAGACAAAGCCGCGGGAGGAGCAGTACAACAGCACGTACCGTGTG
GTCAGCGTCCTCACCGTCCTGCACCAGGACTGGCTGAATGGCAAGGA
GTACAAGTGCAAGGTCTCCAACAAAGCCCTCCCAGCCCCCATCGAGAA
AACCATCTCCAAAGCCAAAGGGCAGCCCCGAGAACCACAGGTGTACAC
CCTGCCCCCATCCCGGGATGAGCTGACCAAGAACCAGGTCAGCCTGA
CCTGCCTGGTCAAAGGCTTCTATCCCAGCGACATCGCCGTGGAGTGGG
AGAGCAATGGGCAGCCGGAGAACAACTACAAGACCACGCCTCCCGTG
CTGGACTCCGACGGCTCCTTCTTCCTCTACAGCAAGCTCACCGTGGAC
AAGAGCAGGTGGCAGCAGGGGAACGTCTTCTCATGCTCCGTGATGCAT
GAGGCTCTGCACAACCACTACACGCAGAAGAGCCTCTCCCTGTCTCCG
GGTAAATTTTGGGTGCTGGTGGTGGTTGGTGGAGTCCTGGCTTGCTAT
AGCTTGCTAGTAACAGTGGCCTTTATTATTTTCTGGGTGAGGAGTAAGT
AA

CAR T-cell transduction efficiency by using the PG13-packaging cells versus the HEK 293T VECs

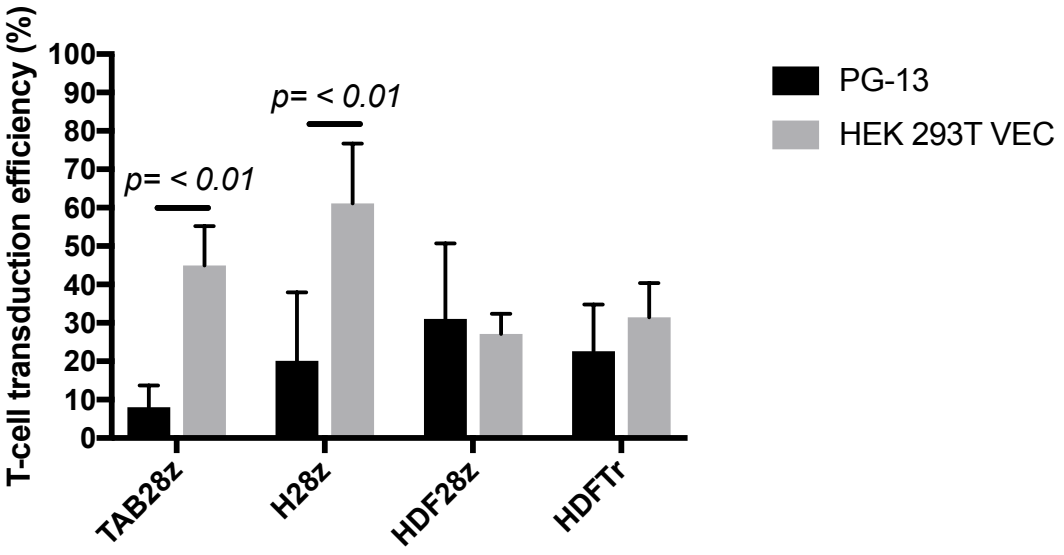

Supplementary Figure 1: T-cell transduction efficiency by using PG-13 or HEK 293T VEC cells. Isolated PBMCs from healthy volunteers were isolated and activated 48h afterwards with CD3/CD28 paramagnetic beads. At 48h post T-cell activation, cells were transduced to express either the TAB28z, H28z, HDF28z or HDFTr CAR. For the purpose of T-cell transduction viral supernanant from either PG-13 or HEK 293T VEC retroviral packaging cells was used which carry the CAR transgene. At day 5 post transduction, the CAR T-cell transduction efficiency was evaluated with flow cytometry. Statistical analysis was performed with multiple t-tests.

Bibliography

1. Torre, L. A. *et al.* Global Cancer Statistics, 2012. *CA a cancer J. Clin.* **65,** 87–108 (2015).
2. Ferlay, J. *et al.* Cancer incidence and mortality worldwide: Sources, methods and major patterns in GLOBOCAN 2012. *Int. J. Cancer* **136,** E359–E386 (2015).
3. Cancer Research UK. The Twenty Most Common Cancers, 2014. Cancer Research UK statistics.
4. Cancer Research UK. *The 20 Most Common Causes of Cancer Death in 2014, Cancer Research UK statistics*.
5. Cancer Research UK. Breast cancer mortality statistics | Cancer Research UK. Available at: http://www.cancerresearchuk.org/health-professional/cancer-statistics/statistics-by-cancer-type/breast-cancer/mortality#heading-Two. (Accessed: 17th September 2017)
6. Cancer Research UK. *Age-specific Incidence Rates of Breast Bancer , Cancer Research UK statistics*.
7. Singletary, S. E. Rating the Risk Factors for Breast Cancer. *Ann. Surg.* **237,** 474–482 (2003).
8. Antoniou, A. *et al.* Average Risks of Breast and Ovarian Cancer Associated with BRCA1 or BRCA2 Mutations Detected in Case Series Unselected for Family History: A Combined Analysis of 22 Studies. *Am. J. Hum. Genet* **72,** 1117–1130 (2003).
9. Chlebowski, R. T. *et al.* Ethnicity and Breast Cancer: Factors Influencing Differences in Incidence and Outcome. *JNCI J. Natl. Cancer Inst.* **97,** 439–448 (2005).
10. Smigal, C. *et al.* Trends in Breast Cancer by Race and Ethnicity: Update 2006. *CA. Cancer J. Clin.* **56,** 168–183 (2006).
11. Trichopoulos, D., MacMahon, B. & Cole, P. Menopause and breast cancer risk. *J. Natl. Cancer Inst.* **48,** 605–13 (1972).
12. Brinton, L. A., Schairer, C., Hoover, R. N. & Fraumeni, J. F. Menstrual Factors and Risk of Breast Cancer. *Cancer Invest.* **6,** 245–254 (1988).
13. Brinton, L. A., Hoover, R. & Fraumeni, J. F. Reproductive factors in the aetiology of breast cancer. *Br. J. Cancer* **47,** 757–762 (1983).
14. White, E. Projected changes in breast cancer incidence due to the trend toward delayed childbearing. *Am. J. Public Health* **77,** 495–7 (1987).
15. Ellison, R. C., Zhang, Y., McLennan, C. E. & Rothman, K. J. Exploring the relation of alcohol consumption to risk of breast cancer. *Am. J. Epidemiol.* **154,** 740–7 (2001).
16. Tretli, S. Height and weight in relation to breast cancer morbidity and mortality. A prospective study of 570,000 women in Norway. *Int. J. Cancer* **44,** 23–30 (1989).

17. Lahmann, P. H. *et al.* Long-term weight change and breast cancer risk: the European prospective investigation into cancer and nutrition (EPIC). *Br. J. Cancer* **93,** 582–9 (2005).
18. Ng, A. K. & Travis, L. B. Radiation therapy and breast cancer risk. *J. Natl. Compr. Canc. Netw.* **7,** 1121–8 (2009).
19. Boice, J. D., Preston, D., Davis, F. G. & Monson, R. R. Frequent chest X-ray fluoroscopy and breast cancer incidence among tuberculosis patients in Massachusetts. *Radiat. Res.* **125,** 214–22 (1991).
20. Thune, I., Brenn, T., Lund, E. & Gaard, M. Physical activity and the risk of breast cancer. *N. Engl. J. Med.* **336,** 1269–1275 (1997).
21. Calle, E. E. *et al.* Breast cancer and hormone replacement therapy: Collaborative reanalysis of data from 51 epidemiological studies of 52,705 women with breast cancer and 108,411 women without breast cancer. *Lancet* **350,** 1047–1059 (1997).
22. Nelson, H. D., Humphrey, L. L., Nygren, P., Teutsch, S. M. & Allan, J. D. Postmenopausal Hormone Replacement Therapy. *JAMA* **288,** 872 (2002).
23. Beaber, E. F. *et al.* Recent oral contraceptive use by formulation and breast cancer risk among women 20 to 49 years of age. *Cancer Res.* **74,** 4078–4089 (2014).
24. Dupont, W. D. *et al.* Breast cancer risk associated with proliferative breast disease and atypical hyperplasia. *Cancer* **71,** 1258–65 (1993).
25. Maxwell, K. N. & Domchek, S. M. Familial breast cancer risk. *Curr. Breast Cancer Rep.* **5,** 170–182 (2013).
26. Reis-Filho, J. S. & Pusztai, L. Gene expression profiling in breast cancer: Classification, prognostication, and prediction. *Lancet* **378,** 1812–1823 (2011).
27. Weigelt, B. & Reis-Filho, J. S. Histological and molecular types of breast cancer: is there a unifying taxonomy? *Nat. Rev. Clin. Oncol.* **6,** 718–730 (2009).
28. Tavassoli, F. a *et al.* Intraductal proliferative lesions. *World Heal. Organ. Classif. Tumours. Pathol. Genet. Tumours Breast Female Genit. Organs.* 63–74 (2003).
29. Sotiriou, C. & Pusztai, L. Gene-expression signatures in breast cancer. *N. Engl. J. Med.* **360,** 790–800 (2009).
30. Weigelt, B., Baehner, F. L. & Reis-Filho, J. S. The contribution of gene expression profiling to breast cancer classification, prognostication and prediction: a retrospective of the last decade. *J. Pathol.* **220,** 263–80 (2010).
31. Perou, C. M. *et al.* Molecular portraits of human breast tumours. *Nature* **406,** 747–752 (2000).
32. Sorlie, T. *et al.* Gene expression patterns of breast carcinomas distinguish tumor subclasses with clinical implications. *Proc. Natl. Acad. Sci. U. S. A.* **98,** 10869–10874 (2001).
33. Weigelt, B. *et al.* Molecular portraits and 70-gene prognosis signature are preserved throughout the metastatic process of breast cancer. *Cancer Res.* **65,** 9155–8 (2005).

34. Sorlie, T. *et al.* Repeated observation of breast tumor subtypes in independent gene expression data sets. *Proc. Natl. Acad. Sci.* **100,** 8418–8423 (2003).
35. Carey, L. A. *et al.* Race, Breast Cancer Subtypes, and Survival in the Carolina Breast Cancer Study. *JAMA* **295,** 2492 (2006).
36. Nielsen, T. O. *et al.* A comparison of PAM50 intrinsic subtyping with immunohistochemistry and clinical prognostic factors in tamoxifen-treated estrogen receptor-positive breast cancer. *Clin. Cancer Res.* **16,** 5222–5232 (2010).
37. Rouzier, R. *et al.* Breast cancer molecular subtypes respond differently to preoperative chemotherapy. *Clin. Cancer Res.* **11,** 5678–5685 (2005).
38. Parker, J. S. *et al.* Supervised risk predictor of breast cancer based on intrinsic subtypes. *J. Clin. Oncol.* **27,** 1160–7 (2009).
39. Bauer, K. R., Brown, M., Cress, R. D., Parise, C. A. & Caggiano, V. Descriptive analysis of estrogen receptor (ER)-negative, progesterone receptor (PR)-negative, and HER2-negative invasive breast cancer, the so-called triple-negative phenotype: a population-based study from the California cancer Registry. *Cancer* **109,** 1721–8 (2007).
40. Eroles, P., Bosch, A., Alejandro Pérez-Fidalgo, J. & Lluch, A. Molecular biology in breast cancer: Intrinsic subtypes and signaling pathways. *Cancer Treat. Rev.* **38,** 698–707 (2012).
41. Paik, S. *et al.* A multigene assay to predict recurrence of tamoxifen-treated, node-negative breast cancer. *N. Engl. J. Med.* **351,** 2817–26 (2004).
42. van de Vijver, M. J. *et al.* A gene-expression signature as a predictor of survival in breast cancer. *N. Engl. J. Med.* **347,** 1999–2009 (2002).
43. Fan, C. *et al.* Concordance among gene-expression-based predictors for breast cancer. *N. Engl. J. Med.* **355,** 560–9 (2006).
44. National Institute for Health and Care Excellence (NICE). Early and locally advanced breast cancer overview - NICE Pathways. Available at: https://pathways.nice.org.uk/pathways/early-and-locally-advanced-breast-cancer. (Accessed: 4th September 2017)
45. National Institute for Health and Care Excellence (NICE). Advanced breast cancer overview - NICE Pathways. Available at: https://pathways.nice.org.uk/pathways/advanced-breast-cancer. (Accessed: 4th September 2017)
46. Kapteijn, B. A. *et al.* Identification and biopsy of the sentinel lymph node in breast cancer. *Eur. J. Surg. Oncol.* **24,** 427–30 (1998).
47. Turner, R. R., Ollila, D. W., Krasne, D. L. & Giuliano, A. E. Histopathologic validation of the sentinel lymph node hypothesis for breast carcinoma. *Ann. Surg.* **226,** 271-6-8 (1997).
48. Krag, D. N., Weaver, D. L., Alex, J. C. & Fairbank, J. T. Surgical resection and

radiolocalization of the sentinel lymph node in breast cancer using a gamma probe. *Surg. Oncol.* **2,** 335–9; discussion 340 (1993).

49. Alex, J. C. & Krag, D. N. Gamma-probe guided localization of lymph nodes. *Surg. Oncol.* **2,** 137–43 (1993).
50. Ahmed, M., Purushotham, A. & Douek, M. Novel techniques for sentinel lymph node biopsy in breast cancer: a systematic review. *Lancet Oncol.* **15,** e351–e362 (2014).
51. Hanahan, D. & Weinberg, R. A. Hallmarks of cancer: The next generation. *Cell* **144,** 646–674 (2011).
52. Zhang, H., Tombline, G. & Weber, B. L. BRCA1, BRCA2, and DNA Damage Response: Collision or Collusion? *Cell* **92,** 433–436 (1998).
53. Easton, D. F., Ford, D. & Bishop, D. T. Breast and ovarian cancer incidence in BRCA1-mutation carriers. Breast Cancer Linkage Consortium. *Am. J. Hum. Genet.* **56,** 265–71 (1995).
54. Farmer, H. *et al.* Targeting the DNA repair defect in BRCA mutant cells as a therapeutic strategy. *Nature* **434,** 917–21 (2005).
55. Mateo, J. *et al.* DNA-Repair Defects and Olaparib in Metastatic Prostate Cancer. *N. Engl. J. Med.* **373,** 1697–1708 (2015).
56. Ledermann, J. A. *et al.* Overall survival in patients with platinum-sensitive recurrent serous ovarian cancer receiving olaparib maintenance monotherapy: an updated analysis from a randomised, placebo-controlled, double-blind, phase 2 trial. *Lancet Oncol.* **17,** 1579–1589 (2016).
57. Ledermann, J. *et al.* Olaparib Maintenance Therapy in Platinum-Sensitive Relapsed Ovarian Cancer. *N. Engl. J. Med.* **366,** 1382–1392 (2012).
58. Fong, P. C. *et al.* Inhibition of Poly(ADP-Ribose) Polymerase in Tumors from BRCA Mutation Carriers. *N. Engl. J. Med.* **361,** 123–134 (2009).
59. Bryant, H. E. *et al.* Specific killing of BRCA2-deficient tumours with inhibitors of poly(ADP-ribose) polymerase. *Nature* **434,** 913–917 (2005).
60. Dobzhansky, T. Genetics of Natural Populations. Xiii. Recombination and Variability in Populations of Drosophila Pseudoobscura. *Genetics* **31,** 269–290 (1946).
61. Ashworth, A., Lord, C. J. & Reis-Filho, J. S. Genetic interactions in cancer progression and treatment. *Cell* **145,** 30–38 (2011).
62. Slamon, D. J. *et al.* Human breast cancer: correlation of relapse and survival with amplification of the HER-2/neu oncogene. *Science* **235,** 177–82 (1987).
63. De Laurentiis, M. *et al.* A meta-analysis on the interaction between HER-2 expression and response to endocrine treatment in advanced breast cancer. *Clin. Cancer Res.* **11,** 4741–8 (2005).
64. Harris, C. A., Ward, R. L., Dobbins, T. A., Drew, A. K. & Pearson, S. The efficacy of HER2-targeted agents in metastatic breast cancer: a meta-analysis. *Ann. Oncol.* **22,** 1308–17 (2011).

65. Phillips, G. D. L. *et al.* Targeting HER2-Positive Breast Cancer with Trastuzumab-DM1, an Antibody–Cytotoxic Drug Conjugate. *Cancer Res* **68,** 9280–90 (2008).
66. Junttila, T. T., Guangmin Li, B., Kathryn Parsons, B., Gail Lewis Phillips, B. & Mark Sliwkowski, B. X. Trastuzumab-DM1 (T-DM1) retains all the mechanisms of action of trastuzumab and efficiently inhibits growth of lapatinib insensitive breast cancer. doi:10.1007/s10549-010-1090-x
67. Verma, S. *et al.* Trastuzumab Emtansine for HER2-Positive Advanced Breast Cancer. *n engl j med* **36719367,** 1783–91 (2012).
68. National Cancer Institute (NIH). FDA Approval for Ado-Trastuzumab Emtansine - National Cancer Institute. Available at: https://www.cancer.gov/about-cancer/treatment/drugs/fda-ado-trastuzumab-emtansine. (Accessed: 22nd September 2017)
69. Rusnak, D. W. *et al.* The effects of the novel, reversible epidermal growth factor receptor/ErbB-2 tyrosine kinase inhibitor, GW2016, on the growth of human normal and tumor-derived cell lines in vitro and in vivo. *Mol. Cancer Ther.* **1,** 85–94 (2001).
70. Wood, E. R. *et al.* A unique structure for epidermal growth factor receptor bound to GW572016 (Lapatinib): Relationships among protein conformation, inhibitor off-rate, and receptor activity in tumor cells. *Cancer Res.* **64,** 6652–6659 (2004).
71. National Cancer Institute (NIH). FDA Approval for Lapatinib Ditosylate - National Cancer Institute. Available at: https://www.cancer.gov/about-cancer/treatment/drugs/fda-lapatinib. (Accessed: 20th September 2017)
72. Cameron, D. *et al.* A phase III randomized comparison of lapatinib plus capecitabine versus capecitabine alone in women with advanced breast cancer that has progressed on trastuzumab: Updated efficacy and biomarker analyses. *Breast Cancer Res. Treat.* **112,** 533–543 (2008).
73. Schwartzberg, L. S. *et al.* Lapatinib plus Letrozole as First-Line Therapy for HER-2+ Hormone Receptor-Positive Metastatic Breast Cancer. *Oncologist* **15,** 122–129 (2010).
74. Miller, K. *et al.* Paclitaxel plus Bevacizumab versus Paclitaxel Alone for Metastatic Breast Cancer. **26,** (2007).
75. National Cancer Institute (NIH). FDA Approval for Bevacizumab - National Cancer Institute. *National Cancer Institute* (2013). Available at: https://www.cancer.gov/about-cancer/treatment/drugs/fda-bevacizumab. (Accessed: 30th September 2017)
76. Gianni, L. *et al.* AVEREL: A randomized phase III trial evaluating bevacizumab in combination with docetaxel and trastuzumab as first-line therapy for her2-positive locally recurrent/metastatic breast cancer. *J. Clin. Oncol.* **31,** 1719–1725 (2013).
77. Miller, K. D. *et al.* Randomized phase III trial of capecitabine compared with bevacizumab plus capecitabine in patients with previously treated metastatic breast cancer. *J. Clin. Oncol.* **23,** 792–799 (2005).

78. U.S Food and Drug Administration. Drug Safety and Availability - Avastin (bevacizumab) Information. Available at: https://www.fda.gov/Drugs/DrugSafety/ucm193900.htm. (Accessed: 30th September 2017)
79. Muenst, S. *et al.* Expression of programmed death ligand 1 (PD-L1) is associated with poor prognosis in human breast cancer. **146,** 15–24 (2014).
80. Sabatier, R. *et al.* Prognostic and predictive value of PDL1 expression in breast cancer. *Oncotarget* **6,** (2014).
81. Ghebeh, H. *et al.* The B7-H1 (PD-L1) T Lymphocyte-Inhibitory Molecule Is Expressed in Breast Cancer Patients with Infiltrating Ductal Carcinoma: Correlation with Important High-Risk Prognostic Factors. *Neoplasia* **8,** 190–198 (2006).
82. Mittendorf, E. A. *et al.* PD-L1 expression in triple-negative breast cancer. *Cancer Immunol. Res.* **2,** 361–70 (2014).
83. Soliman, H., Khalil, F. & Antonia, S. PD-L1 expression is increased in a subset of basal type breast cancer cells. *PLoS One* **9,** (2014).
84. Rugo, H. *et al.* Abstract S5-07: Preliminary efficacy and safety of pembrolizumab (MK-3475) in patients with PD-L1–positive, estrogen receptor-positive (ER+)/HER2-negative advanced breast cancer enrolled in KEYNOTE-028. *Cancer Res.* **76,** S5-7-S5-7 (2016).
85. Emens, L. A. *et al.* Abstract PD1-6: Inhibition of PD-L1 by MPDL3280A leads to clinical activity in patients with metastatic triple-negative breast cancer. *Cancer Res.* **75,** PD1-6-PD1-6 (2015).
86. Hoffmann-La Roche. A Study of Atezolizumab in Combination With Nab-Paclitaxel Compared With Placebo With Nab-Paclitaxel for Participants With Previously Untreated Metastatic Triple-Negative Breast Cancer (IMpassion130) - Full Text View - ClinicalTrials.gov. Available at: https://clinicaltrials.gov/show/NCT02425891. (Accessed: 22nd September 2017)
87. Genentech, I. A Study of Atezolizumab Administered in Combination With Bevacizumab and/or With Chemotherapy in Participants With Locally Advanced or Metastatic Solid Tumors - Full Text View - ClinicalTrials.gov. Available at: https://clinicaltrials.gov/show/NCT01633970. (Accessed: 22nd September 2017)
88. Nanda, R. *et al.* Pembrolizumab in Patients With Advanced Triple-Negative Breast Cancer: Phase Ib KEYNOTE-012 Study. *J. Clin. Oncol.* **34,** 2460–7 (2016).
89. Merck Sharp & Dohme Corp. Study of Pembrolizumab (MK-3475) Monotherapy for Metastatic Triple-Negative Breast Cancer (MK-3475-086/KEYNOTE-086). *clinicaltrials.gov* 2015–2018 (2015).
90. Vonderheide, R. H. *et al.* Tremelimumab in Combination with Exemestane in Patients with Advanced Breast Cancer and Treatment-Associated Modulation of Inducible Costimulator Expression on Patient T Cells. doi:10.1158/1078-0432.CCR-10-0505

91. Cesar Augusto Santa-Maria, N. U. MEDI4736 and Tremelimumab in Treating Patients With Metastatic HER2 Negative Breast Cancer - Full Text View - ClinicalTrials.gov. Available at: https://clinicaltrials.gov/ct2/show/NCT02536794. (Accessed: 23rd September 2017)
92. clinicaltrials.gov. Search of: chimeric antigen receptors | Breast Cancer - List Results - ClinicalTrials.gov. Available at: https://clinicaltrials.gov/ct2/results?cond=Breast+Cancer+&term=chimeric+antigen+receptors&cntry1=&state1=&recrs=#wrapper. (Accessed: 23rd September 2017)
93. Hollingsworth, M. A. & Swanson, B. J. Mucins in cancer: protection and control of the cell surface. *Nat. Rev. Cancer* **4,** 45–60 (2004).
94. Kufe, D. Mucins in cancer: function, prognosis and therapy. *Nat. Rev. Cancer* **9,** 874–885 (2009).
95. Gendler, S., Taylor-Papadimitriou, J., Duhig, T., Rothbard, J. & Burchell, J. A highly immunogenic region of a human polymorphic epithelial mucin expressed by carcinomas is made up of tandem repeats. *J. Biol. Chem.* **263,** 12820–3 (1988).
96. Asker, N., Axelsson, M. A., Olofsson, S. O. & Hansson, G. C. Dimerization of the human MUC2 mucin in the endoplasmic reticulum is followed by a N-glycosylation-dependent transfer of the mono- and dimers to the Golgi apparatus. *J. Biol. Chem.* **273,** 18857–63 (1998).
97. Gum, J. R., Hicks, J. W., Toribara, N. W., Siddiki, B. & Kim, Y. S. Molecular cloning of human intestinal mucin (MUC2) cDNA. Identification of the amino terminus and overall sequence similarity to prepro-von Willebrand factor. *J. Biol. Chem.* **269,** 2440–2446 (1994).
98. Godl, K. *et al.* The N terminus of the MUC2 mucin forms trimers that are held together within a trypsin-resistant core fragment. *J. Biol. Chem.* **277,** 47248–56 (2002).
99. Verdugo, P., Aitken, M., Langley, L. & Villalon, M. J. Molecular mechanism of product storage and release in mucin secretion. II. The role of extracellular Ca++. *Biorheology* **24,** 625–33 (1987).
100. Kesimer, M., Makhov, A. M., Griffith, J. D., Verdugo, P. & Sheehan, J. K. Unpacking a gel-forming mucin: a view of MUC5B organization after granular release. *Am. J. Physiol. - Lung Cell. Mol. Physiol.* **298,** (2009).
101. Singh, R. & Bandyopadhyay, D. MUC1: A target molecule for cancer therapy. *Cancer Biol. Ther.* **6,** 481–486 (2014).
102. Nath, S. & Mukherjee, P. MUC1: A multifaceted oncoprotein with a key role in cancer progression. *Trends in Molecular Medicine* **20,** 332–342 (2014).
103. Ligtenbergs, M. J. L. *et al.* Cell-associated Episialin Is a Complex Containing Two Proteins Derived from a Common Precursor. *J. Biol. Chem.* **267,** (1992).
104. Levitin, F. *et al.* The MUC1 SEA module is a self-cleaving domain. *J. Biol. Chem.* **280,** 33374–33386 (2005).

105. Gendler, S. J. *et al.* Molecular cloning and expression of human tumor-associated polymorphic epithelial mucin. *J. Biol. Chem.* **265,** 15286–93 (1990).
106. Müller, S. *et al.* High density O-glycosylation on tandem repeat peptide from secretory MUC1 of T47D breast cancer cells. *J. Biol. Chem.* **274,** 18165–72 (1999).
107. Lan, M. S., Batra, S. K., Qi, W. N., Metzgar, R. S. & Hollingsworth, M. A. Cloning and sequencing of a human pancreatic tumor mucin cDNA. *J. Biol. Chem.* **265,** 15294–15299 (1990).
108. Hanisch, F. G. & Müller, S. MUC1: the polymorphic appearance of a human mucin. *Glycobiology* **10,** 439–449 (2000).
109. Litvinov, S. V. & Hilkens, J. The epithelial sialomucin, episialin, is sialylated during recycling. *J. Biol. Chem.* **268,** 21364–21371 (1993).
110. Thathiah, A., Blobel, C. P. & Carson, D. D. Tumor necrosis factor-α converting enzyme/ADAM 17 mediates MUC1 shedding. *J. Biol. Chem.* **278,** 3386–3394 (2003).
111. Thathiah, A. & Carson, D. D. MT1-MMP mediates MUC1 shedding independent of TACE/ADAM17. *Biochem. J* **382,** 363–373 (2004).
112. Kufe, D. MUC1-C oncoprotein as a target in breast cancer: activation of signaling pathways and therapeutic approaches. *Oncogene* **32,** 1073–1081 (2012).
113. Li, Y., Liu, D., Chen, D., Kharbanda, S. & Kufe, D. Human DF3/MUC1 carcinoma-associated protein functions as an oncogene. *Oncogene* **22,** 6107–6110 (2003).
114. Huang, L. *et al.* MUC1 Oncoprotein Blocks Glycogen Synthase Kinase 3B–Mediated Phosphorylation and Degradation of B-Catenin. *Cancer Res* **65,** 10413–22 (2005).
115. Schroeder, J. A. *et al.* MUC1 overexpression results in mammary gland tumorigenesis and prolonged alveolar differentiation. *Oncogene* **23,** 5739–5747 (2004).
116. Kardon, R. *et al.* Bacterial conjunctivitis in Muc1 null mice. *Invest. Ophthalmol. Vis. Sci.* **40,** 1328–35 (1999).
117. McAuley, J. L. *et al.* MUC1 cell surface mucin is a critical element of the mucosal barrier to infection. *J. Clin. Invest.* **117,** 2313–24 (2007).
118. Desouza, M. M. *et al.* MUC1/episialin: a critical barrier in the female reproductive tract. *J. Reprod. Immunol.* **45,** 127–158 (1999).
119. Lillehoj, E. P., Kim, H., Chun, E. Y., Kim, K. C. & Chul, K. Pseudomonas aeruginosa stimulates phosphorylation of the airway epithelial membrane glycoprotein Muc1 and activates MAP kinase.
120. Finn, O. J., Beatty, P. L., Plevy, S. E. & Sepulveda, A. R. Cutting Edge: Transgenic Expression of Cutting Edge: Transgenic Expression of Human MUC1 in IL-10 ⁻/⁻ Mice Accelerates Inflammatory Bowel Disease and Progression to Colon Cancer 1. *J Immunol Ref.* **179,** 735–739 (2007).
121. Ligtenberg, M. J. L., Buijs, F., Vos, H. L. & Milkens2, J. Suppression of Cellular Aggregation by High Levels of Episialin. *CANCER Res.* **52,** 2318–2324 (1992).
122. Wesseling, J., Van Der Valk, S. W. & Hilkens, J. A Mechanism for Inhibition of E-

Cadherin-mediated Cell-Cell Adhesion by the Membrane-associated Mucin Episialin/MUC1. *Mol. Biol. Cell* **7,** 565–577 (1996).

123. Pimental, R. A., Julian, J., Gendler, S. J. & Carson, D. D. Synthesis and Intracellular Trafficking of Muc-1 and Mucins by Polarized Mouse Uterine Epithelial Cells*.
124. Zaretsky, J. Z. *et al.* Expression of genes coding for pS2, c-erbB2, estrogen receptor and the H23 breast tumor-associated antigen. A comparative analysis in breast cancer. *FEBS Lett.* **265,** 46–50 (1990).
125. Hinoda, Y. *et al.* Increased expression of MUC1 in advanced pancreatic cancer. *J. Gastroenterol.* **38,** 1162–6 (2003).
126. Utsunomiya, T. *et al.* Expression of MUC1 and MUC2 mucins in gastric carcinomas: its relationship with the prognosis of the patients. *Clin. Cancer Res.* **4,** 2605–14 (1998).
127. Dong, Y. *et al.* Expression of MUC1 and MUC2 mucins in epithelial ovarian tumours. *J. Pathol.* **183,** 311–7 (1997).
128. Takahashi, T. *et al.* Expression of MUC1 on myeloma cells and induction of HLA-unrestricted CTL against MUC1 from a multiple myeloma patient. *J. Immunol.* **153,** 2102–9 (1994).
129. Dyomin, V. G. *et al.* MUC1 is activated in a B-cell lymphoma by the t(1;14)(q21;q32) translocation and is rearranged and amplified in B-cell lymphoma subsets. *Blood* **95,** 2666–71 (2000).
130. Thompson, F. *et al.* Clonal chromosome abnormalities in human breast carcinomas. I. Twenty-eight cases with primary disease. *Genes. Chromosomes Cancer* **7,** 185–93 (1993).
131. Bièche, I. & Lidereau, R. A gene dosage effect is responsible for high overexpression of the MUC1 gene observed in human breast tumors. *Cancer Genet. Cytogenet.* **98,** 75–80 (1997).
132. Lacunza, E. *et al.* MUC1 oncogene amplification correlates with protein overexpression in invasive breast carcinoma cells. *Cancer Genet. Cytogenet.* **201,** 102–110 (2010).
133. Zaretsky, J. Z. *et al.* Analysis of the promoter of the MUC1 gene overexpressed in breast cancer. *FEBS Lett.* **461,** 189–195 (1999).
134. Lagow, E. L. & Carson, D. D. Synergistic stimulation of MUC1 expression in normal breast epithelia and breast cancer cells by interferon-gamma and tumor necrosis factor-alpha. *J. Cell. Biochem.* **86,** 759–772 (2002).
135. Iorio, M. V *et al.* MicroRNA gene expression deregulation in human breast cancer. *Cancer Res.* **65,** 7065–7070 (2005).
136. Rajabi, H. *et al.* Mucin 1 oncoprotein expression is suppressed by the miR-125b oncomir. *Genes and Cancer* **1,** 62–68 (2010).
137. Yamada, N. *et al.* MUC1 expression is regulated by DNA methylation and histone H3 lysine 9 modification in cancer cells. *Cancer Res.* **68,** 2708–2716 (2008).

138. Dalziel, M. *et al.* The relative activities of the C2GnT1 and ST3Gal-I glycosyltransferases determine O-glycan structure and expression of a tumor-associated epitope on MUC1. *J. Biol. Chem.* **276,** 11007–15 (2001).
139. Brockhausen, I. & Yang, J. Mechanisms underlying aberrant glycosylation of MUC1 mucin in breast cancer cells. *Eur. J. …* **617,** 607–617 (1995).
140. Burchell, J. *et al.* An alpha2,3 sialyltransferase (ST3Gal I) is elevated in primary breast carcinomas. *Glycobiology* **9,** 1307–11 (1999).
141. Picco, G. *et al.* Over-expression of ST3Gal-I promotes mammary tumorigenesis. *Glycobiology* **20,** 1241–1250 (2010).
142. Altschuler, Y. *et al.* Clathrin-mediated Endocytosis of MUC1 Is Modulated by Its Glycosylation State. *Mol. Biol. Cell* **11,** 819–831 (2000).
143. Kufe, D. *et al.* Differential reactivity of a novel monoclonal antibody (DF3) with human malignant versus benign breast tumors. *Hybridoma* **3,** 223–32 (1984).
144. Ramasamy, S. *et al.* The MUC1 and galectin-3 oncoproteins function in a microRNA-dependent regulatory loop. *Mol. Cell* **27,** 992–1004 (2007).
145. Bitler, B. G., Goverdhan, A. & Schroeder, J. A. MUC1 regulates nuclear localization and function of the epidermal growth factor receptor. *J. Cell Sci.* **123,** 1716–23 (2010).
146. Pochampalli, M., El Bejjani, R. & Schroeder, J. MUC1 is a novel regulator of ErbB1 receptor trafficking. *Oncogene* **26,** 1693–1701 (2007).
147. Sahraei, M. *et al.* MUC1 regulates PDGFA expression during pancreatic cancer progression. *Oncogene* **31,** (2012).
148. Pandey, P., Kharbanda, S. & Kufe, D. Association of the DF3/MUC1 breast cancer antigen with Grb2 and the Sos/Ras exchange protein. *Cancer Res.* **55,** 4000–3 (1995).
149. Kitamoto, S. *et al.* MUC1 enhances hypoxia-driven angiogenesis through the regulation of multiple proangiogenic factors. *Oncogene* **32,** (2012).
150. Beatson, R. *et al.* MUC1 modulates the tumor immune microenvironment through the engagement of Siglec-9. *Nat. Immunol.* **17,** 1273–1281 (2017).
151. Lüttges, J., Feyerabend, B., Buchelt, T., Pacena, M. & Klöppel, G. The mucin profile of noninvasive and invasive mucinous cystic neoplasms of the pancreas. *Am. J. Surg. Pathol.* **26,** 466–71 (2002).
152. Nakamori, S., Ota, D. M., Cleary, K. R., Shirotani, K. & Irimura, T. MUC1 mucin expression as a marker of progression and metastasis of human colorectal carcinoma. *Gastroenterology* **106,** 353–61 (1994).
153. Rahn, J. J., Dabbagh, L., Pasdar, M. & Hugh, J. C. The importance of MUC1 cellular localization in patients with breast carcinoma: an immunohistologic study of 71 patients and review of the literature. *Cancer* **91,** 1973–82 (2001).
154. Pitroda, S. P., Khodarev, N. N., Beckett, M. A., Kufe, D. W. & Weichselbaum, R. R. MUC1-induced alterations in a lipid metabolic gene network predict response of human breast cancers to tamoxifen treatment. *Proc. Natl. Acad. Sci. U. S. A.* **106,**

5837–41 (2009).

155. Safi, F., Kohler, I., Röttinger, E. & Beger, H. The value of the tumor marker CA 15-3 in diagnosing and monitoring breast cancer. A comparative study with carcinoembryonic antigen. *Cancer* **68,** 574–82 (1991).
156. Steinberg, W. The clinical utility of the CA 19-9 tumor-associated antigen. *Am. J. Gastroenterol.* **85,** 350–5 (1990).
157. Winter, J. M. *et al.* A Novel Survival-Based Tissue Microarray of Pancreatic Cancer Validates MUC1 and Mesothelin as Biomarkers. *PLoS One* **7,** e40157 (2012).
158. Rivalland, G., Loveland, B. & Mitchell, P. Update on Mucin-1 immunotherapy in cancer: a clinical perspective. *Expert Opin. Biol. Ther.* **15,** 1773–1787 (2015).
159. Barnd, D. L., Lan, M. S., Metzgar, R. S. & Finn, O. J. Specific, major histocompatibility complex-unrestricted recognition of tumor-associated mucins by human cytotoxic T cells. *Proc. Natl. Acad. Sci. U. S. A.* **86,** 7159–63 (1989).
160. Jerome, K. R. *et al.* Cytotoxic T-lymphocytes derived from patients with breast adenocarcinoma recognize an epitope present on the protein core of a mucin molecule preferentially expressed by malignant cells. *Cancer Res.* **51,** 2908–16 (1991).
161. Hiltbold, E. M. *et al.* The mechanism of unresponsiveness to circulating tumor antigen MUC1 is a block in intracellular sorting and processing by dendritic cells. *J. Immunol.* **165,** 3730–3741 (2000).
162. Melero, I. *et al.* Therapeutic vaccines for cancer: an overview of clinical trials. *Nat. Rev. Clin. Oncol.* **11,** 509–24 (2014).
163. Hossain, M. K. & Wall, K. A. Immunological Evaluation of Recent MUC1 Glycopeptide Cancer Vaccines. *Vaccines* **4,** 1–13 (2016).
164. Cai, H. *et al.* Synthesis of Tn/T Antigen MUC1 Glycopeptide BSA Conjugates and Their Evaluation as Vaccines. *European J. Org. Chem.* **2011,** 3685–3689 (2011).
165. Kim, S. K. *et al.* Comparison of the effect of different immunological adjuvants on the antibody and T-cell response to immunization with MUC1-KLH and GD3-KLH conjugate cancer vaccines. *Vaccine* **18,** 597–603 (1999).
166. Kaiser, A. *et al.* A synthetic vaccine consisting of a tumor-associated sialyl-T NMUC1 tandem-repeat glycopeptide and tetanus toxoid: induction of a strong and highly selective immune response. *Angew. Chemie - Int. Ed.* **48,** 7551–7555 (2009).
167. Palitzsch, B. *et al.* A Synthetic Glycopeptide Vaccine for the Induction of a Monoclonal Antibody that Differentiates between Normal and Tumor Mammary Cells and Enables the Diagnosis of Human Pancreatic Cancer. *Angew. Chemie Int. Ed.* **55,** 2894–2898 (2016).
168. Apostolopoulos, V., Pietersz, G. A. & Mckenzie, I. F. C. Cell-mediated immune responses to MUCl fusion protein coupled to mannan. **14,** 930–938 (1996).
169. Apostolopoulos, V. & Thalhammer, T. Targeting antigens to dendritic cell receptors for vaccine development. *J. drug …* **2013,** (2013).

170. Vassilaros, S. *et al.* Up to 15-year clinical follow-up of a pilot Phase III immunotherapy study in stage II breast cancer patients using oxidized mannan-MUC1. *Immunotherapy* **5,** 1177–82 (2013).
171. Apostolopoulos, V. *et al.* Pilot phase III immunotherapy study in early-stage breast cancer patients using oxidized mannan-MUC1 [ISRCTN71711835]. *Breast Cancer Res.* **8,** R27 (2006).
172. Karanikas, V. *et al.* Mannan Mucin-1 Peptide Immunization: Influence of Cyclophosphamide and the Route of Injection. *J. Immunother. (1991).* **24,** 172–183 (2001).
173. Samuel, J. *et al.* Immunogenicity and antitumor activity of a liposomal MUC1 peptide-based vaccine. *Int. J. Cancer* **75,** 295–302 (1998).
174. Butts, C. *et al.* Tecemotide (L-BLP25) versus placebo after chemoradiotherapy for stage III non-small-cell lung cancer (START): a randomised, double-blind, phase 3 trial. *Lancet Oncol.* **15,** 59–68 (2014).
175. Mitchell, P. *et al.* Tecemotide in unresectable stage III non-small-cell lung cancer in the phase III START study: updated overall survival and biomarker analyses. *Ann. Oncol.* **26,** 1134–1142 (2015).
176. Dreicer, R. *et al.* MVA-MUC1-IL2 vaccine immunotherapy (TG4010) improves PSA doubling time in patients with prostate cancer with biochemical failure. *Invest. New Drugs* **27,** 379–386 (2009).
177. Arriola, E. & Ottensmeier, C. TG4010: a vaccine with a therapeutic role in cancer. *Immunotherapy* **8,** 511–519 (2016).
178. Lohmueller, J. J. *et al.* Antibodies elicited by the first non-viral prophylactic cancer vaccine show tumor-specificity and immunotherapeutic potential. *Sci. Rep.* **6,** 31740 (2016).
179. Lohmueller, J. & Finn, O. J. Current modalities in cancer immunotherapy: Immunomodulatory antibodies, CARs and vaccines. *Pharmacology and Therapeutics* (2017). doi:10.1016/j.pharmthera.2017.03.008
180. Ibrahim, N. K. *et al.* Randomized Phase II Trial of Letrozole plus Anti-MUC1 Antibody AS1402 in Hormone Receptor–Positive Locally Advanced or Metastatic Breast Cancer. *Clin. Cancer Res.* **17,** (2011).
181. Hird, V. *et al.* Adjuvant therapy of ovarian cancer with radioactive monoclonal antibody. *Br. J. Cancer* **68,** 403–6 (1993).
182. Verheijen, R. H. *et al.* Phase III trial of intraperitoneal therapy with yttrium-90-labeled HMFG1 murine monoclonal antibody in patients with epithelial ovarian cancer after a surgically defined complete remission. *J. Clin. Oncol.* **24,** 571–8 (2006).
183. Oei, A. L. *et al.* Decreased intraperitoneal disease recurrence in epithelial ovarian cancer patients receiving intraperitoneal consolidation treatment with yttrium-90-labeled murine HMFG1 without improvement in overall survival. *Int. J. Cancer* **120,**

2710–2714 (2007).

184. Ocean, A. J. *et al.* Fractionated radioimmunotherapy with 90Y-clivatuzumab tetraxetan and low-dose gemcitabine is active in advanced pancreatic cancer. *Cancer* **118,** 5497–5506 (2012).

185. Moreno, M. *et al.* High level of MUC1 in serum of ovarian and breast cancer patients inhibits huHMFG-1 dependent cell-mediated cytotoxicity (ADCC). doi:10.1016/j.canlet.2007.06.016

186. Marincola, F. M. *et al.* Loss of HLA haplotype and B locus down-regulation in melanoma cell lines. *J. Immunol.* **153,** 1225–37 (1994).

187. Koopman, L. A., Corver, W. E., Van Der Slik, A. R., Giphart, M. J. & Fleuren, G. J. Multiple Genetic Alterations Cause Frequent and Heterogeneous Human Histocompatibility Leukocyte Antigen Class I Loss in Cervical Cancer. *J. Exp. Med* **191,** 961–975 (2000).

188. Cabrera, T. *et al.* High Frequency of Altered HLA Class I Phenotypes in Laryngeal Carcinomas. *Hum. Immunol.* **61,** 499–506 (2000).

189. Cabrera, T. *et al.* High frequency of altered HLA class I phenotypes in invasive colorectal carcinomas. *Tissue Antigens* 114–123 (1998).

190. Cabrera, T. *et al.* High frequency of altered HLA class I phenotypes in invasive breast carcinomas. *Hum. Immunol.* **50,** 127–134 (1996).

191. Hanahan, D. & Weinberg, R. A. Hallmarks of Cancer: The Next Generation. *Cell* **144,** 646–674 (2011).

192. Mantovani, A., Sozzani, S., Locati, M., Allavena, P. & Sica, A. Macrophage polarization: tumor-associated macrophages as a paradigm for polarized M2 mononuclear phagocytes. *TRENDS Immunol.* **23,** (2002).

193. Zou, W. Regulatory T cells, tumour immunity and immunotherapy. *Nat. Rev. Immunol.* **6,** 295–307 (2006).

194. Ostrand-Rosenberg, S. & Sinha, P. Inflammation and Cancer Myeloid-Derived Suppressor Cells: Linking Myeloid-Derived Suppressor Cells: Linking Inflammation and Cancer 1. *J Immunol Ref.* **18218284499,** 4499–4506 (2009).

195. Pickup, M., Novitskiy, S. & Moses, H. L. The roles of TGFβ in the tumour microenvironment. *Nat. Publ. Gr.* **13,** (2013).

196. Robert, C. *et al.* Ipilimumab plus Dacarbazine for Previously Untreated Metastatic Melanoma. *N Engl J Med* **364,** 2517–26 (2011).

197. Hodi, F. S. *et al.* Improved Survival with Ipilimumab in Patients with Metastatic Melanoma. *n engl j med* **3638363,** 711–23 (2010).

198. National Cancer Institute (NIH). FDA Approval for Ipilimumab - National Cancer Institute. Available at: https://www.cancer.gov/about-cancer/treatment/drugs/fda-ipilimumab. (Accessed: 24th September 2017)

199. U.S Food and Drug Administration. FDA approves Yervoy to reduce the risk of

melanoma returning after surgery. Available at: https://www.fda.gov/NewsEvents/Newsroom/PressAnnouncements/ucm469944.htm. (Accessed: 24th September 2017)

200. Keytruda (pembrolizumab) FDA Approval History - Drugs.com. Available at: https://www.drugs.com/history/keytruda.html. (Accessed: 24th September 2017)
201. Opdivo (nivolumab) FDA Approval History - Drugs.com. Available at: https://www.drugs.com/history/opdivo.html. (Accessed: 24th September 2017)
202. U.S Food and Drug Administration. FDA approves first cancer treatment for any solid tumor with a specific genetic feature. (2017). Available at: https://www.fda.gov/newsevents/newsroom/pressannouncements/ucm560167.htm. (Accessed: 24th September 2017)
203. Rosenberg, S. A. *et al.* Use of tumor-infiltrating lymphocytes and interleukin-2 in the immunotherapy of patients with metastatic melanoma. A preliminary report. *N. Engl. J. Med.* **319,** 1676–80 (1988).
204. List results of engineered TCRs - ClinicalTrials.gov. *clinicaltrials.gov* Available at: https://clinicaltrials.gov/ct2/results?cond=&term=engineered+TCRs&cntry1=&state1=&recrs=. (Accessed: 7th October 2017)
205. Adaptimmune. Press Release :: Investors :: Adaptimmune. Available at: http://ir.adaptimmune.com/phoenix.zhtml?c=253991&p=irol-newsArticle&ID=2175118. (Accessed: 7th October 2017)
206. Johnson, L. A. *et al.* Gene therapy with human and mouse T-cell receptors mediates cancer regression and targets normal tissues expressing cognate antigen. *Blood* **114,** 535–46 (2009).
207. Morgan, R. A. *et al.* Cancer regression and neurological toxicity following anti-MAGE-A3 TCR gene therapy. *J. Immunother.* **36,** 133–51 (2013).
208. Porter, D. L. *et al.* Chimeric Antigen Receptor Modified T Cells Directed Against CD19 (CTL019 cells) Have Long-Term Persistence and Induce Durable Responses In Relapsed, Refractory CLL. in *55th ASH Annual Meeting and Exposition* (2013).
209. Porter, D. L. *et al.* Randomized, Phase II Dose Optimization Study Of Chimeric Antigen Receptor Modified T Cells Directed Against CD19 (CTL019) In Patients With Relapsed, Refractory CLL. in *55th ASH Annual Meeting and Exposition* (2013).
210. Kochenderfer, J. N., Dudley, M. E., Kassim, S. H., Karpenter, R. O. & Yang, J. C. Effective Treatment Of Chemotherapy-Refractory Diffuse Large B-Cell Lymphoma With Autologous T Cells Genetically-Engineered To Express An Anti-CD19 Chimeric Antigen Receptor. in *55th ASH Annual Meeting and Exposition* (2013).
211. Maude, S. L. *et al.* Chimeric Antigen Receptor T Cells for Sustained Remissions in Leukemia. *N. Engl. J. Med.* **371,** 1507–1517 (2014).
212. Gross, G., Eshhar, Z. & Waks, T. Expression of immunoglobulin-T-cell receptor chimeric molecules as functional receptors with antibody-type specificity. *Proc. Natl.*

Acad. Sci. U. S. A. **86,** 10024–8 (1989).

213. Eshhar, Z. & Gross, G. Chimeric T cell receptor which incorporates the anti-tumour specificity of a monoclonal antibody with the cytolytic activity of T cells: a model system for immunotherapeutical approach. *Br. J. Cancer. Suppl.* **10,** 27–9 (1990).
214. Guest, R. *et al.* TheRoleofExtracellularSpacerRegionsinthe OptimalDesignofChimericImmuneReceptors EvaluationofFourDifferentscFvsandAntigens. *J. Immunother. (1991).* **28,** (2005).
215. Gong, M. C. *et al.* Cancer patient T cells genetically targeted to prostate-specific membrane antigen specifically lyse prostate cancer cells and release cytokines in response to prostate-specific membrane antigen. *Neoplasia* **1,** 123–7 (1999).
216. Maher, J., Brentjens, R. J., Gunset, G., Rivière, I. & Sadelain, M. Human T-lymphocyte cytotoxicity and proliferation directed by a single chimeric TCRzeta /CD28 receptor. *Nat. Biotechnol.* **20,** 70–5 (2002).
217. Zhao, Y. *et al.* A herceptin-based chimeric antigen receptor with modified signaling domains leads to enhanced survival of transduced T lymphocytes and antitumor activity. *J. Immunol.* **183,** 5563–74 (2009).
218. U.S Food & Drug Administration. *Approved Drugs - FDA approves tisagenlecleucel for B-cell ALL and tocilizumab for cytokine release syndrome*. (Center for Drug Evaluation and Research).
219. U.S Food & Drug Administration. *KYMRIAH Prescribing information*.
220. Maude, S. L., Barrett, D., Teachey, D. T. & Grupp, S. A. Managing Cytokine Release Syndrome Associated With Novel T Cell-Engaging Therapies. doi:10.1097/PPO.0000000000000035
221. Beatty, G. L. *et al.* Mesothelin-specific chimeric antigen receptor mRNA-engineered T cells induce anti-tumor activity in solid malignancies. *Cancer Immunol. Res.* **2,** 112–20 (2014).
222. Louis, C. U. *et al.* Antitumor activity and long-term fate of chimeric antigen receptor-positive T cells in patients with neuroblastoma. *Blood* **118,** 6050–6 (2011).
223. van Schalkwyk, M. C. I. *et al.* Design of a phase I clinical trial to evaluate intratumoral delivery of ErbB-targeted chimeric antigen receptor T-cells in locally advanced or recurrent head and neck cancer. *Hum. Gene Ther. Clin. Dev.* **24,** 134–42 (2013).
224. Noy, R. & Pollard, J. W. Tumor-Associated Macrophages: From Mechanisms to Therapy. *Immunity* **41,** 49–61 (2014).
225. Olumi, A. F. *et al.* Carcinoma-associated Fibroblasts Direct Tumor Progression of Initiated Human Prostatic Epithelium. *CANCER Res.* **59,** 5002–5011 (1999).
226. Gabrilovich, D. I. & Nagaraj, S. Myeloid-derived suppressor cells as regulators of the immune system. *Nat. Rev. Immunol.* **9,** 162–174 (2009).
227. Powell, D. R. & Huttenlocher, A. Neutrophils in the Tumor Microenvironment. *Trends Immunol.* **37,** 41–52 (2016).

228. Sica, A. *et al.* Autocrine Production of IL-10 Mediates Defective IL-12 Production and NF- B Activation in Tumor-Associated Macrophages. *J. Immunol.* **164,** 762–767 (2000).
229. Biswas, S. K. *et al.* A distinct and unique transcriptional program expressed by tumor-associated macrophages (defective NF-κB and enhanced IRF-3/STAT1 activation). *Blood* **107,** 2112–2122 (2006).
230. Curiel, T. J. *et al.* Specific recruitment of regulatory T cells in ovarian carcinoma fosters immune privilege and predicts reduced survival. *Nat. Med.* **10,** 942–949 (2004).
231. Liu, J. *et al.* Tumor-associated macrophages recruit CCR6+ regulatory T cells and promote the development of colorectal cancer via enhancing CCL20 production in mice. *PLoS One* **6,** (2011).
232. Rodriguez, P. C. *et al.* L-Arginine Consumption by Macrophages Modulates the Expression of CD3 Chain in T Lymphocytes. *J. Immunol.* **171,** 1232–1239 (2003).
233. Pegram, H. J. *et al.* Tumor-targeted T cells modified to secrete IL-12 eradicate systemic tumors without need for prior conditioning. *Blood* **119,** 4133–4141 (2012).
234. Yeku, O. O., Purdon, T. J., Koneru, M., Spriggs, D. & Brentjens, R. J. Armored CAR T cells enhance antitumor efficacy and overcome the tumor microenvironment. *Sci. Rep.* **7,** 10541 (2017).
235. John, L. B. *et al.* Anti-PD-1 antibody therapy potently enhances the eradication of established tumors by gene-modified T cells. *Clin. Cancer Res.* **19,** 5636–5646 (2013).
236. Chong, E. A. *et al.* PD-1 blockade modulates chimeric antigen receptor (CAR)-modified T cells: Refueling the CAR. *Blood* **129,** 1039–1041 (2017).
237. Ren, J. *et al.* Multiplex genome editing to generate universal CAR T cells resistant to PD1 inhibition. *Clin. Cancer Res.* **23,** 2255–2266 (2017).
238. Lim, W. A. & June, C. H. The Principles of Engineering Immune Cells to Treat Cancer. *Cell* **168,** 724–740 (2017).
239. Kawalekar, O. U. *et al.* Distinct Signaling of Coreceptors Regulates Specific Metabolism Pathways and Impacts Memory Development in CAR T Cells. *Immunity* **44,** 380–390 (2016).
240. Eyquem, J. *et al.* Targeting a CAR to the TRAC locus with CRISPR/Cas9 enhances tumour rejection. *Nature* **543,** 113–117 (2017).
241. Long, A. H. *et al.* 4-1BB costimulation ameliorates T cell exhaustion induced by tonic signaling of chimeric antigen receptors. *Nat. Med.* 1–13 (2015). doi:10.1038/nm.3838
242. Shum, T. *et al.* Constitutive signaling from an engineered IL-7 receptor promotes durable tumor elimination by tumor redirected T-cells. *Cancer Discov.* CD-17-0538 (2017). doi:10.1158/2159-8290.CD-17-0538
243. Craddock, J. A. *et al.* Enhanced tumor trafficking of GD2 chimeric antigen receptor T cells by expression of the chemokine receptor CCR2b. *J. Immunother.* **33,** 780–8 (2010).

244. Moon, E. K. *et al.* Expression of a functional CCR2 receptor enhances tumor localization and tumor eradication by retargeted human T cells expressing a mesothelin-specific chimeric antibody receptor. *Clin. Cancer Res.* **17,** 4719–4730 (2011).
245. Di Stasi, A. *et al.* T lymphocytes coexpressing CCR4 and a chimeric antigen receptor targeting CD30 have improved homing and antitumor activity in a Hodgkin tumor model. *Blood* **113,** 6392–6402 (2009).
246. Scheuermann, R. H. & Racila, E. CD19 antigen in leukemia and lymphoma diagnosis and immunotherapy. *Leuk. Lymphoma* **18,** 385–397 (1995).
247. Uckun, F. M. *et al.* Detailed Studies on Expression and Function of CD19 Surface Determinant by Using B43 Monoclonal Antibody and the Clinical Potential of Anti-CD19 Immunotoxins. *Blood* **71,**
248. Kochenderfer, J. N. *et al.* B--cell depletion and remissions of malignancy along with cytokine- associated toxicity in a clinical trial of anti-CD19 chimeric-antigen- receptor–transduced T cells. *Blood* **119,** 2709–2720 (2012).
249. Kochenderfer, J. N. *et al.* Eradication of B-lineage cells and regression of lymphoma in a patient treated with autologous T cells genetically engineered to recognize CD19. *Blood* **116,** 4099–4102 (2010).
250. Kochenderfer, J. N., Yu, Z., Frasheri, D., Restifo, N. P. & Rosenberg, S. A. Adoptive transfer of syngeneic T cells transduced with a chimeric antigen receptor that recognizes murine CD19 can eradicate lymphoma and normal B cells. **116,** 3875–3886 (2010).
251. Quartier, P. *et al.* Early and prolonged intravenous immunoglobulin replacement therapy in childhood agammaglobulinemia: a retrospective survey of 31 patients. *J. Pediatr.* **134,** 589–96 (1999).
252. Lamers, C. H. J. *et al.* Treatment of metastatic renal cell carcinoma with autologous T-lymphocytes genetically retargeted against carbonic anhydrase IX: first clinical experience. *J. Clin. Oncol.* **24,** e20-2 (2006).
253. Lamers, C. H. *et al.* Treatment of metastatic renal cell carcinoma with CAIX CAR-engineered T cells: clinical evaluation and management of on-target toxicity. *Mol Ther* **21,** 904–912 (2013).
254. Yan, M. *et al.* HER2 expression status in diverse cancers: review of results from 37,992 patients. *Cancer Metastasis Rev.* **34,** 157–64 (2015).
255. Press, M. F., Cordon-Cardo, C. & Slamon, D. J. Expression of the HER-2/neu proto-oncogene in normal human adult and fetal tissues. *Oncogene* **5,** 953–62 (1990).
256. Morgan, R. A. *et al.* Case report of a serious adverse event following the administration of T cells transduced with a chimeric antigen receptor recognizing ERBB2. *Mol. Ther.* **18,** 843–51 (2010).
257. Ahmed, N. *et al.* Human Epidermal Growth Factor Receptor 2 (HER2) -Specific

Chimeric Antigen Receptor-Modified T Cells for the Immunotherapy of HER2-Positive Sarcoma. *J. Clin. Oncol.* **33,** 1688–96 (2015).

258. Ahmed, N. *et al.* Immunotherapy for Osteosarcoma: Genetic Modification of T cells Overcomes Low Levels of Tumor Antigen Expression. *Mol. Ther.* **17,** 1779–1787 (2009).
259. Hammarstrom. The carcinoembryonic anigen (CEA) family: structures, suggested functions and expression in normal and malignant tissues. *Semin. CANCER BI OLOGY* **9,** (1999).
260. Parkhurst, M. R. *et al.* Characterization of genetically modified T-cell receptors that recognize the CEA:691-699 peptide in the context of HLA-A2.1 on human colorectal cancer cells. *Clin. Cancer Res.* **15,** 169–80 (2009).
261. Parkhurst, M. R. *et al.* T cells targeting carcinoembryonic antigen can mediate regression of metastatic colorectal cancer but induce severe transient colitis. *Mol. Ther.* **19,** 620–6 (2011).
262. Carpenter, R. O. *et al.* B-cell maturation antigen is a promising target for adoptive T-cell therapy of multiple myeloma. *Clin. Cancer Res.* **19,** 2048–2060 (2013).
263. Ali, S. A. *et al.* T cells expressing an anti-B-cell maturation antigen chimeric antigen receptor cause remissions of multiple myeloma. *Blood* **128,** 1688–1700 (2016).
264. Dutour, a *et al.* In Vitro and In Vivo Antitumor Effect of Anti-CD33 Chimeric Receptor-Expressing EBV-CTL against CD33 Acute Myeloid Leukemia. *Adv. Hematol.* **2012,** 683065 (2012).
265. Pizzitola, I. *et al.* Chimeric antigen receptors against CD33/CD123 antigens efficiently target primary acute myeloid leukemia cells in vivo. *Leukemia* 1–10 (2014). doi:10.1038/leu.2014.62
266. Mardiros, A. *et al.* T cells expressing CD123-specific chimeric antigen receptors exhibit specific cytolytic effector functions and antitumor effects against human acute myeloid leukemia. *Blood* **122,** 3138–3148 (2013).
267. Wang, Q. *et al.* Treatment of CD33-directed chimeric antigen receptor-modified T cells in one patient with relapsed and refractory acute myeloid leukemia. *Mol. Ther.* **23,** 184–91 (2015).
268. Cellectis. Cellectis Reports Clinical Hold of UCART123 Studies | Cellectis. Available at: http://www.cellectis.com/en/press/cellectis-reports-clinical-hold-of-ucart123-studies/. (Accessed: 1st October 2017)
269. Wilkie, S. *et al.* Dual targeting of ErbB2 and MUC1 in breast cancer using chimeric antigen receptors engineered to provide complementary signaling. *J. Clin. Immunol.* **32,** 1059–70 (2012).
270. Kloss, C. C., Condomines, M., Cartellieri, M., Bachmann, M. & Sadelain, M. Combinatorial antigen recognition with balanced signaling promotes selective tumor eradication by engineered T cells. *Nat. Biotechnol.* **31,** 71–5 (2013).

271. Lanitis, E. *et al.* Chimeric Antigen Receptor T Cells with Dissociated Signaling Domains Exhibit Focused Antitumor Activity with Reduced Potential for Toxicity In Vivo. *Cancer Immunol. Res.* **1,** 43–53 (2013).
272. Roybal, K. T. *et al.* Precision Tumor Recognition by T Cells with Combinatorial Antigen-Sensing Circuits. *Cell* **164,** 770–779 (2016).
273. Morsut, L. *et al.* Engineering Customized Cell Sensing and Response Behaviors Using Synthetic Notch Receptors. *Cell* 780–791 (2016). doi:10.1016/j.cell.2016.01.012
274. Roybal, K. T. *et al.* Engineering T Cells with Customized Therapeutic Response Programs Using Synthetic Notch Receptors. *Cell* **167,** 419–432 (2016).
275. Fedorov, V. D., Themeli, M. & Sadelain, M. PD-1- and CTLA-4-based inhibitory chimeric antigen receptors (iCARs) divert off-target immunotherapy responses. *Sci. Transl. Med.* **5,** 215ra172 (2013).
276. Fitzgerald, J. C. *et al.* Cytokine Release Syndrome After Chimeric Antigen Receptor T Cell Therapy for Acute Lymphoblastic Leukemia. *Crit. Care Med.* **45,** e124–e131 (2017).
277. Prudent, V. & Breitbart, W. S. Chimeric antigen receptor T-cell neuropsychiatric toxicity in acute lymphoblastic leukemia. doi:10.1017/S147895151600095X
278. Davila, M. L., Kloss, C. C., Gunset, G. & Sadelain, M. CD19 CAR-Targeted T Cells Induce Long-Term Remission and B Cell Aplasia in an Immunocompetent Mouse Model of B Cell Acute Lymphoblastic Leukemia. *PLoS One* **8,** (2013).
279. Juno Therapeutics. News Release | Juno Therapeutics. Available at: http://ir.junotherapeutics.com/phoenix.zhtml?c=253828&p=irol-newsArticle&ID=2250772. (Accessed: 26th September 2017)
280. Di Stasi, A. *et al.* Inducible apoptosis as a safety switch for adoptive cell therapy. *N Engl J Med* **365,** 1673–1683 (2011).
281. Zhou, X. *et al.* Inducible caspase-9 suicide gene controls adverse effects from alloreplete T cells after haploidentical stem cell transplantation. *Blood* **125,** 4103–4113 (2015).
282. Wu, C.-Y., Roybal, K. T., Puchner, E. M., Onuffer, J. & Lim, W. A. Remote control of therapeutic T cells through a small molecule-gated chimeric receptor. *Science (80-.).* **350,** aab4077-aab4077 (2015).
283. Cheever, M. a *et al.* The prioritization of cancer antigens: a national cancer institute pilot project for the acceleration of translational research. *Clin. Cancer Res.* **15,** 5323–37 (2009).
284. Curry, J. M. *et al.* The use of a novel MUC1 antibody to identify cancer stem cells and circulating MUC1 in mice and patients with pancreatic cancer. *J. Surg. Oncol.* (2013). doi:10.1002/jso.23316
285. Moore, L. J. *et al.* Antibody-Guided In Vivo Imaging for Early Detection of Mammary Gland Tumors. *Transl. Oncol.* **9,** 295–305 (2016).

286. OncoTAb. About OncoTAb - OncoTAb. Available at: https://www.oncotab.com/about/. (Accessed: 12th September 2017)
287. Taylor-Papadimitriou~, J. *et al.* Monoclonal Antibodies To Epithelium-Specific Components of the Human Milk Fat Globule Membrane: Production and Reaction With Cells in Culture. *Int. J. Cancer* **28,** 17–21 (1981).
288. Burchell, J. Detection of the tumour-associated antigens recognized by the monoclonal antibodies HMFG-1 and HMFG-2 in serum from patients with breast cancer. *Int. J. Cancer* **768,** 763–768 (1984).
289. Epenetos, A. A., Canti, G., Curling, M., Bodmer, W. F. & Taylor-Papadimitriou, J. Use of two epithelium-specific monoclonal antibodies for diagnosis in serous effusions. *Lancet* 1004–1006 (1982).
290. Abramenko, I. V., Gluzman, D. F., Sklyarenko, L. M., Pisnyachevskaya, G. V. & Pinchouk, V. G. Immunocytochemical staining of cells in 153 pleural effusions with a panel of monoclonal antibodies and lectins. *Anticancer Res.* **11,** 629–634 (1991).
291. Epenetos, A. A. *et al.* TARGETING OF IODINE-123-LABELLED TUMOUR-ASSOCIATED MONOCLONAL ANTIBODIES TO OVARIAN, BREAST, AND GASTROINTESTINAL TUMOURS. *Lancet* **320,** 999–1004 (1982).
292. Epenetos, A. A. *et al.* 123I radioiodinated antibody imaging of occult ovarian cancer. *Cancer* **55,** 984–987 (1985).
293. Riviere, I., Brose, K. & Mulligan, R. C. Effects of retroviral vector design on expression of human adenosine deaminase in murine bone marrow transplant recipients engrafted with genetically modified cells. *Proc. Natl. Acad. Sci.* **92,** 6733–6737 (1995).
294. Brewin, J. *et al.* Generation of EBV-specific cytotoxic T cells that are resistant to calcineurin inhibitors for the treatment of posttransplantation lymphoproliferative disease. **114,** 4792–4803 (2009).
295. Wilkie, S. *et al.* Retargeting of human T cells to tumor-associated MUC1: the evolution of a chimeric antigen receptor. *J. Immunol.* **180,** 4901–9 (2008).
296. Whilding, L. M. *et al.* Targeting of Aberrant ??v??6 Integrin Expression in Solid Tumors Using Chimeric Antigen Receptor-Engineered T Cells. *Mol. Ther.* **25,** 259–273 (2017).
297. Neve, R. M. *et al.* A collection of breast cancer cell lines for the study of functionally. *Cancer Cell* **10,** 515–527 (2009).
298. Kenny, P. A. *et al.* The morphologies of breast cancer cell lines in three-dimensional assays correlate with their profiles of gene expression. *Mol. Oncol.* **1,** 84–96 (2007).
299. Roy, C. *et al.* An analytical study of the dimerization of in vitro generated RNA of Moloney murine leukemia virus MoMuLV. *Nucleic Acids Res.* **18,** 7287–92 (1990).
300. Coffin, J. M., Hughes, S. H. & Varmus, H. E. *Retroviruses*. *Retroviruses* (Cold Spring Harbor Laboratory Press, 1997).
301. Nisole, S. *et al.* Early steps of retrovirus replicative cycle. *Retrovirology* **1,** 9 (2004).
302. Roe, T., Reynolds, T. C., Yu, G. & Brown, P. O. Integration of murine leukemia virus

DNA depends on mitosis. *EMBO J.* **12,** 2099–108 (1993).

303. Stake, M. S., Bann, D. V, Kaddis, R. J. & Parent, L. J. Nuclear trafficking of retroviral RNAs and Gag proteins during late steps of replication. *Viruses* **5,** 2767–95 (2013).
304. Ory, D. S., Neugeborent, B. A. & Mulligantt, R. C. A stable human-derived packaging cell line for production of high titer retrovirus / vesicular stomatitis virus G pseudotypes. **93,** 11400–11406 (1996).
305. Miller, A., Garcia, J. & Suhr, N. Von. Construction and properties of retrovirus packaging cells based on gibbon ape leukemia virus. *J. …* **65,** 2220–2224 (1991).
306. Persons, D. a, Mehaffey, M. G., Kaleko, M., Nienhuis, a W. & Vanin, E. F. An improved method for generating retroviral producer clones for vectors lacking a selectable marker gene. *Blood Cells. Mol. Dis.* **24,** 167–82 (1998).
307. Ghani, K. & Wang, X. Efficient human hematopoietic cell transduction using RD114- and GALV-pseudotyped retroviral vectors produced in suspension and serum-free media. *Hum. gene …* **974,** 966–974 (2009).
308. Parente-Pereira, A. C., Wilkie, S., Van der Stegen, S. J. C., Davies, D. M. & Maher, J. Use of retroviral-mediated gene transfer to deliver and test function of chimeric antigen receptors in human T-cells. *J. Biol. Methods* **1,** 7 (2014).
309. Kingsley, D. M., Kozarsky, K. F., Hobbie, L. & Krieger, M. Reversible Defects in O-Linked Glycosylation and LDL Receptor Expression in a UDP-GaWDP-GalNAc 4-Epimerase Deficient Mutant. *Cell* **44,** 749–759 (1966).
310. Bäckström, M. *et al.* Recombinant MUC1 mucin with a breast cancer-like O-glycosylation produced in large amounts in Chinese-hamster ovary cells. *Biochem. J.* **376,** 677–86 (2003).
311. Link, T. *et al.* Bioprocess development for the production of a recombinant MUC1 fusion protein expressed by CHO-K1 cells in protein-free medium. *J. Biotechnol.* **110,** 51–62 (2004).
312. Beatson, R. *et al.* The Breast Cancer-Associated Glycoforms of MUC1, MUC1-Tn and sialyl-Tn, Are Expressed in COSMC Wild-Type Cells and Bind the C-Type Lectin MGL. *PLoS One* **10,** e0125994 (2015).
313. Louis, K. S. & Siegel, A. C. Cell Viability Analysis Using Trypan Blue: Manual and Automated Methods. in 7–12 (2011). doi:10.1007/978-1-61779-108-6_2
314. Mosmann, T. Rapid colorimetric assay for cellular growth and survival: Application to proliferation and cytotoxicity assays. *J. Immunol. Methods* **65,** 55–63 (1983).
315. Riss, T. L. *et al. Cell Viability Assays*. *Assay Guidance Manual* (Eli Lilly & Company and the National Center for Advancing Translational Sciences, 2004).
316. Taylor-Papadimitriou, J. *et al.* Monoclonal antibodies to epithelium-specific components of the human milk fat globule membrane: production and reaction with cells in culture. *Int. J. cancer* **28,** 17–21 (1981).
317. Arklie, J., Taylor-Papadimitriou, J., Bodmer, W., Egan, M. & Millis, R. Differentiation

antigens expressed by epithelial cells in the lactating breast are also detectable in breast cancers. *Int. J. Cancer* **28,** 23–29 (1981).

318. Burchell, J. Detection of the tumour-associated antigens recognized by the monoclonal antibodies HMFG-1 and HMFG-2 in serum from patients with breast cancer. *Int. J. Cancer* **768,** 763–768 (1984).
319. Burchell, J., Durbin, H. & Taylor-Papadimitriou, J. Complexity of expression of antigenic determinants, recognized by monoclonal antibodies HMFG-1 and HMFG-2, in normal and malignant human mammary epithelial cells. *J. Immunol.* **131,** 508–13 (1983).
320. Burchell, J. *et al.* Development and Characterization of Breast Cancer Reactive Monoclonal Antibodies Directed to the Core Protein of the Human Milk Mucin. *Cancer Res.* 5476–5482 (1987).
321. Sørensen, A. L. *et al.* Chemoenzymatically synthesized multimeric Tn/STn MUC1 glycopeptides elicit cancer-specific anti-MUC1 antibody responses and override tolerance. *Glycobiology* **16,** 96–107 (2006).
322. Beverley, P. C. L. & Callard, R. E. Distinctive functional characteristics of human „T" lymphocytes defined by E rosetting or a monoclonal anti-T cell antibody. *Eur. J. Immunol.* **11,** 329–334 (1981).
323. Evans, R. L. *et al.* Thymus-dependent membrane antigens in man: Inhibition of cell-mediated lympholysis by monoclonal antibodies to TH2 antigen. *Immunology* **78,** 544–548 (1981).
324. Smith, S. H., Brown, M. H., Rowe, D., Callard, R. E. & Beverley, P. C. L. Functional subsets of human helper-inducer cells defined by a new monoclonal antibody, UCHL1. *Immunology* **58,** 63–70 (1986).
325. May, K. F. *et al.* Anti-human CTLA-4 monoclonal antibody promotes T-cell expansion and immunity in a hu-PBL-SCID model: a new method for preclinical screening of costimulatory monoclonal antibodies. *Blood* **105,** 1114–20 (2005).
326. the BD LSR Fortessa cytometer. Available at: http://www.bdbiosciences.com/ds/is/tds/23-9141.pdf. (Accessed: 9th July 2017)
327. Leonard D. Shultz, Bonnie L. Lyons, Lisa M. Burzenski, Bruce Gott, Xiaohua Chen, Stanley Chaleff, Malak Kotb, Stephen D. Gillies, Marie King, Julie Mangada, D. L. & Handgretinger, G. and R. Human Lymphoid and Myeloid Cell Development in NOD/LtSz-scid IL2R null Mice Engrafted with Mobilized Human Hemopoietic Stem Cells. *J. Immunol.* **174,** 6477–6489 (2005).
328. The Jackson Laboratory. NOD scid gamma (NSG). Available at: https://www.jax.org/strain/005557. (Accessed: 10th July 2017)
329. Shaner, N. C. *et al.* Improved monomeric red, orange and yellow fluorescent proteins derived from Discosoma sp. red fluorescent protein. *Nat. Biotechnol.* **22,** 1567–1572 (2004).

330. Donnelly, M. L. L. *et al.* Analysis of the aphthovirus 2A/2B polyprotein 'cleavage' mechanism indicates not a proteolytic reaction, but a novel translational effect: A putative ribosomal 'skip'. *J. Gen. Virol.* **82,** 1013–1025 (2001).
331. Tomayko, M. M. & Reynolds, C. P. Determination of subcutaneous tumor size in athymic (nude) mice. *Cancer Chemother. Pharmacol.* **24,** 148–54 (1989).
332. Kimura, T. & Finn, O. J. MUC1 immunotherapy is here to stay. *Expert Opin. Biol. Ther.* **13,** 35–49 (2013).
333. Roulois, D., Grégoire, M. & Fonteneau, J. F. J. MUC1-specific cytotoxic T lymphocytes in cancer therapy: induction and challenge. *Biomed Res. Int.* **2013,** 871936 (2012).
334. Kondo, H. *et al.* Adoptive immunotherapy for pancreatic cancer using MUC1 peptide-pulsed dendritic cells and activated T lymphocytes. *Anticancer Res.* **28,** 379–387 (2008).
335. Maher, J. & Wilkie, S. CAR mechanics: driving T cells into the MUC of cancer. *Cancer Res.* **69,** 4559–62 (2009).
336. Posey, A. D., Clausen, H. & June, C. H. Distinguishing Truncated and Normal MUC1 Glycoform Targeting from Tn-MUC1-Specific CAR T Cells: Specificity Is the Key to Safety. *Immunity* **45,** 947–948 (2016).
337. Posey, A. D. *et al.* Engineered CAR T Cells Targeting the Cancer-Associated Tn-Glycoform of the Membrane Mucin MUC1 Control Adenocarcinoma. *Immunity* **44,** 1444–1454 (2016).
338. You, F. *et al.* Phase 1 clinical trial demonstrated that MUC1 positive metastatic seminal vesicle cancer can be effectively eradicated by modified Anti-MUC1 chimeric antigen receptor transduced T cells. *Sci. China* **59,** 386–397 (2016).
339. PersonGen BioTherapeutics (Suzhou) Co., L. CAR-T Cell Immunotherapy in MUC1 Positive Solid Tumor - Full Text View - ClinicalTrials.gov. Available at: https://clinicaltrials.gov/ct2/show/NCT02617134?term=muc1+chimeric+antigen+receptors&rank=2. (Accessed: 5th August 2017)
340. PersonGen BioTherapeutics (Suzhou) Co., L. Phase I/II Study of Anti-Mucin1 (MUC1) CAR T Cells for Patients With MUC1+ Advanced Refractory Solid Tumor - Full Text View - ClinicalTrials.gov. Available at: https://clinicaltrials.gov/ct2/show/NCT02587689?term=muc1+chimeric+antigen+receptors&rank=4. (Accessed: 5th August 2017)
341. PersonGen BioTherapeutics (Suzhou) Co., L. CAR-pNK Cell Immunotherapy in MUC1 Positive Relapsed or Refractory Solid Tumor. Available at: https://clinicaltrials.gov/ct2/show/NCT02839954?term=muc1+chimeric+antigen+receptors&rank=1. (Accessed: 5th August 2017)
342. Shanghai Cell Therapy Research Institute. CTLA-4 and PD-1 Antibodies Expressing MUC1-CAR-T Cells for MUC1 Positive Advanced Solid Tumor - Full Text View - ClinicalTrials.gov. Available at:

https://clinicaltrials.gov/ct2/show/NCT03179007?term=muc1+chimeric+antigen+receptors&rank=3. (Accessed: 5th August 2017)

343. Taylor-Papadimitriou, J., Burchell, J., Miles, D. . W. & Dalziel, M. MUC1 and cancer. *Biochim. Biophys. Acta - Mol. Basis Dis.* **1455,** 301–313 (1999).
344. Walsh, M. D., Luckie, S. M., Cummings, M. C., Antalis, T. M. & McGuckin, M. a. Heterogeneity of MUC1 expression by human breast carcinoma cell lines in vivo and in vitro. *Breast Cancer Res. Treat.* **58,** 255–266 (1999).
345. Bear, A. S. *et al.* Replication-Competent Retroviruses in Gene-Modified T Cells Used in Clinical Trials: Is It Time to Revise the Testing Requirements? **20,** (2012).
346. Scholler, J. *et al.* Decade-long safety and function of retroviral-modified chimeric antigen receptor T cells. *Sci. Transl. Med.* **4,** 132ra53 (2012).
347. Pinku Mukherjee. Tumor specific antibodies and uses therefor. (2010).
348. Sorensen, A. L. *et al.* Chemoenzymatically synthesized multimeric Tn/STn MUC1 glycopeptides elicit cancer-specific anti-MUC1 antibody responses and override tolerance. *Glycobiology* **16,** 96–107 (2005).
349. Ruella, M. *et al.* Dual CD19 and CD123 targeting prevents antigen-loss relapses after CD19-directed immunotherapies. *J. Clin. Invest.* **126,** 3814–3826 (2016).
350. Brunner, K. T., Mauel, J., Cerottini, J.-C. & Chapuis, B. Quantitative Assay of the Lytic Action of Immune Lymphoid Cells on 5"Cr-Labelled Allogeneic Target Cells In vitro; Inhibition by Isoantibody and by Drugs. *Immunology* **14,** (1968).
351. Gertner-dardenne, J. Standard 4-hours Chromium-51 (51Cr) Release Assay. *BIO-PROTOCOL* **2,** (2012).
352. Korzeniewski, C. & Callewaert, D. M. An enzyme-release assay for natural cytotoxicity. *J. Immunol. Methods* **64,** 313–320 (1983).
353. Decker, T. & Lohmann-Matthes, M. L. A quick and simple method for the quantitation of lactate dehydrogenase release in measurements of cellular cytotoxicity and tumor necrosis factor (TNF) activity. *J. Immunol. Methods* **115,** 61–69 (1988).
354. Corporation, P. CytoTox 96(R) Non-Radioactive Cytotoxicity Assay Technical Bulletin TB163. 608–277
355. Coombe, D. R., Nakhoul, A.-M., Stevenson, S. M., Peroni, S. E. & Sanderson, C. J. Expressed luciferase viability assay (ELVA) for the measurement of cell growth and viability. *J. Immunol. Methods* **215,** 145–150 (1998).
356. Karimi, M. A. *et al.* Measuring cytotoxicity by bioluminescence imaging outperforms the standard chromium-51 release assay. *PLoS One* **9,** e89357 (2014).
357. Nakagawa, Y., Watari, E., Shimizu, M. & Takahashi, H. One-step simple assay to determine antigen-specific cytotoxic activities by single-color flow cytometry. *Biomed. Res.* **32,** 159–166 (2011).
358. Qin, L. *et al.* Incorporation of a hinge domain improves the expansion of chimeric antigen receptor T cells. doi:10.1186/s13045-017-0437-8

359. Hudecek, M. *et al.* The non-signaling extracellular spacer domain of chimeric antigen receptors is decisive for in vivo antitumor activity. *Cancer Immunol. Res.* **3,** 125–135 (2014).
360. Hombach, A., Hombach, A. & Abken, H. Adoptive immunotherapy with genetically engineered T cells: modification of the IgG1 Fc 'spacer' domain in the extracellular moiety of chimeric antigen receptors avoids 'off-target' activation and unintended initiation of an innate immune response. *Gene Ther.* **17,** 1206–121391 (2010).
361. Frigault, M. J. *et al.* Identification of chimeric antigen receptors that mediate constitutive or inducible proliferation of T cells. *Cancer Immunol. Res.* **3,** 356–367 (2015).
362. Murphy, K. & Weaver, K. *Janeway's Immunobiology*. (Garland Science).
363. Anderson, M. S. *et al.* Projection of an immunological self shadow within the thymus by the aire protein. *Science* **298,** 1395–401 (2002).
364. Moran, A. E. *et al.* T cell receptor signal strength in Treg and iNKT cell development demonstrated by a novel fluorescent reporter mouse. *J. Exp. Med.* **208,** 1279–89 (2011).
365. Liu, G. Y. *et al.* Low Avidity Recognition of Self-Antigen by T Cells Permits Escape from Central Tolerance. *Immunity* **3,** 407–415 (1995).
366. Redmond, W. L. & Sherman, L. A. Review Peripheral Tolerance of CD8 T Lymphocytes. *Immunity* **22,** 275–284 (2005).
367. Ohashi, P. S. et al. Ablation of 'tolerance' and induction of diabetes by virus infec- tion in viral antigen transgenic mice. *Cell* **65,** 305–317 (1991).
368. Mueller, D. L. Mechanisms maintaining peripheral tolerance. *Nature Immunology* **11,** 21–27 (2010).
369. Hernandez, J., Aung, S., Redmond, W. L. & Sherman, L. A. Phenotypic and functional analysis of CD8(+) T cells undergoing peripheral deletion in response to cross-presentation of self-antigen. *J. Exp. Med.* **194,** 707–17 (2001).
370. Hawiger, D. *et al.* Dendritic cells induce peripheral T cell unresponsiveness under steady state conditions in vivo. *J. Exp. Med.* **194,** 769–79 (2001).
371. Rocha, B., Grandien, A. & Freitas, A. A. Anergy and exhaustion are independent mechanisms of peripheral T cell tolerance. *J. Exp. Med.* **181,** 993–1003 (1995).
372. Mamalaki, C. *et al.* T cell deletion follows chronic antigen specific T cell activation in vivo. *Int. Immunol.* **5,** 1285–92 (1993).
373. Francisco, L. M. *et al.* PD-L1 regulates the development, maintenance, and function of induced regulatory T cells. *J. Exp. Med.* **206,** 3015–29 (2009).
374. Moon, E. K. *et al.* Multifactorial T-cell hypofunction that is reversible can limit the efficacy of chimeric antigen receptor-transduced human T cells in solid tumors. *Clin. Cancer Res.* **20,** 4262–4273 (2014).
375. Agrawal, B. & Longenecker, B. M. MUC1 mucin-mediated regulation of human T cells.

Int. Immunol. **17,** 391–399 (2005).

376. Chang, J. F., Zhao, H. L., Phillips, J. & Greenburg, G. The epithelial mucin, MUC1, is expressed on resting T lymphocytes and can function as a negative regulator of T cell activation. *Cell. Immunol.* **201,** 83–88 (2000).
377. Agrawal, B., Krantz, M. J., Parker, J. & Longenecker, B. M. Expression of MUC1 mucin on activated human T cells: implications for a role of MUC1 in normal immune regulation. *Cancer Res.* **58,** 4079–81 (1998).
378. Correa, I. *et al.* Form and pattern of MUC1 expression on T cells activated in vivo or in vitro suggests a function in T-cell migration. *Immunology* **108,** 32–41 (2003).
379. Simms, P. E. & Ellis, T. M. Utility of flow cytometric detection of CD69 expression as a rapid method for determining poly- and oligoclonal lymphocyte activation. *Clin. Diagn. Lab. Immunol.* **3,** 301–4 (1996).
380. Tarp, M. A. *et al.* Identification of a novel cancer-specific immunodominant glycopeptide epitope in the MUC1 tandem repeat. *Glycobiology* **17,** 197–209 (2006).
381. Fattorossi, A. *et al.* Constitutive and Inducible Expression of the Epithelial Antigen MUC1 (CD227) in Human T Cells. *Exp. Cell Res.* **280,** 107–118 (2002).
382. Green, D. R., Droin, N. & Pinkoski, M. Activation-induced cell death in T cells. *Immunol. Rev.* **193,** 70–81 (2003).
383. Kunkele, A. *et al.* Functional Tuning of CARs Reveals Signaling Threshold above Which CD8+ CTL Antitumor Potency Is Attenuated due to Cell Fas-FasL-Dependent AICD. *Cancer Immunol. Res.* **3,** 368–379 (2015).
384. Gargett, T. *et al.* GD2-specific CAR T Cells Undergo Potent Activation and Deletion Following Antigen Encounter but can be Protected From Activation-induced Cell Death by PD-1 Blockade. *Mol. Ther.* **24,** 1135–1149 (2016).
385. Lavrsen, K. *et al.* Aberrantly glycosylated MUC1 is expressed on the surface of breast cancer cells and a target for antibody-dependent cell-mediated cytotoxicity. *Glycoconj. J.* **30,** 227–36 (2013).
386. Hillerdal, V., Ramachandran, M., Leja, J. & Essand, M. Systemic treatment with CAR-engineered T cells against PSCA delays subcutaneous tumor growth and prolongs survival of mice. *BMC Cancer* **14,** 30 (2014).
387. Shuk-Yee Lo, A., Xu, C., Murakami, A. & Marasco, W. A. Regression of established renal cell carcinoma in nude mice using lentivirus-transduced human T cells expressing a human anti-CAIX chimeric antigen receptor. *Mol. Ther. – Oncolytics* **1,** 14003 (2014).
388. Huang, X. *et al.* IGF1R- and ROR1-Specific CAR T Cells as a Potential Therapy for High Risk Sarcomas. *PLoS One* **10,** e0133152 (2015).
389. Zhou, X. *et al.* Cellular immunotherapy for carcinoma using genetically modified EGFR-specific T lymphocytes. *Neoplasia* **15,** 544–53 (2013).
390. Parente-Pereira, A. C. *et al.* Synergistic Chemoimmunotherapy of Epithelial Ovarian

Cancer Using ErbB-Retargeted T Cells Combined with Carboplatin. *J. Immunol.* **191,** 2437–45 (2013).

391. Klampatsa, A. *et al.* Intracavitary ???T4 immunotherapy??? of malignant mesothelioma using pan-ErbB re-targeted CAR T-cells. *Cancer Lett.* **393,** 52–59 (2017).
392. Tasian, S. K. *et al.* Optimized depletion of chimeric antigen receptor T cells in murine xenograft models of human acute myeloid leukemia. *Blood* **129,** (2017).
393. Chen, K. H. *et al.* Preclinical targeting of aggressive T-cell malignancies using anti-CD5 chimeric antigen receptor. *Leukemia* (2017). doi:10.1038/leu.2017.8
394. Davila, M. L. *et al.* Efficacy and Toxicity Management of 19-28z CAR T Cell Therapy in B Cell Acute Lymphoblastic Leukemia. **6,** (2015).
395. Grupp, S. a. *et al.* Chimeric Antigen Receptor–Modified T Cells for Acute Lymphoid Leukemia. *N. Engl. J. Med.* **368,** 1509–1518 (2013).
396. Cheadle, E. J. *et al.* Differential role of Th1 and Th2 cytokines in autotoxicity driven by CD19-specific second-generation chimeric antigen receptor T cells in a mouse model. *J. Immunol.* **192,** 3654–65 (2014).
397. Tran, E. *et al.* Immune targeting of fibroblast activation protein triggers recognition of multipotent bone marrow stromal cells and cachexia. *J. Exp. Med.* **210,** 1125–35 (2013).
398. Kalaitsidou, M., Kueberuwa, G., Schütt, A. & Gilham, D. E. CAR T-cell therapy: toxicity and the relevance of preclinical models. *Immunotherapy* **7,** 487–497 (2015).
399. Song, D.-G. *et al.* Effective adoptive immunotherapy of triple-negative breast cancer by folate receptor-alpha redirected CAR T cells is influenced by surface antigen expression level. *J. Hematol. Oncol.* **9,** 56 (2016).
400. Sun, M. *et al.* Construction and evaluation of a novel humanized HER2-specific chimeric receptor. *Breast Cancer Res.* **16,** R61 (2014).
401. Cao, Y. *et al.* Design of Switchable Chimeric Antigen Receptor T Cells Targeting Breast Cancer. *Angew. Chemie - Int. Ed.* (2016). doi:10.1002/anie.201601902
402. Manning, H. C., Buck, J. R. & Cook, R. S. Mouse Models of Breast Cancer: Platforms for Discovering Precision Imaging Diagnostics and Future Cancer Medicine. *J. Nucl. Med.* **57 Suppl 1,** 60S–8S (2016).
403. Close, D. M., Xu, T., Sayler, G. S. & Ripp, S. In vivo bioluminescent imaging (BLI): noninvasive visualization and interrogation of biological processes in living animals. *Sensors (Basel).* **11,** 180–206 (2011).
404. Kim, J.-B. *et al.* Non-Invasive Detection of a Small Number of Bioluminescent Cancer Cells In Vivo. *PLoS One* **5,** e9364 (2010).
405. Zinn, K. R. *et al.* Non-invasive bioluminescence imaging in small animals. *ILAR J.* **49,** 103–15 (2008).
406. Wallace, J. *et al.* Humane Endpoints and Cancer Research. *ILAR J.* **41,** 87–93 (2000).

407. Workman, P. *et al.* Guidelines for the welfare and use of animals in cancer research. *Br. J. Cancer* **102,** 1555–1577 (2010).
408. Khalil, A. A. *et al.* The Influence of Hypoxia and pH on Bioluminescence Imaging of Luciferase-Transfected Tumor Cells and Xenografts. *Int. J. Mol. Imaging* **2013,** 287697 (2013).
409. Black, P. C. *et al.* Validating bladder cancer xenograft bioluminescence with magnetic resonance imaging: the significance of hypoxia and necrosis. *AUTHORS. J. Compil. BJU Int. Investig. Urol.* (2010). doi:10.1111/j.1464-410X.2010.09424.x
410. Moriyama, E. H. *et al.* In vitro influence of hypoxia on bioluminescence imaging in brain tumor cells. doi:10.1117/12.696720
411. Jensen, M. M., Jørgensen, J. T., Binderup, T. & Kjær, A. Tumor volume in subcutaneous mouse xenografts measured by microCT is more accurate and reproducible than determined by 18F-FDG-microPET or external caliper. *BMC Med. Imaging* **8,** 16 (2008).
412. Girit, I. C., Jure-Kunkel, M. & McIntyre, K. W. A structured light-based system for scanning subcutaneous tumors in laboratory animals. *Comp. Med.* **58,** 264–70 (2008).
413. Parente-Pereira, A. C. *et al.* Trafficking of CAR-Engineered human T cells following regional or systemic adoptive transfer in SCID beige mice. *J. Clin. Immunol.* **31,** 710–718 (2011).
414. Albelda, S. M. *et al.* Augmentation of CAR T cell trafficking and antitumor efficacy by blocking protein kinase A (PKA) localization. *Cancer Immunol. Res.* 1–12 (2016). doi:10.1158/2326-6066.CIR-15-0263
415. Kershaw, M. H. *et al.* A phase I study on adoptive immunotherapy using gene-modified T cells for ovarian cancer. *Clin. Cancer Res.* **12,** 6106–15 (2006).
416. Carpenito, C. *et al.* Control of large, established tumor xenografts with genetically retargeted human T cells containing CD28 and CD137 domains. *Proc. Natl. Acad. Sci.* **106,** 3360–3365 (2009).
417. Park, J. R. *et al.* Adoptive transfer of chimeric antigen receptor re-directed cytolytic T lymphocyte clones in patients with neuroblastoma. *Mol. Ther.* **15,** 825–33 (2007).
418. Song, D.-G. *et al.* In vivo persistence, tumor localization, and antitumor activity of CAR-engineered T cells is enhanced by costimulatory signaling through CD137 (4-1BB). *Cancer Res.* **71,** 4617–27 (2011).
419. Gregoire-Gauthier, J. *et al.* Use of immunoglobulins in the prevention of GvHD in a xenogeneic NOD/SCID/γc− mouse model. *Bone Marrow Transplant.* **47,** 439–450 (2012).
420. Ali, N. *et al.* Xenogeneic Graft-versus-Host-Disease in NOD-scid IL-2Rγnull Mice Display a T-Effector Memory Phenotype. *PLoS One* **7,** e44219 (2012).
421. Rijn, R. S. Van *et al.* A new xenograft model for graft-versus-host disease by intravenous transfer of human peripheral blood mononuclear cells in RAG2-/- yc-/-

double-mutant mice. *Immunobiology* **102,** 2522–2531 (2003).

422. King, M. A. *et al.* Human peripheral blood leucocyte non-obese diabetic-severe combined immunodeficiency interleukin-2 receptor gamma chain gene mouse model of xenogeneic graft-versus-host-like disease and the role of host major histocompatibility complex. *Clin. & Exp. Immunol.* **157,** 104–118 (2009).
423. Adusumilli, P. S. *et al.* Regional delivery of mesothelin-targeted CAR T cell therapy generates potent and long-lasting CD4-dependent tumor immunity. *Sci. Transl. Med.* **6,** 261ra151-261ra151 (2014).
424. Ross, D. T. *et al.* Systematic variation in gene expression patterns in human cancer cell lines. *Nat. Genet.* **24,** 227–235 (2000).
425. Spicer, A. P., Parry, G., Patton, S. & Gendler, S. J. Molecular cloning and analysis of the mouse homologue of the tumor-associated mucin, MUC1, reveals conservation of potential o-glycosylation sites, transmembrane, and cytoplasmic domains and a loss of minisatellite-like polymorphism. *J. Biol. Chem.* **266,** 15099–15109 (1991).
426. Wang, L. X. J. *et al.* Tumor ablation by gene-modified T cells in the absence of autoimmunity. *Cancer Res.* **70,** 9591–9598 (2010).
427. Moon, E. K. *et al.* Blockade of programmed death 1 augments the ability of human T cells engineered to target NY-ESO-1 to control tumor growth after adoptive transfer. *Clin. Cancer Res.* **22,** 436–447 (2016).
428. Valitutti, B. S., Müller, S., Salio, M. & Lanzavecchia, A. Degredation of T Cell Receptor (TCR)-CD3-Zeta Complexes after Antigenic Stimulation. *J. Exp. Med* **185,** 1859–1864 (1997).
429. Agrawal, B. & Krantz, M. Cancer-associated MUC1 mucin inhibits human T-cell proliferation, which is reversible by IL-2. *Nat. Med.* (1998).
430. Gimmi, C. D. *et al.* Breast cancer-associated antigen, DF3/MUC1, induces apoptosis of activated human T cells. *Nat Med* **2,** 1367–1370 (1996).
431. Fisher, J. P. H. *et al.* Effective combination treatment of GD2-expressing neuroblastoma and Ewing's sarcoma using anti-GD2 ch14.18/CHO antibody with Vγ9Vδ2+ γδT cells. *Oncoimmunology* **5,** e1025194 (2016).
432. Du, S. H. *et al.* Co-expansion of cytokine-induced killer cells and Vγ9Vδ2 T cells for CAR T-cell therapy. *PLoS One* **11,** (2016).
433. Fisher, J. *et al.* Avoidance of On-Target Off-Tumor Activation Using a Co-stimulation-Only Chimeric Antigen Receptor. *Mol. Ther.* **25,** 1234–1247 (2017).
434. Ren, X. *et al.* Modification of cytokine-induced killer cells with chimeric antigen receptors (CARs) enhances antitumor immunity to epidermal growth factor receptor (EGFR)-positive malignancies. *Cancer Immunol. Immunother.* **64,** (2015).
435. Budde, L. E. *et al.* Combining a CD20 Chimeric Antigen Receptor and an Inducible Caspase 9 Suicide Switch to Improve the Efficacy and Safety of T Cell Adoptive Immunotherapy for Lymphoma. *PLoS One* **8,** e82742 (2013).

436. Taylor-Papadimitriou, J. *et al.* MUC1 and the immunobiology of cancer. *J. Mammary Gland Biol. Neoplasia* **7,** 209–221 (2002).
437. Davis, S. J. & van der Merwe, P. A. The kinetic-segregation model: TCR triggering and beyond. *Nat. Immunol.* **7,** 803–9 (2006).
438. Wild, M. K. *et al.* Dependence of T cell antigen recognition on the dimensions of an accessory receptor-ligand complex. *J. Exp. Med.* **190,** 31–41 (1999).
439. James, J. R. & Vale, R. D. Biophysical mechanism of T-cell receptor triggering in a reconstituted system. *Nature* **487,** 64–9 (2012).
440. Cordoba, S. P. S. *et al.* The large ectodomains of CD45 and CD148 regulate their segregation from and inhibition of ligated T-cell receptor. *Blood* **121,** 4295–4302 (2013).
441. Gendler, S., Taylor-Papadimitriou, J., Duhig, T., Rothbard, J. & Burchell, J. A Highly Immunogenic Region of a Human Polymorphic Epithelial Mucin Expressed by Carcinomas Is Made Up of Tandem Repeats*. *J. Biol. Chem.* **263,** 12820–12823 (1988).